TRW REPORT
34129-6001-UT-00

NASA CR 165153

DEPRIMING OF ARTERIAL HEAT PIPES: AN INVESTIGATION OF CTS THERMAL EXCURSIONS

(NASA-CR-165153) DEPRIMING OF ARTERIAL HEAT PIPES: AN INVESTIGATION OF CTS THERMAL EXCURSIONS Final Report, Sept. 1978 - Aug. 1980 (TRW Defense and Space Systems Group) 214 p HC A10/MF A01 CSCL 20D G3/34

N80-32688

Unclas
28773

FINAL REPORT

AUGUST 20, 1980

D. Antoniuk
D. K. Edwards

TRW SALES NO. 34129.000
CONTRACT NAS 3-21740

Prepared for
NASA-LEWIS RESEARCH CENTER
CLEVELAND, OHIO, 44135

TRW
DEFENSE AND SPACE SYSTEMS GROUP
ONE SPACE PARK • REDONDO BEACH • CALIFORNIA

1. Report No.	2. Government Accession No.	3. Recipient's Catalog No.
CR 165153		

4. Title and Subtitle	5. Report Date
DEPRIMING OF ARTERIAL HEAT PIPES: An Investigation of CTS Thermal Excursions	August 1980
	6. Performing Organization Code
7. Author(s)	8. Performing Organization Report No.
D. Antoniuk and D. K. Edwards	34129-6001-UT-00
	10. Work Unit No.
9. Performing Organization Name and Address	11. Contract or Grant No.
TRW Defense and Space Systems Group One Space Park Redondo Beach, California 90278	NAS3-21740
	13. Type of Report and Period Covered
12. Sponsoring Agency Name and Address	Final (9/78 to 8/80)
NASA Lewis Research Center 21000 Brookpark Road Cleveland, Ohio 44135	14. Sponsoring Agency Code
	6133

15. Supplementary Notes

16. Abstract

This final report describes the analyses and experimentation performed to determine the cause(s) and/or contributing factor(s) responsible for four (4) thermal excursions of the Transmitter Experiment Package (TEP) on the Communications Technology Satellite (CTS) during its eclipse season in 1977. These so-called "anomolies" were the result of the depriming of the arteries in all three (3) heat pipes in the Variable Conductance Heat Pipe System (VCHPS) which cooled the TEP. The determined cause of the depriming of the heat pipes was the formation of bubbles of the nitrogen/helium control gas mixture in the arteries during the thaw portion of a freeze/thaw cycle of the inactive region of the condenser section of the heat pipe. Conditions such as suction freezeout or heat pipe turn-on, which moved these bubbles into the active region of the heat pipe, contributed to the depriming mechanism. Methods for precluding, or reducing the probability of, this type of failure mechanism in future applications of arterial heat pipes are also included in the report.

17. Key Words (Suggested by Author(s))	18. Distribution Statement
Arterial heat pipes; thermal control; artery depriming mechanisms; Communications Technology Satellite (Hermes).	Unclassified - unlimited STAR category

19. Security Classif. (of this report)	20. Security Classif. (of this page)	21. No. of Pages	22. Price*
Unclassified	Unclassified	216	

*For sale by the National Technical Information Service, Springfield, Virginia 22161

CONTENTS

CONTENTS (Continued)

1.0 INTRODUCTIONS

1.1 CTS THERMAL ANOMALIES

The Communication Technology Satellite (CTS) was launched into an equatorial geosynchrouous orbit in January, 1976 and is stationed at 116° longitude. After completing nearly four years of operation, the CTS mission has recently been terminated.

The major payload on the CTS is the Transmitter Experiment Package (TEP) which consists of a high power travelling wave tube (TWT), a power processing system (PPS) and a variable conductance heat pipe system (VCHPS) shown schematically in Figure 1-1. Heat produced in the tube collector is directly radiated to space, whereas power dissipated in the PPS is first conducted to the TEP saddle and the spacecraft south panel from where it is radiatively rejected.

The temperature control of the TWT is provided primarily by a variable conductance heat pipe (VCHP)/Radiator system which transports and rejects most of the heat dissipated in the tube body. Mounting details of the tube body to heat pipe evaporator saddle and the spacecraft south panel are sketched in Figure 1-2. As shown there are several interfaces through which the heat must flow to reach the heat pipes. Normally, heat reaching the aluminum baseplate is mostly absorbed by the heat pipes and is transported axially to the VCHP radiator. A fraction of it, however, is conducted to the spacecraft south panel where it is radiated to space.

The VCHP system, shown in Figure 1-3, consists of three stainless steel/methanol dual artery heat pipes whose variable conductance is achieved with the help of external cold wicked reservoirs loaded with a 10 percent helium/90 percent nitrogen gas mixture. Figure 1-3 shows the six positions in the VCHP/radiator system at which temperatures are measured in flight. The Transmitter Experiment Package is instrumented with four additional temperature sensors, two located on the Multistage Depressed Collector (MDC) and two sensors located on and near the tube body.

The CTS is the first spacecraft to rely on heat pipes to control the thermal performance of a major onboard system. The Transmitter Experiment Package has performed satisfactorily except on four occasions in 1977, March 16, March 23, April 11, and September 10 when measured tube body

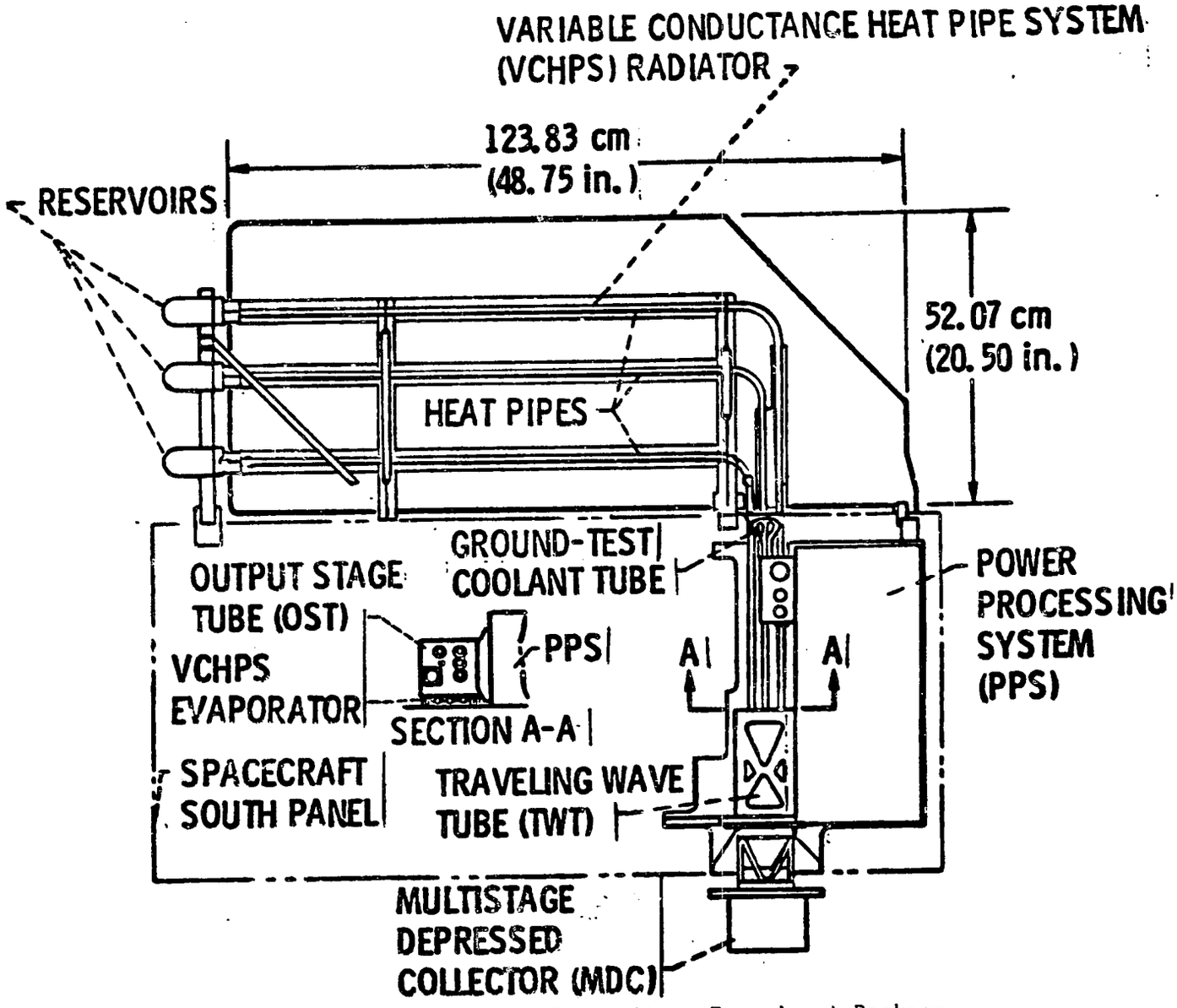

Figure 1-1. CTS Transmitter Experiment Package

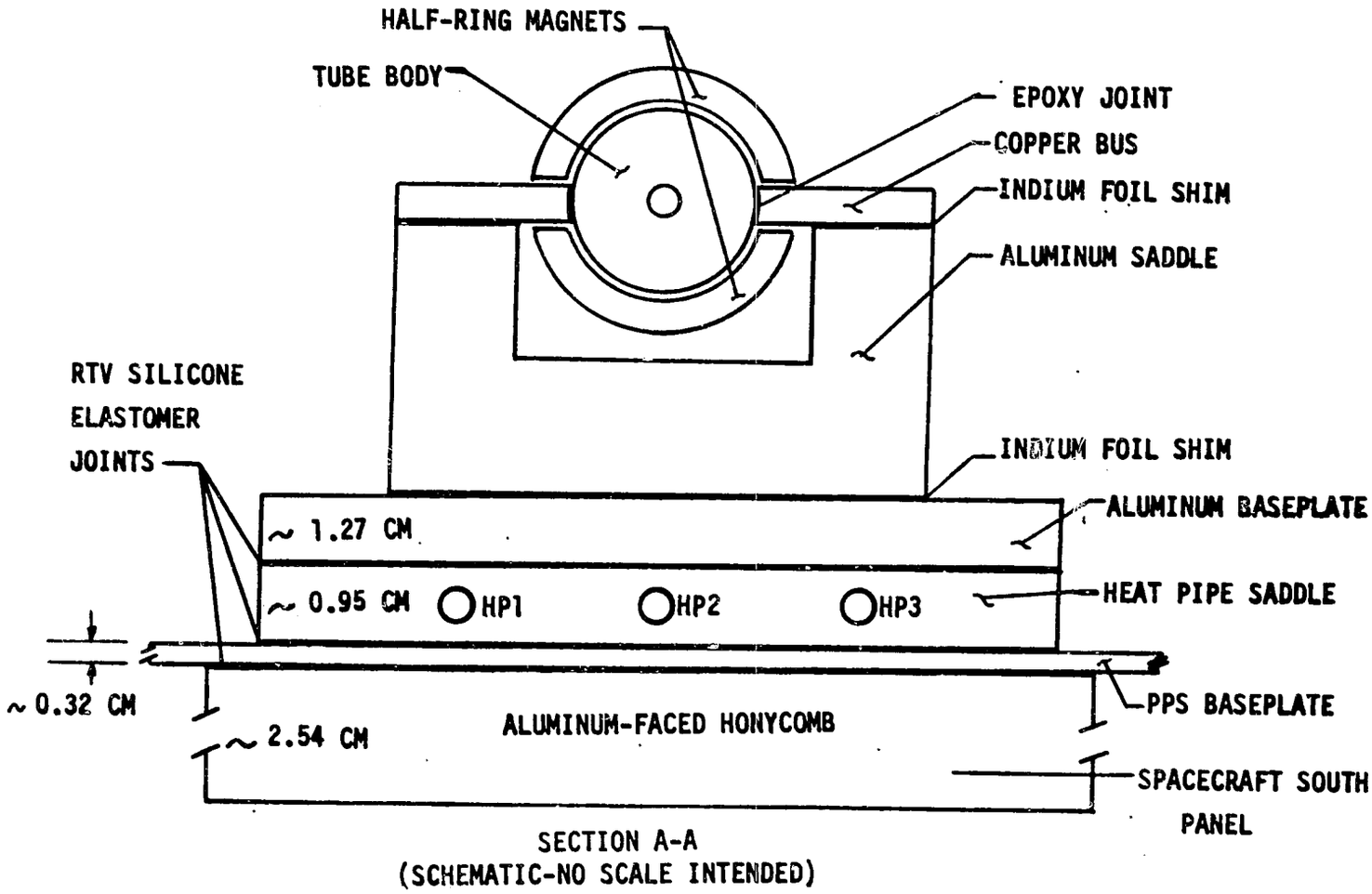

Figure 1-2. Mounted CTS OST

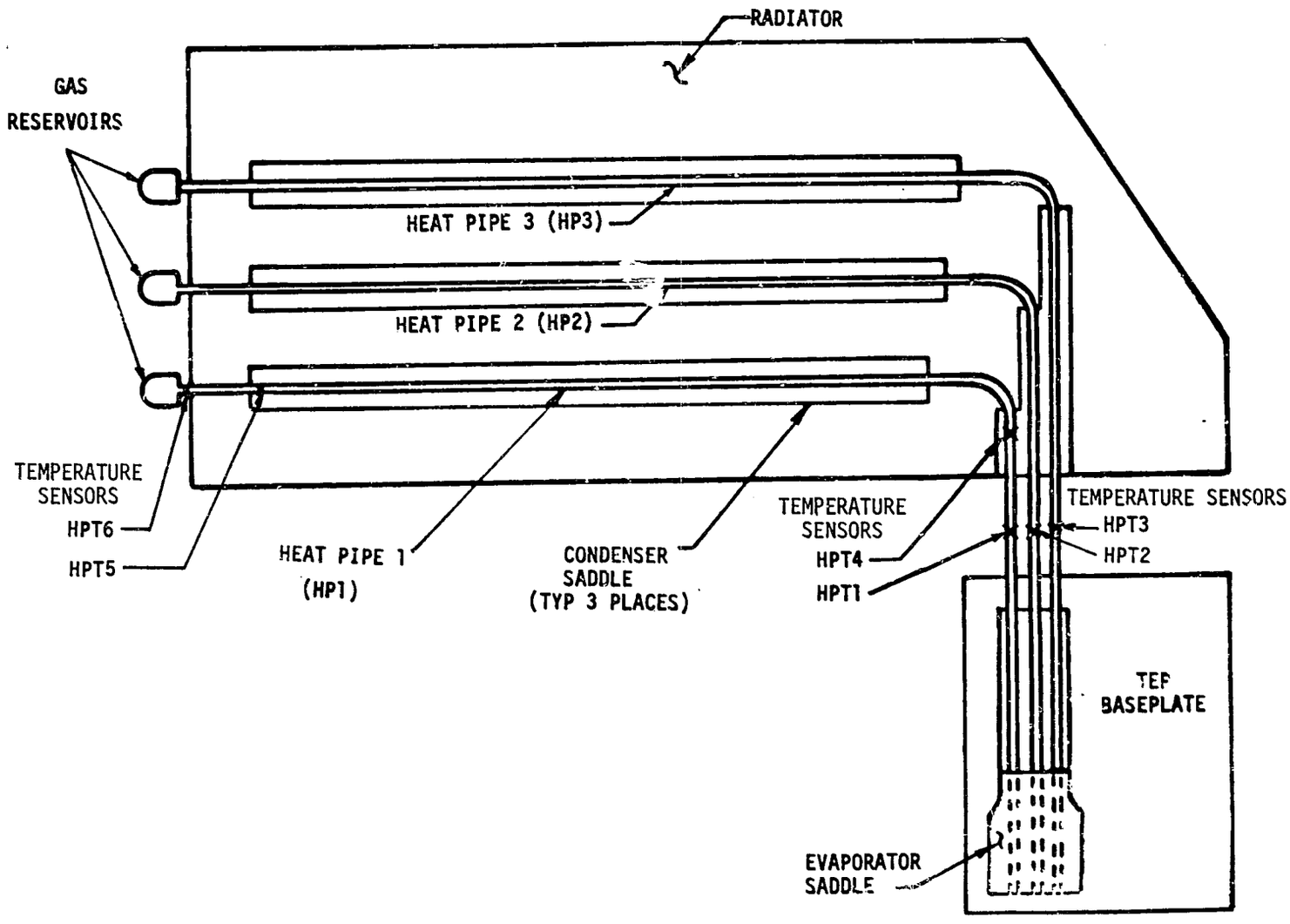

Figure 1-3. Flight Instrumentation Variable Conductance Heat Pipe System

temperatures displayed sudden, rapid increases not normal for the TEP operating conditions and inconsistent with the design of the thermal control systems. The anomalous behavior of the TEP in these four occasions are referred to as the "CTS Thermal Anomalies" of days 75, 82, 101, and 253 respectively.

During all the anomalies, the continuous increase of the tube body temperatures was reversed by reducing the output power without damage to TEP. Operation of the TWT at the reduced power resulted subsequently in the recovery of the thermal control system with no evidence of degradation or changes in its performance.

After the fourth anomaly (day 253), the TEP was successfully operated at somewhat reduced power (below the open artery capacity of the heat pipes), and no further anomalies were detected.

1.2 REVIEW OF PREVIOUS WORK

Following the first occurrence (day 75), the CTS anomalies were the subject of investigations both at NASA Lewis Research Center (LeRC) and at TRW in an effort to understand the cause of the thermal failures, focussing particular attention on the VCHPS since it is in the thermal path from the tube body to space. The work performed at LeRC and preliminary studies conducted at TRW are documented in References 1 and 2, respectively.

LeRC's investigation included the use of flight-type TEP components in ambient and vacuum ground tests, analytical studies, flight data review, and CTS on-orbit tests. The objectives were to determine the most probable cause of the anomalies and to identify procedures or TEP operating modes which would preclude damage to the TWT in the event of recurring anomalies or of continuous degraded capacity of the thermal control system.

From the review of flight data for both normal and anomalous days the following observations about the anomalies were made:

1) All occurred after relatively long periods at constant, although differing, TWT RF power levels or heat rejection rates from the tube baseplate.

2) All the anomalies took place near the Spring and Fall equinox periods during which sun angle with respect to the VCHPS radiator is relatively small and during the orbit quadrant where the CTS is almost directly between Earth and Sun in which case the VCHPS surface becomes increasingly shadowed by the spacecraft itself.

3) All the anomalies, except on day 253, were characterized by being preceded by temperatures measured at the extremity of heat pipe number 1 (HP1 with sensor HPT5. See Figure 1-3) being at or below -98 C, the methanol freezing point.

4) All the thermal anomalies were preceded or accompanied by a sudden abnormal but small increase in the difference in measured temperatures between the adiabatic sections of heat pipe number 3 and 1, ΔT_{1-3}. This increase in ΔT_{1-3} was followed by a second increase, and at the outset of unstable tube body temperature rise, ΔT_{3-1} was observed to drop to a lower level.

Tests were performed with a TWT almost identical to the one outboard CTS. The results indicated that the anomalies could not have been caused by thermal interface failure inasmuch that: a) it is improbable that a failed interface could recover its integrity completely after an anomaly, and b) it was demonstrated that an interface failure results in tube body temperature rates higher than those observed during the anomalies.

Vacuum tests that most closely approximated anomalous temperature profiles were those in which the tube base plate cooling was abruptly reduced from that required for thermal equilibrium at normal operating temperatures. These test results suggested that the reduction in heat transfer capability of the variable conductance heat pipe system is, to a high degree of certainty, the cause of the thermal anomalies.

Room-ambient tests at LeRC with a flight-type VCHPS indicated that ΔT_{3-1} increases are caused by depriming of heat pipe 1 (HP1) or heat pipe (HP1) and heat pipe 2 (HP2). The temperature difference between the adiabatic sections of heat pipe 3 (HP3) and HP1 was found to depend on the priming states of the heat pipe arteries. The measured temperature differences ΔT_{3-1} were:

a) $\Delta T_{3-1} \doteq 1.1$C, all heat pipes are primed

b) $\Delta T_{3-1} \doteq 5.1$C, HP1 is deprimed

c) $\Delta T_{3-1} \doteq 7.8$C, HP1 and HP2 deprimed

d) $\Delta T_{3-1} \doteq 2.3$C, all heat pipes deprimed

These values for ΔT_{3-1} are consistent with the temperature levels observed during anomalous days and tend to confirm the postulate that the anomalies are initiated by depriming of HP1, followed by depriming of HP2, and the onset of tube body unstable temperature rise caused finally by depriming of HP3.

On day 253, while LeRC personnel were performing experiments on-board CTS, the fourth anomaly occurred. This event gave the unique opportunity to establish the stable VCHPS heat rejection capacity beyond which the tube body temperature becomes unstable. It was found the open artery capacity of the VCHPS is approximately 106 watts.

The comprehensive investigative work performed at LeRC made significant contributions to the understanding of the CTS thermal anomalies. The most significant contribution is the fact that convincing evidence was made available to establish that the thermal anomalies were caused by unexpected reductions in the VCHPS heat transfer capability resulting from depriming of the heat pipe arteries.

The first preliminary investigation of the CTS thermal anomalies conducted at TRW is documented in Reference 2. This investigation, performed in direct support of LeRC efforts, focussed particular attention at the identification and analysis of potential artery depriming mechanisms.

Selection of depriming mechanisms was based on the premise that they must be consistent with three key observations:

1) All the anomalies occurred during the eclipse season.

2) These anomalies are sporadic. Similar conditions on successive days can yield an anomaly one day but not the next.

3) The anomalies are triggered by depriming of arteries in HP1.

In the early study, among a number of postulated mechanisms, only three were identified which could be associated with eclipse seasons:

I) Condenser freezing

II) Marangoni flow

III) Gas evolution in the arteries due to rapid chilling

It was argued that under certain conditions freezing of CTS arteries could lead to depriming. Arterial failure could result from the transfer of mass from the evaporator to the frozen condenser where it would freeze and not be available for circulation. This transfer of mass could be effected by vapor diffusion, by liquid pumping in fillets due to reduction of specific volume as it cools and/or by Marangoni flow. The fact that the CTS-type heat pipes will not fail due to condenser freezing when operated under no load or at high heat loads, led to the argument that the condenser freezing mechanism will work if the pipe is operated at the right load, not too high, not too low. However, several factors implied that, although condenser freezing can lead to artery depriming, it could not be the primary cause of the anomalies.

These factors are the fact that on day 253 an anomaly occurred before the radiator portion of HP1 approached freezing conditions, and the fact that with all pipes primed HP3 should freeze and deprime first since it carries least load and its radiator portion radiates from both sides, however, HP1 failed first. An additional factor is the fact that after the anomalies the VCHPS recovers before the radiator begins to warm up. It was thus argued that if sufficient excess fluid was frozen to cause artery depriming there would be none available to rewet the evaporator. Therefore, condenser freezing was ruled out.

Marangoni Flow (surface tension flow due to temperature gradients along the a VCHP gas-blocked region) could induce a flow along fillets and excess fluid reservoirs toward the condenser end along the vapor-liquid interfaces. No flow, however could be induced in the wick and arteries which have structure to support the surface tension gradient. It was argued that Marangoni Flow could influence the VCHP in two ways:

1) If the condenser end is frozen, Marangoni Flow toward that end would increase freezing under load. However, condenser freezing was argued not to be the primary mechanism for depriming.

2) If the heat pipe is not frozen, Marangoni Flow will cause a pressure drop along fillets and natural reservoirs reducing their pumping capacity. However, the reduction must be small, otherwise anomalies due to Marangoni Flow effects would occur on consecutive days under similar conditions, not sporadically. It was argued, however, that once deprimed,

the open artery capacity could be measurably influenced by Marangoni Flow.

In view of the fact that the control gases helium and nitrogen, particularly helium, have solubilities in methanol decreasing with decreasing temperature and pressure, it was argued that this behavior could give rise to a potential depriming mechanism which is consistent with sporadic occurrences during the eclipse seasons. This mechanism is gas evolution within the arteries during heat pipe chilldown.

It was postulated that when TEP ceases to operate several hours before an eclipse, the gas blocks the entire length of the heat pipes. During this off period, liquid in the arteries becomes saturated with gas surrounding the arteries at the gas-blocked condenser temperature and evaporator pressure. When the CTS enters eclipse, the heat pipes experienced rapid chilldown which causes the temperature and pressure to drop rendering the liquid in the arteries sufficiently supersaturated in dissolved gas to cause gas bubble nucleation within the arteries.

In the early study, it was postulated that gas would evolve at unspecified nucleating sites leading to numerous small bubbles, some of which would coalesce to form fewer but larger bubbles with intrinsic longer lifetimes. When the TEP is reactivated, the heat pipes would turn on leading to the establishment of a gas/vapor front and a build-up of stress in the active portion. It was postulated then that if the local liquid stress exceeds a critical level for a bubble before this bubble is redissolved or vented, the arteries would deprime. Of the three potential mechanisms for artery depriming considered in this early study, gas evolution was argued to be the most plausible inasmuch that it ties the anomalies to eclipse seasons when the VCHP system experiences rapid chilldowns. Furthermore, it also provided an explanation for the sporadic occurrences within eclipse seasons since, it depends on the operating conditions before and after the eclipse and on bubble nucleation and aglomeration which are statistical phenomena.

Although no attempts were made at that time to analytically treat the gas evolution scenario, a simple experiment was performed to determine whether gas bubbles would be nucleated in the arteries under CTS conditions.

The experimental setup consisted of a short section of CTS-type arterial wick inserted into a glass tube sealed at one end and valved at the other. The tube was filled with appropriate amounts of 10 percent He/90 percent N_2 gas and methanol simulating CTS design parameters. The tube was then subjected to temperature reduction under hydrostatic stress in excess of open artery capacity. The imposed stress was equivalent to increased supersaturation which would enhance the probability of bubble nucleation. Experiments at temperature reduction rates of -1.71 C/Min and -0.9 C/Min yielded negative results even though the cooling rates were about twice those observed in orbit, and the imposed hydrostatic stress enhanced the probability of bubble nucleation.

The results of this experiment lead to the conclusion that the gas evolution mechanism could not have caused artery depriming under conditions experienced by the CTS.

Thus, this preliminary investigation at TRW was unsuccessful in its quest for a single or sequential series of mechanisms for artery depriming consistent with all flight data. However, depriming due to gas evolution within the arteries was regarded as qualitatively consistent with all the observed anomalies and warranted further investigation.

1.3 PHASE I STUDIES

In view of the fact that previous investigations of the CTS thermal anomalies convincingly established depriming of the heat pipes in the VCHP system as the cause of the anomalies but failed to identify the mechanism or sequential series of mechanisms that led to depriming of the arteries, TRW (under contract to NASA LeRC - Contract NAS3-21740) undertook a two-step investigation of the hydrodynamic characteristics of CTS-type heat pipes.

This section of the report summarizes the work performed during Phase I and refers to attached appendices (documents generated during Phase I) for further details.

The first task performed was to identify mechanisms which under a wide range of feasible conditions could lead to depriming of the heat pipe arteries. Ten mechanisms were postulated which are briefly described and classified in four basic groups in Figure 1-4. Also shown are comments on

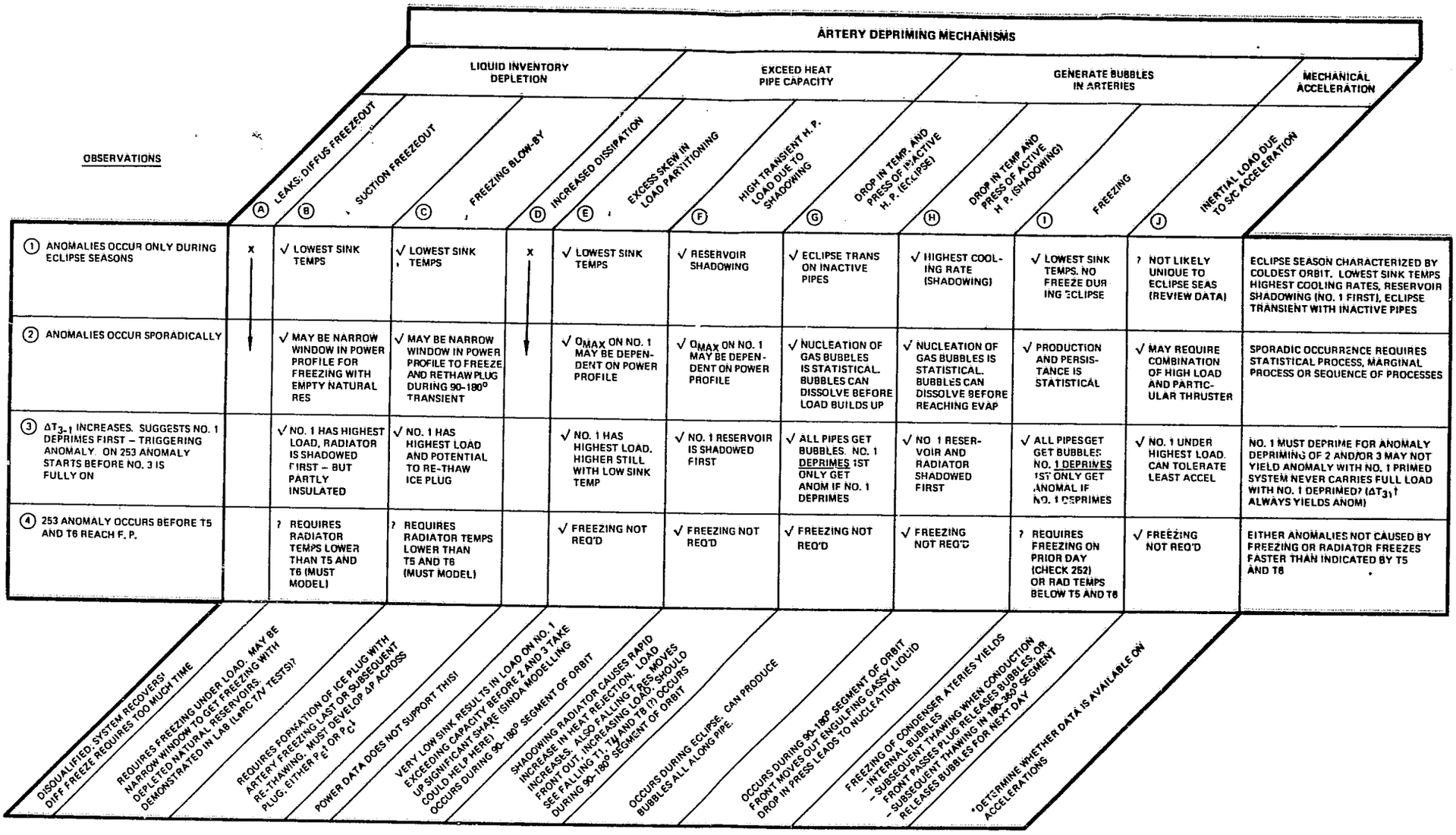

Figure 1-4. Observations on Postulated Artery Depriming Mechanisms

the postulated mechanisms in light of observed characteristics of the anomalies and flight data. The approach in Phase I to investigate the potential of these mechanisms is shown in Figure 1-5.

The basic approach has been, for a given depriming mechanism, to conduct analyses in the following sequential order with the implementation of each succeeding task being contingent upon the results of the previous one:

a) Analytical "back-of-the-envelope" calculations and/or flight data review.

b) Calculations with more realistic analytical models.

c) Bench-scale experiments such as with glass heat pipe.

d) Experiments with CTS SN009 heat pipe which is similar to heat pipe 1 on the CTS.

e) Correlations of experimental data with thermal (SINDA) and heat pipe (VCHPDA) analytical models results.

Tasks a, b, c, and d were performed by TRW, whereas task e was the result of a joint effort with LeRC in which the experimental data generated at TRW facilities were correlated with the results of steady state and transient thermal analyses of TEP performed at LeRC. The LeRC study is briefly reviewed in Appendix A.4.1.

Mechanisms Exceeding Heat Pipe Capacity

The arteries in a heat pipe can certainly be caused to deprime if the imposed heat load exceeds the designed heat transfer capacity of the heat pipe. Exceeding the heat pipe capacity can be the result of increased dissipation by TEP, excess skew in load partitioning on the VCHPS, and high transient heat pipe load due to condenser and/or reservior shadowing.

Increased Dissipation (Column D of Figure 1-4). This is clearly not the cause of artery depriming since:

1) TEP power dissipation exceeding designed levels is not supported by flight power data

2) The heat loads are well below the system capacity when all three heat pipes are primed. In fact a single primed heat pipe can carry the maximum designed dissipation heat load.

INVESTIGATION AREA	EXPERIMENT	ANALYSIS	COMPUTER MODELLING
SUCTION AND BLOW-BY FREEZING B AND C	SN 009: FREEZE CONDENSER AS FUNCTION OF S. S. LOAD AND TILT. ALSO AS PART OF TRANSIENT POWER INCREASE IF DE-PRIMING OBSERVED (1-G EFFECTS ON BLOW-BY?)		• MODIFY SINDA MODEL FOR CORRECT GAS AND LIQUID INVENT. ALSO, RESISTANCES, DIMENSIONS, ETC. (GET LeRC MODEL FROM LOU GEDEON), ADD SUBROUTINE TO DECOUPLE RES FROM COND WITH ICE PLUG • RUN SINDA TO DETERMINE GAS FRONT POSITIONS AND TEMP DISTRIB ON ANOMALY DAYS • MODIFY MULTIWICK TO INCLUDE MARANGONI FLOW AND FREEZING • RUN MULTIWICK TO ESTABLISH INVENTORY DISTRIBUTION AND STRESS AS FUNCTION OF FREEZING PROCESS
BUBBLE PRODUCTION G, H AND I	GLASS TEST SECTION AND/OR GLASS HEAT PIPE: TRY TO PRODUCE BUBBLES IN He-SATURATED METHANOL BY CHILLING, BY FREEZING, BY SUDDEN DROP IN PRESSURE (IONIZING RADIATION?)	CALCULATE NUMBER OF CRITICAL SIZE BUBBLES WHICH CAN BE GENERATED DUE TO SUPERSATURATION IN RAPID CHILLDOWN. CONSIDER BOTH TEMPERATURE AND PRESSURE EFFECTS GUIDANCE ON TEST CONDITIONS	
SUDDEN COOLING F	SN 009: RAPIDLY CHILL/FREEZE CONDENSER AND/OR RESERVOIR TO SEE IF PIPE CAN BE DEPRIMED YES DO PARAMETRIC LAB TESTS TO DETERMINE LEAST SEVERE CONDITIONS NECESSARY TO DEPRIME PIPES	FIRST ORDER CALCULATION OF INCREASE IN LOAD DUE TO COOLING-INDUCED EXPANSION OF FRONT IF SIGNIFICANT	SINDA CALCULATIONS: ARE MINIMUM NECESSARY CONDITIONS FEASIBLE. DOES THERE EXIST A WINDOW IN POWER PROFILE (LOW LOAD – EXCESS RESERVOIRS FULL OF LIQUID TO HANDLE TRANSIENT, HIGH LOAD – RADIATOR NEARLY FULL ON WITH LITTLE POTENTIAL FOR LOAD INCREASE, OR – RES ON NO. 1 MUST BE SHADOWED WITH HIGH LOAD ON 1 BUT 2 AND 3 NOT ON SIGNIFICANTLY)
EXCESS SKEW IN LOAD PARTITIONING E			SINDA MODELLING: CALCULATE LOAD ON H. P. NO. 1 THROUGHOUT ORBITAL TRANSIENT MULTIWICK: CALCULATE CAPACITY OF H. P. NO. 1 THROUGHOUT ORBITAL TRANSIENT USING SINDA OUTPUT FOR GAS FRONT AND TEMP DISTRIBUTIONS
INERTIAL ACCELERATION LOAD J		EXAMINE S/C ACCELEROMETER DATA, IF AVAILABLE	
DEPRIMING SEQUENCE		EXAMINE FLIGHT DATA IN DETAIL. DAY 253; ΔT_{3-2} AND ΔT_{2-1} ON ANOMALY AND NORMAL DAYS; CORRELATION OF T1, T2, T3 WITH BODY TEMP INDICATING PRIMED STATE	

Figure 1-5. Approach to Investigate Potential Depriming Mechanisms

3) On many days preceding and/or following the anomalies, higher heat loads were accommodated without difficulty.

Excess Skew in Load Partitioning (Column E of Figure 1-4). The three heat pipes of the VCHPS on CTS are designed to turn on sequentially so as to balance the load between them at full-on design conditions. However, very low sink temperatures during equinox conditions could result in the load of heat pipe HP1 exceeding transiently its capacity before HP2 and HP3 take up a significant share of the load. Failure of HP1 by the above mechanism or by any other could then result in a rapid transfer of load to HP2 which, due to inertial effects associated with rapid load transfer, could fail leading to a rapid transfer of load to HP3, yielding, perhaps, a "domino effect" failure of the whole system.

Failure of HP1 due to excess skew in load partitioning is discounted since LeRC transient thermal results for periods preceding the four anomalies indicate the maximum load on HP1 never exceeds 80 watts, a load that is well below its primed heat transfer capacity.

In Appendix A.1 flight data are analyzed to determine whether there exists a regularity in the depriming sequence associated with the anomalies, and the possibility of a "domino effect" failure of the system is investigated experimentally.

The analysis of flight data showed that these exists some regularity in the depriming sequence as follows: HP1 deprimes first, HP2 deprimes next followed by depriming of HP3. (On days 89 and 253 the temperature data suggest that heat pipe 2 or 3 was deprimed, while HP1 carried the load.) Experimentally, attempts were made to deprime the SN009 heat pipe with rapid increases of load, simulating, under more stringent conditions, rapid sequential load transfer as heat pipes deprime.

Tests performed for both high (-18C) and low (-96C) sink temperatures and at 2.5 cm evaporator tilt, indicated no measurable rate effect attributable to fluid inertia and thus argued against a "domino effect".

High Transient Heat Pipe Load Due to Condenser and/or Reservoir Shadowing (Column F of Figure 1-4). Sudden shadowing cools the heat pipe reservoir which causes the vapor/gas front to move toward the reservoir end of the radiator increasing the active portion of the condenser which

causes the heat load on the pipe to increase. In addition, shadowing of the VCHPS radiator increases the load on the heat pipes due to a drop in the effective environment temperature.

Although both effects will eventually lead to cooling of the heat source, movement of the gas/vapor front reducing the active condenser section, and reequilibration at the dissipation load, the transient peak may be sufficient to exceed the heat pipe capacity and deprime the arteries.

An examination of flight data corresponding to periods preceding and including the onset of the four anomalies shows a scenario of decreasing temperatures of the gas reservoirs and on sections of the VCHP system radiator. Telemetry data for temperature sensors HPT5 and HPT6 (see Figure 1-3) show that at these locations the temperature drop monotonically prior to the anomalies.

In order to explore the potential of this postulated mechanism for artery depriming, the transient loads possible under typical orbital conditions were estimated using a simplified analytical model of the VCHP system. The description of the model and the basis for the transient loads calculations are presented in Appendices A.2.1 and A.2.2, which address the effects of shadowing of the reservoir and condenser, respectively. The analytical estimates show, that under some assumed cooling rates, the instantaneous heat loads may be as much as 45 percent larger than steady state conditions would indicate. These analytical results were found significant enough to warrant further tests on the SN009 heat pipe.

Appendix A.2.3 describes a series of tests performed on the SN009 heat pipe during which the condenser or the gas reservoir was cooled at various rates while the evaporator was maintained at a constant heat load. In tests loads of 100 and 150 watts and cooling of the condenser at approximately 2.8 C/Min produced no depriming. No depriming was observed either in tests with 125 watts and at a condenser cooling rate of approximately 3.9 C/Min. Thus, depriming due to rapid chilldown of the condenser was not demonstrated.

During tests in which the gas reservoir was cooled repeatedly at successively higher rates depriming was observed. With 100 watts at the evaporator and the inactive condenser at -18 C, depriming occurred when the reservoir was cooled at the threshold rate of approximately -3.2 C/Min.

Although depriming due to rapid chilldown of the reservoir was demonstrated, the required rates were substantially higher than those observed during the anomalies. This fact eliminates the postulated sudden cooling mechanism as a potential cause of the CTS anomalies.

Mechanisms for Depletion of Liquid Inventory

Another possible cause of artery depriming in a heat pipe is depletion of liquid inventory, either depletion of total heat pipe inventory such as that resulting from a leak, or depletion of liquid from the active portion of the pipe such as could result from diffusion freezeout, suction freeze-out or freezing blow by. Suction freezeout is the loss of liquid from freezing. Freezing blowby is the loss of liquid from the thawing of an ice plug allowing a high pressure evaporator to blow liquid from the active pipe into a low pressure gas reservoir.

Loss of inventory due to leaks will cause permanent changes in heat pipe performance, an event that is not supported by the observed complete recovery of the system following an anomaly. Diffusion freezeout is the transfer of inventory in the vapor phase from the active pipe into the frozen section where the vapor condenses and freezes. It is too slow a transfer process to have been effective during the time available prior to the anomalies.

Suction Freezeout (Column B of Figure 1-4). Suction freezeout has long been recognized as an artery depriming mechanism. Depriming occurs due to depletion of evaporator liquid because of the local density increase as a freezing front moves toward the evaporator end of the pipe. It is necessary, however, that the condenser freeze while the heat pipe is under load so that the natural liquid reservoirs in the evaporator do not contain excess liquid. Such excess liquid would satisfy the demand of the freezing process without stressing the arteries to failure. Suction freezeout is a viable explanation for depriming on anomaly days 75, 82, and 101. But not on day 253, since the results of steady state and transient calculations on the CTS model performed at LeRC indicate no freezing on this day at the time of the anomaly.

This depriming mechanism was investigated analytically in the previous TRW's study[2] where the mechanism is referred to as "Condenser Freezing".

The results of this investigation made in light of flight data and observation about the anomalies were summarized in Section 1.2 of this report.

In Phase I of this program, suction freezeout was subjected to experimental investigation with tests on the SN009 heat pipe. Several attempts to deprime the arteries by freezing the condenser while the SN009 heat pipe was under hydrostatic and thermal load were unsuccessful.

The experimental results support the conclusion of the previous investigation[2] which states that although suction freezeout or condenser freezing can and may lead to artery depriming, it is not the primary cause of the anomalies.

Freezing Blowby (Column C of Figure 1-4). The CTS heat pipes contain substantial amounts of excess liquid. Such excess inventory is required for successful priming of the arteries in earth gravity testing. In zero gravity a slug of excess liquid generally bridges the condenser vapor spaces, acting as a moving membrane between portions of the non-condensible control gas. Subfreezing radiator temperatures can cause the slug of liquid to become an immobilized plug of ice separating the active section of the pipe from its gas reservoir. If during a transient a pressure differential develops across the ice plug, with the pressure higher on the evaporator side, and then the plug partially thaws, this pressure difference can blow liquid from the evaporator to the reservoir side and deplete the active pipe inventory causing the arteries to deprime.

Because freezing blowby requires freezing, this mechanism can not be the cause of the fourth anomaly, since freezing had not occurred immediately preceding the anomaly on day 253. However, freezing blowby could account for some of the anomalies during which freezing occurred.

To explore experimentally the depriming potential of this mechanism, it was first necessary to develop means of forming an ice plug in the laboratory in the absence of the natural slugging of excess liquid expected in zero gravity. Appendix A.3 describes a successful technique that was developed to form an ice plug in the SN009 heat pipe, and the procedure followed during the blowby tests. Three tests were performed during which depriming occurred each time. The results of these tests clearly established

that freezing blowby is a bonafide depriming mechanism and a candidate to explain at least some of the anomalies.

The latter statement is supported, to a certain extent, by some results from the CTS model analyses which showed that ice plugs formed in all the heat pipes on day 82 several hours prior to the onset of the anomaly. In addition, the results showed that the pressure on the evaporator side would have been higher than on the reservoir side when the plugs thawed forty five minutes before the last heat pipe deprimed. The significance of these calculated results is that they show conditions for freezing blowby may have existed on at least one day of the anomalies.

Mechanisms for Bubble Nucleation

The presence of gas inside the arteries of the heat pipe has long been recognized as detrimental to the stable operation of the pipe. Because the solubilities of nitrogen and, particularly, helium in methanol, decrease with decreasing temperature and pressure, there exists the potential of bubble nucleation within the arteries in CTS-type heat pipes as they undergo rapid temperature reduction. This potential is compounded by the decrease in pressure that results from temperature reduction in the closed heat pipe environment. Liquid methanol saturated with gas can become supersaturated with gas when undergoing rapid temperature and pressure reduction, an event that enhances the potential of bubble nucleation.

Bubbles that might nucleate inside the arteries during the transient cooldown of the heat pipes after the power is turned off and the spacecraft enters into eclipse, can coalesce to form fewer but larger bubbles. If, as the result of their size and the rather slow process of gas diffusion back into surrounding liquid, the bubbles survive until the heat pipes are once again activated under load, some bubbles might be convected into high-stress liquid regions where they can grow in size and consequently deprime an artery.

The process of bubble coalescense and migration is recognized as statistical in nature.

The above postulated mechanism was examined during a previous TRW investigation;[2] however, experiments under simulated anomaly conditions failed to induce bubble nucleation.

Despite these results, this mechanism was reexamined during the current program due to the fact that the postulated conditions for the mechanism to be activated can be supported by flight data corresponding to all the anomalies, and the probabilistic nature of the mechanism bears positive correlation to the sporadic occurrences of the anomalies. In addition, a thorough examination required the performance of experiments simulating more realistically the operating characteristics and anomaly conditions of the CTS heat pipes and investigation of the potential of other mechanisms, particularly freezing-thawing, to induce bubble nucleation.

Bubble Nucleation Due to Temperature and Pressure Reduction (Columns G and H on Figure 1-4). An analysis of the potential for bubble formation was performed based on fundamentals described in Appendix A.5.1. Sample calculations were made for two cases (1) a condenser depressurization case where the evaporator temperature is dropped at constant gas-blocked condenser temperature and (2) a condenser chilldown case where the gas-blocked condenser is cooled at constant total pressure.

The sample calculations presented in Appendix A.5.2 showed the possibility for bubble formation upon (1) depressurization by reduction in heat pipe loading and reservoir chilling and (2) condenser chilldown. Depressurization showed greater potential, for approximately 500,000 bubbles/cm^3 were found possible, compared to only one of equal size resulting from condenser chilldown. The above calculations, based on two hypothetical cases, were followed by a number of calculations for various anomaly conditions. The predicted number of bubbles of varying critical size was found substantial for all anomaly conditions considered in the analysis.

In order to verify qualitatively the above analytical results, a series of simple experiments were formulated which are described in Appendix A.5.3. Tests were performed with a glass vessel half filled with liquid methanol containing a short section of mesh screen artery laying on its bottom. The vessel was instrumented to permit continuous monitoring of temperature and pressure. The liquid methanol was saturated with either helium or nitrogen at room temperature subsequent to which three series of tests were performed. In the first two series of tests the saturated methanol was subjected to various rates of temperature and/or pressure reduction. During the tests bubble nucleation in the bulk of the liquid

or on the surface of the artery mesh screen was never observed. These results suggested that temperature and pressure reduction are not potential mechanisms for bubble generations in CTS-type heat pipes. In the last series of tests with the glass vessel, the saturated methanol was subjected to several freeze/thaw cycles. Large numbers of bubbles were observed streaming from the ice surface.

Bubble Generation Due to Freezing (Column I of Figure 1-4). The results of the glass vessel tests were of paramount importance, for they identified freezing and thawing of gas-saturated methanol in the arteries as a potential mechanism for bubble formation in the arteries. The fact that freezing occurred preceding three of the four anomalies and sometime during the 24 hours before all of them, the involvement of ice-generated bubbles in the four thermal anomalies was shown to be a distinct possibility.

To explore this bubble nucleation mechanism in a realistic heat pipe environment, a series of tests were performed with an existing glass heat pipe. The pipe contains a slab wick with a CTS-type artery attached to one side and permits observations on the behavior of the artery in an operational heat pipe. For the tests the heat pipe was gas loaded with a 90 percent N_2/10 percent He gas mixture at a pressure equivalent to that in the CTS heat pipes. The experiments performed on the glass heat pipe are documented in Appendix A.5.4.

The results of bubble nucleation experiments showed that each time the artery in the condenser section underwent freezing and thawing bubbles were observed inside the arteries although the number of bubbles, their size and location along the artery varied from test to test. The time required for the bubbles to disappear by diffusion was found to vary enormously depending on their size. Small spherical bubbles dissolved within hours, while elongated bubbles required up to several weeks.

Additional experiments were conducted with this heat pipe during which the gas/vapor front was forced to move into the previously frozen condenser section in attempts to incorporate ice-generated bubbles into the active condenser and cause depriming. A number of deprimings were observed, but they were sporadic, probabilistic in nature. These results

conclusively demonstrated that: 1) Control gas is liberated from saturated methanol every time the heat pipe goes through a freeze/thaw cycle, 2) the number, size, and durability of gas bubbles generated within the arteries have a statistical variation and are influenced by bubble coalescence, and 3) arterial bubbles can lead to depriming if they migrate or are convected into the active region of the pipe under normal load conditions. Thus, it is clear that freezing and thawing of the condenser can, but does not necessarily, lead to artery depriming, depending on subsequent history.

Attempts to induce arterial failure in the SN009 heat pipe due to the ice-generated-bubble mechanism were partially successful. Depriming was not observed in several tests when the heat pipe was brought under a heat load immediately after the condenser had gone through a freeze/thaw cycle. However, depriming was discovered on two occasions after the SN009 heat pipe had been left unattended under hydrostatic load for several hours during which time the condenser froze following the termination of a normal freeze/thaw cycle.

The results of tests with the SN009 and glass heat pipes clearly indicated that in order to establish the statistics of this artery failure mode, repeated experiments would be required.

SUMMARY

In the course of Phase I of this program, numerous depriming mechanisms were postulated and subjected to analytical and experimental investigation. Several mechanisms were convincingly rendered highly improbable causes of artery failure on CTS. Four mechanisms, however, were identified as potential candidates to explain the anomalies and are listed in decreasing likelihood in Table 1.

It was argued during this Phase of the study that potential depriming mechanisms must be consistent with three key observations about the anomalies:

1) The anomalies occur only during the radiator eclipse season when condenser freezing may be realized.

2) The anomalies are sporadic. Similar conditions on successive days can yield an anomaly on one day and not on any of several similar days.

Table 1. Summary of Potential Depriming Mechanisms from Phase I.

ARTERY DEPRIMING RESULTS FROM:	ANALYTICALLY	EXPERIMENTALLY		
		FLASK	GLASS H.P	SN-009 H.P
I. BUBBLE NUCLEATION DUE TO:				
a) FREEZE/THAW	—	YES	YES	?
b) PRESSURE REDUCTION	YES	NO	NO	—
c) TEMP REDUCTION	YES	NO	NO	—
II. FREEZING BLOW-BY	YES	—	—	YES
III. RADIATOR/RESERVOIR RAPID COOLING	YES	—	—	YES
IV. SUCTION FREEZE-OUT	YES	—	—	NO (?)

3) On day 253 condenser freezing did not occur immediately prior to the onset of the anomaly.

In light of the above observation, the following comments can be made on the mechanisms listed on Table 1.

Suction freezeout is not a statistical depriming mechanism and cannot account for the anomaly on day 253. Artery depriming due to suction freezeout was not demonstrated with the SN009 heat pipe which seems to indicate that none of the other anomalies could have been caused by this mechanism alone. This mechanism can only be considered a potential contributing factor to some of the anomalies.

The sudden cooling mechanisms could account in principle for all the anomalies, however, they are not statistical in nature. Furthermore, tests with the SN009 heat pipe showed that the cooling rates required to fail the arteries far exceed those indicated by flight data. Thus, this artery failure mode can be assigned a low probability of success and only be considered a contributing factor to some of the anomalies.

Artery depriming due to freezing blowby was verified in repeated experiments with SN009 heat pipe, establishing freezing blowby as a bonafide potential depriming mechanism. Analyses of the CTS thermal model

for day 82 predicted the formation of ice plugs in the CTS heat pipes and calculated pressure differential across the barrier (pressure higher on evaporator side) which were sustained until the ice plugs thawed. These predicted results tend to indicate that conditions for blowby may be present on some of the anomaly days. Although freezing blowby is not a statistical mechanism and can not be the cause of the anomaly on day 253, it can not be totally discounted.

In view of the results of glass flask and glass heat pipe experiments, the ice-generated bubble mechanism appears to be a prime candidate for explaining all four CTS anomalies. It is consistent with (1) their seasoned occurrence (eclipse conditions are necessary to cause condenser freezing), (2) their sporadic occurrence (due to the statistical nature of bubble population and behavior), and (3) the lack of freezing on day 253 (bubbles were generated by a freeze/thaw process during day 252).

1.4 OBJECTIVES OF PHASE II STUDIES

The Phase I studies demonstrated that bubbles are generated each time liquid methanol containing dissolved gas undergoes freezing and thawing, and that these bubbles may result in artery depriming if inducted into the active portion of the heat pipe. This depriming mechanism was demonstrated on the glass heat pipe. However, depriming due to ice-generated bubbles was not conclusively demonstrated on the SN009 heat pipe. Because the SN009 heat pipe is similar in overall dimensions and performance characteristics to heat pipe number 1 onboard CTS, the need to demonstrate depriming on the SN009 due to bubbles became apparent in order to demonstrate beyond a reasonable doubt that the postulated bubble mechanism is the cause of the thermal anomalies.

The Phase I studies also warranted further study of the behavior of bubbles inside arteries, particularly their lifetimes, owing to the fact that the probability of arterial failure due to bubbles induction into high stress regions is positively correlated to longer bubbles lifetimes.

As a result a second phase of this program was continued. The second phase was necessary to bring the CTS-anomaly studies to the satisfactory conclusion envisioned at the outset.

The objectives of Phase II were:

1. To analyze the diffusion process for non-condensible control gases in arteries and to determine lifetimes of bubbles of various sizes at various temperature levels and rates of change of temperature level and for various selected control gases.

2. To run continuous cyclic freeze/thaw tests on the SN009 heat pipe for five consecutive days in an effort to produce artery depriming by freeze-thaw bubble formation. The successful triggering of a failure would establish that freeze-thaw bubble formation is the logical cause of the CTS thermal anomalies.

3. To propose concepts to avert artery depriming.

2.0 ANALYSIS OF BUBBLE LIFETIMES IN HEAT PIPE ARTERIES

2.1 THE SPHERICAL BUBBLE MODEL

Consistent with Phase II objectives 1 and 3, it is desired to calculate how fast vapor bubbles in heat pipe arteries might grow or collapse and how the kind of gas used affects the growth/collapse rates. The first model selected for such calculations is the one-dimensional spherical annulus, the domain $R_1 < r < R_2$ as shown in Figure 2-1.

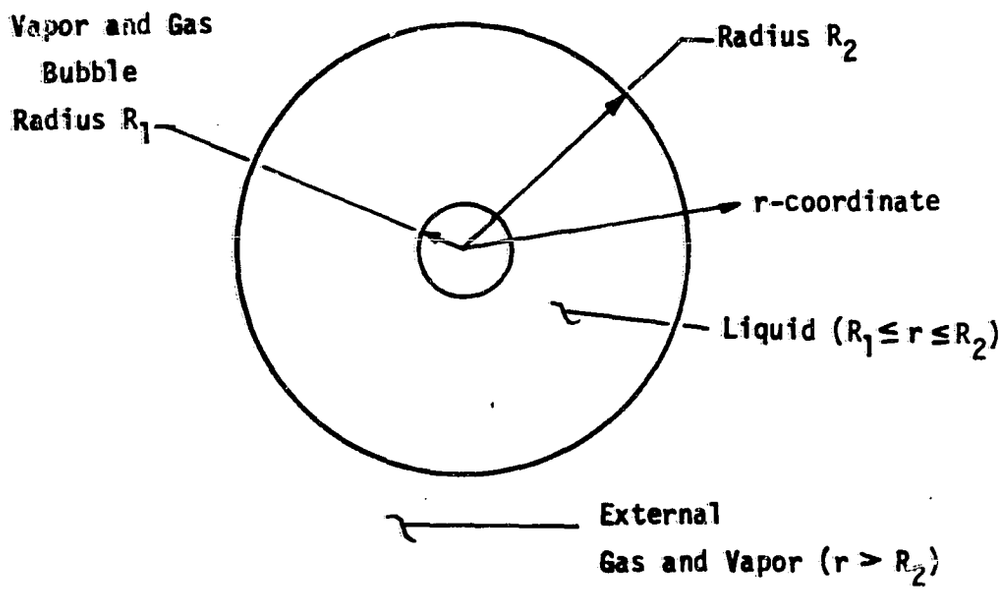

Figure 2-1. Spherical Bubble Model

The vapor-and-gas-filled bubble ($r < R_1$) has uniform composition, because gas-phase diffusivities exceed liquid phase diffusivities by several orders of magnitude. The external gas $r > R_2$ has known pressure and composition. The interface at R_2 is considered to be a screen like the wall of an artery so that the pressure difference across the interface is uncoupled from that otherwise dictated by surface tension and R_2. At $r=R_1$ no screen exists, so the vapor-to-liquid pressure difference is $2\sigma/R_1$ where σ is surface tension.

The following heat pipe scenario is postulated: The heat pipe pictured in Figure 2-2 operates with an active section at 300K and a gas-blocked condenser at 250K long enough for the artery liquid to saturate with the gas. Then as pictured in Figure 2-3 the condenser is briefly frozen and then thawed to 180K. Upon thawing of the gas-blocked condenser, there are, as has been observed experimentally, large numbers of minute bubbles released from the ice, but most diffuse back into solution. A few are postulated to condense to form the bubble of prescribed size $R_{1,0}$. The noncondensible gas compositions in the bubble and in the liquid were taken to be the same, the same as that in the saturated liquid at 250 K. The condenser then warms up at a prescribed rate as pictured in Figure 2-3, affecting the vapor composition in the external gas. Because thermal diffusion proceeds at a much higher rate than mass diffusion (Prandtl number is much smaller than Schmidt number), the artery liquid is assumed to be in thermal equilibrium with the condenser temperature, and the vapor composition of the internal gas is also affected.

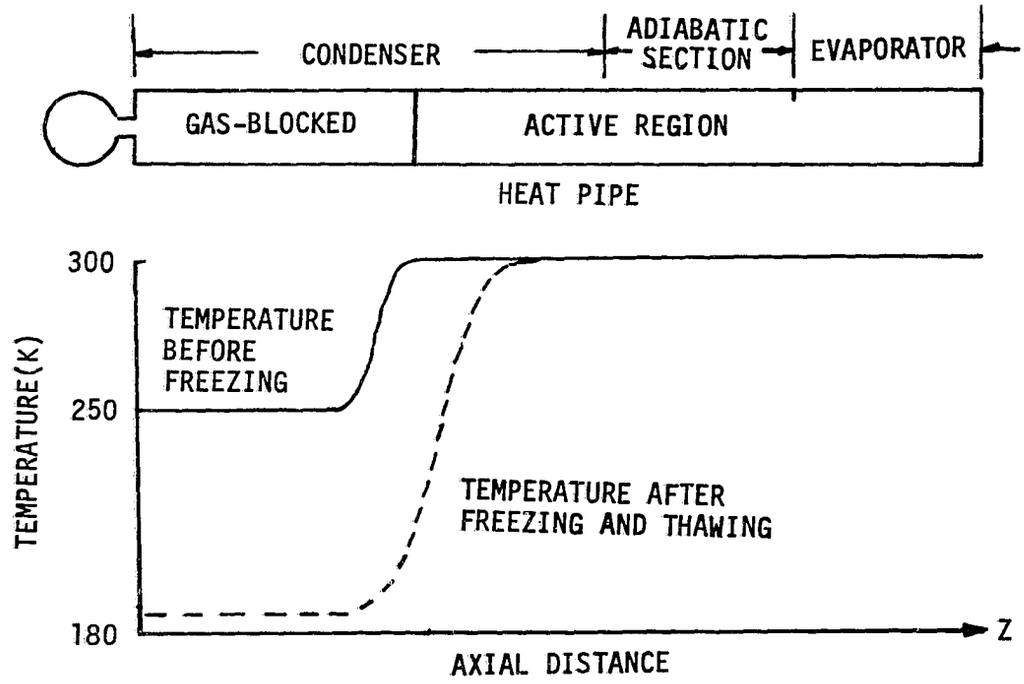

Figure 2-2. Axial Temperature Profile

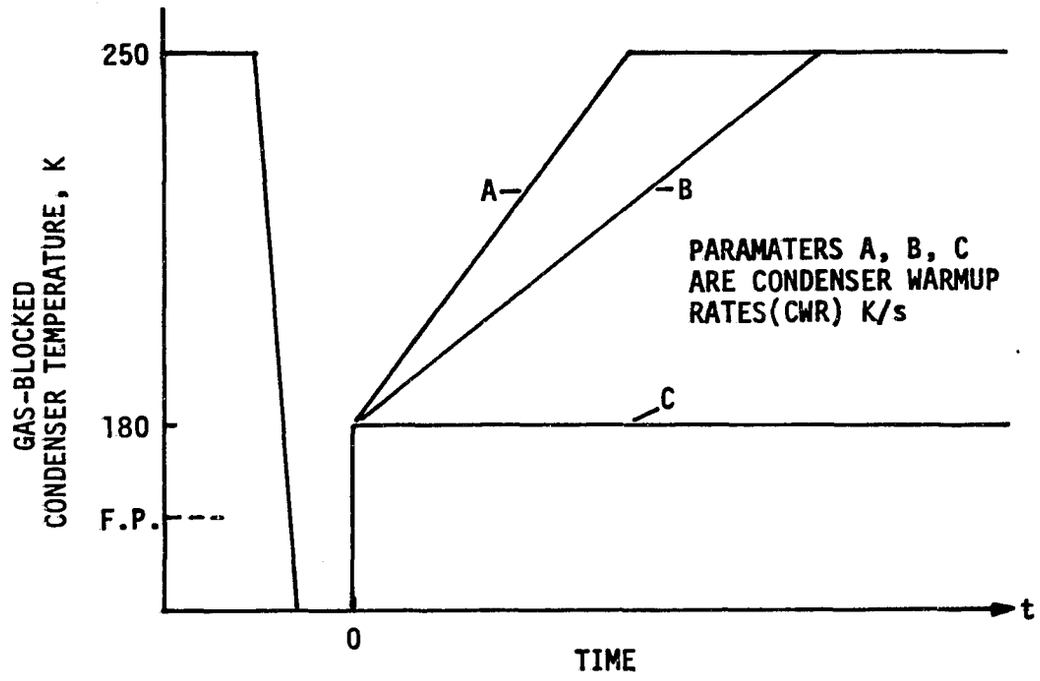

Figure 2-3. Postulated Gas-Blocked Condenser Temperature History

2.2 GOVERNING EQUATIONS FOR THE SPHERICAL BUBBLE

Within the liquid, conservation of mass species i takes the form.

$$\frac{\partial x_i}{\partial t} + v \frac{\partial x_i}{\partial r} = D_i \left(\frac{\partial^2 x_i}{\partial r^2} + \frac{2}{r} \frac{\partial x_i}{\partial r} \right) \tag{2-1}$$

where i = 2 to n (i=1 is reserved for the liquid). The quantity x_i is the mole fraction of species i, and r is the radius. The assumption has been made that the solution is dilute and isothermal, so the molar concentration c is constant at that of the liquid, and the diffusivity D_i for species i in the liquid is unaffected by the other dilute species present. The radial velocity v is caused entirely by growth or collapse of the central bubble, because the diffusion mass transfer rates are so low, conservation of mass dictates

$$v = \left(\frac{R_1}{r} \right)^2 \frac{dR_1}{dt} \tag{2-2}$$

Within the central bubble the gas is assumed to be uniform in composition and pressure, because the gas-phase diffusivities are high compared to the liquid-phase values, and inertia forces are negligible for the small changes in bubble growth or collapse rate. Accordingly the gas-phase species equations equivalent to Eq. (2-1) are not used explicitly. Rather, they are replaced by the simple expression

$$\frac{dw_i}{dt} = -4\pi R_1^2 N_{i,1} \tag{2-3}$$

where w_i is the molar content of species i within the bubble and $N_{i,1}$ is the molar flux for species i at $r=R_1$, given by Fick's Law on the liquid side of the bubble meniscus as

$$N_{i,1} = c\, D_i \left.\frac{\partial x_i}{\partial r}\right|_{r=R_1} \qquad i=2,n \tag{2-4}$$

where c is liquid molar concentration (g-moles/cm^3).

The molar content of the bubble is given by

$$w_i = \frac{4}{3}\pi R_1^3 P_i/R\,T_c \qquad i=2,n \tag{2-5}$$

where T_c is the condenser temperature, and R is the universal gas constant. Similarly the conservation of momentum equation is replaced by a quasi-hydrostatic balance equation

$$\sum_{i=1}^{n} P_i = P_{liq} + 2\sigma/R_1 \tag{2-6}$$

The partial pressures within the bubble are given by Raoult's and Henry's Laws. Since x_1 is nearly unity, Raoult's Law gives simply

$$P_1 = P_v(T_c) \tag{2-7}$$

while Henry's Law is

$$P_i = C_i(T_c)\, x_i \qquad i=2,n \tag{2-8}$$

Outside the liquid at $r=R_2$ the total pressure of the vapor and gas is $P_v(T_{ev})$ where T_{ev} is the evaporator temperature. The gas pressure in the

gas-blocked condenser is

$$P_g = P_v\,(T_{ev}) - P_v\,(T_c) \tag{2-9}$$

The gas composition is specified by Y_i , i=2 to n, where Y_i is the mole fraction of species i in the noncondensible. For example, if 2 is helium and 3 is nitrogen, Y_2 might be 0.10 and Y_3 0.90 for a 10 percent helium, 90 percent nitrogen gas mixture. The saturation values of x_i at $r = R_2$ are

$$x_i = Y_i\,P_g/G_i\,(T_c) \tag{2-10}$$

The initial conditions at t=0 are specified by a uniform set of x_i, i=2 to n, for the initial liquid composition, a set of Y_i in the gas bubble and the initial radius R_1 of the bubble. From these there can be derived the set of w_i, i=2 to n. First, from Eqs. (2-6) and (2-7)

$$P_g = P_{liq} + 2\sigma\,(T_c)/R_1 - P_v\,(T_c) \tag{2-11}$$

Then from the gas law

$$W_g = \frac{4}{3}\,\pi R_1^3\,P_g/RT_c \tag{2-12a}$$

where

$$w_g = \sum_{i=2}^{n} w_i \tag{2-12b}$$

Finally

$$w_i = Y_i\,w_g \tag{2-13}$$

2.3 TRANSFORMATION AND NUMERICAL SOLUTION

It is convenient to anchor the spatial coordinate to the bubble interface and make the coordinate dimensionless with respect to $R_2 - R_1$.

$$\eta = \frac{r - R_1(t)}{R_2(t) - R_1(t)} \tag{2-14}$$

where $R_2(t)$ is given by

$$\frac{4}{3}\pi R_2^3 - \frac{4}{3}\pi R_1^3 = \frac{4}{3}\pi R_{2,0}^3 - \frac{4}{3}\pi R_{1,0}^3 \qquad (2\text{-}15)$$

Velocity v given by Equation (2-2) becomes

$$v = \left(\frac{R_1}{R_1+\eta\Delta R}\right)^2 \dot{R}_1 \qquad (2\text{-}16)$$

Partial derivatives with respect to r at constant t (and thus at constant R_1 and $\Delta R = R_2 - R_1$) are given by

$$\frac{\partial x_i}{\partial r} = \frac{\partial x_i}{\partial \eta}\frac{1}{\Delta R} \qquad (2\text{-}17)$$

The partial derivative with respect to t at constant r must be transformed to one with respect to t at constant η

$$\left.\frac{\partial x_i}{\partial t}\right|_r = \left.\frac{\partial x_i}{\partial t}\right|_\eta + \left.\frac{\partial x_i}{\partial \eta}\right|_t \left.\frac{\partial \eta}{\partial t}\right|_r \qquad (2\text{-}18)$$

$$\left.\frac{\partial \eta}{\partial t}\right|_r = -\frac{1}{\Delta R}\dot{R}_1 - \frac{(r-R_1)}{\Delta R^2}\dot{\Delta R} \qquad (2\text{-}19)$$

Hence Equation (2-1) becomes

$$\left.\frac{\partial x_i}{\partial t}\right|_\eta + \left.\frac{\partial x_i}{\partial \eta}\right|_t \left(-\frac{1}{\Delta R}\dot{R}_1 - \frac{\eta}{\Delta R}\dot{\Delta R}\right) + \left(\frac{R_1}{R_1+\eta\Delta R}\right)^2 \frac{\dot{R}_1}{\Delta R}\frac{\partial x_i}{\partial \eta}$$

$$= D_i\left(\frac{1}{\Delta R^2}\frac{\partial^2 x_i}{\partial \eta^2} + \frac{2}{R_1+\eta\Delta R}\frac{1}{\Delta R}\frac{\partial x_i}{\partial \eta}\right)$$

Collecting terms gives

$$\frac{\partial x_i}{\partial t} + \left(\frac{R_1^2\dot{R}_1}{(R_1+\eta\Delta R)^2\Delta R} - \frac{(1+\eta)\dot{R}_1}{\Delta R} - \frac{2D_i}{(R_1+\eta\Delta R)\Delta R}\right)\frac{\partial x_i}{\partial \eta} - \frac{D_i}{\Delta R^2}\frac{\partial^2 x_i}{\partial \eta^2} = 0 \qquad (2\text{-}20)$$

Since large values of $\partial x_i/\partial\eta$ are expected near $\eta = 0$, computational efficiency is improved by transforming the η coordinate to z so as to expand the region near $\eta = 0$ relative to the region near η=1. A negative

value of the parameter γ in the following coordinate transformation achieves the desired result.

$$z = \frac{1 - e^{\gamma\eta}}{1 - e^{\gamma}} \tag{2-21}$$

After transformation Equation (2-20) is in the form of

$$\frac{\partial x_i}{\partial t} + F \frac{\partial x_i}{\partial z} + G \frac{\partial^2 x_i}{\partial z^2} = 0 \tag{2-22}$$

where F and G are functions of z, R_1, $\dot{R}_1$, D_i, and γ (recall that R_2 and hence ΔR is given by Equation (2-15)).

Equation (2-22) is solved numerically in finite difference form. Let subscript j denote z location and superscript o and oo denote values at $t-\Delta t$ and $t-2\Delta t$ respectively. The species subscript i is dropped to avoid confusion. The temporal derivative is approximated as

$$\frac{\partial x_i}{\partial t} = \frac{1}{\Delta t} \left[a_1 x_j + a_2 x_j^{o} + a_3 x_j^{oo}\right] \tag{2-23}$$

where for constant time increment Δt, $a_1 = 3/2$, $a_2 = -2$, and $a_3 = 1/2$. The spatial derivatives are

$$\frac{\partial x_i}{\partial z} = \frac{x_{j+1} - x_{j-1}}{2\Delta z} \tag{2-24}$$

$$\frac{\partial^2 x_j}{\partial z^2} = \frac{x_{j+1} + x_{j-1} - 2x_j}{(\Delta z)^2} \tag{2-25}$$

Equation (2-22) takes the form

$$x_j = A_j x_{j+1} + B_j x_{j-1} + C_j, \quad j = 2,N \tag{2-26}$$

where $z_2 = 0$ and $z_N = 1$. The coefficients A_j, B_j, and C_j may be calculated at any time step in terms of the previous known sets x_j^o and x_j^{oo} and the known values of R_1, $\dot{R}_1$, D_i, γ, and z_j. The new set of x_j values is computed by means of Gaussian elimination in which

$$x_j = A_j^* \, x_{j+1} + B_j^* \tag{2-27}$$

Equations (2-26) and (2-27) combine to permit the forward (j=2, 3, ...) calculation of A_j^* and B_j^*.

$$A_2^* = 0 \ , \ B_2^* = B_2 \, x_1 + C_2 \tag{2-28a,b}$$

$$A_j^* = A_j/(1 - B_j \, A_{j-1}^*) \tag{2-28c}$$

$$B_j^* = (B_j \, B_{j-1}^* + C_j)/(1 - B_j \, A_{j-1}^*) \tag{2-28d}$$

Then Equation (2-27) allows the backward (j=N-1, N-2, ...) calculation of x_j starting with the prescribed boundary value x_n.

Appendix B.1 contains the listing of the program used to calculate $x(z_j,t)$ and $R_1(t)$.

2.4 THE ELONGATED BUBBLE MODEL

When a bubble grows so that its radius (R_1) reaches the artery radius, further growth occurs through elongation of the bubble within the artery. In the absence of a priming foil, the artery wall prevents meniscus coalescence, and a sheath of liquid is retained about the elongated bubble. Mass transfer of species i (i=2 to n) can occur through the sheath and into or out of the end-cap liquid. Equations (2-5) and (2-12) become

$$w_i = (\tfrac{4}{3} \pi \, R_a^3 + \pi R_a^2 L) \, P_i/RT_c \tag{2-29}$$

$$w_g = (\tfrac{4}{3} \pi \, R_a^3 + \pi R_a^2 L) \, P_g/RT_c \tag{2-30}$$

while Equations (2-6) through (2-11) and (2-13) remain unchanged.

Equation (2-3) and (2-4) are well approximated by

$$\frac{dw_i}{dt} = cD_i \, [(2\pi R_a L \, \varepsilon/\tau \Delta R) + (F/R_a)] \, \Delta x_i \tag{2-31}$$

where Δx_i is the difference in mole fraction between that of the inside liquid at the bubble-liquid interface and that of the outside liquid at the condenser-gas-liquid interface. The quantity ε is the artery screen

void fraction, τ is its tortuosity, and F is the conduction shape factor for a hemispherial bubble of radius R_a in a semi-infinite cylinder of radius $R_a + \Delta R$. For the CTS heat pipe arteries $R_a \doteq 0.0127$ cm, $\varepsilon \doteq 0.37$, $R_a/\Delta R \doteq 8$, and $F \doteq 8$.

Equation (2-31) was integrated numerically with Equation (2-30) used to find L in a Runge-kutta type algorithm.

2.5 PROPERTIES USED IN CALCULATIONS

Figures 2-4 (Ref. 3) shows the solubility data used for the calculations. Shown versus temperature is the mole fraction in the liquid for a partial pressure of 1 atm, that is the reciprocal of Henry's constant in atm^{-1}. The variation with temperature will be shown to be quite significant. For now, merely note that methane and argon become less soluble in methanol with increasing temperature (as does air in water) while helium becomes less soluble with decreasing temperature. The solubility of nitrogen in methanol is nearly independent of temperature. Helium is seen to be only sparingly soluble while methane is quite soluble in methanol.

Figure 2-5 (Ref. 4) shows the diffusivity of argon and helium in liquid methanol versus reciprocal temperature. The theory shown in the figure agreed poorly with experimental data, and it was decided to fit the experimental data with an Arrhenius relation. Since data were lacking and theory seemed dubious, it was decided to use the experimental helium fit for helium diffusivity and the experimental argon fit for the diffusivity of argon, nitrogen, and methane. Thus the calculated results for the latter two gases should be regarded as only qualitatively correct. When reliable data for these latter two gases become available, a minor time-scale expansion or contraction will be necessary to adjust for the approximate values of diffusivity used.

2.6 RESULTS FOR THE SPHERICAL BUBBLE

Figures 2-6 through 2-9 show the calculated results for the spherical bubbles. Each of the four figures is for a different gas: helium, argon, methane, and 10 percent He 90 percent N_2, respectively. For a given condenser warmup rate and initial bubble size, helium bubbles are seen to persist for very much longer times than argon bubbles. Methane bubbles disappear much faster than even argon bubbles. The explanation is simply

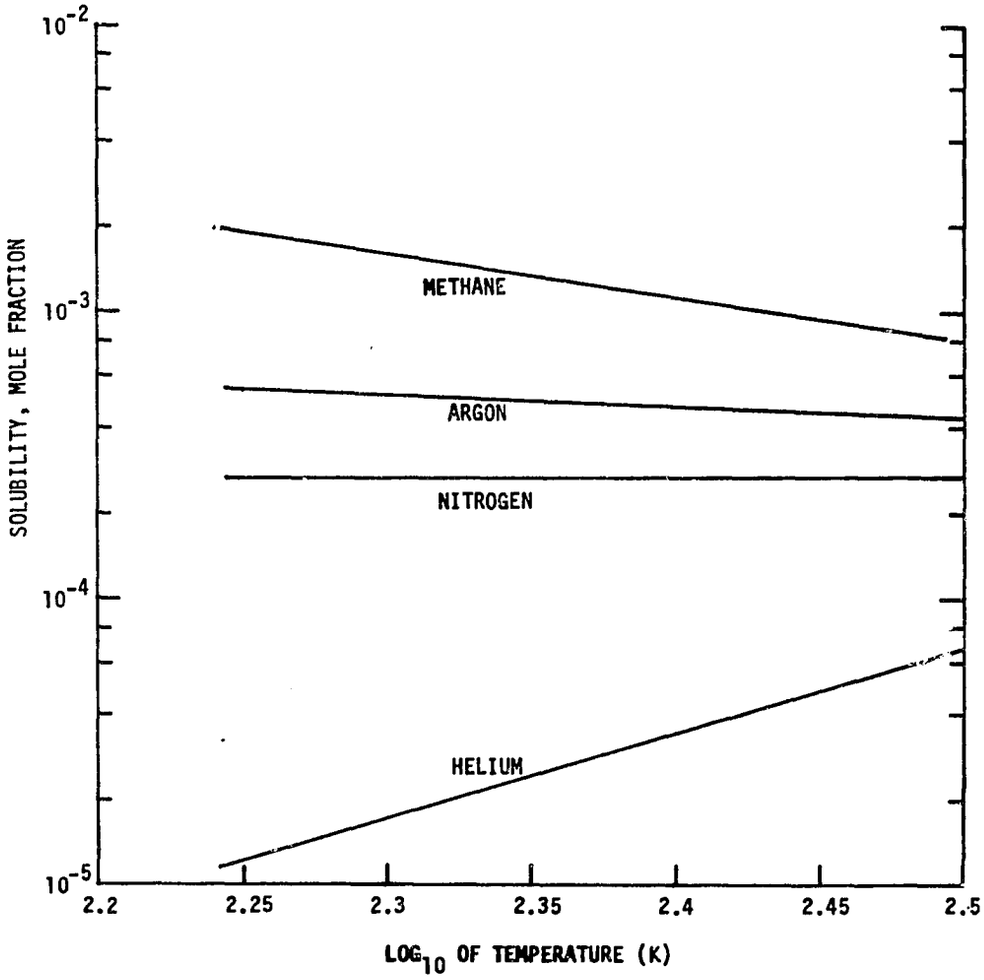

Figure 2-4. Solubility of Various Gases in Methanol as Function of Temperature (from Reference 3)

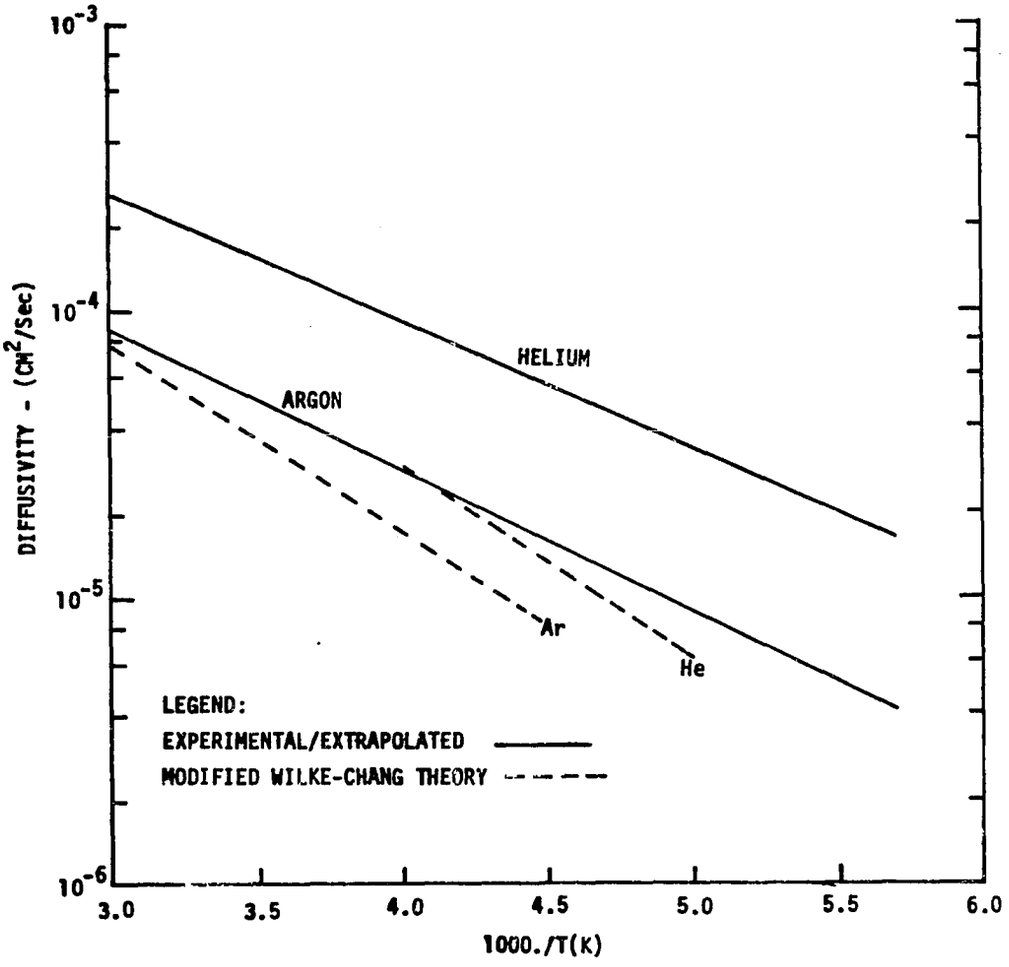

Figure 2-5. Diffusivity of Helium and Argon in Methanol as Function of Temperature (from Reference 4)

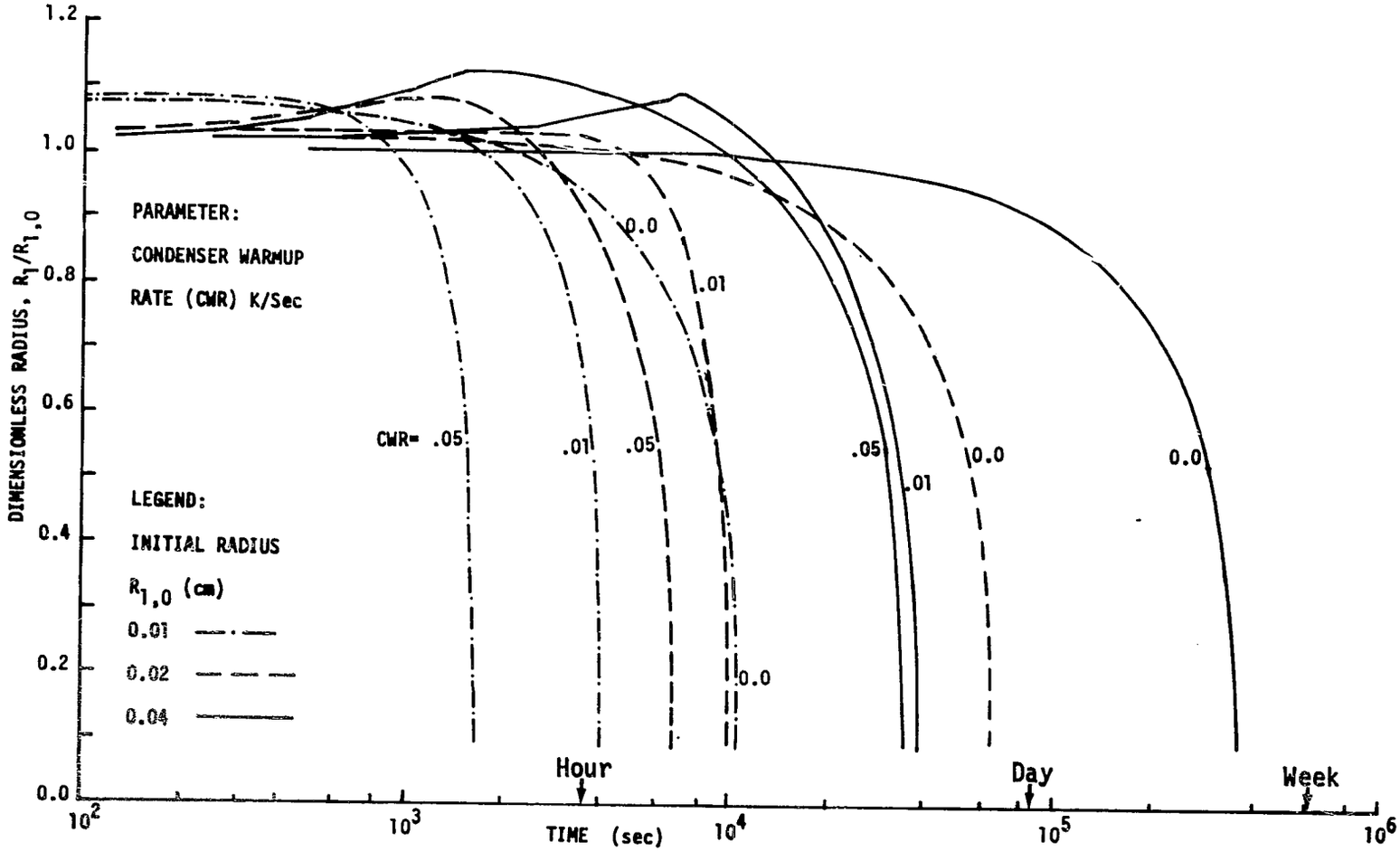

Figure 2-6. Spherical Bubble Radius History, Helium Gas

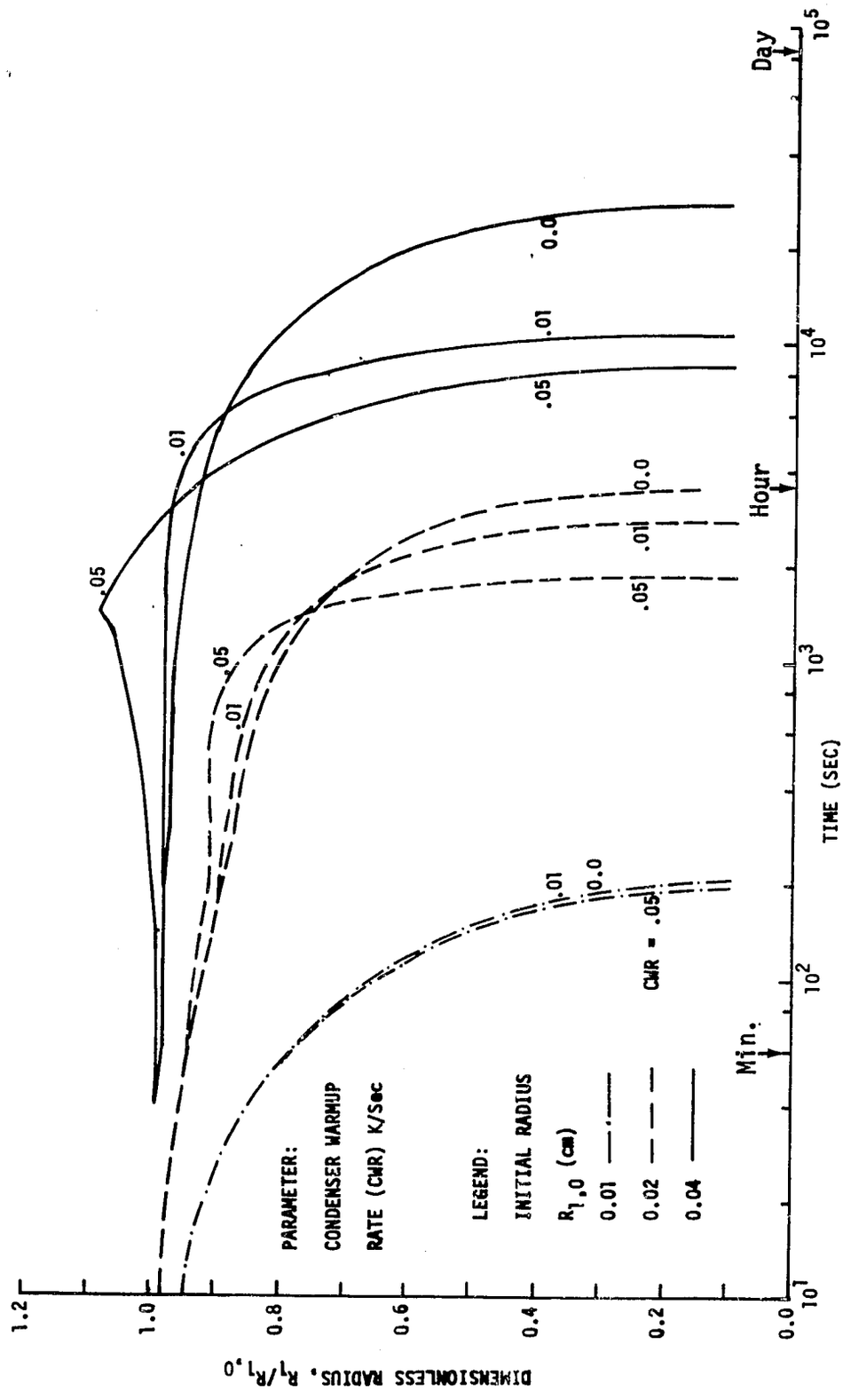

Figure 2-7. Spherical Bubble Radius History, Argon Gas

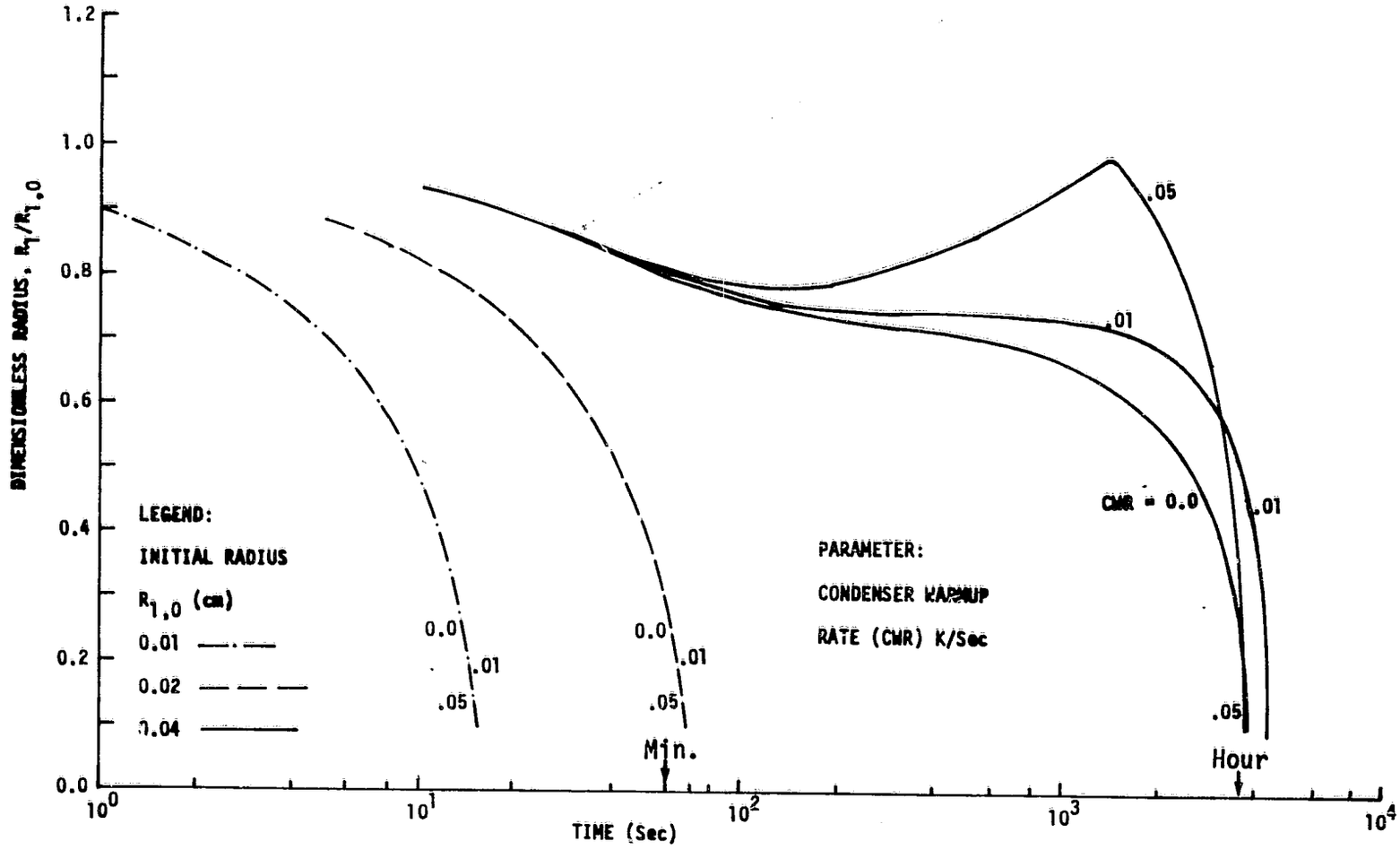

Figure 2-8. Spherical Bubble Radius History, Methane Gas

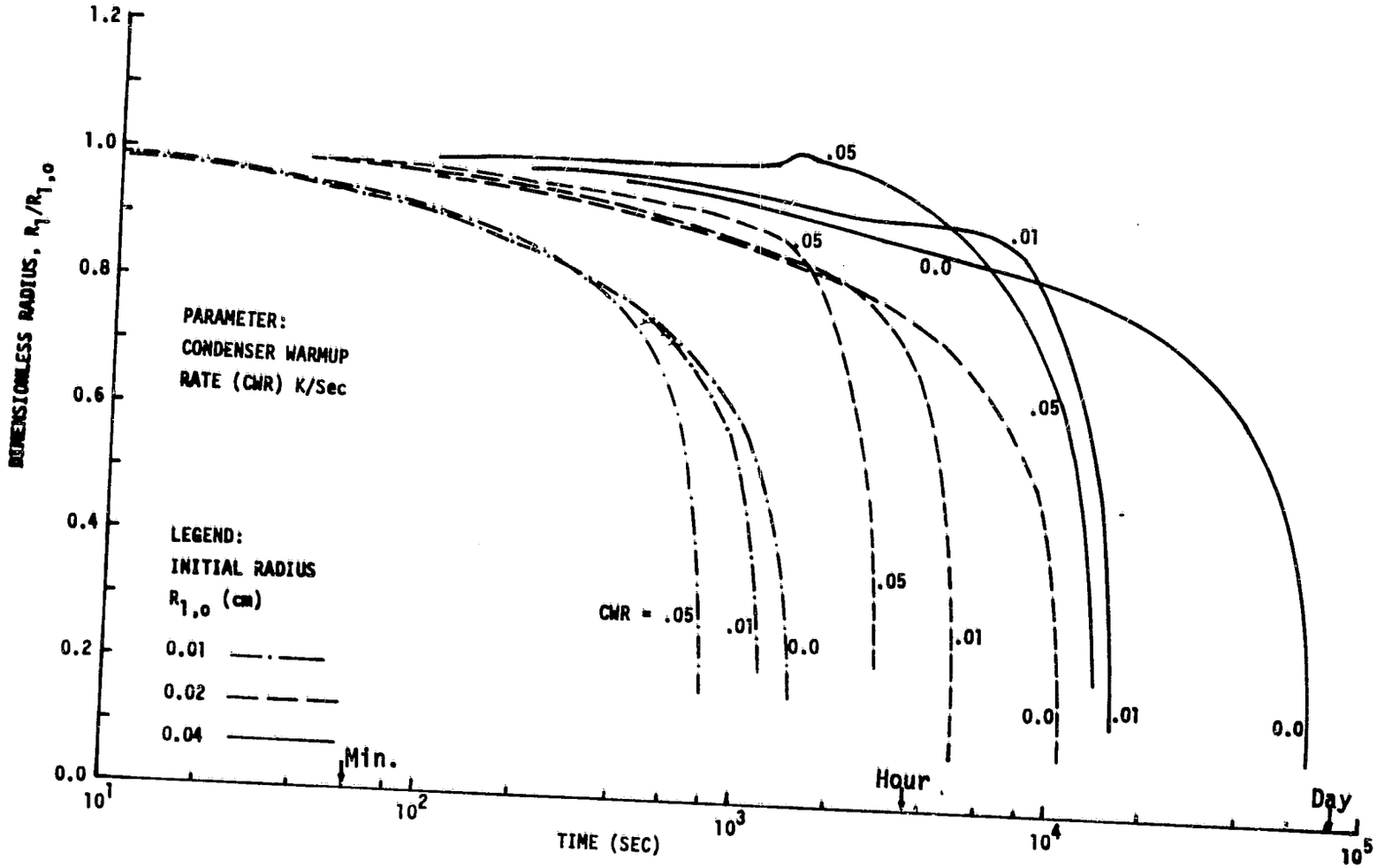

Figure 2-9. Spherical Bubble Radius History, 10% Helium/90% Nitrogen Gas

that, despite its higher diffusivity, the solubility of helium in methanol is low; hence the values of $cD_i \Delta x_i$ are low for helium. Because of the helium component, the 90%N_2 - 10%He noncondensible gas mixture displays long bubble lifetimes.

For a given gas and condenser warmup rate, small bubbles disappear much faster than large bubbles. In the small bubble the gas pressure is larger due to surface tension, so the values of x_i are larger. The mass transfer coefficient area product decreases with size as R_1, but the volume of gas remaining decreases as R_1^3.

With helium gas in a bubble of a certain initial size, increasing the condenser warmup rate increases the solubility and diffusivity of the helium and hastens the reabsorption of the bubble, despite a decreased surface tension, and an increased pressure of methanol vapor which tends to swell the bubble.

With argon the increase in diffusivity with increasing temperature causes the same type of behavior as in the case of helium but to a lesser degree. With methane, however, the increase in diffusivity offsets the decrease in solubility and lessened surface tension, so that the time to reabsorb small bubbles is nearly independent of condenser warmup rate. A complex behavior is seen for the large bubble and high condenser warmup rate. In that case, the fall in solubility of methane and the increase in methanol vapor pressure combine to cause the methane gas and methanol vapor bubble to swell before ultimately collapsing.

Table 2-1 summarizes the bubble lifetime results. Note the much longer times necessary for helium-containing bubbles to be reabsorbed.

2.7 RESULTS FOR THE ELONGATED BUBBLE

Figures 2-10 through 2-13 show calculated results for the elongated bubbles. Again each figure is for a different gas or gas mixture. Again helium-containing bubbles are seen to persist to a much longer time, while methane bubbles are most readily reabsorbed. Again an increase in condenser warmup rate strongly hastens the reabsorption of helium bubbles and weakly hastens the reabsorption of argon and methane bubbles. Bubble swelling, elongation in this case, is seen in all cases, because reabsorption is initially slower than for small spherical bubbles. A final

Table 2-1. Calculated Spherical Bubbles Lifetimes

Gas/Gas Mixture	Initial Radius (cm)	Condenser Warm-up Rate (K/sec)		
		0.0	0.01	0.05
		Time, in seconds, at which bubble radius reaches 1/10 of initial radius.		
Methane CH_4	0.01	15	15	15
	0.02	68	68	68
	0.04	3775	4362	3712
Helium He	0.01	10717	4055	1658
	0.02	64411	9998	6782
	0.04	371408	38651	35409
Argon Ar	0.01	208	204	194
	0.02	3614	2790	1884
	0.04	27890	10740	8460
CTS Mixture 90% N_2/10% He	0.01	1514	1216	782
	0.02	10777	4950	2823
	0.04	67520	16038	14150

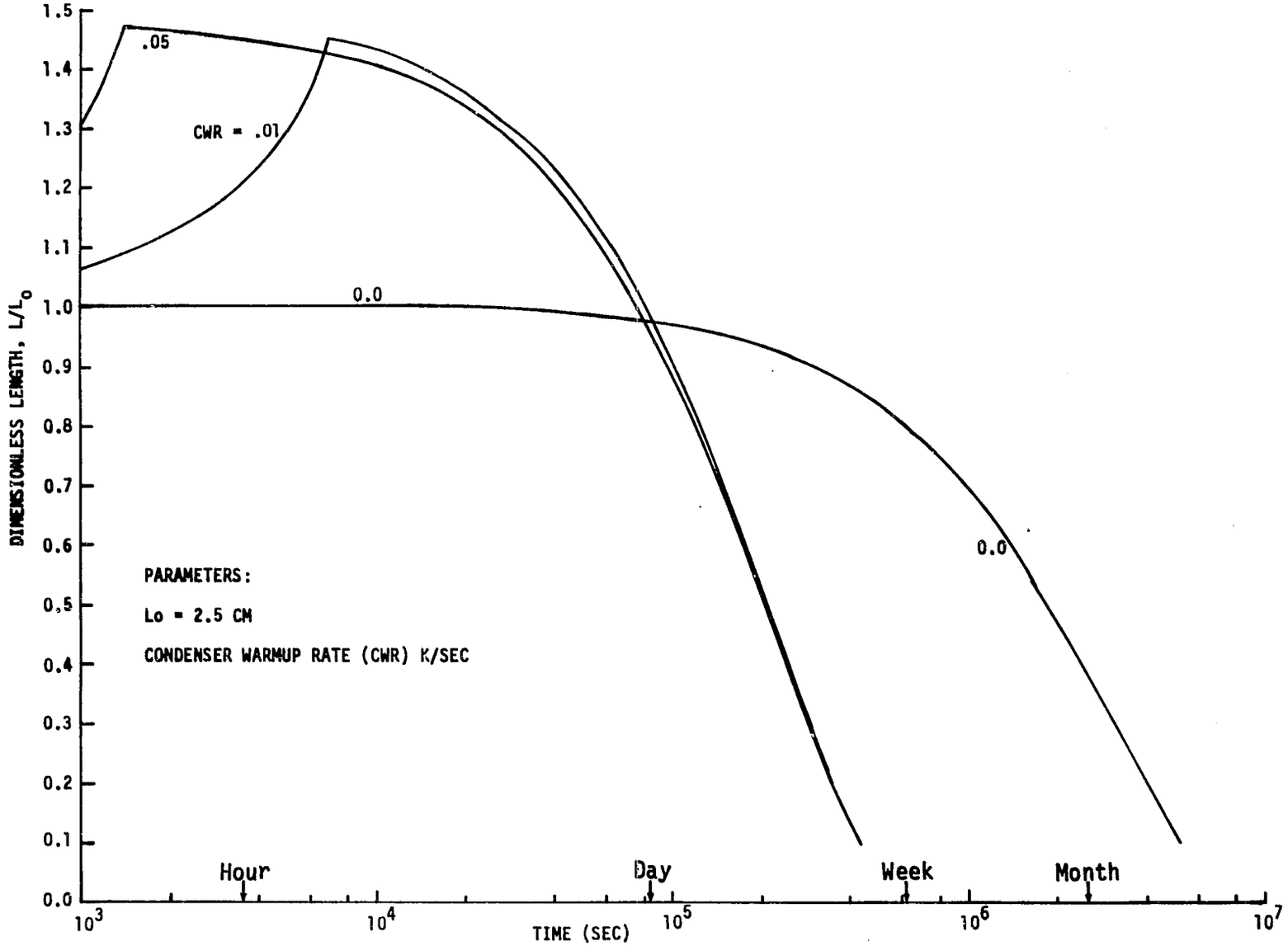

Figure 2-10. Elongated Bubble Length History, Helium Gas

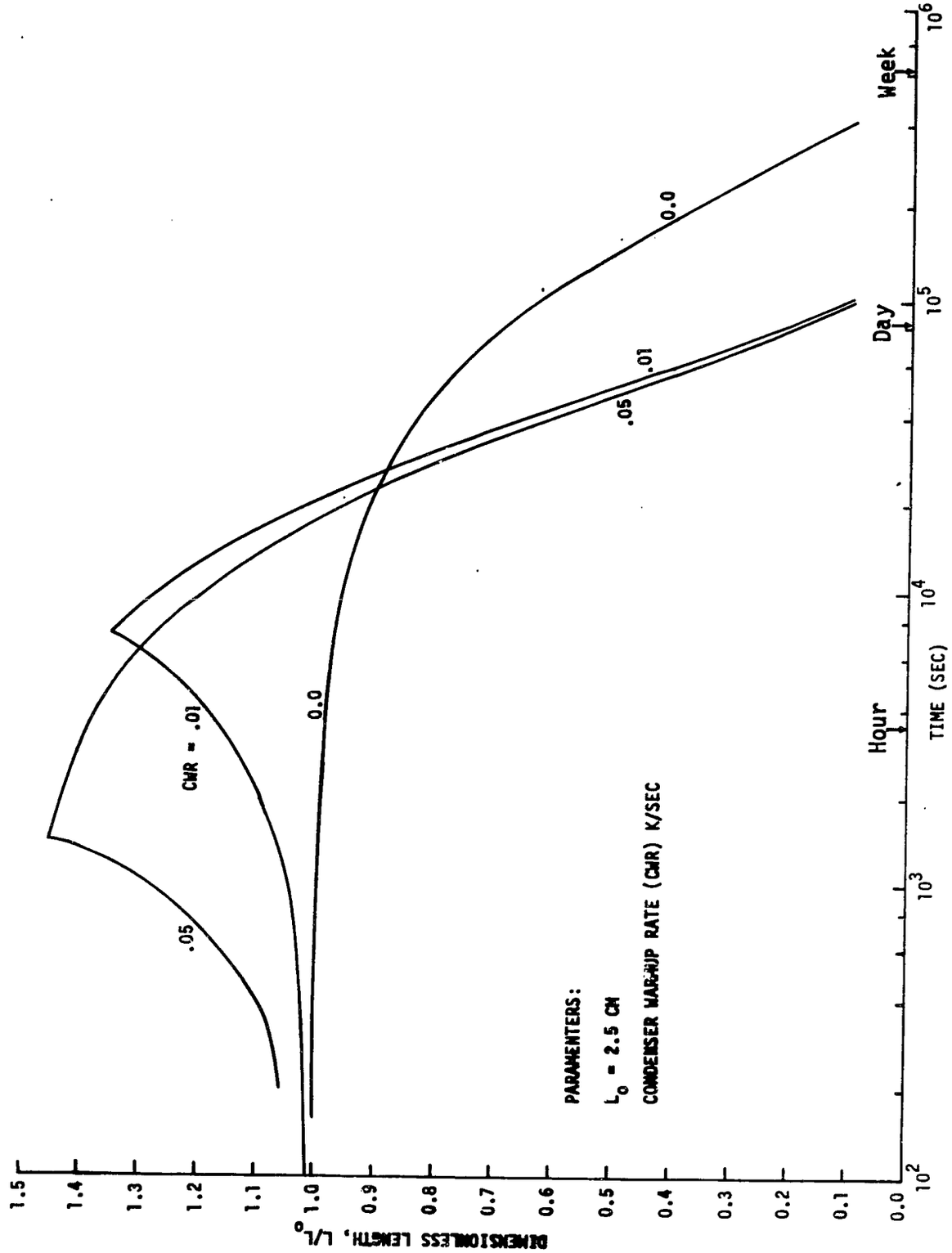

Figure 2-11. Elongated Bubble Length History, Argon Gas

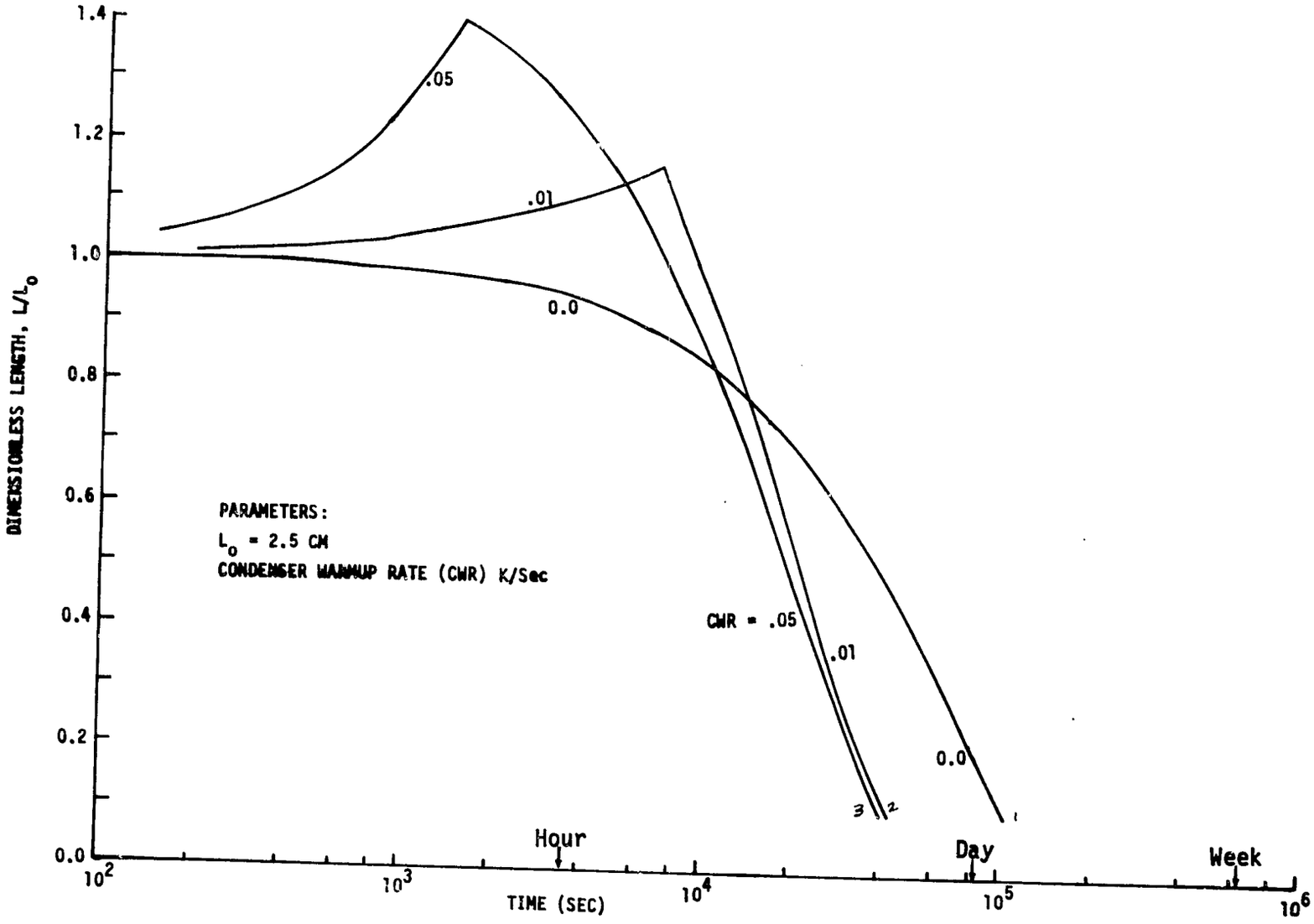

Figure 2-12. Elongated Bubble Length History, Methane Gas

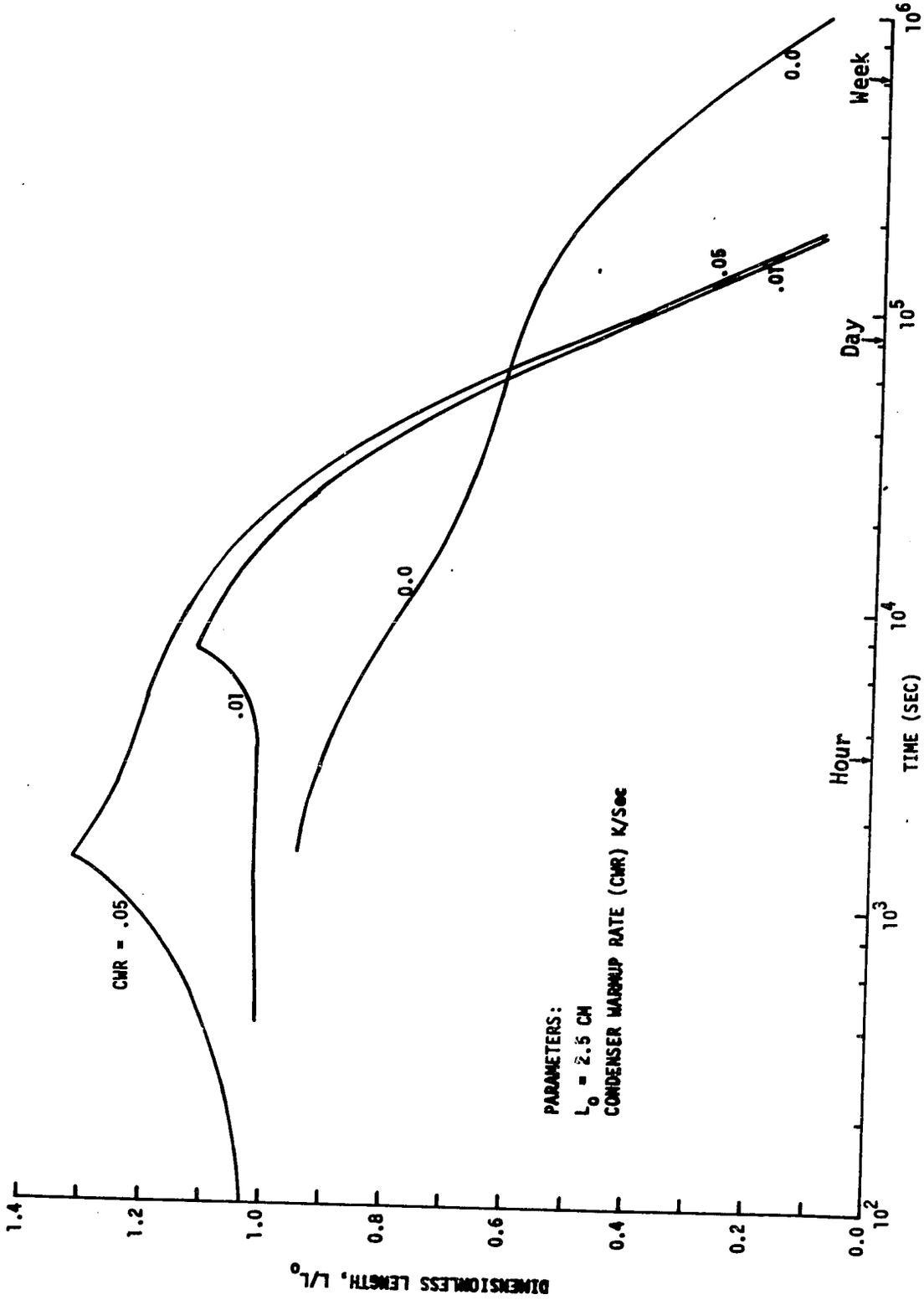

Figure 2-13. Elongated Bubble Length History, 10% Helium/90% Nitrogen Gas

observation is that the helium in the helium-nitrogen gas mixture becomes the residual gas in the bubble at long times and low condenser warmup rates and requires a long time to diffuse out of the bubble.

Table 2-2 summarizes the calculations of the elongated bubble lifetimes.

Table 2-2. Calculated Elongated Bubbles Lifetimes

Gas/Gas Mixture	Initial Length CM	Condenser Warm-up Rate (K/sec)		
		0.0	0.01	0.05
		Time, in seconds, at which bubble length reaches 1/10 of initial length.		
Methane CH_4	2.5	110,070	42,655	40,555
Helium He	2.5	5,069,500	436,000	432,300
Argon Ar	2.5	406,600	101,600	99,000
CTS Mixture 90% N_2/10% He	2.5	998,800	182,560	186,440

2.8 SIGNIFICANCE OF THE ANALYTICAL/NUMERICAL RESULTS

The CTS heat pipes contained 90%N_2 - 10%He control gas. The helium was added to facilitate leak detection. In retrospect, that decision appears to have been unfortunate. For should gas bubbles be created by freezing in the gas-blocked condenser and should they coalesce into bubbles approaching.0.8 mm in diameter, their lifetimes are seen to be on the order of 20 hours when the condenser warmup rate is slow. Larger sausage bubbles are seen to persist hundreds of hours, that is, some ten days or more. Such bubbles, if present through cyclic freezing and thawing may be enlarged through a fractionation process reminiscent of the making of New England applejack. With each freezing episode dissolved gas is forced out

of the ice into the bubble. A large bubble can persist many days even after freezing no longer occurs provided it is in the gas-blocked region. When the heat pipe is powered up, and the gas front approaches the bubble, Marangoni Flow brings the bubble into the active condenser, and condensate flow sweeps it up the pipe toward the evaporator to a location where the local vapor-liquid pressure difference exceeds the capillary pressure of the artery, and the artery deprimes.

The results suggest that methane would make a good control gas, because methane bubbles up to 0.8 mm in diameter are reabsorbed in approximately one hour. Thus there is little likelihood that a 24 hour periodic freezing and thawing could create a large bubble, and the small bubbles released from thawing ice would be reabsorbed before the approach of the gas front.

3.0 CYCLIC FREEZE/THAW TESTS ON SN009 HEAT PIPE

3.1 TEST OBJECTIVES

Phase II objective 2 was to simulate an anomaly with the SN009 heat pipe by cyclic freezing and thawing of the condenser during a 5-day extended continuous test period. The goals of the tests were (a) to demonstrate the generation and collection of bubbles in the arteries and their migration or induction into the active section of the heat pipe where their presence could result in depriming of at least a single artery, and (b) to establish by test data analysis that freezing blowby or suction freezeout rather than bubble formation was not the cause of the observed heat pipe failure.

3.2 APPARATUS AND TEST PROCEDURE

The test assembly described in Figure 3-1 is similar to the one used for tests on the SN009 heat pipe during Phase I of this program. As shown, the heat load is applied on the heat pipe over a 0.305 meter long section by means of an attached 4.0 kg heated aluminum block.

The heat pipe condenser, 0.91 meter long, is mounted on an aluminum plate whose area and thermal mass corresponds approximately to the effective portion of the CTS radiator. This plate is coupled to the sink through 0.32 centimeters of cork over a 0.1045 square meter area. Tape heaters attached along the plate allow changing the condenser temperatures even with a constant temperature sink.

A cooling coil with tape heaters is attached to the gas reservoir for purposes of controlling its temperature independently from the rest of the heat pipe assembly.

The heat pipe test assembly is instrumented with seventeen temperature sensors, the location of which are shown in Figure 3-2. The sensors are connected to a 24-channel strip chart recorder which allows monitoring these temperatures at 1.5 minute intervals.

The test procedure in Table 3-1 outlines the basic steps for conducting the cyclic freeze/thaw tests on the SN009 heat pipe. Steps 1 through 5 represent the original procedure for repriming the heat pipe and adjusting the operating parameters in preparation for the commencement of a new cycle. As indicated in the procedure, the selected evaporator elevation and heat

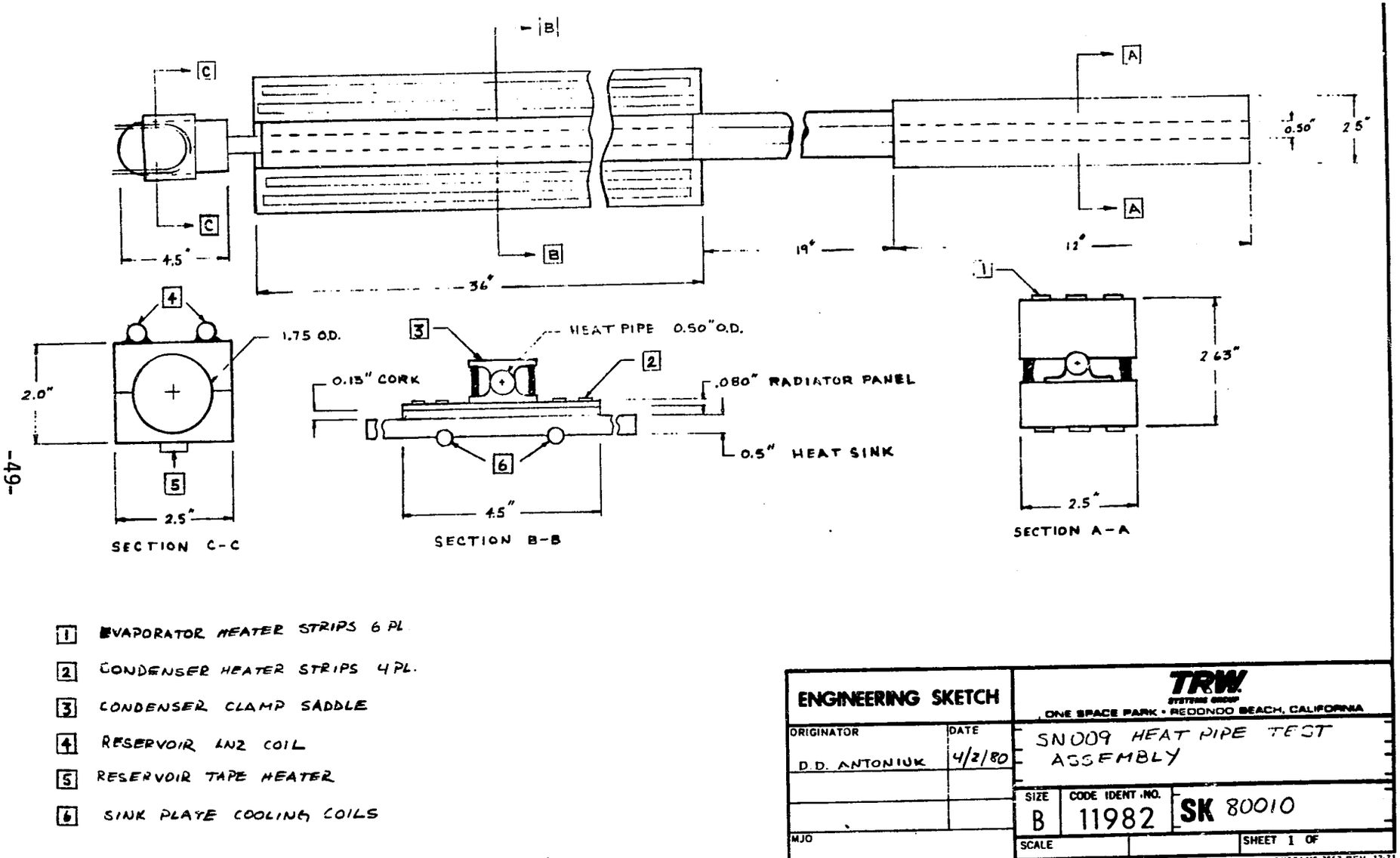

Figure 3-1. Engineering Sketch of SN009 Heat Pipe Test Assembly

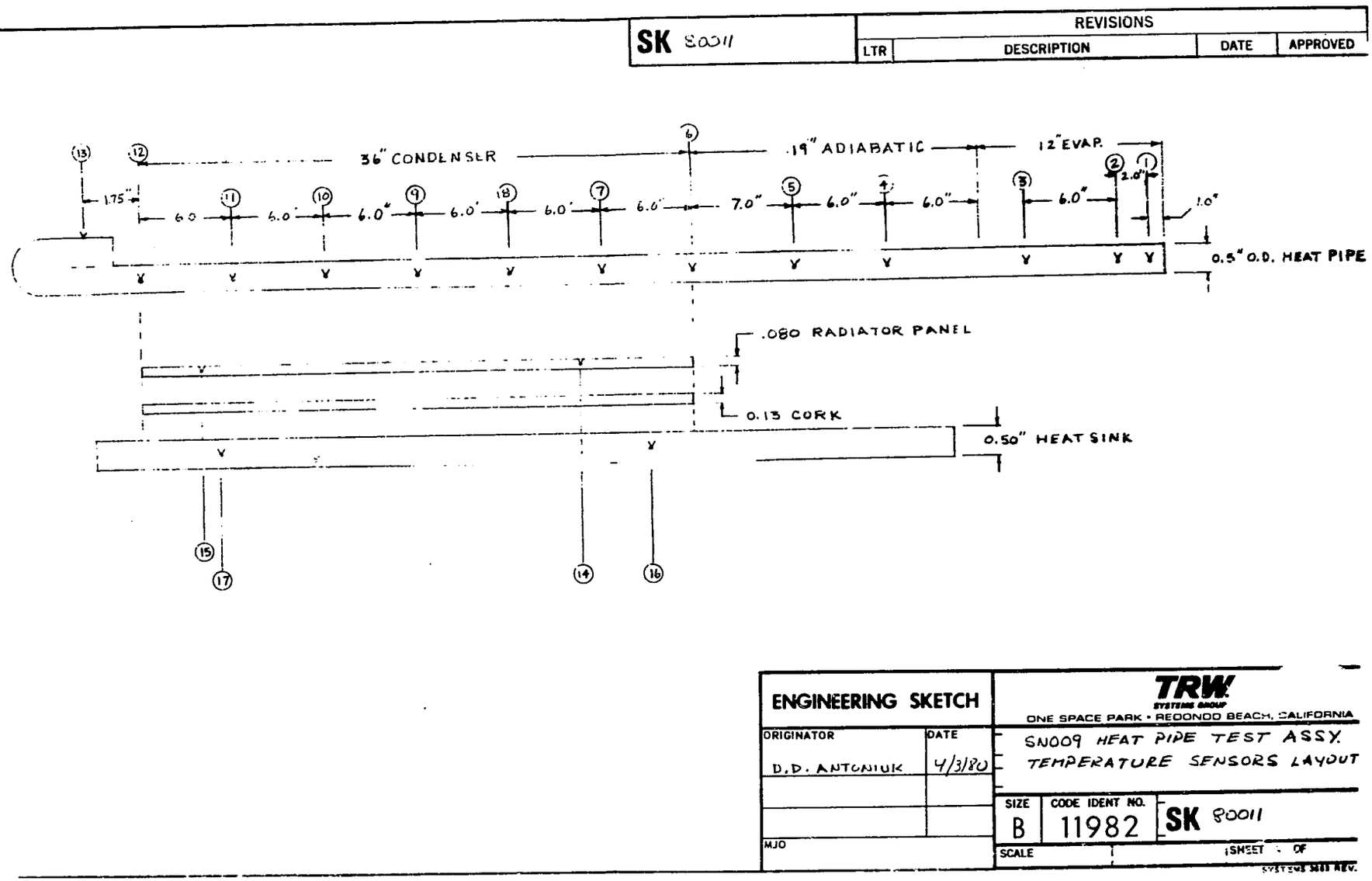

Figure 3-2. Locations of Thermocouples on SN009 Test Assembly

Table 3-1. SN009 Heat Pipe Freeze/Thaw Cyclic Test Procedure Outline

Using the test assembly described in SK80010 and SK80011, perform the cyclic tests for a period of 120 continuous hours in accordance with the following procedure:

1. Level heat pipe to within 1.0 mm.
2. Isothermalize heat pipe to within 1°C and wait 30 minutes.
3. Elevate evaporator end 1.2 cm above condenser.
4. Apply 130 watts to evaporator heater and verify artery priming. If arteries are primed, proceed with Step 5, otherwise, repeat Steps 1 through 4.
5. Reduce sink plate, inactive condenser and gas reservoir temperatures to the following levels:
   a) Sink plate: lower than -145°C (-229°F)
   b) Inactive condenser: -40°C ±5°C
   c) Gas reservoir: -95°C ±5°C (-139°F)

   Reservoir temperature reduction rates should not exceed -2°C/min (-3.6°F/min).
6. Simultaneously, reduce temperatures in inactive condenser section below -102°C (-152°F) and increase gas reservoir temperature to -40°C ±5°C over a period of approximately 25 minutes. Maintain subfreezing condenser temperatures for at least 12 minutes. If heat pipe fails, repeat Steps 1 through 6.
7. Increase inactive condenser temperatures to -40°C ±5°C over a period of approximately 20 minutes and simultaneously start reducing gas reservoir temperature to -95°C over a period of 180 to 200 minutes. At no time should the reservoir cooling rate exceed -2°C/min. If heat pipe fails, repeat Steps 1 through 7.
8. Repeat Steps 6 through 8.

load on the heat pipe for the tests are 1.25 centimeters and 130 watts, respectively.

The tilt on the pipe is meant to minimize the contribution of excess fluid inventory to the pumping capacity of the pipe and to compensate to a certain extent for that component of the buoyancy force vector tending to keep the bubbles against the upper walls of the arteries.

Although heat loads over 90 watts are known to be in excess of the heat pipe one-artery capacity, the higher heat load of 130 watts is chosen in order to enhance the migration of bubbles toward the evaporator by virtue of higher fluid flow rates inside the arteries.

Steps 6 through 8 of an idealized freezing/thawing test cycle are shown graphically in Figure 3-3 where segments (B-C), (B-D), and (B-E) represent different condenser warmup rates. These steps are described in conjunction with the figure in what follows.

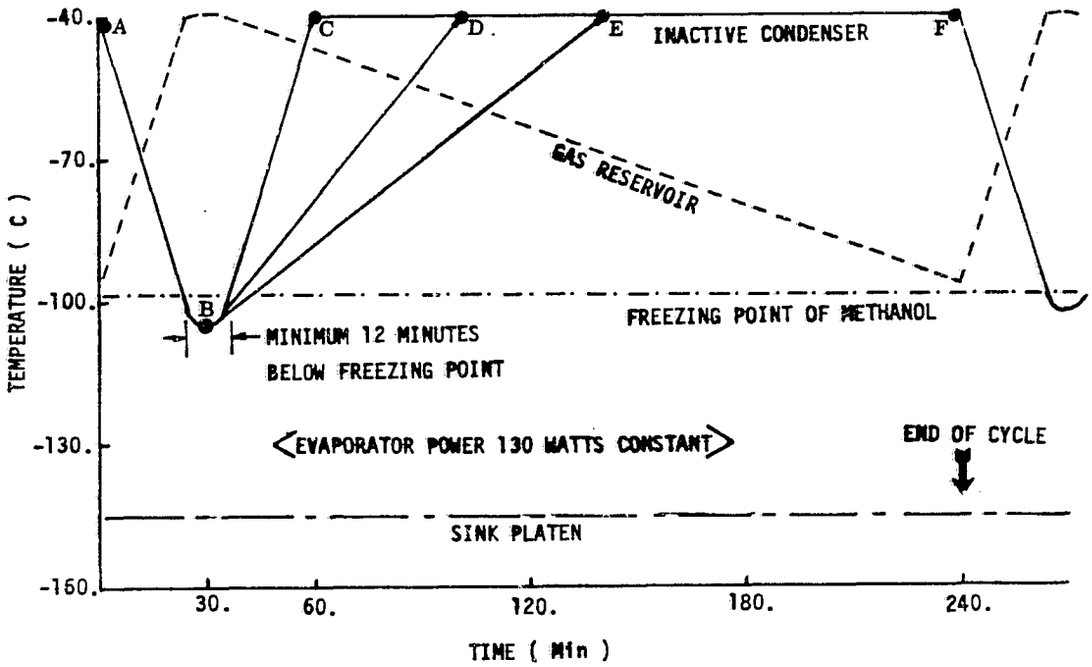

Figure 3-3. Idealized Freezing/Thawing Cycle "A"

By turning off the heaters on the condenser plate, the inactive condenser section is allowed to cool from -40°C (Point A) to below the freezing point of methanol (B) at a rate of approximately -4°C/min. Simultaneously, heat is applied to the gas reservoir to raise its temperature from about -95°C to -40°C in approximately 25 minutes. During this period of the test cycle, the advancement of the gas front toward the evaporator resulting from reduced condenser temperatures is further enhanced by the increasing temperature of the gas reservoir, the net effect of the above being to inactivate temporarily a portion of the condenser to allow the liquid in the arteries to freeze. Subfreezing temperatures in the inactive condenser are maintained for ten minutes to ensure complete freezing inside the arteries.

Failure of the heat pipe during condenser freezing could be attributed to be the result of either suction freezeout or the bubbles mechanism. If this event is repeatable in every cycle, then artery depriming will be, with a high degree of certainty, due to suction freezeout. On the other hand, sporadic failure of the heat pipe during condenser freezing will be consistent with the recognized statistical nature of the bubbles mechanism. If no evidence of heat pipe burnout is observed through the end of the freezing process, the test cycle continues with Step 7, otherwise, Steps 1 through 6 are repeated.

During Step 7, (e.g., B-C) power is applied to heaters on the condenser plate to thaw the inactive condenser and raise its temperature in approximately 25 minutes to -40°C where it is held within ±5°C for the remainder of the 240-minute test cycle. About the time the inactive condenser starts to thaw (B+), cooling of the gas reservoir is initiated and allowed to continue through the end of the cycle (F) at an average rate of 0.3°C/min. Reservoir cooling rates are not permitted to exceed 2°C/min to preclude the sudden cooling mechanism from taking place.

During this period of the test cycle, (e.g., B-C) rising condenser temperatures will cause the gas/vapor front to advance toward the reservoir end of the condenser, thawing the previously inactive section of the pipe and presumably engulfing into the active section bubbles that were generated during the freeze/thaw process. The simultaneous and continuous reduction of the gas reservoir temperature will have two significant effects

on the bubbles mechanism. First, it will cause a continuous movement of the gas front toward the reservoir during which additional bubbles will be induced into the active portion of the heat pipe where their migration toward the evaporator is enhanced. Second, reservoir cooling will tend to diminish the pressurization of the heat pipe resulting from increasing condenser temperatures and will cause subsequently, after the condenser reaches a steady state, (e.g., C) a continuous decrease of the total pressure in the heat pipe.

Exploratory analyses using the spherical bubble model indicate that pressure reduction in the heat pipe environment can significantly increase bubbles lifetimes. Longer bubble lifetimes are certainly a factor enhancing the potential of the bubble mechanism to deprime the arteries.

A heat pipe failure observed about the time the inactive condenser undergoes thawing (B+) could be attributed to either the postulated freezing blowby or the bubbles mechanism. The fact that artery depriming due to freezing blowby is not statistical in nature requires in order to consider the freezing blowby mechanism the culprit, that failures during the thawing process (B+) occur at every cycle. Sporadic heat pipe failures during the thawing process or at any other time during the test cycles will be considered to be the result of bubble migration and growth in the arteries. If no evidence of heat pipe burnout is observed by the end of the 240-minute test cycle, (F) Steps 6 and 7 are repeated for the remainder of the 120-hour continuous test period.

3.3 TEST RESULTS

The cyclic tests on the SN009 heat pipe were performed from April 14 to April 19, 1980. A total of twenty seven partial and complete cycles were achieved during which seventeen burnouts or heat pipe failures were observed. A summary of the test results is presented in Figure 3-4. It shows the temperatures at nine different locations along the heat pipe at the end of the cooling period (Condition 'A') and those observed near the time of burnout or at the end of a cycle (Condition 'B').

The tests commenced at 0600 hours when the heat pipe was tilted 1.25 cm and 130 watts were applied to the evaporator block. After having established that both arteries were primed, cooling of the condenser was

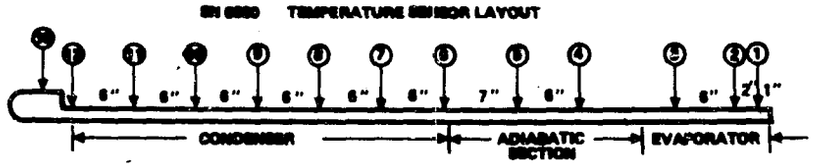

RUN S/N	CONDITION 'A' TEMPERATURES AT END OF COOLING PERIOD SENSOR TEMPERATURE (C)									CONDITION 'B' TEMPERATURES AT BURNOUT OR AT END OF CYCLE SENSOR TEMPERATURE (C)									TIME FROM 'A' to 'B' (MIN)	MAXIMUM C.W.R.* (C/MIN)	COMMENT/OBSERVATION
	⑯	⑫	⑪	⑩	⑨	⑧	⑦	⑤	①	⑯	⑫	⑪	⑩	⑨	⑧	⑦	⑤	①			
1	-40	-. 4	-132	-121	-65	6	31	32	34	-46	-	-79	-43	-	-	32	-	38	11	5.0	Burnout
2	-46	-125	-146	-140	-96	19	29	31	33	-96	-59	-63	4	27	29	31	31	34	190	5.0	Normal Cycle
3	-48	-103	-127	-121	-73	10	29	31	33	-44	-71	-71	-44	21	31	34	35	38	12	4.7	Burnout
4	-40	-101	-119	-111	-59	21	31	32	34	-36	-59	-51	-3	31	35	36	37	39	12.5	5.3	Burnout.
5	-33	-	-136	-131	-88	21	31	32	34	-39	-	-87	-72	8	31	34	34	36	10	5.3	Burnout
6	-37	-123	-124	-122	-75	9	29	32	33	-91	-40	-41	2	27	29	31	31	34	180	2.2	Normal Cycle
7	-47	-133	-136	-132	-99	-9	28	31	32	-94	-41	-42	8	27	29	31	32	39	180	2.5	Normal Cycle
8	-42	-126	-127	-121	-75	9	29	31	33	-42	-101	-102	-90	-37	27	31	34	36	10	3.6	Burnout
9	-51	-126	-128	-122	-75	11	28	31	32	-57	-68	-69	-41	23	30	33	34	36	45	2.2	Burnout
10	-56	-123	-125	-114	-68	6	28	31	32	-53	-101	-102	-86	-26	25	31	32	34	15	2.2	Burnout
11	-46	-140	-142	-137	-93	-1	26	31	32	-43	-107	-108	-99	-49	24	31	32	36	12	3.3	Burnout
12	-49	-132	-133	-126	-82	-6	28	31	32	-51	-103	-106	-91	-29	23	31	32	35	22	1.4	Burnout
13	-53	-126	-128	-117	-71	2	28	31	32	-51	-109	-111	-97	-43	21	29	31	37	32	0.9	Burnout
14	-48	-126	-127	-121	-74	11	28	31	32	-41	-117	-118	-111	-68	18	29	32	36	12	0.8	Burnout
15	-54	-107	-121	-108	-60	23	29	31	33	-53	-72	-69	-38	23	31	33	34	36	70	0.8	Burnout
16	-56	-107	-122	-111	-66	23	28	31	32	-58	-107	-112	-98	-42	21	29	31	34	15	0.8	Burnout
17	-48	-114	-136	-127	-94	-11	28	31	32	-52	-108	-118	-107	-56	13	28	31	36	15	1.7	Burnout
18	-48	-105	-124	-113	-71	13	28	31	32	-94	-57	-39	16	27	29	31	31	33	275	0.4	Normal Cycle
19	-93	-99	-96	-74	-26	26	27	28	30	-112	-56	-36	19	27	29	30	31	32	215	1.7	Normal — Non-freezing Test Cycles
20	-101	-98	-96	-75	-32	24	27	28	29	-96	-57	-39	14	26	29	30	31	33	180	6.7	Normal — Non-freezing Test Cycles
21	-100	-97	-94	-71	-10	21	26	28	29	-62	-51	-39	12	28	31	33	34	36	230	6.7	Normal — Non-freezing Test Cycles
22	-80	-126	-128	-108	-58	22	26	28	29	-68	-54	-42	2	28	31	32	33	35	190**	Rapid Condenser Warmup Under No Load	Normal — Power off after Freezing/Power on after Thawing
23	-79	-131	-134	-118	-73	21	26	28	30	-71	-47	-34	3	29	32	33	34	36	15**		Burnout — Power off after Freezing/Power on after Thawing
24	-68	-147	-154	-147	-107	-26	21	28	30	-64	-51	-39	8	27	31	33	34	36	183**		Normal — Power off after Freezing/Power on after Thawing
25	-46	-99	-118	-105	-54	18	29	31	33	-80	-73	-65	-34	23	29	30	31	33	180	0.4	Normal Cycle
26	-40	-100	-120	-113	-69	12	29	32	34	-71	-124	-126	-113	-66	21	28	29	31	30	0.2	Burnout
27	-69	-121	-124	-111	-63	3	27	29	31	-84	-73	-63	-31	24	29	31	32	34	165	—	Burnout when CWR increased from 0.19 to 5 C/Min.

*C.W.R.: Condenser Warm-up Rate (dT_{11}/dt)

**Time from end of warm-up period.

Figure 3-4. Summary of SN009 Heat Pipe Freeze/Thaw Cyclic Tests

initiated by turning the radiator heaters off. This process continued until subfreezing temperatures in the inactive condenser section, as indicated by temperature sensors 10, 11 and 12, were realized. These sensors showed minimum temperatures of -120C, -132C and -114C respectively prior to the initiation of the condenser warm-up period. Approximately eleven minutes after the radiator heaters were turned on, the heat pipe failed. About the time of the failure, the condenser warm-up rate (CWR) was about 9F/min and the minimum temperature in the condenser section, shown by sensor 11, was -79C which is 19C above the freezing point of methanol, thus well past point B^+ in Figure 3-3.

Subsequent to burnout, the heat pipe was leveled and allowed to reach close to isothermal conditions over a period of two hours. The pipe was then tilted 1.25 cm and 130 watts were applied to the evaporator, but the heat pipe failed to sustain the load. The above priming procedure was repeated with similar results.

The inability of the heat pipe to hold the load after two priming attempts was postulated to be the result of the presence of residual bubbles in the arteries. It was decided then to modify the procedure to prime the pipe, by requiring that the evaporator end be raised 61 cm for one minute before leveling the pipe. The high tilt would presumably eject all the liquid and residual bubbles from the arteries. After the pipe was leveled for thirty minutes, 130 watts were applied to the evaporator raised 1.25 cm. This time priming of the arteries was verified and the second cycle was started. The latter procedure for priming the heat pipe was followed through the rest of the test period with successful results.

Cycle number 2 was the first complete normal cycle and was followed by three burnouts observed during the condenser warm-up periods of cycles 3, 4 and 5, at which times the CWR was, approximately 5C/min (9F/min).

The partial history of selected temperatures along the heat pipe during normal cycle 2 is shown in Figure 3-5. It can be seen that prior to condenser warmup the ice front almost reaches the locations of sensor 9, i.e., approximately 18 inches of the condenser end were frozen. During the warmup period of the cycle the figure shows the gas front moved close to sensor 10 which indicates that a portion of the previously frozen condenser became part of the active condenser section.

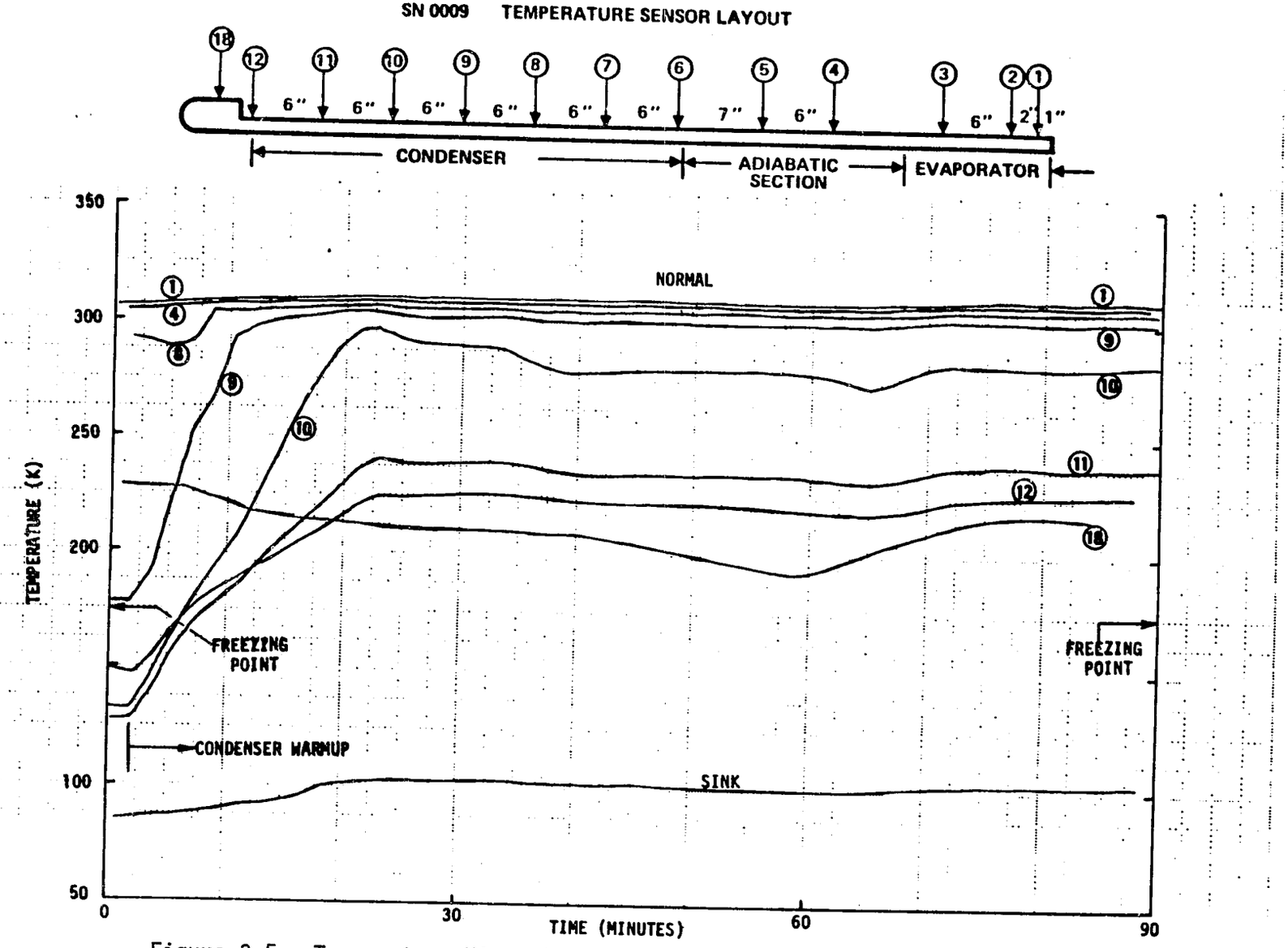

Figure 3-5. Temperature Histories During SN009 Heat Pipe Cyclic Test No. 2

The large proportion of failures, four out of five, was attributed to rapid thawing and warming of the inactive condenser, events which were originally postulated to result in the formation of bubbles inside the arteries and in their rapid induction into the active portion of the condenser before the bubbles could vent by diffusion. Once in the active portion of the pipe, these bubbles would grow and deprime the artery.

A typical temperature history of the four cycles during which depriming was observed is that of cycle 4 shown in Figure 3-6. As shown, the ice front was located somewhere between sensors 9 and 10 at the end of the cooling period of the test cycle. During the warmup period depriming is observed apparently at the time the gas front reached the previous location of the ice front. The fact that depriming occurred approximately 9 minutes after the inactive condenser completely thawed, the possible involvement of freezing blowby in these heat pipe failures can be discounted, therefore it can be argued that depriming can only be the result of bubbles.

In order to determine the effect of condenser warm-up rates on the frequency of heat pipe failures, the CWR during the next six cycles was reduced an average of fifty percent. The results were that the heat pipe performed normally during two consecutive complete cycles, cycles 6 and 7, at the reduced CWR of about 2.2C/min. The following four cycles, however, resulted in burnouts during condenser warmup at rates varying from 2.2C/min to 3.6C/min. The variation in these CWRs was not intentional but rather the result of the limited heater control capability of the test assembly.

The typical partial temperature history of normal cycles 6 and 7 is that of cycle 6 shown in Figure 3-7. The temperature history of cycle 11 shown in Figure 3-8 is similar to that of cycles 8 and 10. As in most previous cycles, the ice front can be seen located between sensor 9 and 10 at the end of the cooling period. Figure 3-8 shows however, that depriming occurred under significantly different condenser conditions in most cycles at the lower condenser warmup rate: 1) the inactive condenser was still partially frozen (last 12 inches) and 2) temperatures of sensors 8 and 9 indicate the gas/vapor front never reached the previously frozen region.

Because the condenser was not completing the thawing process at the time of burnout, freezing blowby can be discounted as the cause of pipe

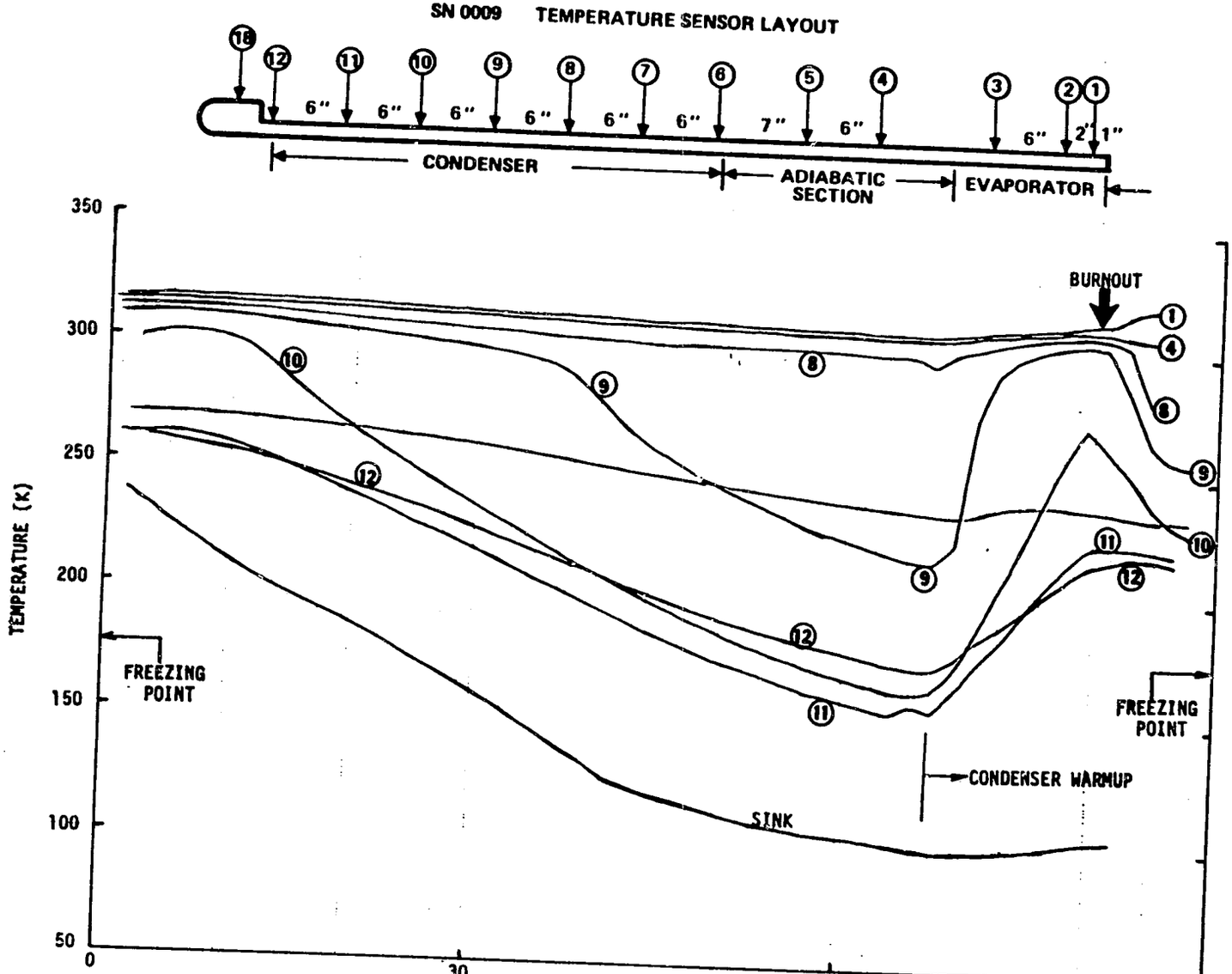

Figure 3-6. Temperature Histories During SN009 Heat Pipe Cyclic Test No. 4

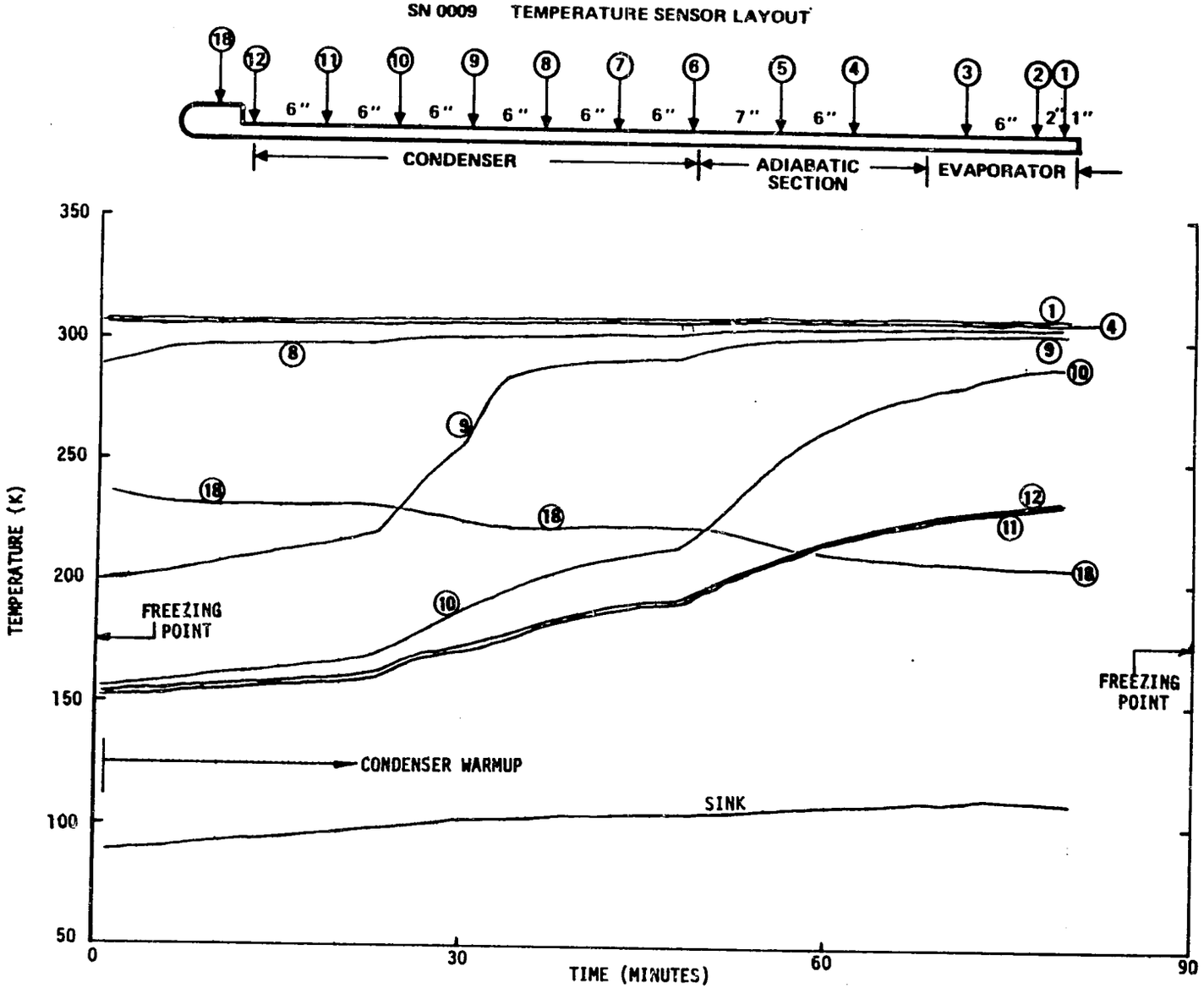

Figure 3-7. Temperature Histories During SN009 Heat Pipe Cyclic Test No. 6

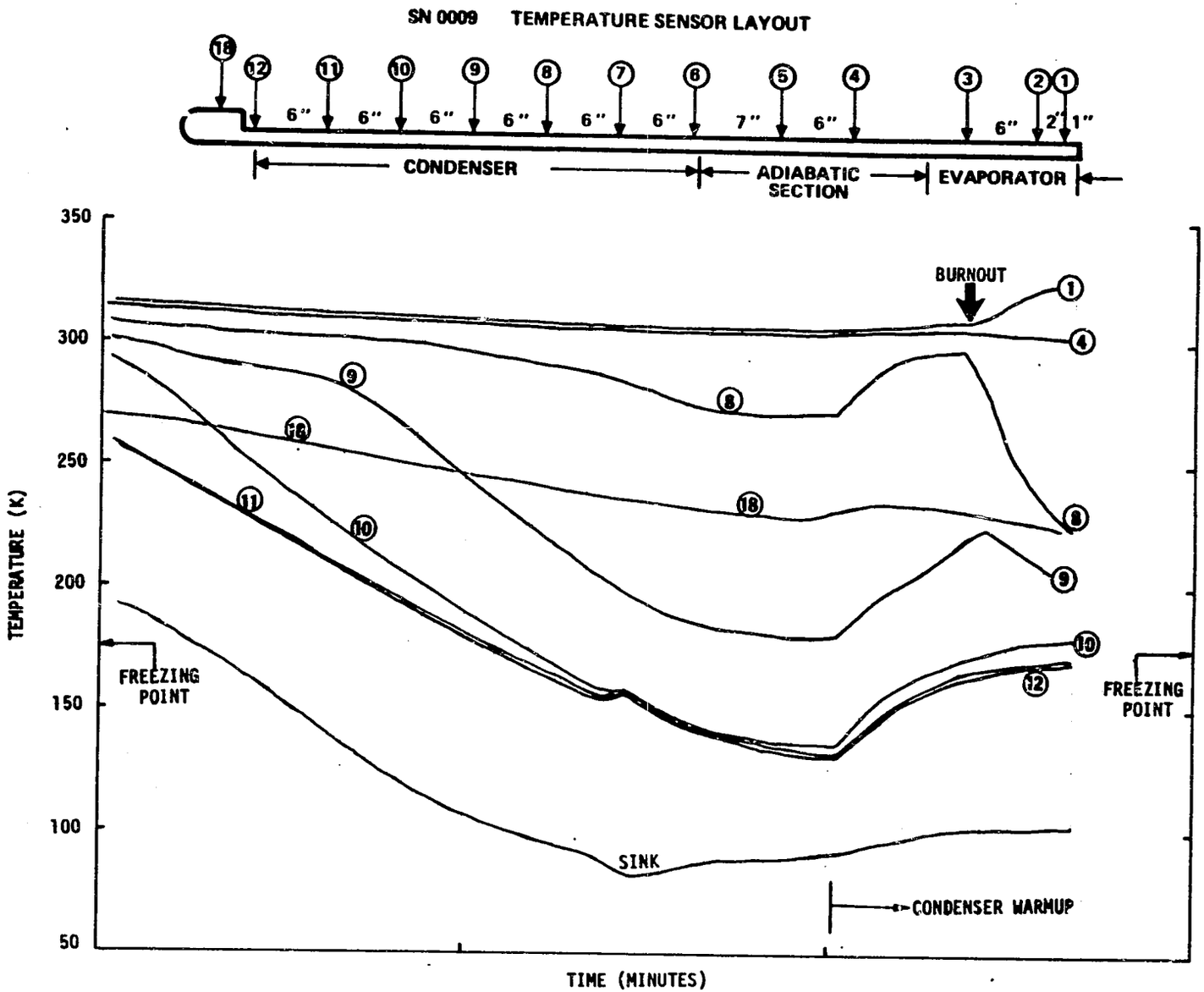

Figure 3-8. Temperature Histories During SN009 Heat Pipe Cyclic Test No. 11

failure which, then can be attributed only to be the result of bubbles. However, the fact that portions of the previously frozen condenser section were never incorporated into the active heat pipe section, a condition that was postulated to be necessary to induce bubbles into the evaporator, seems to indicate that other mechanisms such as Marangoni Flow were involved to move bubbles into the active portion of the condenser where further growth or movement would be expected.

It was postulated that depriming due to bubbles released in the inactive section occurred as follows. During the cooling period the freezing front moves toward the evaporator expelling bubbles which are then locked inside the ice and building stress on the arteries due to suction freeze-out. This process continues until the end of the cooling period when the imposed stress on the arteries due to freezeout reaches a maximum level. This increase in stress is accompanied by a reduction of the hydrodynamic stress which results from shrinkage of the effective length due to advancement of the gas/vapor front toward the evaporator.

This imposed stress on the arteries due to suction freezeout is either overcompensated by the reduced hydrodynamic stress or the unused pumping capacity of the artery, for no heat pipe failures were observed during the cooling periods of the test cycles. During the warmup period, the advancement of the gas/vapor front toward the reservoir end results in increased hydrodynamic stress as the effective length expands, and in the propagation of a conduction heat wave which causes the ice front to recede and release liquid and bubbles upon thawing. Although the release of the liquid reduces the stress that came from suction freezeout, there remains sufficient back stress on the arteries in the gas-blocked region to induce growth of the released bubbles. These bubbles agglomerate and then reach the active section due to continuing growth and/or Marangoni Flow.

Whereas depriming during cycles 8, 10, and 11 occurred 10 to 12 minutes into the warmup period before the gas/vapor front reached previously frozen sections, depriming in cycle 9, as shown in Figure 3-9, occurred approximately 45 minutes into the warmup period, 25 minutes after the condenser completely thawed. An interpretation of the data seems to indicate that bubbles first released about the previous location of the ice front somewhere between sensors 9 and 10 were subsequently incorporated into the

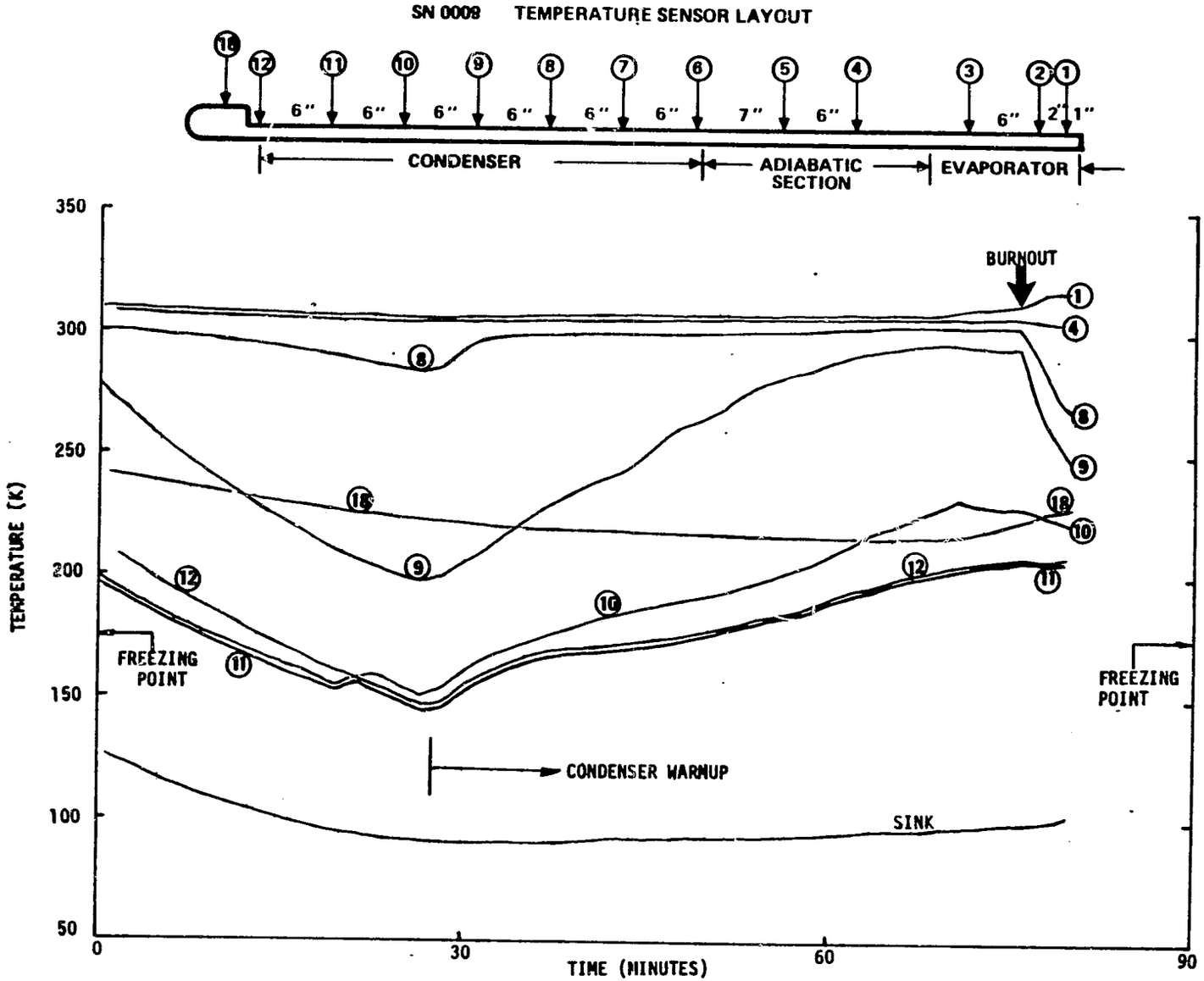

Figure 3-9. Temperature Histories During SN009 Heat Pipe Cyclic Test No. 9

active portion and caused depriming when the gas/vapor front reached that location 45 minutes later.

During test cycles 12 through 18, the heat pipe inactive condenser was warmed up at even lower rates ranging from 0.4C/min to 1.7C/min. Burnouts were observed in all these cycles, except in cycle 18 which had the lowest CWR of 0.4C/min.

The temperature history of cycle 13 is shown in Figure 3-10. It can be seen that depriming occurred before the gas/vapor reached previously frozen sections and while the last 12 inches of the condenser were below the freezing point. Similar observations can be made of deprimings observed during cycles 12, 14, 16 and 17.

Depriming during cycle 15, as shown in Figure 3-11, occurred under different conditions. It can be seen that when the gas/front apparently reached previously frozen areas a burnout was triggered. At this time the condenser had been completely thawed for approximately 40 minutes.

Normal freezing cycle 18, was followed by three cycles during which the inactive condenser was rapidly cooled to temperatures just above the freezing point and then warmed at rates as high as 6.7C/min. The idealized nonfreezing cycle is described graphically in Figure 3-12. These nonfreezing test cycles were performed to support the hypothesis that the frequency of failures due to bubbles could be greatly diminished if freezing and thawing did not occur in every cycle. The fact that the heat pipe evidenced normal operation during these cycles tends to support the above. The typical temperature history of a nonfreezing test cycle is that for cycle 19 shown in Figure 3-13.

During test cycles 22 through 24, the inactive condenser was rapidly cooled below the freezing point with the heat pipe operating under 130 watts. Subfreezing condenser temperatures were maintained for at least ten minutes subsequent to which the evaporator heaters were turned off and the inactive condenser was rapidly warmed. When the inactive condenser temperatures reached about -40C the evaporator heaters were turned on again. The idealized cycle is described graphically in Figure 3-14. A burnout was observed during the second cycle, cycle 23, 15 minutes after the heat load

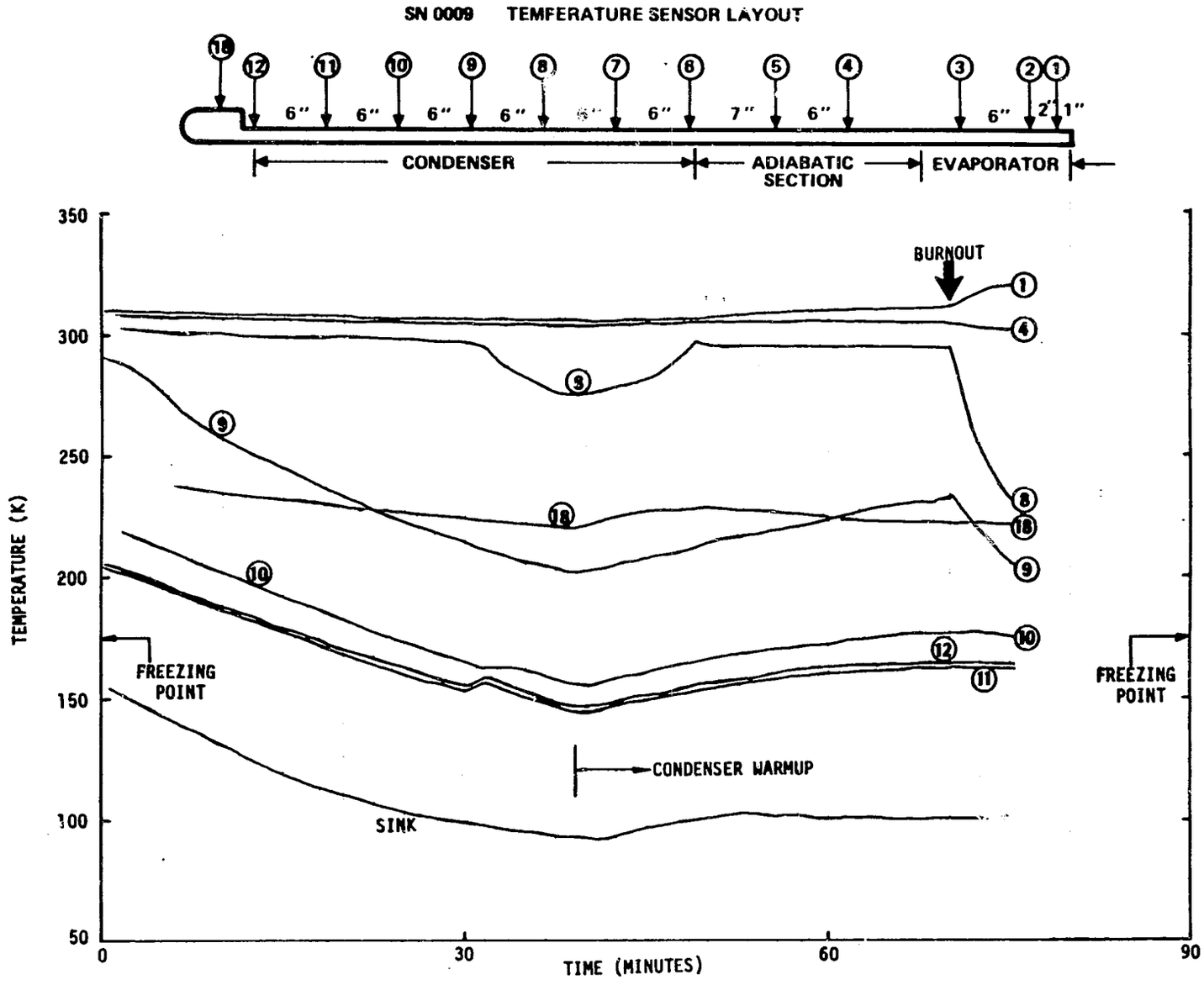

Figure 3-10. Temperature History During SN009 Heat Pipe Cyclic Test No. 13

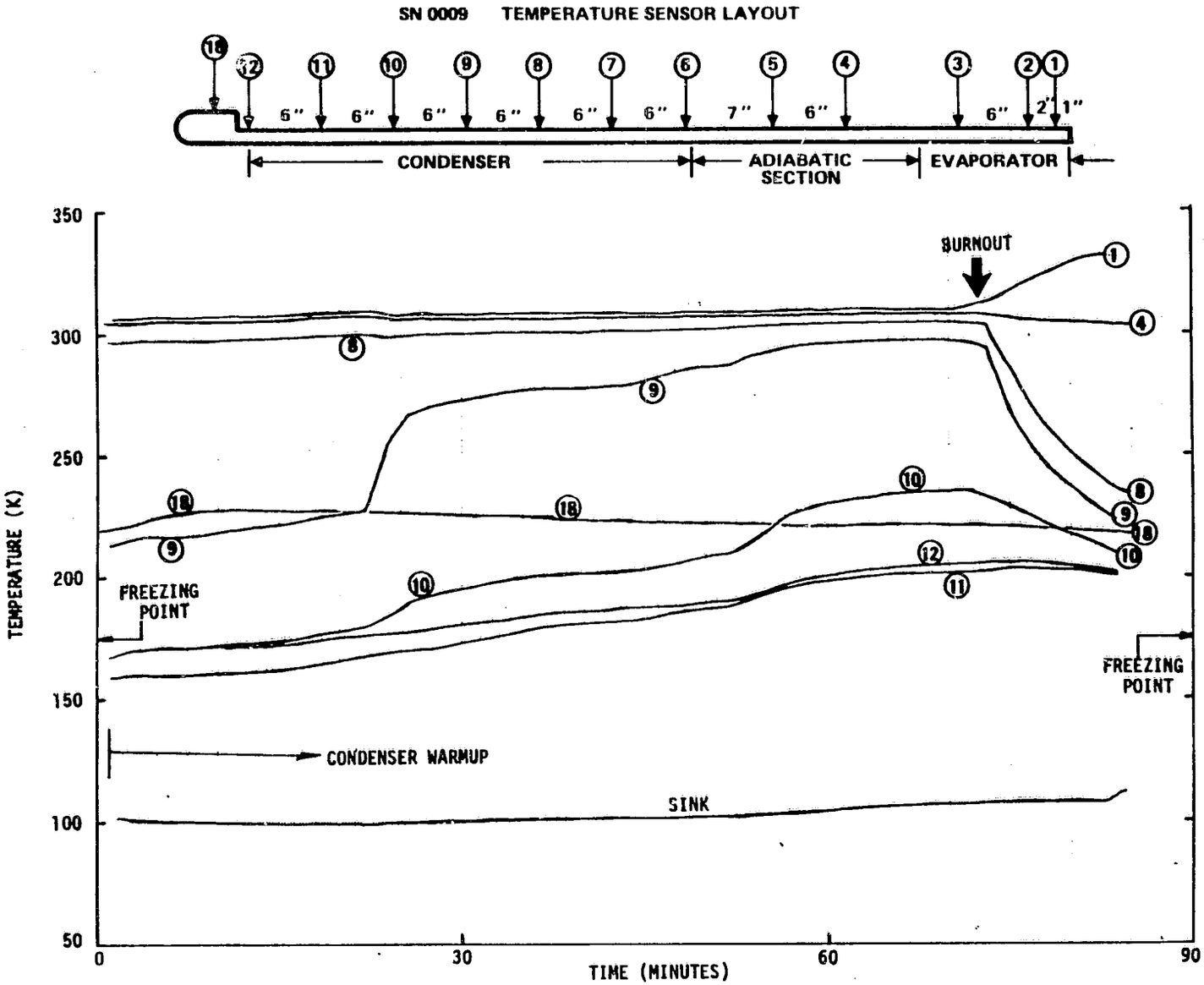

Figure 3-11. Temperature History During SN009 Heat Pipe Cyclic Test No. 15

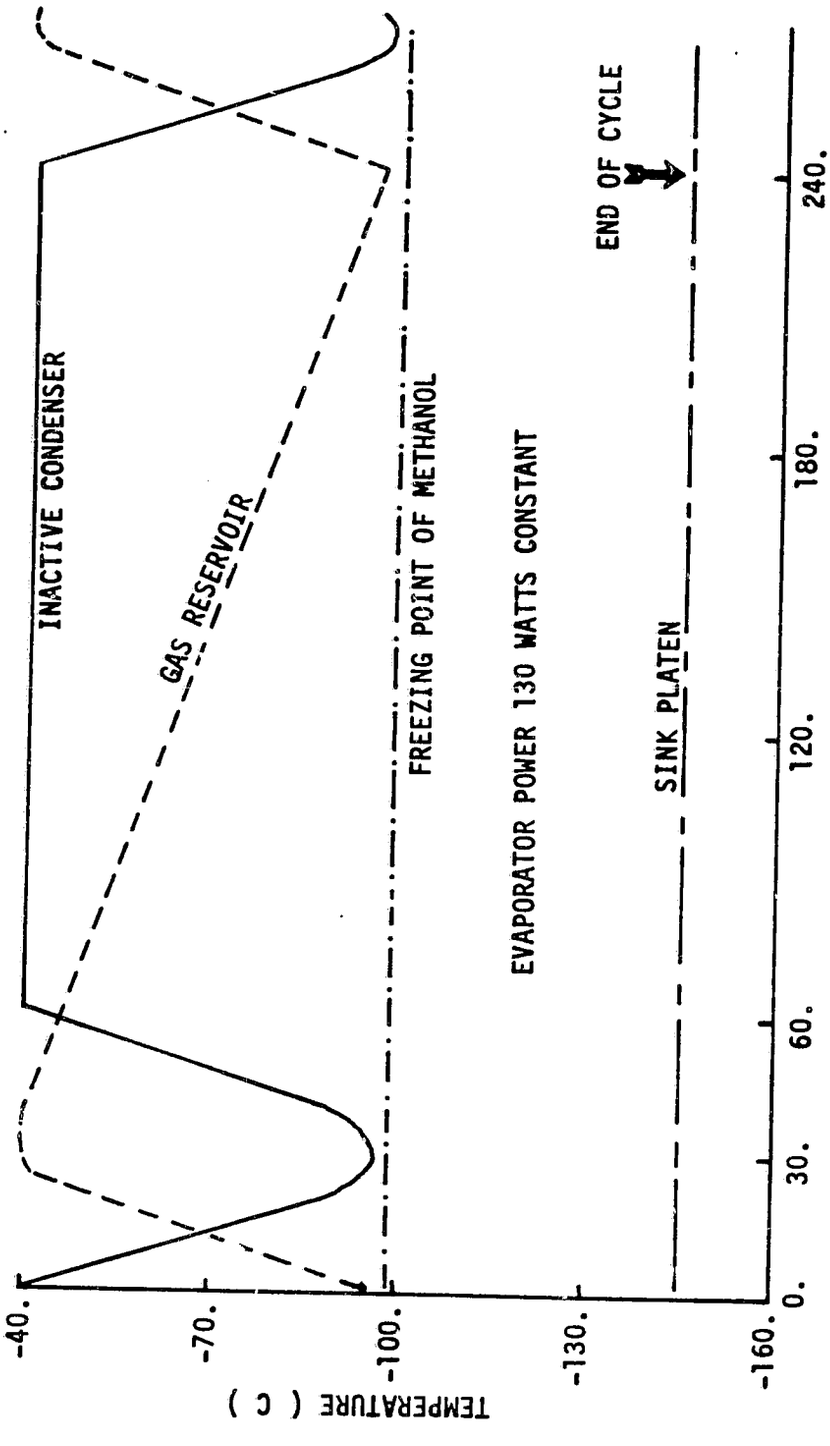

Figure 3-12. Idialized Nonfreezing Cycle "B"

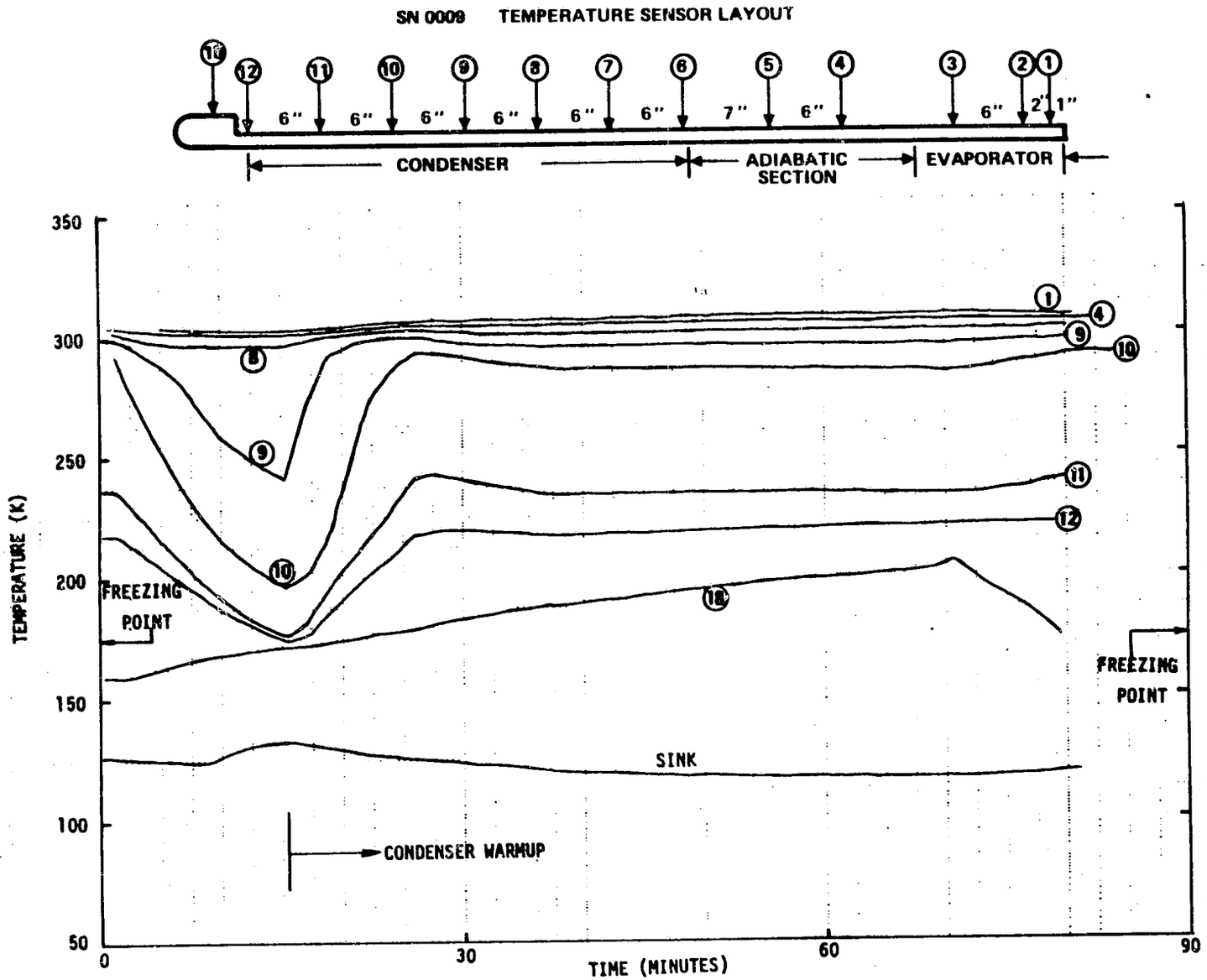

Figure 3-13. Temperature History During SN009 Heat Pipe Cyclic Test No. 19

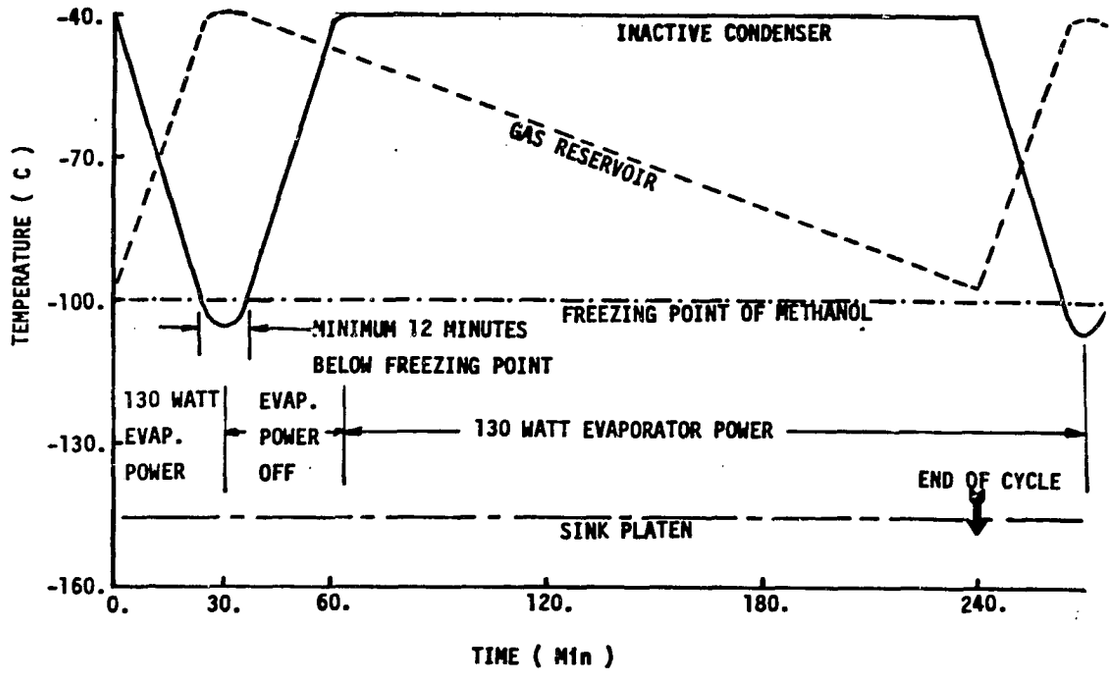

Figure 3-14. Idialized Freezing/Thawing Cycle "C"

was reestablished. This can be seen in Figure 3-15 which shows that depriming occurred apparently when the gas/vapor front reached the previously frozen condenser section.

In the last three cycles of the test program, the heat pipe, under a continuous load of 130 watts, was subjected to condenser warmup rates ranging from 0.2C/min to 0.4C/min. Cycle 25 with the higher CWR of 0.4C/min was normal. Burnouts were observed in the next two cycles. The last heat pipe failure during cycle 27, however, is worth noting since it occurred 165 minutes into the warmup period when the CWR was increased from 0.2C/min to 5C/min. The temperature history of this cycle is shown in Figure 3-16. Although the cooling period of the cycle is not shown in this figure, Figure 3-2 indicates the ice front prior to warmup was located somewhere between sensor 9 and 10. Figure 3-16 shows the gas/vapor front at the end of the slow warmup period was located between sensors 8 and 9. As the warmup rate was increased, it can be seen that the gas front rapidly moved between sensors 9 and 10 seemingly reaching the previously frozen section and triggering a burnout.

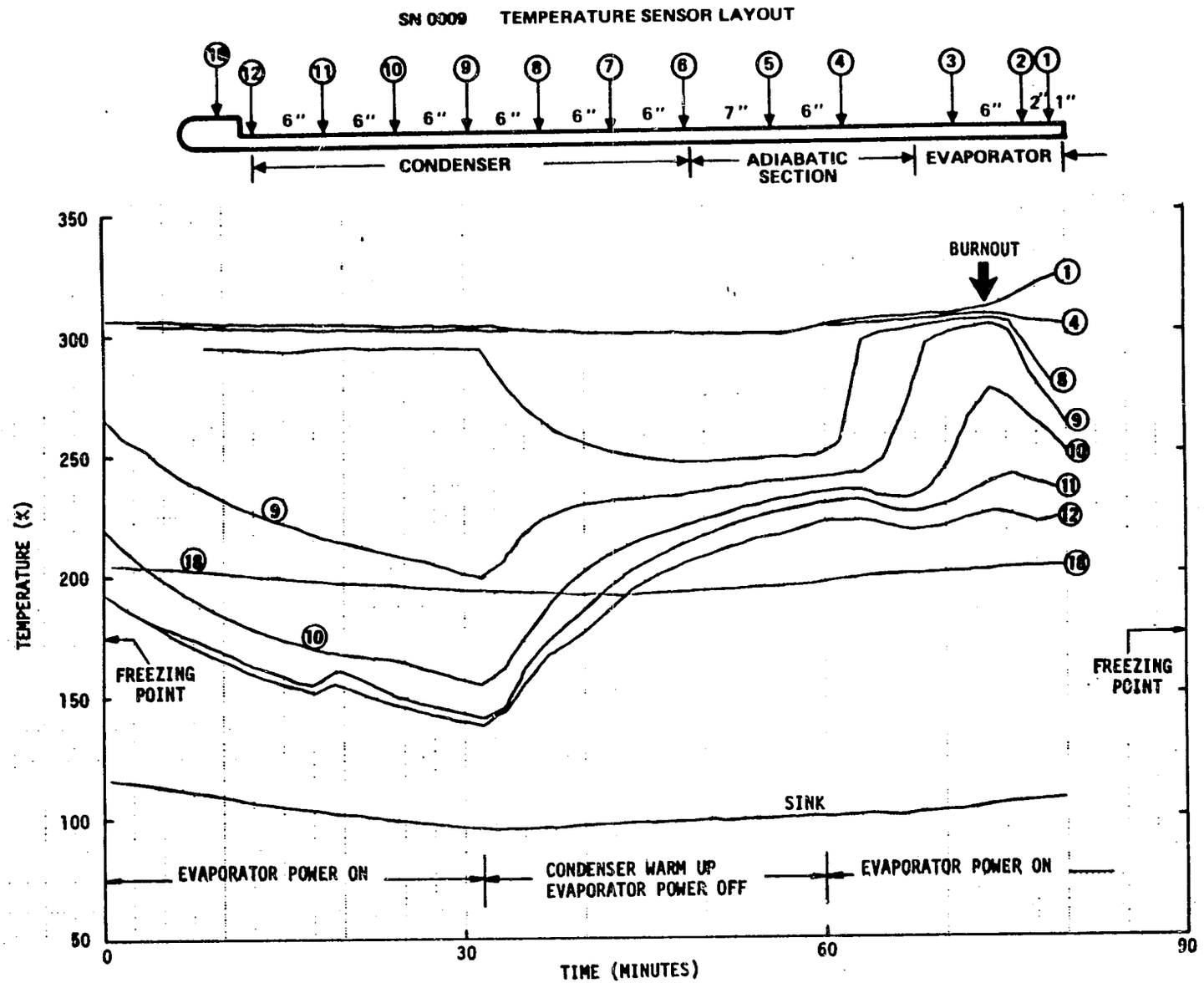

Figure 3-15. Temperature Histories During SN009 Heat Pipe Cyclic Test No. 23

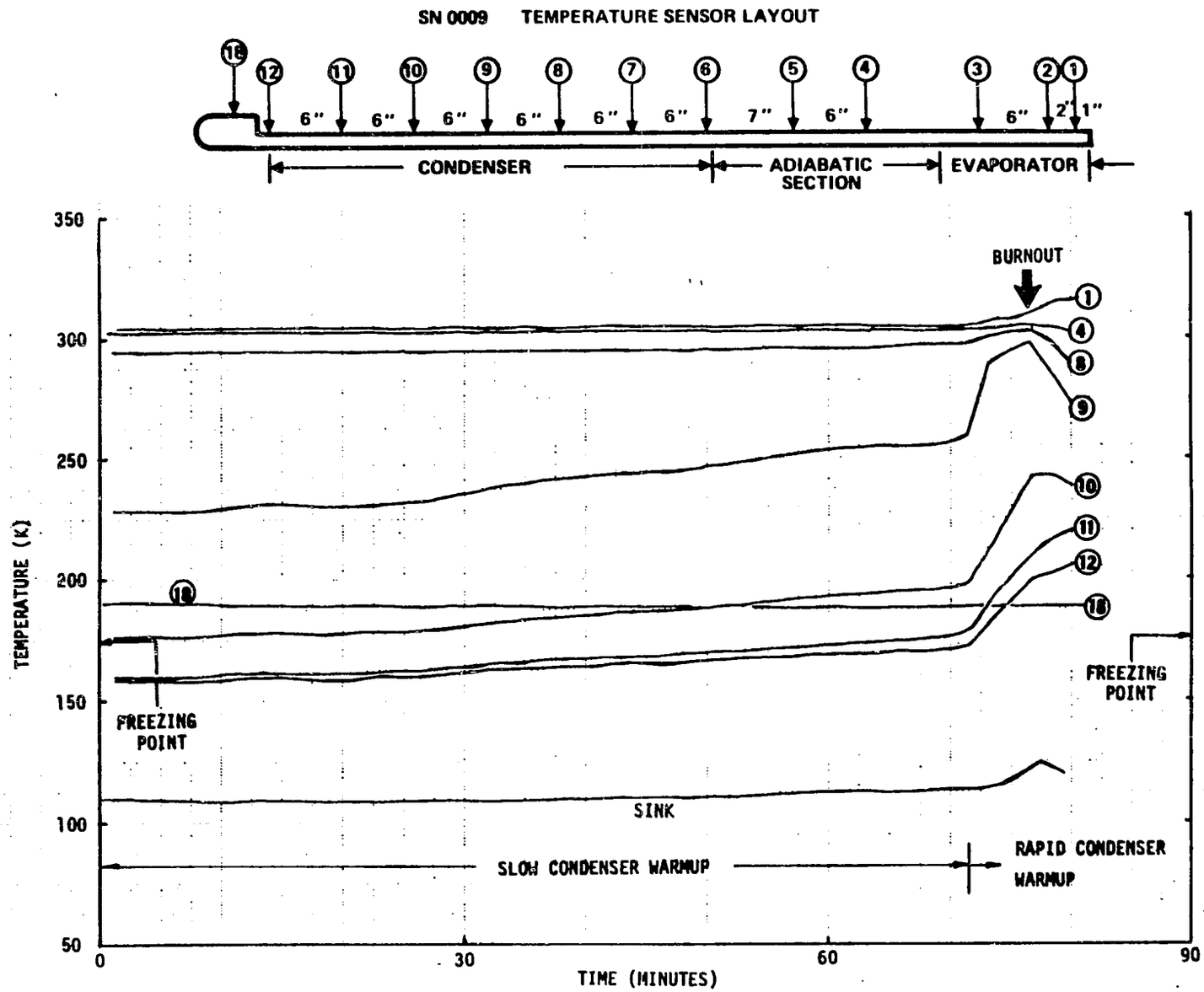

Figure 3-16. Temperature Histories During SN009 Heat Pipe Cyclic Test No. 27

Following this final burnout, the heat pipe was leveled and left undisturbed over the weekend. Fifty-five hours later, when 130 watts were applied to the evaporator, the heat pipe failed to hold the load, an event seemingly pointing to the survival of bubbles from the last freeze/thaw cycle as the probable cause of artery depriming. The temperature histories of cycles not shown in this section can be found in Appendix B.2.

3.4 SIGNIFICANCE OF TESTS RESULTS

The results of the cyclic tests on the SN009 heat pipe clearly established that thawing the frozen condenser of an arterial heat pipe under high load is an operating mode that results in arterial failure with significant frequency. Out of twenty one freezing and thawing cycles under high load, sixteen cycles resulted in heat pipe failures. Although thawing the condenser under high load enhances the probability of artery depriming, it is not a necessary condition. This proposition is supported by the fact that out of three cycles in which the condenser was thawed under no heat load one cycle (number 23) resulted in artery failure subsequent to thawing when the heat load was reestablished on the pipe.

In twenty four freezing and thawing cycles no heat pipe failures occurred during condenser freezing. The lack of failures during freezing when the suction freezeout mechanism has its greatest potential to deprime the arteries seems to indicate that none of the observed failures during the test cycles can be solely attributed to this mechanism. Even though bubbles are known to be released during freezing they are immobilized inside the ice structure rendering a failure during freezing due to bubbles an unlikely event.

All the observed anomalies occurred during or following condenser warmup periods. The fact that the inactive condenser was either completely thawed or still frozen along a considerable length when deprimings occurred, it can be argued that the freezing blowby mechanism could not account for any of the heat pipe failures observed during the cyclic tests.

Since neither suction freezeout nor freezing blowby were the sole cause of any of the observed heat pipe failures, it can be concluded only that all the anomalies during the cyclic tests on the SN009 heat pipe were the result of the freezing/thawing bubble mechanism.

The freezing and thawing process is required for bubbles to form inside the arteries. Periodic freezing and thawing replenishes the bubble population which enhances the probability of artery depriming due to bubbles. The results of three normal successive cycles without freezing supports the above.

The presence of bubbles in the arteries is necessary for depriming to occur. However, depriming does not necessarily occur when bubbles are present. This statement is supported by the fact that out of 24 freeze/thaw test cycles seven were normal (i.e., no failure occurred). These test results indicate that the occurrence of the observed heat pipe failures is random, which is consistent with the demonstrated statistical nature of the bubble mechanism.

During the freeze/thaw process bubbles are generated in the gas-blocked condenser section. It was postulated at the outset of the cyclic tests that the active condenser length had to expand into the previously frozen section. However, in roughly half the failures the active condenser length had not yet reached the previously frozen section.

The results of the tests seem to indicate that there exists some correlation between the condenser warm-up rate and the incidence of heat pipe failures. The reduction of the condenser warm-up rate used in the first five cycles by approximately 50 percent was followed by the only two consecutive normal cycles observed during the tests. In addition, during cycle 27 depriming occurred almost two hours into the warm-up period following a rapid and large increase in the condenser warm-up rate.

Deprimings observed during cycles with high warm up rates occurred after the condenser had completely thawed and soon after the active condenser length reached the previously frozen section. On the other hand, most heat pipe failures during cycles with low warm up rates occurred while portions of the condenser were still frozen and before the active condenser length ever reached the previously frozen section. The latter failures are attributed to movement of bubbles into the active condenser helped by suction freezeout and/or Marangoni flow.

The results of several unsuccessful attempts to reprime the heat pipe after the first freeze/thaw cycle indicate that a depriming does not clear

out all the bubbles. Consequently bubbles form during a single freeze/thaw process can result in repeated successive failures due to residual bubbles.

Numerous deprimings observed during the tests occurred 10 to 30 minutes after freezing conditions in the condenser ceased to exist. Following the last freezing and thawing test cycle, the SN009 heat pipe deprimed 52 hours later when the normal heat load was reestablished. This heat pipe failure can only be attributed to be the result of bubbles generated during the last freeze/thaw cycle of the test program.

These results indicate that ice-generated bubbles can last a long time, and therefore freezing at the very time of the CTS anomalies was not necessary. Thus the anomaly on day 253 can be attributed to ice-generated bubbles from day 252 or earlier.

4.0 CONCEPTS TO AVERT ARTERY DEPRIMING

4.1 NONCONDENSIBLE CONTROL GAS SELECTION

Unquestionably the simplest and most effective concept to avert arterial depriming is the selection of a control gas that would preclude the formation of bubbles when the liquid methanol undergoes freezing and thawing. This concept is unfortunately unrealizable, for the freeze/thaw process, being a degasifying process, will result always in the formation of bubbles regardless of the noncondensible control gas selected.

Nucleation experiments performed during Phase I, showed that a large number of minute bubbles are initially released during freezing and thawing. Most of them rapidly disappear owing to their size, but others coalesce forming fewer but larger bubbles whose lifetimes strongly depend on their sizes. Larger bubbles have longer lifetimes which enhance the probability of further coalescence which results in bubbles of even longer lifetimes which can then survive until the gas/vapor front moves into previously frozen sections or until suction freezeout and/or Marangoni flow succeed in making them grow and transporting them into the active section of the heat pipe.

The above observations indicate that reducing bubble lifetimes by proper selection of a control gas can decrease to a certain extent the probability of bubble coalescence and of their induction into the active section of the heat pipe. The results of the bubble lifetime analysis in Section 2.0, show, for example, that a spherical CTS control gas bubble (90% N_2/10% He) of 0.8 mm in diameter (i.e., half the CTS artery diameter) under some assumed conditions has a lifetime of about 19 hours compared to a lifetime of less than one hour for a methane bubble of the same size. The rapid dissolution of methane bubbles suggests the selection of methane for the control gas.

Although the selection of a new control gas, such as methane, will result in bubble lifetimes significantly shorter than in the CTS heat pipes which will diminish to a certain extent the probability of depriming, this concept cannot guarantee that depriming will be averted. However, the use of methane in conjunction with other steps to avoid depriming should enhance the effectiveness of those steps.

4.2 OPERATIONAL PROCEDURE FOR START-UP OF A FROZEN CONDENSER

Since the bubbles leading to arterial depriming are formed by a freeze/thaw process, the avoidance of freezing will avert artery depriming. Selection of sun angle and radiator radiation properties or the use of heaters could prevent freezing in many missions. However, in missions to outer planets, avoidance of freezing may be costly or even impossible. Even when the condenser has been frozen, it is possible to thaw the heat pipe and restore it to a primed and serviceable state, provided proper procedure is followed.

The key to successful restoration of a previously frozen heat pipe is dissolution or venting of the freeze/thaw generated bubbles. Venting is discussed in Section 4.3. Dissolution requires leaving the condenser in a quiescent state somewhat above the freezing point for a time long enough to allow the bubbles to collapse. This time depends upon the control gas, the size of the largest bubble, and the pressure and temperature in the gas-blocked condenser. The advantage of methane as a control gas has been discussed. It has a high solubility-diffusivity product leading to more rapid bubble dissolution. Since the bubble agglomeration mechanism appears to be statistical, and it is not clear that a laboratory test at 1-g is a good indicator of agglomeration at zero-g, it is presently difficult to predict with certainty the size of the largest bubble and thus the time required for it to collapse. However, start-up can be attempted earlier than necessary merely to test whether a sufficiently long time has been allowed to elapse. If depriming occurs, the heat pipe is returned to a quiescent state for more time to pass. In the attempt at operation, at least one bubble was vented. Thus successive attempts at start up contribute to the bubble clearing process.

High pressure during the bubble collapse period hastens it. With an actively controlled heat pipe, the gas reservoir and evaporator could both be heated somewhat to raise the gas-blocked condenser pressure. It should be noted that the restart procedure would have to be used each time a segment of the gas-blocked condenser freezes and is thawed.

4.3 MECHANICAL MODIFICATIONS

In a gas-controlled arterial heat pipe it has been found that a priming foil at the end of the evaporator is necessary for successful priming [5]. Without it, gas in the pipe can be trapped inside the artery during priming. With the priming foil and with a gentle heating of the evaporator bubbles trapped in the evaporator are transported to the foil and vented.

The priming foil shown in Figure 4-1 consists of a very thin metallic membrane with one or more holes no larger than the effective pumping pore diameter needed for the capillary flow in the active pipe. The size of the vent hole and the thickness of the foil must be such that the meniscus of a bubble of arterial size contacts the meniscus attached to the outer corners of the vent hole. Meniscus coalescence then ruptures the liquid

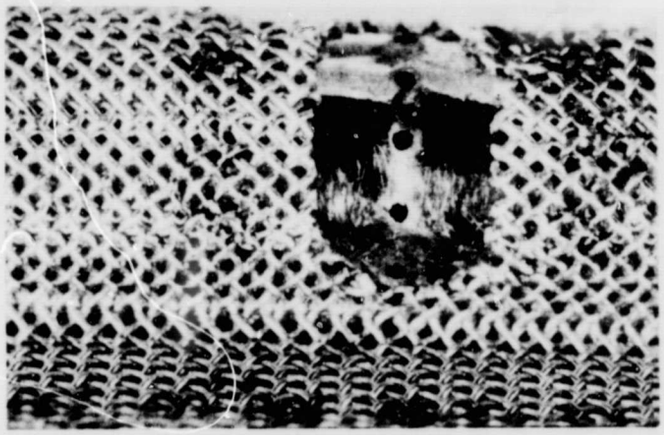

Fiugre 4-1. Segment of an Artery with a Priming or Venting Foil

film bridging the vent hole and allows the gas to be vented. It should be noted that the heat load during venting must be less than the open-artery capacity of the heat pipe.

The same principle can be applied to the condenser region or even to the entire pipe [5] as long as the local stress does not exceed the capillary pumping capability of the artery at that point and time. Thus a location in the condenser (or perhaps even in the adiabatic section) can be identified where under restart heat load the local stress is below this limit. At that location a screen across the artery can be placed to filter out and collect small bubbles tending to move toward the evaporator. On the condenser side of the screen a priming foil would be placed (venting holes located one artery radius from the screen) to allow venting of the collected gas should the gas volume reach arterial size.

The bubble-filter/venting-foil concept should allow a normal start up from a frozen condenser state and permit continuous normal operation of the heat pipe even though the gas-blocked condenser is undergoing periodic freezing and thawing.

5.0 CONCLUSIONS

Evidence strongly suggests that bubbles generated through freezing and thawing of methanol in the gas-blocked condenser arteries were responsible for the CTS thermal anomalies. Out of the 24 freeze/thaw cyclic tests with the SN009 heat pipe, 17 deprimings were observed. While some of the tests were conducted under conditions where probability of depriming was high, others were conducted where the probability was low, thus emphasizing a statistical variation in the freeze-thaw bubble mechanism.

Most often depriming occurred while the gas-blocked condenser was still frozen along a portion of its length but some occurred 10 to 30 minutes after thawing was completed. In one test depriming occurred 52 hours after thawing.

Analytical-numerical studies of bubble collapse show bubble lifetimes to be strongly dependent upon bubble size and control gas composition. The helium in the CTS control gas mixture causes long bubble lifetimes when the bubbles are of arterial size. Selection of methane as a control gas would significantly shorten bubble lifetime for equal sized bubbles.

At the present level of understanding, selection of methane for control gas cannot ensure avoidance of bubble depriming. Prevention of freezing in the gas-blocked condenser by active or passive control should avert depriming. Should avoidance of freezing be inconvenient or not feasible, either installation of a bubble-filter/priming foil element at the condenser-adiabatic section interface or adoption of an appropriate thawing and bubble clearing procedure would probably allow successful heat pipe operation.

6.0 REFERENCES

1. R.E. Alexovich and A.N. Curren, "Thermal Anomalies of the Transmitter Experiment Package on the Communication Technology Satellite," NASA Technical Paper 1410, April, 1979.

2. B.D. Marcus, "CTS TEP Thermal Anomalies — Heat Pipe System Performance," NASA Contract NAS3-21012, November 30, 1977.

3. E.W. Saaski, "Heat Pipe Temperature Control Utilizing a Soluble Gas Absorption Reservoir," NASA Report CR 137,792, February 1976.

4. E.W. Saaski, "Investigation of Bubbles in Arterial Heat Pipes," NASA Report CR 114,531, December 1972.

5. J.E. Eninger, "Menisci Coalescence as a Mechanism for Venting Gas from Heat-Pipe Arteries," AIAA Paper No. 74-748, July 1974.

APPENDIX A.1
EXCESS SKEW IN LOAD PARTITIONING

The three heat pipes of the CTS VCHP system are designed to turn on sequentially so as to balance the load between them at full-on design conditions. However, a build up of tolerances on gas inventory during manufacture, and very low sink temperature during equinox conditions may result in the load on heat pipe No. 1 exceeding its capacity before Nos. 2 and 3 take up a significant share. Failure of No. 1 by the above mechanism or by any other could then result in a rapid transfer of load to No. 2, etc., perhaps yielding a "domino effect" failure of the whole system.

The first step in investigating this was to further review the flight data to search for regularity in the depriming sequence associated with the anomalies. Toward this end, NASA LeRC personnel provided computer plots of pertinent flight data for subsequent review.

Experimentally, attempts were made to deprime the SN009 heat pipe with rapid load increases, simulating rapid sequential load transfer as pipes deprime.

The tasks performed in this investigation are summarized below.

Flight Data Analysis to Determine Depriming Sequence

Computer plots and tabulations of CTS telemetered data were provided for days 75, 82, 89, 101 and 253 of 1977. Day 89 was a so-called "normal" day whereas the others were the four anomaly days.

Flight data had already been examined in a previous study effort. However, the new data included overlay plots of all pertinent data on single pages, and values of ΔT_{3-2} and ΔT_{2-1} in addition to ΔT_{3-1} provided earlier. It was hoped that this data format might shed additional light on the system behavior, particularly the sequence in which the heat pipes deprimed on the anomaly days.

Unfortunately, the telemetry increment in the temperatures was 1.8C to 1.9C, which is of the same magnitude as the normal values of ΔT between pipes as well as the changes in temperature which accompany depriming. Consequently, it is very difficult to distinguish between

actual physical phenomena and telemetry noise. In view of this limitation, the data tentatively suggests the following:

Day 75: It appears that heat pipe No. 1 deprimed first, yielding increased values for ΔT_{2-1} and ΔT_{3-1}. Several hours later heat pipe No. 2 deprimed, followed almost immediately by heat pipe No. 3 and the sudden rise in body temperature.

Day 82: The data is particularly unclear this day, but as with day 75, it appears that heat pipe No. 1 failed first, followed by Nos. 2 and 3.

Day 89: No anomaly occurred on this day. However, the data suggests that heat pipe No. 2 was deprimed, causing No. 3 to carry a greater load.

Day 101: The data indicates the failure sequence was 1:2:3, as with day 75.

Day 253: In this case, heat pipe No. 3 did not even "turn-on" until the anomaly began, and apparently could not prevent it. Thus, it had to be deprimed from the start. In fact, the data suggests that heat pipes 2 and 3 deprimed first, with the anomalous increase in body temperature corresponding to the depriming of No. 1.

Specific interpretation of the depriming sequences is covered in the SN009 heat pipe test discussion that follows. However, one item of note bears discussion. If bubble nucleation within the arteries is a cause of the anomalies, then the statistical nature of the mechanism should yield one heat pipe failed occurrences far more often than two or three heat pipe failed occurrences. Day 89, in which No. 2 appears deprimed, while Nos. 1 and 3 are primed, may be such a day.

Rapid Increases in Load Tests on SN009 Heat Pipe

Extensive testing was performed with the SN009 heat pipe. The first series of tests were to determine whether there exists significant inertial effects on heat pipe capacity which could contribute to a "domino effect" failure of all three CTS pipes. That is, if heat pipe No. 1

deprimed, most of the load it had carried would be suddenly transferred to No. 2, etc. If the capacity of a heat pipe were substantially lower for the sudden application of load than for gradual application (due to fluid inertia), the probability of a sequential failure of all three pipes would be enhanced.

In order to maximize the rate of load transfer into the heat pipe evaporator, attached heater blocks normally used to simulate the thermal mass of a heat source were removed and tape heaters were placed on the heat pipe saddle over a 30-cm long section of the pipe which was then properly insulated. Testing was done for both high (-18C) and low (-96C) sink temperatures with the heat pipe evaporator elevated 2.5 cm. Heat loads ranging from 100 to 150 watts were rapidly applied resulting in no heat pipe failures. The results indicated essentially no rate effect attributable to fluid inertia. This argued against the postulated "domino effect" failure of the whole VCHP system.

APPENDIX A.2.1

INSTANTANEOUS HEAT FLOW AFTER HEAT PIPE RESERVOIR ECLIPSE

TRW
DEFENSE AND SPACE SYSTEMS GROUP
ONE SPACE PARK • REDONDO BEACH • CALIFORNIA 90278

INTEROFFICE CORRESPONDENCE 8715.10-78-6

TO: E. E. Luedke CC: Distribution DATE: 18 October 1978

SUBJECT: Instantaneous Heat Flow After Heat Pipe Reservoir Eclipse

FROM: D. K. Edwards
BLDG 01 MAIL STA. 1230 EXT. 52850

INTRODUCTION

When a gas-controlled heat pipe's reservoir experiences an eclipse, the gas partial density within the reservoir rises, and the gas front retreats until the evaporator temperature drops sufficiently to establish a new equilibrium. During the transient, the evaporation from the warm end may exceed the capacity of the axial wicking, and arterial depriming may occur. It is desired to estimate the instantaneous heat flow during such a transient for comparison to the burnout heat flow capacity.

RESERVOIR COOLING RATE

The reservoir temperature versus time may be known from measurement. It is set by a heat balance between the surrounds and the thermal capacity. Let the mass of the reservoir be M and its specific heat c. Conductive coupling to the radiator is KA/L, and insulation is modelled with massless radiation shielding.

$$-m\,c\,\frac{dT}{dt} = A_R F\left[\sigma T^4 - \frac{\alpha}{\varepsilon}\,\bar{q}\right] - \frac{KA}{L}\left[T - T_c\right] \qquad (1)$$

Before eclipse $\bar{q}$ is high, and the quasi-equilitrium temperature is given by setting the left-hand side to zero. After $\bar{q}$ is reduced, T, cools at the rate given by Eq. (1).

FLOW VELOCITY INTO RESERVOIR

When a wicked reservoir of volume V cools at a rate of -dT/dt, the vapor partial pressure inside the reservoir falls. Since the total pressure is fixed at the evaporator end (neglecting vapor flow pressure drop), the partial pressure of the gas rises. Furthermore, the gas temperature falls (assuming thermal equilibrium). These two effects increase the gas partial density. The rate at which the partial density times the volume rises must come from the flow of gas from the heat pipe radiator into the reservoir.

$$\frac{d}{dt}\left(\rho_g V\right) = \rho_{gc}\, v\, A_c \qquad (2)$$

$$\rho_g = \frac{P - P_v(T)}{R_g T} \qquad (3)$$

Differentiating Eq.(3) gives

$$\frac{d\rho_g}{dt} = \frac{P-Pv}{R_g T}\,\frac{1}{T}\left(\frac{-dT}{dt}\right) + \frac{1}{R_g T}\,\frac{dPv}{dT}\left(\frac{-dT}{dt}\right) + \frac{1}{R_g T}\,\frac{dP}{dt}$$

Substituting into Eq.(2) then gives

$$v = \frac{V}{\rho_{gc} A_c}\left(\frac{1}{R_g T}\right)\left\{\left[\frac{P-Pv}{T} + \frac{dPv}{dT}\right]\left(-\frac{dT}{dt}\right) + \frac{dP}{dt}\right\} \qquad (4)$$

Let dPv/dT be approximated from the Clausius - Clapeyron equation

$$P_v = P_o e^{-(\Delta h/RT_o)\,(T_o/T-1)}$$

$$\frac{dP_v}{dT} = P_v\left(\frac{\Delta h}{RT^2}\right)$$

Then Eq.(4) becomes

$$v = \frac{V}{A_c} \left(\frac{Tc/T}{P-P_{vc}}\right) \left\{ \left[\frac{P}{T} + \frac{Pv}{T} \left(\frac{\Delta h}{RT} - 1\right)\right] \left(-\frac{dT}{dt}\right) + \frac{dP}{dt} \right\} \quad (5)$$

The total pressure P is the vapor pressure at the evaporator temperature T_v.

$$\frac{dP}{dt} = \frac{dPv}{dTv}\left(\frac{dTv}{dt}\right) = -\frac{dPv}{dTv}\left(-\frac{dTv}{dt}\right) \quad (6)$$

The evaporator temperature in turn is set by a heat balance upon it. The worst case occurs when the evaporator is well-coupled thermally to a large thermal mass. In this worst case dP/dt may fall only very slowly compared to the other terms. Measured data may be used to evaluate dTv/dt. A crude model is a one-capacity model.

$$M_{ev}C_{ev}\frac{dTv}{dt} = \dot{Q}_{elec.} - \dot{Q}_{elec.} - \dot{Q}_{hp} - A\mathcal{F}(\sigma T_v^4 - \sigma T_s^4) \quad (7)$$

The last term in the equation models heat leak to surrounds at temperature T_s

HEAT FLOW

The instantaneous heat flow through the pipe $\dot{Q}_{hp}$ is fixed by the length of active condenser and the rate of advancement of the gas front.

$$\dot{Q}_{hp} = \dot{Q}_{static} + \dot{Q}_{dynamic} \quad (8)$$

The static load is that caused by condensation on the gas-free condenser wall

$$\dot{Q}_{static} = \varepsilon P L_c n (\sigma T_v^4 - \frac{\alpha}{\varepsilon} q_c^-) \quad (9)$$

where the length L_c is fixed by a gas inventory m_g

$$m_g = \rho_g V + \rho_{gc} A_c (L - L_c) \qquad (10)$$

The dynamic load is proportional to the velocity v at which the front advances

$$\dot{Q}_{dynamic} = \rho_f c_f A_f v \eta (T_v - T_c) \qquad (11)$$

where ρ_f is the condenser fin density, c_f its specific heat, A_f its area (volume per unit length), and η is not the radiating fin effectiveness, because of the fourth power dependence of the black body radiosity. The appropriate value of η is between the radiating fin effectiveness and the fourth root of that value, depending upon the ratio of $(T_c/T_v)^4$.

EXAMPLE

For example consider the CTS heat pipe 1 on Day 75. The following data are available

Time	Vapor Temp.	Gas-Blocked Temp.	Gas Reservoir Temp.
t	T_v	T_c	T
min	°C	°C	°C
460	27.5	-93	-68
470	28	-94	-71
480	29	-95.5	-74

From these data one can estimate $-dT/dt = 18$ K/hr and $dT_v/dt = 4.5$K/hr. The following vapor pressure data pertain

	Temperature	Pressure	Latent Heat
	K	N/m^2	J/k_g
Tv	300	19500	1.15×10^6
T	205	~13	1.2×10^6
T_c	180	~1.5	1.2×10^6

For a 90% N_2 10% He mixture the mean molecular weight is 25.6 and Rg = 8314.3/25.6 = 325 J/kg K. The density of the gas in the gas-blocked condenser is

$$\rho_{gc} = \frac{P_{gc}}{RT} = \frac{19500}{(325)(180)} = 0.333 \text{ kg/m}^3$$

Other parameters needed are

$$\left.\frac{\Delta h}{RT}\right|_{T = 205} = \frac{1.2 \times 10^6}{(206)\ (205)} = 22.51$$

$$\left.\frac{\Delta h}{RT}\right|_{T = 300} = \frac{1.15 \times 10^6}{(260)\ (300)} = 14.74$$

The pertinent parameters of the pipe itself are understood to be as follows:

Reservoir Volume	V	8.70 $inch^3$	1.426×10^{-4}	m^3
Pipe Vapor Area	A_c	0.1245 in^2	8.03×10^{-5}	m^2

Equation (5) then gives

$$v = \frac{1.426 \times 10^{-4}}{8.03 \times 10^{-5}} \quad \frac{(180/205)}{19500 - 1.5} \left\{ \left[\frac{19500}{205} + \frac{13}{205} (22.5 - 1) \right] (18) \right.$$

$$\left. + \frac{19500}{300} (14.74) (4.5) \right\}$$

$$v = (1.78) (4.50 \times 10^{-5}) \left\{ [95.1 + 1.36] (18) + (958) (4.5) \right\}$$

$$v = 8 \times 10^{-5} \left\{ 1736 + 4311 \right\} = 0.484 \text{ m/hr} = 1.59 \text{ feet/hr}$$

Note that, in this example, the fall of the vapor pressure in the reservoir was a negligible consideration but the rise of vapor pressure in the evaporator was quite significant.

For purposes of an estimate ηA_F is taken to be 0.04 inches by 12 inches. Thus Equation (11) gives

$$\dot{Q}_{dynamic} = (174) (0.21) (.04/12) (12/12) (1.59) (300 - 180) (1.8)$$

$$\dot{Q}_{dynamic} = 41.8 \frac{BTU}{hr} = 12.25 \text{ Watts}$$

DISCUSSION

While a rapid decrease in reservoir temperature has the potential of adding a significant dynamic heat flow to the static load, the example worked here indicates that the decrease must be rapid, much greater than the 18K/hr value used in the example.

APPENDIX A.2.2

INSTANTANEOUS HEAT FLOW AFTER HEAT PIPE RADIATOR ECLIPSE

TRW
SYSTEMS GROUP
ONE SPACE PARK • REDONDO BEACH • CALIFORNIA 90278

INTEROFFICE CORRESPONDENCE 8715.10.2-78-9

TO E. E. Luedke

CC: D. Antoniuk
J. E. Eninger
B. D. Marcus
D. J. Wanous

DATE: 28 November 1978

SUBJECT: Instantaneous Heat Flow After Heat Pipe Radiator Eclipse

FROM: D. K. Edwards
BLDG 01 MAIL STA. 1230 EXT. 52850

Introduction

When a gas-controlled heat pipe's radiator experiences an eclipse, the heat flow in the pipe increases until the evaporator cools to a new equilibrium operating condition. During the transient, the evaporation from the warm end may exceed the capacity of the axial wicking, and arterial depriming may occur. It is desired to estimate the instantaneous heat flow during this transient for comparison to the burnout heat flow capacity. This memo is a companion to one that explored the instantaneous heat flow after heat pipe reservoir eclipse.

A Simplified Thermal Model.

To explore the magnitude of the expected effect and to show the effect of the major parameters, a simplified model is proposed. In this model the heat loss out of the radiator is taken to be

$$\dot{Q}_r = F_{scr} WL(\sigma T_v^4 - \sigma T_e^4)\, e_f \qquad (1)$$

where F_{scr} is the so-called script - F radiant transfer factor (equal to emissivity for an isolated radiator) W is the width or perimeter of the panel per pipe (including both sides if both sides radiate), L is the active length of the vapor in the radiator, T_v is the vapor temperature, T_e is the environmental temperature

$$T_e = \left[\frac{\alpha \bar{q}}{F_{scr}\sigma} \right]^{1/4} \qquad (2)$$

and e_f is the fin efficiency. The vapor filled length is assumed to be given by

$$L = L_{tot} \frac{T_v - T_o}{\Delta T} \qquad (3)$$

where L_{tot} is the total length, T_o is the turn-on point, and ΔT is the control

band width. Equation (1) may be factored into the form

$$\dot{Q} = e_f F_{scr} WL\sigma (T_v^2 + T_e^2)(T_v + T_e)(T_v - T_e)$$

and Eq. (3) may be introduced to write

$$\dot{Q} = \frac{1}{R_r} \left(\frac{T_v - T_o}{\Delta T} \right) (T_v - T_e) \tag{4}$$

where

$$R_r = \frac{1}{e_f F_{scr} WL_{tot} \sigma (T_v^2 + T_e^2)(T_v + T_e)} \tag{5}$$

This latter parameter is insensitive to mild excursions in T_v and T_e since the absolute temperatures appear. In contrast Eq. (4) varies rapidly with T_v, because $(T_v - T_o)$ and $(T_v - T_e)$ change significantly when T_v changes, particularly the former quantity, and $(T_v - T_e)$ changes when T_e changes.

Note that this simplified model neglects the thermal capacity of the radiator on the grounds that it is small compared to that of the heat source. This neglect leads to an overprediction of thermal shock on the heat pipe from sudden changes in environmental temperature T_e.

The heat source is modelled as a single lumped capacity of mass m and specific heat c.

$$mc \frac{dT_h}{dt} = Q_e - \frac{1}{R_e} (T_h - T_v) \tag{6}$$

where T_H is the heat source temperature, Q_e is the net electrical power dissipation, and R_e is the thermal resistance into the heat pipe evaporator. It is the heat flow into the evaporator that concerns us

$$\dot{Q} = \frac{1}{R_e} (T_h - T_v) \tag{7}$$

The heat source thermal capacity mc is assumed to be sufficiently large

that T_h remains constant during the time that the radiator and gas front readjust. In this respect the heat transfer through the heat pipe is assumed quasi-steady.

Analysis Based Upon the Simplified Model

The model in its bare essentials consists only of Eqs.(4) and (7). The heat pipe behavior is determined by the evaporator resistance R_e, the radiator resistance R_r, the turn-on point T_o, and the control band width ΔT. The parameters R_e and R_r may be inferred from observed termperatures at, say, the full-on operating point. Equation (4) shows that

$$R_r = \frac{T_{v,full} - T_e}{Q_{full}} = \frac{T_o - T_e + \Delta T}{Q_{full}} \tag{8}$$

and from Eq.(7)

$$R_e = \frac{T_{h,full} - T_{v,full}}{Q_{full}} \tag{9}$$

Hence

$$\frac{R_e}{R_r} = \frac{T_{h,full} - T_{v,full}}{T_{v,full} - T_e} = r \tag{10}$$

Equating Eqs. (4) and (7) and rearranging gives

$$\Delta T(T_h - T_v) = r(T_v - T_o)(T_v - T_e)$$

This quadratic equation may be solved for T_v, and the result put into Eq.(7). Equations (8) and (9) are also introduced for convenience

$$\dot{Q} = \dot{Q}_{full} \frac{\Delta T_o + \Delta T/r - \sqrt{(T_o - T_e)^2 + 2\,(\Delta T/r)\,\Delta T_o + (\Delta T/r)^2}}{2r(T_o - T_e + \Delta T)} \tag{11}$$

where, to shorten notation,

$$\Delta T_o = 2(T_h - T_e) - (T_o - T_e) \qquad (12)$$

Note that in the form of Eq.(11) neither R_e nor R_r appear explicitly, but only their ratio r.

Sample Parametric Calculations

To show the importance of the parameter r we show three sample calculations, one with r=1, one with r=¼, and another r=1/8. We choose the following nominal values:

$T_o = 20^oC$ $\qquad$ $T_{e,max} = -20^oC$

$\Delta T = 5^oC$ $\qquad$ $T_{e,min} = -110^oC$

$T_h = 30^oC$ $\qquad$ $r = 1, \frac{1}{4}, 1/8$

In order to keep the same nominal value of R_r as T_e is changed, one multiplies by the ratio of $(T_o - T_e + \Delta T)/(T_o - T_e + \Delta T)_{nom.}$ The following results are obtained:

TABLE 1
EFFECT OF EVAPORATOR-TO-RADIATOR RESISTANCE RATIO
ON HEAT PIPE OVERLOAD UPON RADIATOR ECLIPSE

r	T_e °C	$[Q/Q_{Full}][(T_o - T_e + \Delta T)/(T_o - T_e + \Delta T)_{nom}]$	
1	-20	[0.1981][45/45] = 0.1981	8%
	-110	[0.0713][135/45] = 0.2140	
0.25	-20	[0.6074][45/45] = 0.6074	28%
	-110	[0.2571][135/45] = 0.7714	
0.125	-20	[0.9384][45/45] = 0.9384	45%
	-110	[0.4550][135/45] = 1.3651	

Nonlinear Effect

In the preceeding the effect of radiator eclipse was explored in the linearized limit. When the sink temperature changes greatly, the heat flow is affected by the nonlinear variation of T^4 in the radiation terms. A numerical calculation is easily made despite the nonlinearity.

We had

$$\dot{Q} = F_{SCR}\, e_f\, WL_{tot}\, \frac{T_v - T_o}{\Delta T}\, (\sigma T_v^4 - \sigma T_e^3) \tag{13}$$

and

$$Q = \frac{1}{K_e}\, (T_h - T_v) \tag{14}$$

with

$$r = R_e\, F_{SCR}\, e_f\, WL_{tot}\, \sigma (T_v^2 + T_e^2)(T_v + T_e) \tag{15}$$

Equating (13) and (14) and introducing (15) gives

$$(T_h - T_v) = r\, \frac{T_v - T_o}{\Delta T}\, \frac{T_v^4 - T_e^4}{(T_{v,1}^2 + T_{e,1}^2)(T_{v,1} + T_{e,1})} \tag{16}$$

Equation (15) is understood to apply to both the original condition before eclipse when $T_v = T_{v,1}$ and $T_e = T_{e,1}$ and to the conditions after eclipse when T_v and T_e are colder.

Given the value of T_h, the original sink condition $T_{e,1}$, the turn-on point T_o, the band width ΔT, and the value of r based upon the original conditions, Eq. (16) is used to find $T_{v,1}$ and $\dot{Q}_1$ from Eq. (14). Then when $T_{e,1}$ goes to $T_{e,2}$, the equation is used again to find $T_{v,2}$, and $\dot{Q}_2$ is found from Eq. (14).

Consider the example used before:

$T_o = 20^oC$ $T_{e,1} = -20^oC$ $\Delta T = 5^oC$ $T_h = 30^oC$

$r = 1/4$, $T_{e,2} = -110^oC$

In the linearized limit we obtained $\dot{Q}_2/\dot{Q}_1 = 1.28$. Allowing for the non-linearity gives the following values:

Condition 1, By Binary Search

T_v ^oC	LHS ^oK	RHS ^oC
30	0	25
20	10	0
25	5	11.25
22.5	7.5	5.31
23.75	6.25	8.20
23.125	6.875	6.738
23.4375	6.5625	7.4658
23.2813	6.7188	7.1008
23.2031	6.7969	6.9193
23.1641	6.8359	6.8287
23.1836	6.8164	6.8739
23.1738	6.8262	6.8513
23,1690	6.8310	6.8401
23.1665	6.8335	6.8344

Condition 2, By Binary Search

T_v ^oC	LHS	RHS
30	0	46.35
20	10	0.00
25	5	21.55
22.5	7.5	10.38
21.25	8.75	5.095
21.875	8.125	7.714
22.1875	7.8125	9.0422
22.0313	7.9688	8.3767
21.9532	8.0469	8.0455

Ratio of $\dot{Q}_2/\dot{Q}_1 = 8.046/6.834 = 1.18$

This ratio differs appreciably from unity, but somewhat less so than the value obtained with the linearized equation.

Conclusion.

The importance of the ratio of the thermal resistance between the equipment and the evaporator to the thermal resistance between the radiator and the evironment is illustrated. When the ratio is large (near one), the transient load is only a few percent of the base load. When the ratio is small, the transient load is a significant fraction of the base load.

APPENDIX A.2.3
CONDENSER AND/OR RESERVOIR SHADOWING TESTS ON SN009 HEAT PIPE

SN009 heat pipe tests were directed toward examining two potential artery depriming modes: 1) rapid chilldown of the condenser, and 2) rapid chilldown of the reservoir. A large evaporator mass was a requisite contributor during these hypothesized depriming modes and, accordingly, four kilograms of aluminum were attached to the SN009 evaporator.

Two series of rapid condenser chilldown tests were run. In the first, the heat in the condenser sink was cooled to -73C (-100F), while the condenser was heated to maintain -18C (0F). The sink and condenser were coupled through 0.30 centimeters of cork over a 162 in^2 (0.1045 m^2) area. With the heat pipe operating at 100 watts (well above open artery capacity), the condenser heater was turned off allowing the condenser temperature to fall approximately 2.8C/min (5F/min). When no depriming occurred, the tests were repeated with 100 and 150 watts. Depriming at 160 watts under steady state was verified. Thus, cooling the condenser at approximately 2.8C/min (5F/min) produced no depriming.

In the second series, the sink was -129C (-200F). When the condenser heater was turned off, a cooling rate of approximately 3.9C/min (7F/min) was achieved. When no depriming occurred, the test was repeated with 125 watts, and again no depriming was observed. However, when an attempt was made to raise the power level to 150 watts, depriming occurred (at the steady condenser temperature of -18C (0F). The pipe was reprimed, held 100 watts, but failed to retain prime at 125 watts. A third attempt resulted in failure to reprime. It is thought that ice-generated bubbles may have been formed in the earlier transient cooling tests, and these bubbles caused the repeated deprimings. Depriming due to rapid chilldown of the condenser was not demonstrated.

Rapid chilldown of the reservoir was achieved by blowing vapors from boiling liquid nitrogen through a cooling coil block attached to the reservoir. With 100 watts power at the evaporator and the condenser at -18C (0F), the reservoir was cooled repeatedly at successively higher

rates. Depriming did occur at a rate of -3.2C/min (-5.6F/min). Depriming did not occur at rates of -0.8, -1.2, -1.6 and -2.5C/min (-1.5, -2.1, -2.8 and -4.5F/min, respectively).

Although depriming due to reservoir chilldown was demonstrated, the rates required were substantially higher than those indicated by flight data. This argues against reservoir and/or condenser shadowing as the cause of the CTS anomalies.

APPENDIX A.3
FREEZING BLOWBY TESTS ON SN009 HEAT PIPE

Freezing blow-by was hypothesized as a possible depriming mechanism. This requires the formation of an incompletely frozen slug bridging the vapor core during a transient in which the pressure on the evaporator side of the slug is increasing with respect to the reservoir side. The resulting pressure difference across the slug can blow liquid from the evaporator to the reservoir side and deplete the evaporator inventory.

To explore this mechanism, it was first necessary to determine how to perform a meaningful 1-g test in the absence of the natural slugging of excess liquid which occurs in 0-g. A successful technique to form an ice plug in heat pipe SN009 was developed. The procedure is as follows:

a) Instrument the heat pipe with temperature sensors along its length to enable monitoring the location of the gas front.

b) Apply sufficient power to turn the heat pipe on i.e., to move gas front into the condenser section. Maintain the sink temperature a few degrees above the methanol freezing point.

c) Midway along the inactive portion of the condenser, locally code a short (~2.5 cm) section of the pipe to subfreezing temperatures. Periodically raise the reservoir-end of pipe to force excess liquid to pass over the frozen pipe section in order to enhance ice build-up.

d) Apply periodically, a power pulse to gas reservoir to induce a transient temperature/pressure increase in the reservoir while monitoring the temperature profile about the location of the gas front. Formations of all ice plug will decouple the reservoir from the evaporator side of the heat pipe. The presence of an ice barrier blocking the arteries and vapor spaces can then be determined from the temperature profile along the evaporator side of the plug which should not respond to an induced temperature change in the gas reservoir.

Experiments were then directed toward investigating the hypothesized freezing blow-by depriming mechanism. The SN009 heat pipe test was modified such that a small, independently chilled, ice plug heat sink was attached

to the condenser midway along its length. The basic test approach was as follows:

a) The ice plug heat sink was employed to generate a solid plug midway along the condenser.

b) The evaporator power was raised to a value in excess of the open artery heat pipe capacity, raising the temperature and pressure on the upstream side of the ice plug.

c) The ice plug was thawed, allowing the pressure differential to relieve itself by blowing liquid and gas through the thawed region.

If there is liquid communication between the region to thaw first and the arteries, the above sequence of events was hypothesized to lead to depriming of the arteries by pumping them dry. The experiment was run so that this liquid communication condition existed and, in fact, the arteries did deprime. The experiment was run three times, always with the same result. Thus, it has been clearly established that freezing blow-by is a bonafide depriming mechanism and a candidate to explain at least some of the observed anomalies.

To enable modelling the blow-by mechanism, the variable conductance heat pipe subroutine was expanded to include the effects of an ice plug forming in the condenser section of the heat pipe and open or deprimed artery performance. Such a plug decouples the reservoir from the active portion of the heat pipe and alters its control characteristics. It also provides the basis for the freezing blow-by depriming hypothesis; i.e., a pressure difference is established across the ice plug which blows the liquid through as the plug begins to thaw resulting in artery depriming which causes the heat pipe to continue operating with reduced or open artery capacity.

In Appendix A.4.2 a transient thermal analysis of a simple VCHP/ radiator system model is described which shows the effects of an ice plug formed in the heat pipe condenser and subsequent blow-by depriming of the arteries on the performance of the sample VCHP system.

APPENDIX A.4.1
BRIEF REVIEW OF LeRC THERMAL STUDIES

In support of Contract NAS3-21740 (Study of Liquid Dynamics in CTS-Type Heat Pipes), NASA LeRC performed thermal analyses on a 'lump' parameter thermal model of the Transmitter Experiment Package. These efforts were conducted by Louis Gedeon of LeRC and are described in two NASA documents entitled "Comparison of Predicted Versus Measured Temperatures for CTS Thermal Anomalies," dated October 1, 1979, and "Modifications to CTS Thermal Model for TRW Contract NAS3-21740," dated January 9, 1980. A review of this analytical task is presented in the sequel.

The CTS model includes the VCHP system, the traveling wave tube, a power processing system baseplate, the spacecraft forward and part of the south panels, the antenna covers and skirts, and the solar array pallet. TRW's Systems Improved Numerical Differential Analyzer (SINDA) computer program and a Variable Conductance Heat Pipe model subroutine (VCHP2) were utilized to solve the CTS model.

During the first transient calculations with a modified VCHP system model, it was found that the heat pipe model subroutine (VCHP2) was not suitable for transient calculations. An analysis at TRW of the solution algorithm in VCHP2 revealed that the solution scheme, in view of the nonlinear nature of the model, was inadequate since it was susceptible to becoming numerically unstable. As a result of this analysis, a new solution method was formulated which proved to be successful in circumventing numerical instabilities.

This solution approach was incorporated into a new version of the variable conductance heat pipe model subroutine renamed VCHPDA. In addition, two new features were introduced into this version which permit simulating the effects of an ice plug formation in the heat pipes and open or deprimed heat pipe capacity on the performance of the whole VCHP system. The description of the ice plug and open artery analytical models and the solution scheme, as well as, a listing of VCHPDA written in FORTRAN IV computer language are presented in Appendix A.4.2.

Subsequent transient runs of the CTS model using the new subroutine VCHPDA were normal, except that the predicted temperatures were lower than flight temperature data. In order to improve the temperature predictions, additional modifications of input parameters were introduced into the CTS model. Among the changes made were:

1) The solar absorptance and total hemispherical emissivity on the VCHP system radiator were increased and decreased respectively.

2) The reflected sun heat load on the VCHPs radiator was assumed diffuse and was multiplied by a factor varying with time.

3) The south panel emissivity was increased.

4) Numerous view factors and shadowing parameters were modified.

Although some of the above changes are deemed somewhat physically unrealistic, they resulted in general, in temperature predictions remarkably close to flight data. Transient runs were made for normal day 89 and for periods preceeding and including the anomaly of days 75, 82, 101, and 253. The initial conditions were those obtained from steady state calculations using the conditions prevailing prior to the start of a spacecraft eclipse.

For each anomaly day a minimum of two transient runs were made, one assuming normal heat pipe operation prior and during the period of the anomaly, with considerations for ice plug formation, the other run assuming open artery capacity conditions prior and during the anomaly. Additional calculations were made for day 75 and day 253. For day 75, lower open artery capacity values were assumed, and for day 253 a third run was performed in which normal heat pipe operation was assumed from eclipse until the observed time of the anomaly at which time the heat pipes were set for open artery or deprimed capacity operation.

Some significant results from these transient analyses were:

1) On day 253 freezing was not predicted at the time of the anomaly.

2) The maximum calculated heat pipe loads never exceeded 80 watts.

3) The coldest calculated temperature for heat pipe number 1 always occurred near the reservoir end of the condenser where temperature sensor HPT5 is located (see Figure 1-3 in text). Temperatures for heat pipes HP2 and HP3 at similar condenser locations were predicted to be a few degrees colder.

4) Formation of ice plugs in the three heat pipes were calculated on day 82 prior to the anomaly.

5) The profile of the tube body temperature excursion is closely matched on day 253 when the heat pipes were set from normal to open artery capacity operation at the observed time of the anomaly.

APPENDIX A.4.2

GENERALIZED VARIABLE CONDUCTANCE HEAT PIPE MODELING

This appendix presents analytical models, sample problem solution, and listing of subroutine VCHPDA.

TRW
DEFENSE AND SPACE SYSTEMS GROUP
ONE SPACE PARK • REDONDO BEACH • CALIFORNIA 90278

INTEROFFICE CORRESPONDENCE 3715.10.1-79-03

TO: Bruce Marcus

CC: J. T. Bevans
D. K. Edwards
J. E. Eninger
E. E. Luedke

DATE: 6/11/79

SUBJECT: Generalized Variable Conductance Heat Pipe Modeling

FROM: David Antoniuk

BLDG	MAIL STA.	EXT.
01	1230	52850

As the result of efforts carried out under the 1973 IR&D Advanced Thermal Control program, a method to analytically simulate a gas loaded, variable conductance heat pipe (VCHP) was developed and is documented in Reference 1.

A FORTRAN IV computer code was implemented to numerically solve the analytical model. This code which is suitable to interface with general thermal models involving heat pipes, has been used successfully in steady state thermal simulation of systems, e.g., the transmitter experiment package (TEP) variable conductance heat pipe system (VCHP) in the Canadian Technology Satellite (CTS). Subsequent attempts, however, to utilize the VCHP2 subroutine for transient thermal analyses yielded unsuccessful results due to numerical instabilities arising during the gas-vapor front location/vapor temperature calculations.

Recently, as part of the efforts to investigate the thermal anomalies in the CTS spacecraft, the solution scheme in VCHP2 was analyzed in order to uncover the source of the numerical problems. The analysis revealed that the iterative approach of the subroutine to obtain a converged solution starting from an initial guessed gas length/vapor temperature, was inadequate in view of the non-linear natureof the model.

As the result of this analysis, a new analytical method was formulated which under most physically realizable operating modes, unconditionally circumvents numerical instabilities.

In addition, two new features were introduced into the VCHP model which permits simulating the effects of an ice plug formation and open artery capacity on the performance of a VCHP system. The appropriate FORTRAN IV logic to solve the analytical model was incorporated into a revised version of the VCHP2 subroutine, now identified as VCHPDA. A logic flow chart and listing of the computer program are attached.

Basic Analysical Model:

Referring to the configuration of a typical, wicked-reservoir, VCHP in Figure 1, and invoking the ideal gas law and the "flat front" gas theory, the cumulative distribution of the number of moles of non-condensible gas along the length of a VCHP can be written as:

$$Ng(z) = (P_T(z) - P_{v,R}) \frac{V_R}{R \cdot T_R} + \int_0^z \frac{P_T(z) - P_v(z)}{R \cdot T(z)} A(z)\, dz \qquad (1)$$

for $z \leq Lg$

where

Lg - location of gas-vapor front or "gas length"

V_R - reservoir volume

T_R and $T(z)$ - temperatures at vapor-liquid interface in reservoir and along pipe, respectively.

R - universal gas constant

$A(z)$ - gas/vapor space cross sectional area

$P_{v,R}$ and $P_v(z)$ - partial vapor pressure of working fluid at T_R and T respectively.

$P_T(z)$ - total pressure in the VCHP defined in Eq. (2).

$$P_T(z) = P_v(T_v(z)) \qquad (2)$$

where $T_v(z)$ is the vapor temperature in the active section of the pipe.

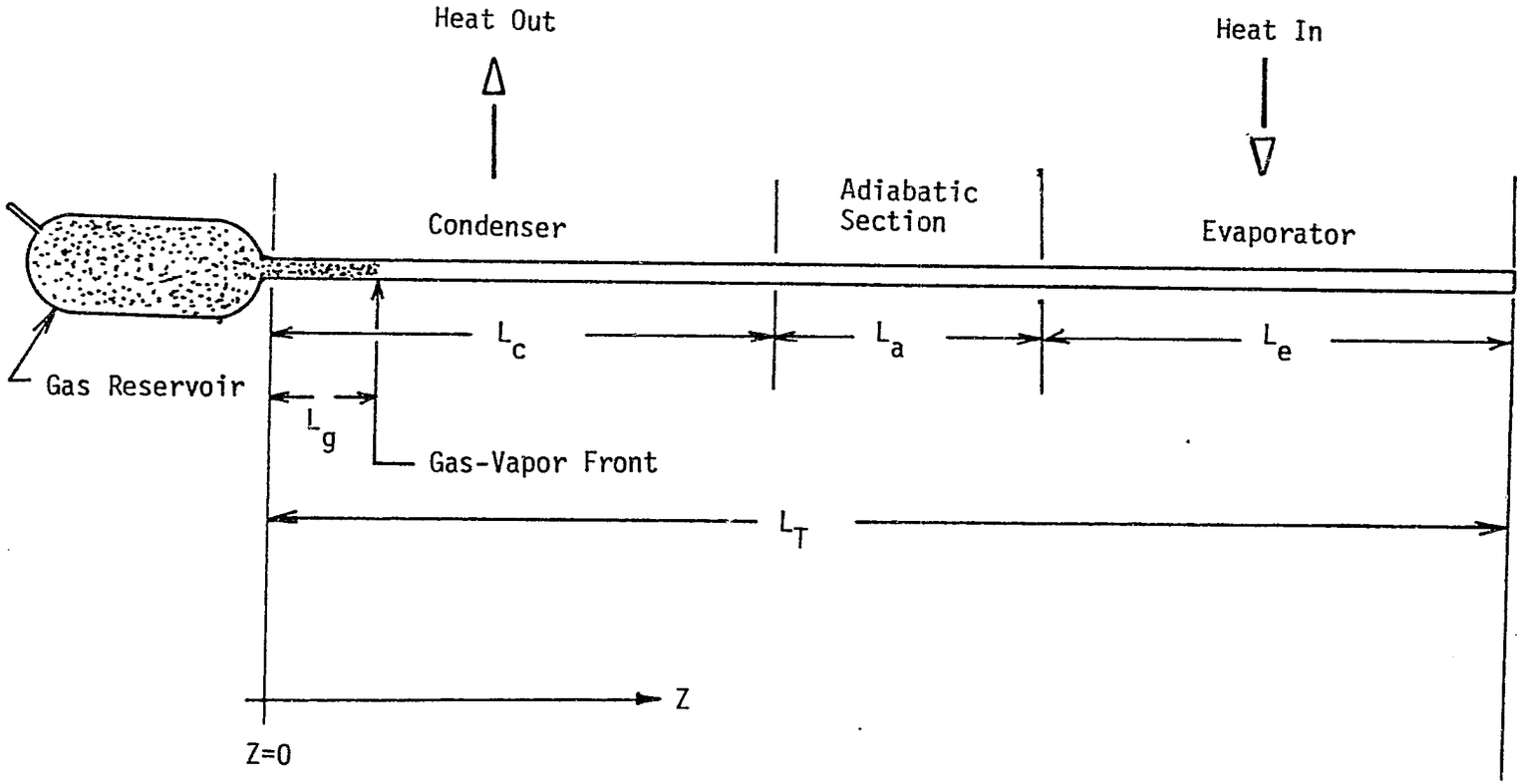

Figure 1. Configuration of Typical VCHP

$$T_v(z) = \int_z^{L_T} h(z')\, T(z')\, P(z')\, dz' \Big/ \int_z^{L_T} h(z')\, P(z')\, dz' \quad (3)$$

where h(z) is the local heat transfer coefficient and $P(z)$, the wetted perimeter. Equations 1, 2 and 3 form a complete non-linear coupled set of equations which enable the calculation of the length of the gas-blocked region and the vapor temperature in the active portion given the temperature distribution along the wall of a VCHP whose configuration conforms to the one sketched in Figure 1.

Solution Scheme:

In order to illustrate the solution procedure incorporated into the current version of subroutine VCHPDA, it is convenient to rearrange Equation (1) as follows:

$$Ng(z) = P_T(z)\, F(z) - N_v(z) \quad (4)$$

where

$$F(z) = \frac{V_R}{R \cdot T_R} + \int_0^z \frac{A(z')}{R \cdot T(z')} \cdot dz' \quad (5)$$

$$Nv(z) = \frac{P_{v,R} \cdot V_R}{R \cdot T_R} + \int_0^z \frac{P_v(z') \cdot A(z')}{R \cdot T(z')} \cdot dz' \quad (6)$$

Resorting to a numerical method to evaluate the integrals F(z), Nv(z) and $P_T(z)$ are calculated stepping out from the reservoir in Δz increments. At each step, Ng(z) is evaluated and compared to the total gas inventory, N_T. The above procedure is continued until $Ng(z) \geq N_T$ at which point a quadratic binary search scheme is applied to find the root of the transcendental equation

$$Ng(z) - N_T = 0 \tag{7}$$

which is satisfied when z = Lg.

To initiate this iterative process, a gas length is approximated by linear interpolation, i.e.,

$$Lg = z + \frac{Ng(z+\Delta z) - N_T}{Ng(z+\Delta z) - Ng(z)} \cdot \Delta z$$

The search is terminated when a prescribed convergence criterion is met, which in the current VCHPDA version is defaulted to

$$\left| \frac{Ng(z) - N_T}{N_T} \right| \leq 10^{-4}$$

Solution to Equation (7) allows the performance of the partially gas-blocked VCHP to be quantified.

The thermal conductance between the vapor and the pipe walls, G(z), can be calculated,

$$G(z) = U(z-Lg)\ h(z)\ P(z) \tag{8}$$

where U is a Heavyside-type function defined as

$$U = \begin{cases} 0.0 & \text{for } (z-Lg) < 0.0 \\ 1.0 & \text{for } (z-Lg) \geq 0.0 \end{cases}$$

and the heat load on the VCHP

$$Q = \left| \int_{Lg}^{L_T} G(z') \cdot (T_v(Lg) - T(z')) \cdot H(T_v(Lg) - T(z')) \cdot dz' \right| \tag{9}$$

where H is similarly defined as

$$H = \begin{cases} 0.0 & \text{for } \{ T_v(Lg) - T(z) \} < 0.0 \\ 1.0 & \text{for } \{ T_v(Lg) - T(z) \} \geq 0.0 \end{cases}$$

The heat load on the heat pipe in terms of power-length can readily be calculated

$$QL = Q \cdot L_{eff} \tag{10}$$

where

$$L_{eff} = \frac{(L_c - Lg)}{2} + L_a + \frac{L_e}{2} \tag{11}$$

The above solution scheme holds provided the VCHP is under load. In the event that $Ng(z) < N_T$ for $z \geq L_T$, the gas length $Lg = L_T$ and the total pressure in the VCHP is calculated by either Equation (1) or (4). Using the latter Equation, the pressure P_T is given by

$$P_T = \left\{ N'_T - N_V(L_T) \right\} / F(L_T) \tag{12}$$

Ice Plug Modelling

Owing to excess fluid inventory, usually present in a VCHP, operation of the heat pipe under subfreezing sink condictions can result in the formation of an ice barrier in the condenser section effectively decoupling the active portion of the pipe from the gas reservoir. Formation of such an "ice plug" can have a significant effect on the performance characteristics of a VCHP. Furthermore, it can, under certain operating conditions, lead to depriming of the arteries by what is referred to as the "freezing blow-by" mechanism. In order to enable to simulate the consequences of such an event, the ice plug model has been developed and is incorporated as an optional operating VCHP mode in subroutine.

It is assumed that in zero-gravity the bulk of the excess fluid resides as a liquid mass in the gas reservoir and as a slug blocking the vapor spaces in the pipe section at and near the coupling between pipe and reservoir. During a transient

analysis, formation of an ice plug in the condenser is subject to the following constraints: a) the gas reservoir temperature must be above freezing conditions, b) the history of the VCHP must show a net decrease of the gas inventory in the reservoir, i.e., gas front and, presumably liquid slug, movement toward the evaporator, and c) subfreezing temperatures at some point along the condenser and/or adiabatic sections.

These conditions for ice plug formation can be stated mathematically,

$$T_R > T_{F.P.} \quad \text{(Freezing temperature of working fluid)} \tag{14}$$

$$\partial Ng_R/\partial t < 0 \tag{15}$$

$$T(z) < T_{F.P.} \tag{16}$$

Provided conditions given by Equations (14) and (15) are met, the solution procedure subsequently involves stepping out from the reservoir end of the pipe in Δz increments in the search of subfreezing temperatures. The point at which conditions, Equation (16), is first satisfied establishes the location of the ice plug which is currently modelled as a barrier of negligible thickness. The location of the ice plug, L_p, is defined by

$$L_p = z \text{ where } T(z) \leq T_{F.P.} \text{ and } T(z-dz) > T_{F.P.} \tag{17}$$

Concurrent calculation of the cummulative gas inventory up to $z = L_p$ (Equation (1)) enables to determine the distribution of the gas on the reservoir and evaporator side of the ice plug which respectively are:

$$Ng_R = Ng(L_p) \tag{18}$$

$$Ng_E = N_T - Ng_R \tag{19}$$

These parameters are stored and used at subsequent times to analyze the characteristics of the two decoupled regions in the VCHP. The solution procedure is then as follows:

I. Calculate total pressure on reservoir side of the plug using Equation (12)

$$P_{T,R} = \left\{ Ng_R - Nv(L_p) \right\} / F(L_p) \qquad (20)$$

II. Perform analysis on the evaporator side of the ice plug resorting to Equations (1) through (12) and appropriately changing the limits of integration and reservoir volume in order to account for the decoupling of the two regions, i.e., set $V_R = 0$ and evaluate the integrals from L_p to $z \leq L_T$.

In addition, calculation of the effective length by Equation (11) requires the condenser length, L_c, be reduced by L_p.

$$L'_c = L_c - L_p \qquad (21)$$

The above procedure yields an estimate of a significant new parameter: the pressure differential across the ice plug, which can result in depriming of an arterial VCHP when liquid contact is established between the two regions.

Open-Artery Capacity Modelling

If a mechanism such as the one described above leads to depriming of an arterial VCHP, the designed capacity of the heat pipe will deminish to what is usually referred to as "open-artery" capacity. In such an operating mode, capillary pumping pressure is substantially reduced and continuous operation of a VCHP at high loads after depriming will generally result in partial evaporator dry-out.

In order to simulate the performance of a VCHP with

open-artery capacity, a model was developed and is currently incorporated in subroutine VCHPDA as an operational operating mode. To exercise this option, a new constraint is introduced into the overall VCHP model. The power-length capacity of the heat pipe, defined in Equation (10), cannot now exceed a prescribed capacity $(QL)_1$, i.e.,

$$QL(z) \leq (QL)_o \tag{22}$$

The effective length, L_{eff}, is calculated by

$$L_{eff} = \frac{L'_c}{2} + L_a + L'_e \tag{23}$$

where, L'_e, is the evaporator length reduced by the length of the dry section of the pipe, L_d.

$$L'_e = L_e - L_d \tag{24}$$

$$L_d = L_T - L_w \tag{25}$$

where, L_w, is the length of the wet portion of the pipe measured from the reservoir end.

Rearranging Equation (22) as

$$QL(z) - (QL)_o = 0.0 \tag{26}$$

the solution procedure involves finding the root of the above Equation which establishes the length of the wet section of the pipe and hence, the dry portion of the evaporator.

The general procedure which requires a double-iterative scheme is as follows:

I. Initialize $L_w = L_T$ (i.e., $L_d = 0.0$) and $Lg = L_T$

II. Calculate gas length, Lg, and vapor temperature, T_v, such that Equation (7) is satisfied

III. Calculate QL(z) for z = L_w and check whether constraint (Equation (22)) is met. If the cneck is positive, the solution to the model has been attained and the procedure is terminated; otherwise, perform step IV.

IV. Holding Lg fixed, and stepping out from the evaporator end of the pipe in ($-\Delta z$) increments, recalculate the vapor temperature using

$$T_v(z) = \int_{Lg}^{z} h(z')\, T(z')\, P(z')\, dz' \Big/ \int_{Lg}^{z} h(z')\, P(z')\, dz' \qquad (27)$$

and subsequently calculate QL(z).

Repeat steps III and IV until $QL(z) \leq (QL)_o$ at which point a quadratic binary search is performed to find the root of Equation (26). To initiate the iterative process, the wet length, L_w, is approximated by linear interpolations as follows:

$$L_w = z + \left\{ \frac{(QL)_o - QL(z)}{QL(z+\Delta z) - QL(z)} \right\} \cdot \Delta z \qquad (28)$$

The search is terminated when a prescribed convergence criterion is satisfied which is defaulted in VCHPDA to

$$\left| \frac{QL(z) - (QL)_o}{(QL)_o} \right| \leq 10^{-4}$$

With the wet length, L_w = z, held fixed a new gas length and vapor temperature are calculated confining the calculations to the wet section of the pipe. Steps II through IV are repeated until

$$\left| \frac{W^{k+1} - W^k}{W^{K+1}} \right| \leq 10^{-4}$$

where W^k is either the gas length, Lg, or wet length, L_w, and superscript 'k' is the iteration number.

Having established the domain of the active section of tne pipe, i.e., $Lg \leq z \leq L_w$, the local thermal conductance, G(z), between the vapor and adjacent pipe walls can now be redefined to reflect the reduction of effective heat transfer area resulting from gas blockage and wall dry-out.

$$G(z) = H(z)\ h(z)\ P(z) \tag{29}$$

where H(z) is defined as

$$H = \begin{cases} 0.0 & \text{for } (z-Lg) < 0.0 \text{ or } (L_w-z) < 0.0 \\ 1.0 & \text{for } (z-Lg) \geq 0 \text{ and } (L_w-z) \geq 0.0 \end{cases} \tag{30}$$

VCHPDA: Computer Program Subroutine Usage

This subroutine solves numerically the analytical VCHP model described in preceeding sections of this report. Its solution logic is written in FORTRAN IV language which is compatible with current Control Data Corporation (CDC) compilers. As a program subroutine, VCHPDA is meant to interact with general lumped parameter thermal systems. In its present form, however, VCHPDA is only suitable for usage in conjunction with TRW's Systems Improved Numerical Differencing Analyzer (SINDA).

The subroutine must be called in VARIABLES 1. In the process of generating a thermal model which involves a VCHP subsystem, the following convention must be followed.

a) Heat pipe wall nodes are numbered and input sequentially stepping out from reservoir end.
b) Wall to vapor conductors are numbered and input sequentially as in a).
c) The vapor of each heat pipe must be declared a boundary node.

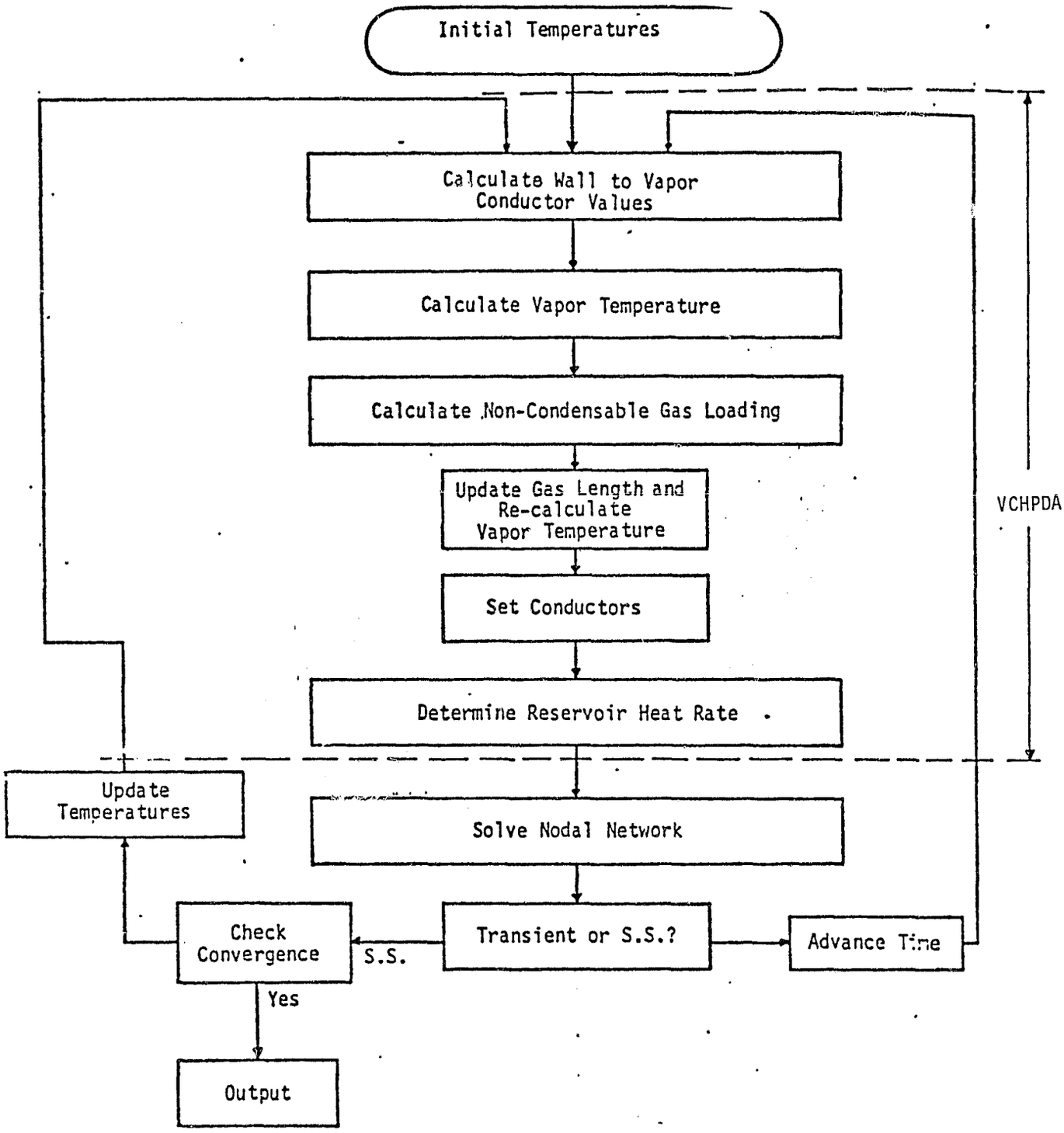

Figure 2. VCHPDA Solution Flowchart

The calling sequence is:

VCHPDA (A1, TN, A3, GN, A2, TJ, TK, QN, K1, K2, TL, A4)

where:

A1 = Working fluid saturation pressure vs temperature array

TN = First node in wall temperature array

A3 = Array of vapor to wall conductors values with no gas input in order starting from the reservoir end (Btu/hr-°F)

GN = First conductor in vapor to wall conductor array

A2 = Heat pipe characteristics array (see below)

TJ = Reservoir temperature node

TK = Control temperature node (for a heated reservoir system)

QN = Reservoir heat input identification (for a heated reservoir system).

K1 = Constant set to zero, fixed point

K2 = Usage flag; 1 = normal calculation usage

-1 = printout of heat pipe data only, used in output calls

TL = Vapor temperature node

A4 = Array of node lengths starting from reservoir end (inches)

Inputs for the heat pipe characteristics array are:

A2(1) = Total heat pipe length (inches)

A2(2) = Number of heat pipe wall nodes (Floating Point Number)

A2(3) = Heat pipe free volume to length ratio (in^3/in)

A2(4) = Reservoir volume (in^3)

A2(5) = Gas NR value (Ft-lb/°R)

A2(6) = Reservior wick flag: 1.0 wicked reservoir

-1.0 un-wicked reservoir

A2(7) = 1.0

A2(8) = Reservoir heater power (Btu/Hr), -1.0 if unheated

A2(9) = Upper temperature setting (°F), (Heated reservoir system)

A2(10) = Lower temperature setting (°F), (Heated reservoir system)

A2(11) = 0.0

A2(12) = Heat pipe identification number (Floating Point Number)

A2(13) = A flag, 0.0 for steady state, 1.0 for transient solutions

A2(14) = Working fluid freezing temperature

A2(15) = A flag, 1.0 to activate ice plug option, 0.0 otherwise

A2(16) = Length of adiabatic section between evaporator and condenser

A2(17) = Specified open artery (deprimed) power-length capacity

A2(18) = A flag, 1.0 to consider deprimed capacity, 0.0 for unrestricted capacity

A2(19) = Length of evaporator section.

Sample Problem

To illustrate the usage of subroutine VCHPDA, the steps involved in solving a simple problem are described in what follows. Consider the heat pipe radiator system sketched in Figure 3. The heat source is a 0.32 Kg aluminum block in which power is uniformly generated. The block is mounted on a 2.5 cm wide saddle that is attached to the heat pipe over a 30 cm-long section. The VCHP is a 1.25 cm O.D., 1.0 meter long aluminum/ammonia heat pipe with a 0.1 litter gas reservoir. Short Al/SS/Al and Al/SS transition sections minimize the coupling by conduction between evaporator and condenser and between reservoir and condenser respectively. Power generated in the heater block is transported by the heat pipe to a radiator panel from which is radiated to a sink.

The system is nodalized as shown in Figure 4. A listing of this model is shown in pages 45 through 47. The FORTRAN version of subroutine VCHPDA is listed in pages 48 through 67.

Steady state, followed by transient solutions were obtained using SINDA. Selected solution outputs are shown in pages 68 through 79. The results are summarized in Figure 5.

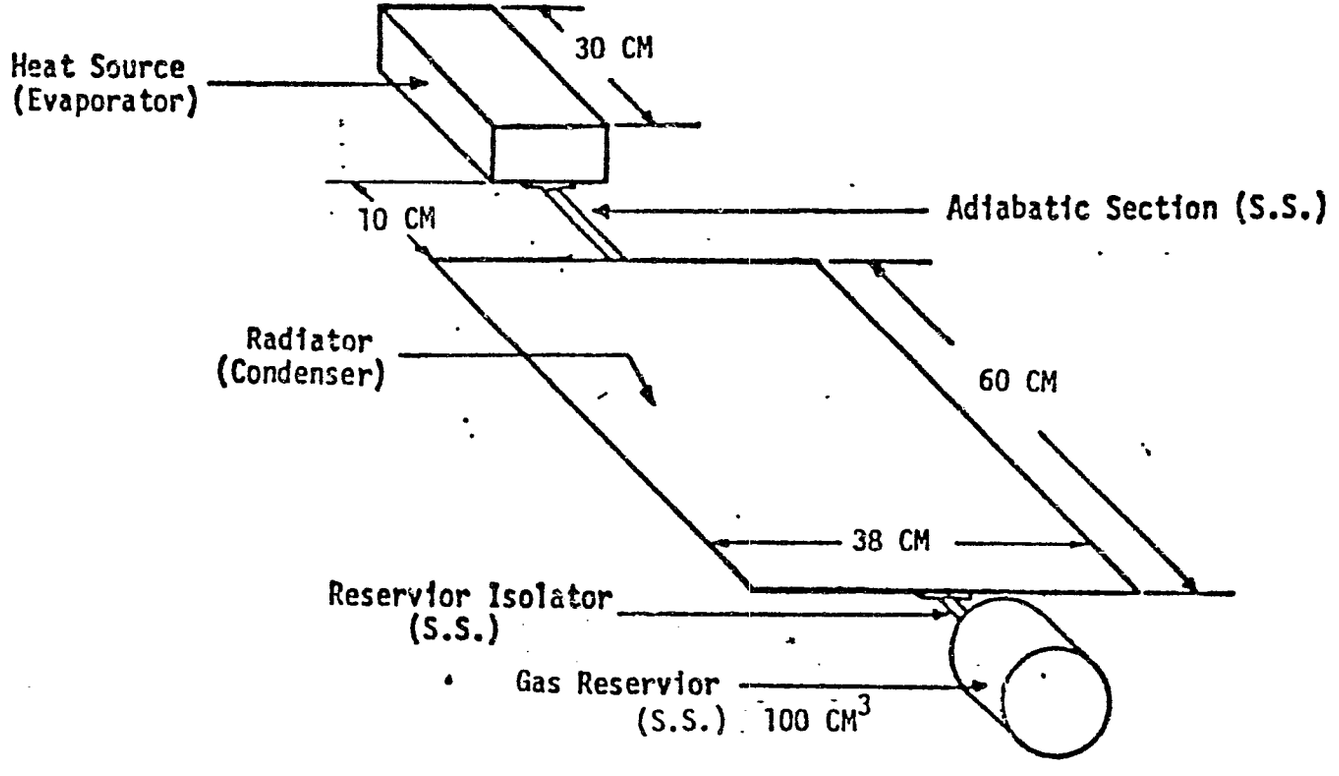

Figure 3. Sample Problem Configuration

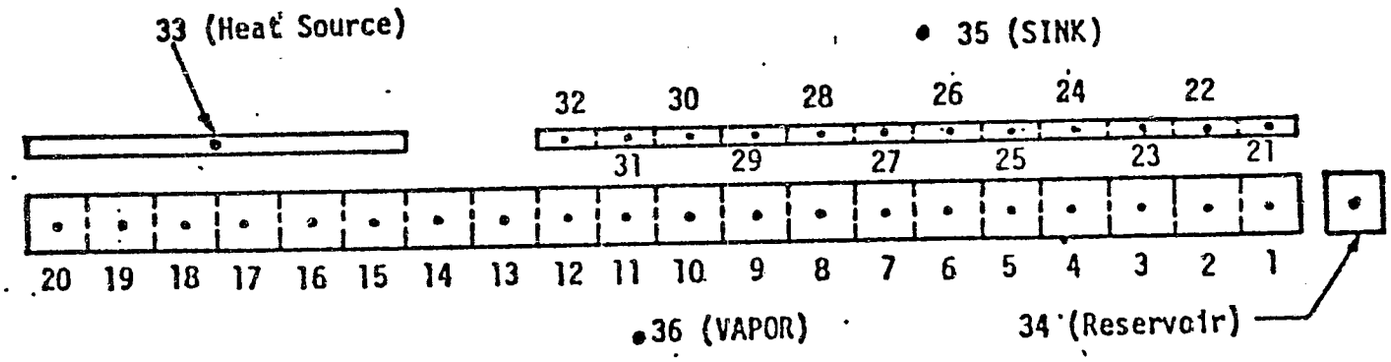

Figure 4. Sample Problem Nodalization

FIGURE 5 VCHP Model Transient Response

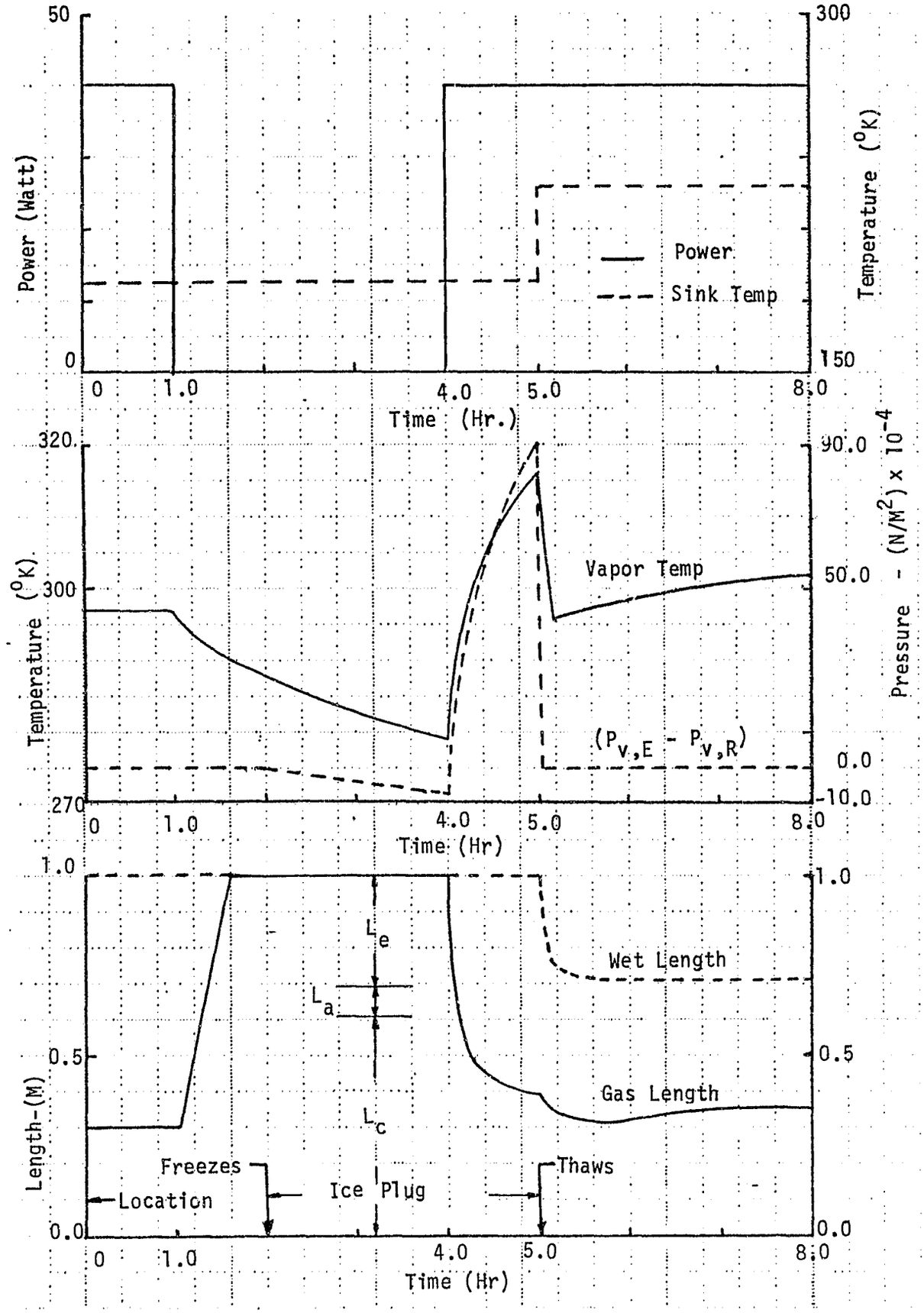

For the first hour after steady state conditions were reached, the VCHP system is shown to transfer 40 watts from the heat source to a sink at 190°K. The vapor temperature remains constant at 296°K and the gas blocks about 3/5 of the condenser section. When the power is turned off, the vapor temperature can be seen to drop resulting in increase gas blockage of the pipe. At 1.5 hours the entire length of the pipe is gas blocked. Although the rate of heat leak from the evaporator is of only one percent of peak power (i.e., 0.40 watt), the vapor, and consequently, the source temperatures undergo a substantial drop during the off period. This is the result of the rather small mass (0.32 Kg) of the source modelled in this problem.

Continuous operation at low sink conditions, causes the inactive condenser to reach subfreezing temperatures and, as shown on the bottom of Figure 5, an ice plug forms at 2 hours, 0.10 meters from the reservoir end of the pipe. The center sketch on the figure shows that a pressure differential develops across the ice plug. This barrier effectively decouples the evaporator from the gas reservoir and causes a large temperature overshoot when the power is turned on at 4.0 hours. Between this time and 5.0 hours, a large pressure differential is sustained across the ice plug. Following a step increase in sink temperature (5.0 hours) simulating a change in solar view factor, the ice plug thaws giving rise to the freezing blow by mechanism which is postulated to cause wicking failure. Continuous operation of the VCHP at 40 watts and deprimed capacity (7.5 watt-meter) is seen to result in partial evaporator dry-out as the heatpipe adjusts its effective length to satisfy the imposed capacity constraint.

References:

Wanous, D. J., "Variable Conductance Heat Pipe Analysis Subroutine, 1973 IR&D Project; Advanced Thermal Control", TRW IOC 8263.135-73-04.

```
BLANK CARD
      BCD 3THERMAL LPCS
      BCD 9 VARIABLE CONDUCTANCE HEAT PIPE TEST CASE
      END
                              ELAPSED TIME =    2.26,   PHASE TIME =    2.26
      BCD 3NODE DATA
      GEN 1,20,1,70.,-1.
          22,70.,-1.
      GEN 23,9,1,70.,174.,.211,7.E-4,1.
          32,70.,-1.
          33,90.,.15
          34,-100.,.04
          -35,-120.,1.
          -36,70.,1.
      END

      RELATIVE NODE NUMBERS                              ACTUAL NODE NUMBERS

       1  THRU   10          23      24      25      26      27      28      29      30      31      33
      11  THRU   20          34       1       2       3       4       5       6       7       8       9
      21  THRU   30          10      11      12      13      14      15      16      17      18      19
      31  THRU   35          20      22      32      35      36
       NODE ANALYSIS...  DIFFUSION =    11,  ARITHMETIC =    22,  BOUNDARY =     2,  TOTAL =    35

                              ELAPSED TIME =    2.34,   PHASE TIME =     .08
      BCD 3CONDUCTOR DATA
      GEN -1,9,1,23,1,35,0,.0346E-8,1.,1.,1.
          -10,22,35,.00822E-8
          -11,32,35,0.00822E-8
          12,2,22,.5
      GEN 13,9,1,3,1,23,1,2.,1.,1.,1.
          22,12,32,.5
      GEN 23,6,1,15,1,33,0,2.56,1.,1.,1.
          29,1,34,.0505
          30,1,2,.0252
          31,2,3,.0777
      GEN 32,8,1,3,1,4,1,0.252,1.,1.,1.
          40,11,12,.0777
          41,12,13,.0252
          42,13,14,.0252
          43,14,15,.0458
      GEN 44,5,1,15,1,16,1,.252
```

```
 CAL -49,34,35,C.5,.64,.1714E-9,1.
 GEN 50,20,1,1,1,36,0,5.,1.,1.,1.
 END

 RELATIVE CONDUCTOR NUMBERS                              ACTUAL CONDUCTOR NUMBERS

  1  THRU    10          1       2       3       4       5       6       7       8       9      10
 11  THRU    20         11      12      13      14      15      16      17      18      19      20
 21  THRU    30         21      22      23      24      25      26      27      28      29      30
 31  THRU    40         31      32      33      34      35      36      37      38      39      40
 41  THRU    50         41      42      43      44      45      46      47      48      49      50
 51  THRU    60         51      52      53      54      55      56      57      58      59      60
 61  THRU    69         61      62      63      64      65      66      67      68      69
 CONDUCTOR ANALYSIS...  LINEAR =    57,  RADIATION =    12,  TOTAL =    69,  CONNECTIONS =    69

                      ELAPSED TIME =    2.54,   PHASE TIME =     .20
 BCD 3CONSTANTS DATA
     NLOOP=300,ARLXCA=0.1,DRLXCA=0.1
 END
 CONSTANTS ANALYSIS...  USER =     0,  ADDED =     0       0       0,  TOTAL =     0

                      ELAPSED TIME =    2.56,   PHASE TIME =     .02
 BCD 3ARRAY DATA
     1,-450.,0.,-170.,.02,-160.,.05,-150.,.1,-140.,.17,-130.,.3,-120.,.5
     -110.,.8,-100.,1.25,-90.,1.88,-80.,2.77,-70.,3.99,-60.,5.62
     -50.,7.75,-40.,10.52,-30.,14.03,-20.,18.45,-10.,23.92,0.,30.62
     10.,38.73,20.,48.47,30.,60.05,40.,73.69,50.,89.64,60.,108.15
     70.,129.47,80.,153.89,90.,181.67,100.,213.11,110.,248.49
     115.,267.76,120.,288.12,125.,309.61,130.,332.28,135.,356.16
     140.,381.29,145.,407.7,150.,435.44,155.,464.53,160.,495.03
     165.,526.97,170.,560.38,175.,595.3,180.,631.7,185.,669.84
     190.,709.53,195.,750.87,200.,793.92
     END
     -2,40.,20.,.115,6.71,.253,1.,12.,-1.,1.,1.,0.,1.,.1,-108.,0.
     4.5,1000.,0.,12.,END $ HEAT PIPE CHARACTERISTICS
     -3,SPACE,20,END
     -4,SPACE,20,END
 END
 ARRAY ANALYSIS...  NUMBER OF ARRAYS =    4  TOTAL LENGTH =   156

                      ELAPSED TIME =    2.66,   PHASE TIME =     .10
                      ELAPSED TIME =    2.76,   PHASE TIME =     .10
```

```
        BCD 3EXECUTION
F       DIMENSION X(300)
F       NDIM=300
F       NTH=0
            STFSQS(5.,20,A3)
            STFSQS(2.,20,A4)
            CINDSL
F           TIMEND=8.
F           OUTPLT=.2
M           A(2+12)=1.
M           A(2+14)=1.
            CNFPDL
        END
                            ELAPSED TIME =     2.87,    PHASE TIME =      .10
        BCD 3VARIABLES 1
M           IF(TIMED.LE.1.0.OR.TIMED.GE.4.0) 033=136.5
M           IF(TIMED.GT.5.0) T35=-50.
            VCHPDA(A1,T1,A3,G50,A2,T34,1.,1.,0,1,T36,A4,TIMED)
F 100   CONTINUE
        END
                            ELAPSED TIME =     2.92,    PHASE TIME =      .05
        BCD 3VARIABLES 2
        END
                            ELAPSED TIME =     2.94,    PHASE TIME =      .02
        BCD 3OUTPUT CALLS
            TOPLIN
            TPRINT
            GPRINT
F 100   CONTINUE
            VCHPDA(A1,T1,A3,G50,A2,T34,1.,1.,0,-1.,T36,A4,TIMED)
            QENDY
        END
                            ELAPSED TIME =     3.02,    PHASE TIME =      .08
```

```
00100       SUBROUTINE VCHPDA(A1,TW,A3,G1,A2,T2,T3,Q,NA,NB,T1,A4,FTIM)
00110 C---------->FILE VCHPDA<----------------
00120 C
00130 C
00140 C     THIS SUBROUTINE IS A NEW VERSION OF THE PREVIOUS VCHP2 SUBROUTINE.
00150 C     THIS SUBROUTINE CONSIDERS THE FORMATION OF AN ICE PLUG WHICH
00160 C     EFFECTIVELY DECOUPLES THE RESERVOIR FROM THE REST OF THE HEAT
00170 C     PIPE. IN ORDER TO CONSIDER THE EFFECT OF AN ICE PLUG ON THE
00180 C     TRANSIENT RESPONSE OF A VARIABLE CONDUCTANCE HEAT PIPE SYSTEM,
00190 C     TWO MORE DATA NEED TO BE INCLUDED AT THE END OF ARRAY =A2=
00200 C     OR AT THE END OF ARRAYS =51=, =52= AND =53= IN THE CTS MODEL.
00210 C     THESE DATA APE:
00220 C
00230 C     A2(14)= FREEZING POINT OF THE WORKIND FLUID
00240 C
00250 C     A2(15)= A FLAG (=1. FOR AND ICE TO BE ALLOWED TO FORM,
00260 C     =0. FOR AN ICE PLUG NOT TO BE CONSIDERED)
00270 C
00280 C
00290 C     IN ADDITION THIS SUBROUTINE CONSIDERS A VARIABLE CONDUCTANCE
00300 C     HEAT PIPE WITH OPEN ARTERY OR REDUCED CAPACITY.
00310 C     IN ORDER TO DETERMINE THE STEADY STATE SOLUTION OR THE THERMAL
00320 C     RESPONSE OF A HEAT PIPE SYSTEM WITH THE HEAT PIPES OPERATING
00330 C     WITH OPEN ARTERY OR REDUCED CAPACITY SEVERAL NEW DATA NEED
00340 C     TO BE INCLUDED AT THE END OF THE ABOVE MENTIONED ARRAYS.
00350 C     THESE ADDITIONAL DATA ARE:
00360 C
00370 C     A2(16)= LENGTH OF THE ADIABATIC SECTION BETWEEN THE EVAPORATOR
00380 C     AND THE CONDENSER
00390 C
00400 C     A2(17)= SPECIFIED OPEN ARTEY CAPACITY IN BTU/HR-INCH
00410 C
00420 C     A2(18)= A FLAG (=1. TO CONSIDER OPERATION OF THE HEAT PIPE
00430 C     WITH OPEN ARTERY CAPACITY, AND =0. TO CONSIDER OPERATION
00440 C     OF THE HEAT PIPE WITH NORMAL OR UNLIMITED CAPACITY)
00450 C
00460 C     A2(19)= LENGTH OF THE EVAPORATOR SECTION
00470 C
00480 C     A2(15)=1. SHOULD USED FOR TRANSIENT RUNS ONLY, HOWEVER
00490 C     A2(18)=1. COULD BE USED FOR STEADY AS WELL AS FOR TRANSIENT
00500 C     RUNS. IN ADDITION A2(15)=1. AND A2(18)=1. COULD BE USED
00510 C     SIMULTANEOUSLY FOR TRANSIENT RUNS.
```

```
00520 C
00530 C
00540 C      IN THE PREVIOUS VCHP2 IT WAS REQUIRED THAT A2(13)=.1 BE
00550 C      USED AS A DAMPING FACTOR FOR STEADY STATE RUNS AND THAT
00560 C      A2(13)=1. BE USED AS A DAMPING FACTOR FOR TRANSIENT SOLUTIONS.
00570 C      IN THIS NEW VERSION THOSE TWO PARAMETERS SHOULD BE USED
00580 C      AS BEFORE ALTHOUGH NOW THEY MERELY FUNCTION AS FLAGS.
00590 C
00600 C      THE PARAMETER ≡NA≡ WHICH WAS USED TO SPECIFY THE NUMBER OF
00610 C      ITERATIONS DESIRED IN THE LOOP TO CALCULATE THE GAS FRONT
00620 C      LOCATION, THE NEW VAPOR-TO-WALL NODE CONDUCTORS AND THE
00630 C      VAPOR TEMPERATURE, IS NOT USED IN THIS NEW VERSION AND
00640 C      HENCE IT CAN BE TREATED AS A DUMMY PARAMETER.
00650 C
00660 C      THE USER WILL NOTICE THAT THERE ARE TWO DIFFERENT OUTPUTS
00670 C      DEPENDING WHETHER AN ICE PLUG HAS FORMED OR WHETHER AN ICE PLUG
00680 C      HAS NOT BEEN CONSIDERED OR HAS THAWED.
00690 C
00700 C      AS BEFORE THE PARAMETER ≡NB≡ IS THE PRINTING FLAG.
00710 C
00720 C      ANY OTHER INPUT PARAMETER REQUIRED TO CALL ≡VCHP2≡ WHICH
00730 C      HAS NOT BEEN MENTIONED ABOVE SHOULD BE CONSIDERED AS BEFORE.
00740
00750 C
00760 C
00770 C
00780 C      A1=FLUID P VS T ARRAY,  TW=WALL TEMP ARRAY,  A3=WALL-VAPOR CONDUCTORS
00790 C      G1=WALL-VAPOR CONDUCTORS CALCULATED, A2=HEAT PIPE CHARACTERISTICS
00800 C      T2=RESERVOIR TEMP,  T3=CONTROL TEMPERATURE,  Q=RESERVOIR HEATER Q
00810 C
00820 C
00830 C
00840        DIMENSION TW(1),A3(1),G1(1),A2(1),A4(1),N1(80),N2(80),F(80),
00850       1 L(80),P(80),PW(80),T(80),FN(10)
00860        REAL L,N1,N2,NGAS,LTOT,LGRE,LGEV,NPEV,NPRE,N23,LP,LPD,LEFF,
00870       1 L1,L2,L3,L4,LCOND
00880        DATA IFREZE/0/
00890        DATA FN/10*0./
00900        IF(FTIM.GT.4.5.AND.IFREZE.EQ.0)A2(18)=1.
00910        CALL FIX(A2(2),N)
00920        NM1=N-1
00930        NP1=N+1
```

```
00940         IF( A2(6).GT.0.) GO TO 102
00950         CALL D1DEG1(TW(1),A1,PVR)
00960         GO TO 101
00970   102   CALL D1DEG1(T2,A1,PVP)
00980   101   CONTINUE
00990         A=A2(3)
01000         LCOND=A2(1)-A2(16)-A2(19)
01010         VR=A2(4)
01020         TR=T2
01030         PVTR=PVR*VR/(TR+460.)/12.
01040         VTR=VR/(TR+460.)/12.
01050         NGAS=A2(5)
01060         IF(A2(13).LT.1.) GO TO 500
01070         IF(IFREZE.EQ.1) GO TO 71
01080         SUM15=0.
01090         SUM610=0.
01100         DO 70 J=1,9
01110         I=10-J
01120         FN(I+1)=FN(I)
01130         IF(I.GT.4) SUM610=SUM610+FN(I+1)
01140         SUM15=SUM15+FN(I+1)
01150   70    CONTINUE
01160         FN(1)=RNR
01170         SUM15=SUM15+FN(1)
01180         SUM15=SUM15-SUM610
01190         IF(SUM15.GT.SUM610) GO TO 500
01200         IF(T2.LT.A2(14)) GO TO 500
01210         GO TO 75
01220   71    DO 72 I=1,10
01230   72    FN(I)=0.
01240         SUM15=0.
01250         SUM610=0.
01260   75    CONTINUE
01270         IF(A2(15).LT.1.) GO TO 500
01280         DO 50 I=1,N
01290         IF(TW(I).LT.A2(14)) GO TO 51
01300   50    CONTINUE
01310         IFREZE=0
01320         GO TO 500
01330   51    IF(IFREZE.EQ.1) GO TO 52
01340         IFREZE=2
01350         GO TO 890
```

```
01360  889    CONTINUE
01370         DO 53 J=1,N
01380         I=NP1-J
01390         IF(TW(I).LT.A2(14)) GO TO 54
01400   53    CONTINUE
01410   54    IFREZE=1
01420         IP1=I+1
01430         IPO=I
01440         N2(IPO)=PSAT*F(IPO)-N1(IPO)
01450         NPEV=NGAS-N2(IPO)
01460         NPRE=N2(IPO)
01470   52    CONTINUE
01480         SUM1=0.
01490         SUM2=0.
01500         SUM3=0.
01510         DO 60 I=1,IPO
01520         CALL D1DEG1(TW(I),A1,PW(I))
01530         SUM1=SUM1+PW(I)*A4(I)*A/(TW(I)+460.)/12.
01540         N1(I)=PVTR+SUM1
01550         SUM2=SUM2+A4(I)*A/(TW(I)+460.)/12.
01560         G1(I)=0.
01570         F(I)=VTP+SUM2
01580         SUM3=SUM3+A4(I)
01590         L(I)=SUM3
01600   60    CONTINUE
01610         LGRE=L(I)
01620         PTOTRE=(NPRE+N1(IPO))/F(IPO)
01630         PGR=PTOTRE-PVR
01640         RNR=PGR*VR/(TR+460.)/12.
01650         IFULL=0
01660         NO=NM1
01670         N3=N
01680         IQ=0
01690         LP=A2(1)
01700         IQQ=-3
01710         IB=0
01720         CLCT=A2(17)
01730   999   CONTINUE
01740         SUM1=0.
01750         SUM2=0.
01760         SUM3=0.
01770         SUMT=0.
```

```
01780       SUMG=0.
01790       DO 61 I=IP1,N3
01800       J=N3+IP1-I
01810       CALL D1DEG1(TW(I),A1,PW(I))
01820       SUM1=SUM1+PW(I)*A4(I)*A/(TW(I)+460.)/12.
01830       N1(I)=SUM1
01840       SUM2=SUM2+A4(I)*A/(TW(I)+460.)/12.
01850       F(I)=SUM2
01860       SUM3=SUM3+A4(I)
01870       L(I)=SUM3
01880       G1(I)=0.
01890       SUMT=SUMT+TW(J)*A3(J)
01900       SUMG=SUMG+A3(J)
01910       T(J)=SUMT/SUMG
01920       CALL D1DEG1(T(J),A1,P(J))
01930  61   CONTINUE
01940       PTOTEV=(NPEV+N1(N3))/F(N3)
01950       CALL D1DEG1(TW(N3),A1,PSAT)
01960       N2(N3)=PSAT*F(N3)-N1(N3)
01970       ICHECK=0
01980       DO 1111 I=IP1,NO
01990       N2(I)=P(I+1)*F(I)-N1(I)
02000  1111 IF(N2(I).GT.NPEV.AND.ICHECK.LT.1) ICHECK=I
02010       IF(ICHECK.EQ.0) GO TO 600
02020       SUMG=0.
02030       SUMGT=0.
02040       DO 62 J=IP1,NO
02050       I=NO+IP1-J
02060       SUMGT=SUMGT+TW(I+1)*A3(I+1)
02070       SUMG=SUMG+A3(I+1)
02080       T(I+1)=SUMGT/SUMG
02090       CALL D1DEG1(T(I+1),A1,P(I+1))
02100       N2(I)=P(I+1)*F(I)-N1(I)
02110       IF(N2(I).LT.NPEV.AND.I.LT.ICHECK) GO TO 601
02120       G1(I+1)=A3(I+1)
02130  62   CONTINUE
02140       FRAC=(N2(I)-NPEV)/N2(I)
02150       G1(I)=FRAC*A3(I)
02160       L(I)=(1.-FRAC)*A4(I)
02170       LGEV=L(I)
02180       XND=(1.-FRAC)*A4(I)
02190       N1(I)=PW(I)*XND*A/(TW(I)+460.)/12.
```

```
02200         F(I)=XND*A/(Tw(I)+460.)/12.
02210         SUMGT=SUMGT+Tw(I)*C1(I)
02220         SUMG=SUMG+G1(I)
02230         TSAT=SUMGT/SUMG
02240         CALL DIDEG1(TSAT,A1,PSAT)
02250         N2(I)=PSAT*F(I)-N1(I)
02260         X4=N2(I)
02270         T1=TSAT
02280         A2(7)=LGEV+LGRE
02290         IF(IFULL.EQ.2) GO TO 1607
02300         IF(A2(18).LT.1.) GO TO 500
02310         CALL QMETER(T1,TW,G1,X5,X6,N3)
02320         QLC=QL(LP,A2(16),A2(7),LCOND,X6,LEFF)
02330         IF(IQ.EQ.-2) GO TO 5002
02340         IF(QLC.LT.A2(17)) GO TO 1353
02350         IQ=-1
02360         QLC=QLC
02370         QLC3=QLG
02380         LP=L(NO)+LGRE
02390         L1=LP
02400         G1(N3)=0.
02410         NO=NO-1
02420         N3=N3-1
02430         IFULL=1
02440         GO TO 999
02450  1353   IF(IQ.EQ.0) GO TO 500
02460         NO=NO+1
02470         N3=N3+1
02480         QLL=QLC
02490         QLC1=QLL
02500         A4N3=A4(N3)
02510         G1N3=A3(N3)
02520         IQ=-2
02530         LP=L(N3)+LGRE
02540         L3=LP
02550         DLP=L3-L1
02560         GO TO 999
02570  5002   IF(IQQ.EQ.0) GO TO 1704
02580         G1(N3)=.5*G1N3
02590         DX=.5*A4N3
02600         LP=L(NO)+DX+LGRE
02610         L2=LP
```

```
      IF(IQQ.EQ.-3) GO TO 1904
1704  IF(IB.EQ.0) QLC2=QLC
      TERM=ABS((QLC-A2(17))/A2(17))
      IF(TERM.LT.1.E-3) GO TO 1903
      IF(IB.EQ.0)
     1 CALL QUADRA(L1,L2,L3,LP,QLC1,QLC2,QLC3,QLCT)
      CALL BINARY(L1,L2,L3,LP,QLC,QLC1,QLC2,QLC3,QLCT,IB)
      DX=LP-(L(NO)+LGPE)
      G1(N3)=DX/DLP*G1N3
1904  A3(N3)=G1(N3)
      A4(N3)=DX
      IQQ=0
      GO TO 999
1803  LPD=A2(1)-LP
      A3(N3)=G1N3
      A4(N3)=A4N3
      IFULL=0
      GO TO 500
601   CONTINUE
      IT=2
      FRAC=(NPEV-N2(I))/(N2(I+1)-N2(I))
      FRAC1=FRAC
      FRAC2=FRAC
      DF1=FRAC
      DF2=1.-FRAC
      DN=PW(I+1)*A/(TW(I+1)+460.)/12.
      DF=A/(TW(I+1)+460.)/12.
927   G1(I+1)=(1.-FRAC)*A3(I+1)
      XND=FRAC*A4(I+1)
      DGT=TW(I+1)*(G1(I+1)-A3(I+1))
      DG=G1(I+1)-A3(I+1)
      TSAT=(SUMGT+DGT)/(SUMG+DG)
      N1(I+1)=N1(I)+DN*XND
      F(I+1)=F(I)+DF*XND
      CALL DIDEG1(TSAT,A1,PSAT)
      N2(I+1)=PSAT*F(I+1)-N1(I+1)
      IF(ABS((N2(I+1)-NPEV)/NPEV).LT.1.E-5) GO TO 602
      IF(IT.EQ.2) GO TO 93
      IF(IT.EQ.1) GO TO 94
95    DF1=DF1/2.
      N23=N2(I+1)-NPEV
      SIGN=N23/ABS(N23)
```

```
03040         FRAC1=FRAC1-SIGN*DF1
03050         FRAC=FRAC1
03060         IT=0
03070         GO TO 927
03080   93    IF(N2(I+1).LT.NPEV) GO TO 94
03090         GO TO 95
03100   94    DF2=DF2/2.
03110         N23=N2(I+1)-NPEV
03120         SIGN=N23/ABS(N23)
03130         FRAC2=FRAC2-SIGN*DF2
03140         FRAC=FRAC2
03150         IT=1
03160         GO TO 927
03170   602   L(I+1)=L(I)+XND
03180         LGEV=L(I+1)
03190         A2(7)=LGRE+LGEV
03200         T1=TSAT
03210         X4=N2(I+1)
03220   1607  IF(A2(18).LT.1.) GO TO 500
03230         IF(IFULL.EQ.1) GO TO 1606
03240         GO TO 1608
03250   1606  N3=N3+1
03260         NO=NO+1
03270         LP=L(N3)+LGRE
03280         IFULL=2
03290         GO TO 999
03300   1608  CONTINUE
03310         CALL QMETER(T1,TW,G1,X5,X6,N3)
03320         QLC=QL(LP,A2(16),A2(7),LCOND,X6,LEFF)
03330         IF(IQ.EQ.-2) GO TO 5001
03340         IF(QLC.LT.A2(17)) GO TO 1453
03350         IQ=-1
03360         QLG=QLC
03370         QLC3=QLG
03380         LP=L(NO)+LGRE
03390         L1=LP
03400         NO=NO-1
03410         G1(N3)=0.
03420         N3=N3-1
03430         GO TO 999
03440   1453  IF(IQ.EQ.0) GO TO 500
03450         NO=NO+1
```

```
03460        N3=N3+1
03470        A4N3=A4(N3)
03480        G1N3=A3(N3)
03490        QLL=QLC
03500        QLC1=QLL
03510        IQ=-2
03520        LP=L(N3)+LGPE
03530        L3=LP
03540        DLP=L3-L1
03550        GO TO 999
03560  5001  IF(IQQ.EQ.0) GO TO 1800
03570        G1(N3)=.5*G1N3
03580        DX=.5*A4N3
03590        LP=L(NO)+DX+LGPE
03600        L2=LP
03610        IF(IQQ.EQ.-3) GO TO 1804
03620  1800  IF(IB.EQ.0) QLC2=QLC
03630        TERM=ABS((QLC-A2(17))/A2(17))
03640        IF(TERM.LT.1.E-3) GO TO 1805
03650        IF(IB.EQ.0)
03660       1 CALL QUADRA(L1,L2,L3,LP,QLC1,QLC2,QLC3,QLCT)
03670        CALL BINARY(L1,L2,L3,LP,QLC,QLC1,QLC2,QLC3,QLCT,IP)
03680        DX=LP-(L(NO)+LGPE)
03690        G1(N3)=DX/DLP*G1N3
03700  1804  A3(N3)=G1(N3)
03710        A4(N3)=DX
03720        IQC=0
03730        GO TO 999
03740  1805  A4(N3)=A4N3
03750        A3(N3)=G1N3
03760        LPO=A2(1)-LP
03770        GO TO 500
03780  600   CONTINUE
03790        X4=NPEV
03800        LGEV=L(N3)
03810        T1=TW(N3)
03820        PSAT=PTOTEV
03830  500   CONTINUE
03840        LTOT=LGPE+LGEV
03850        A2(7)=LTOT
03860        DPV=PSAT-PTOTPE
03870        LPO=A2(1)-LP
```

```
03880       IF(IFREZE.EQ.1) GO TO 501
03890  890  NO=NM1
03900       N4=NP1
03910       N3=N
03920       IQ=0
03930       LP=A2(1)
03940       IQQ=-3
03950       IFULL=0
03960       IR=0
03970  888  SUM1=0.
03980       QLCT=A2(17)
03990       SUM2=0.
04000       SUM3=0.
04010       SUMT=0.
04020       SUMG=0.
04030       DO 110 I=1,N3
04040       CALL D1DEG1(TW(I),A1,PW(I))
04050       SUM1=SUM1+PW(I)*A4(I)*A/(TW(I)+460.)/12.
04060       N1(I)=PVTR+SUM1
04070       SUM2=SUM2+A4(I)*A/(TW(I)+460.)/12.
04080       P(I)=VTP+SUM2
04090       SUM3=SUM3+A4(I)
04100       L(I)=SUM3
04110       G1(I)=0.
04120        J=N3-I
04130        SUMT=SUMT+TW(J+1)*A3(J+1)
04140        SUMG=SUMG+A3(J+1)
04150        T(J+1)=SUMT/SUMG
04160        CALL D1DEG1(T(J+1),A1,P(J+1))
04170  110  CONTINUE
04180       PTOT=(NGAS+N1(N3))/P(N3)
04190       ICHECK=0
04200        DO 111 I=1,NO
04210        N2(I)=P(I+1)*P(I)-N1(I)
04220  111  IF(N2(I).GT.NGAS.AND.ICHECK.LT.1) ICHECK=I
04230       CALL D1DEG1(TW(N3),A1,P(N3))
04240        N2(N3)=P(N3)*P(N3)-N1(N3)
04250        IF(ICHECK.EQ.0) GO TO 1000
04260       CSUM=0.
04270       TGSUM=0.
04280       DO 120 J=1,NO
04290       I=N3-J
```

```
04300         TGSUM=TGSUM+TW(I+1)*A3(I+1)
04310         GSUM=GSUM+A3(I+1)
04320         TSAT=TGSUM/GSUM
04330         CALL DIDEG1(TSAT,A1,P(I+1))
04340         N2(I)=P(I+1)*F(I)-N1(I)
04350         IF(N2(I).LE.NGAS.AND.I.LT.ICHECK) GO TO 2000
04360         G1(I+1)=A3(I+1)
04370  120    CONTINUE
04380         C1(1)=(A4(1)-0.)/A4(1)*A3(1)
04390         A2(7)=0.
04400         T1=TSAT
04410         IF(IFULL.EQ.2) GO TO 607
04420         IF(A2(18).LT.1.) GO TO 121
04430         CALL QMETER(T1,TW,G1,X5,X6,N3)
04440         QLC=QL(LP,A2(16),A2(7),LCOND,X6,LEFF)
04450         IF(IQ.EQ.-2) GO TO 4002
04460         IF(QLC.LT.A2(17)) GO TO 353
04470         IQ=-1
04480         QLG=QLC
04490         LP=L(NO)
04500         G1(N3)=0.
04510         QLC3=QLG
04520         L1=LP
04530         NO=NO-1
04540         N3=N3-1
04550         IFULL=1
04560         GO TO 888
04570  353    IF(IQ.EQ.0) GO TO 121
04580         NO=NO+1
04590         N3=N3+1
04600         QLL=QLC
04610         A4N3=A4(N3)
04620         G1N3=A3(N3)
04630         IQ=-2
04640         LP=L(N3)
04650         QLC1=QLL
04660         L3=LP
04670         DLP=L3-L1
04680         GO TO 888
04690  4002   IF(IQQ.EQ.0) GO TO 704
04700         G1(N3)=.5*G1N3
04710         DX=.5*A4N3
```

```
04720       LP=L(NO)+DX
04730       L2=LP
04740       IF(IQQ.EQ.-3) GO TO 904
04750  704  IF(IB.EQ.0) QLC2=QLC
04760       TERM=ABS((QLC-A2(17))/A2(17))
04770       IF(TERM.LT.1.E-3) GO TO 803
04780       IF(IB.EQ.0)
04790      1 CALL QUADRA(L1,L2,L3,LP,QLC1,QLC2,QLC3,QLCT)
04800       CALL BINARY(L1,L2,L3,LP,QLC,QLC1,QLC2,QLC3,QLCT,IB)
04810       DX=LP-L(NO)
04820       G1(N3)=DX/DLP*G1N3
04830  904  A3(N3)=G1(N3)
04840       A4(N3)=DX
04850       IQQ=0
04860       GO TO 888
04870  803  LPD=A2(1)-LP
04880       A3(N3)=G1N3
04890       A4(N3)=A4N3
04900       IFULL=0
04910       X4=.0
04920       RNR=A2(5)
04930       PGR=PSAT-PVR
04940       GO TO 3000
04950  121  PSAT=P(I+1)
04960       LPD=0.
04970       X4=0.
04980       RNR=A2(5)
04990       PGR=PSAT-PVR
05000       GO TO 3000
05010  1000 PSAT=PTOT
05020       LPD=0.
05030       LEFF=0.
05040        A2(7)=A2(1)
05050       T1=TW(N3)
05060       PGR=PSAT-PVR
05070       RNR=PGR*A2(4)/(T2+460.)/12.
05080       X4=A2(5)-RNR
05090       DO 81 I=1,N3
05100       N2(I)=PSAT*P(I)-N1(I)
05110  81   CONTINUE
05120       GO TO 3000
05130  2000 CONTINUE
```

```
05140          IT=2
05150          FRAC=(NGAS-N2(I))/(N2(I+1)-N2(I))
05160          FRAC1=FRAC
05170          FRAC2=FRAC
05180          DF1=FRAC
05190          DF2=1.-FRAC
05200          DN=PW(I+1)*A/(TW(I+1)+460.)/12.
05210          DF=A/(TW(I+1)+460.)/12.
05220    928   G1(I+1)=(1.-FRAC)*A3(I+1)
05230          XND=FRAC*A4(I+1)
05240          DGT=TW(I+1)*(G1(I+1)-A3(I+1))
05250          DG=G1(I+1)-A3(I+1)
05260          TSAT=(TGSUM+DGT)/(GSUM+DG)
05270          CALL DIDEG1(TSAT,A1,PSAT)
05280          N1(I+1)=N1(I)+DN*XND
05290          F(I+1)=F(I)+DF*XND
05300          N2(I+1)=PSAT*F(I+1)-N1(I+1)
05310          IF(ABS((N2(I+1)-NGAS)/NGAS).LT.1.E-5) GO TO 604
05320          IF(IT.EQ.2) GO TO 97
05330          IF(IT.EQ.1) GO TO 98
05340    99    DF1=DF1/2.
05350          N23=N2(I+1)-NGAS
05360          SIGN=N23/ABS(N23)
05370          FRAC1=FRAC1-SIGN*DF1
05380          FRAC=FRAC1
05390          IT=0
05400          GO TO 928
05410    97    IF(N2(I+1).LT.NGAS) GO TO 98
05420          GO TO 99
05430    98    DF2=DF2/2.
05440          N23=N2(I+1)-NGAS
05450          SIGN=N23/ABS(N23)
05460          FRAC2=FRAC2-SIGN*DF2
05470          FRAC=FRAC2
05480          IT=1
05490          GO TO 928
05500    604   L(I+1)=L(I)+XND
05510          TGSUM=TGSUM+DGT
05520          GSUM=GSUM+DG
05530          A2(7)=L(I+1)
05540          T1=TSAT
05550    607   IF(A2(18).LT.1.) GO TO 605
```

```
05560       IF(IFULL.EQ.1) GO TO 606
05570       GO TO 608
05580  606  N3=N3+1
05590       NO=NO+1
05600       LP=L(N3)
05610       IFULL=2
05620       GO TO 888
05630  608  CONTINUE
05640       CALL OMETER(T1,TW,G1,X5,X6,N3)
05650       QLC=QL(LP,A2(16),A2(7),LCOND,X6,LEFF)
05660       IF(IQ.EQ.-2) GO TO 4001
05670       IF(QLC.LT.A2(17)) GO TO 453
05680       IQ=-1
05690       QLG=QLC
05700       QLC3=QLG
05710       LP=L(NO)
05720       L1=L(NO)
05730       G1(N3)=0.
05740       NO=NO-1
05750       N3=N3-1
05760       GO TO 888
05770  453  IF(IQ.EQ.0) GO TO  605
05780       NO=NO+1
05790       N3=N3+1
05800       A4N3=A4(N3)
05810       G1N3=A3(N3)
05820       QLL=QLC
05830       QLC1=QLL
05840       IQ=-2
05850       LP=L(N3)
05860       L3=L(N3)
05870       DLP=L3-L1
05880       GO TO 888
05890  4001 IF(IQQ.EQ.0) GO TO 800
05900       G1(N3)=.5*G1N3
05910       DX=.5*A4N3
05920       LP=L(NO)+DX
05930       L2=LP
05940       IF(IQQ.EQ.-3) GO TO 804
05950  800  IF(IP.EQ.0) QLC2=QLC
05960       TERM=ABS((QLC-A2(17))/A2(17))
05970       IF(TERM.LT.1.E-3) GO TO 805
```

```
05980         IF(1B.EQ.0)
05990        1 CALL QUADRA(L1,L2,L3,LP,QLC1,QLC2,QLC3,QLCT)
06000         CALL BINARY(L1,L2,L3,LP,QLC,QLC1,QLC2,QLC3,QLCT,IB)
06010         DX=LP-L(NO)
06020         G1(N3)=DX/DLP*G1N3
06030   804   A3(N3)=G1(N3)
06040         A4(N3)=DX
06050         IQQ=0
06060         GO TO 888
06070   805   A4(N3)=A4N3
06080         A3(N3)=G1N3
06090         PGR=PSAT-PVR
06100         LPD=A2(1)-LP
06110         RNR=PGR*A2(4)/(T2+460.)/12.
06120         X4=N2(I+1)-RNR
06130         GO TO 3000
06140   605   PGR=PSAT-PVR
06150         LPD=0.
06160         RNR=PGR*A2(4)/(T2+460.)/12.
06170         X4=N2(I+1)-RNR
06180   3000  CONTINUE
06190         IF(IFREZE.EQ.2) GO TO 889
06200   501   CONTINUE
06210         IF(A2(8).LT.-0.5) GO TO 80
06220 C       IF(A2(11).GT.0.001) GO TO 90
06230 C   CALCULATE RESERVOIR HEATER INPUT
06240         IF(T3.LE.A2(10)) A2(11)=A2(8)
06250         IF(T3.GE.A2(9)) A2(11)=0.0
06260   100   Q=A2(11)
06270   80    CONTINUE
06280   210   IF(N8.GT.0) GO TO 220
06290         CALL METER(T1,TW,G1,X5,X6,N3)
06300         QLC=QL(LP,A2(16),A2(7),LCOND,X6,LEFF)
06310         IF(IFREZE.EQ.1) GO TO 219
06320         WRITE(6,221) A2(12)
06330   221   FORMAT(1HO,15X,17HHEAT PIPE NUMBER ,F2.0,17H  CHARACTERISTICS)
06340         WRITE(6,222) A2(1),A2(3),A2(4)
06350   222   FORMAT(14HOTOTAL LENGTH=,F6.2,2HIN,11H  GAS V/L= ,F5.3,8HIN**3/IN,
06360        C14H  RES VOLUME= ,F6.3,5H IN-3)
06370         WRITE(6,223) A2(5)
06380   223   FORMAT(17H GAS INVENTORY = ,F8.4,8H FT-1B/R,24H RESERVOIR IS     W
06390        CICKED)
```

```
      IF(A2(6).GT.0.0) GO TO 224
      WRITE(6,225)
  225 FORMAT(1H+,46X,3HNCT)
  224 WRITE(6,226) T1,PSAT,A2(7),LPD
  226 FORMAT(14H VAPOR TEMP = ,F7.2,18H F  TOTAL PRESS = ,F7.2,18H PSIA
     C GAS LGTH = ,F6.2,2HIN,2X,15HDRY EVAP LGTH= ,F6.2,3H IN)
      WRITE(6,227) T2,PGR
  227 FORMAT(17H RESERVOIR TEMP= ,F7.2,21H F   RES GAS PRESS=  ,F7.2,5H
     CPSIA)
      WRITE(6,228) X5,X6,LEFF,QLC
  228 FORMAT(10H SUM QIN= ,F8.2,20H BTU/HR,  SUM QOUT= ,F8.2,7H BTU/HR,
     14X,6HLEFF= ,F6.2,8H  INCHES,2X,6HQLEFF=,F7.1,12H BTU-INCH/HR)
      X10=A2(5)-RNR-X4
      WRITE(6,230) RLR,X4,X10
  230 FORMAT(19H RESERVOIR GAS NR= ,F9.6,15H HEAT PIPE NP= ,F9.6,11H RES
     CIDUAL= ,F9.6)
      GO TO 420
  219 CONTINUE
      WRITE(6,200) A2(12)
  200 FORMAT(1H0,15X,16HHEAT PIPE NUMBER,F2.0,16H CHARACTERISTICS)
      WRITE(6,201) A2(1),A2(3),A2(4)
  201 FORMAT(14H TOTAL LENGTH=,F6.2,2HIN, 9H GAS V/L=,F5.3,
     1 8HIN**3/IN,13H RES VOLUME= ,F6.3,6H IN**3)
      WRITE(6,202) A2(5)
  202 FORMAT(16H GAS INVENTORY= ,F8.4,8H FT-LB/R,
     122HRESERVOIR IS    WICKED)
      IF(A2(6).GT.0.) GO TO 203
      WRITE(6,204)
  204 FORMAT(1H+,46X,3HNCT)
  203 LTOT=LGRE+LGEV
      WRITE(6,205) LCPE,LTOT,LPD
  205 FORMAT(23H LOCATION OF ICE PLUG= ,F6.2,3H IN,
     1 23H POSITION OF GAS FRONT=,F6.2,3H IN,2X,15HDRY EVAP LGTH= ,
     2F6.2,3H IN)
      RES=NPEV-X4
      WRITE(6,206) NPRE,X4,RES
  206 FORMAT(18H GAS IN RES SIDE= ,F9.6,19H GAS IN EVAP SIDE= ,F9.6,
     1 15H GAS RESIDUAL= ,F9.6)
      WRITE(6,207) PTOTRE,PSAT,DPV
  207 FORMAT(28H TOTAL PRESSURE IN RES SIDE=,F7.2,5H PSIA,
     130H TOTAL PRESSURE ON EVAP SIDE= ,F7.2,5H PSIA,2X,
     2 8HPEV-PRE=,F7.2,5H PSIA)
```

```
      WRITE(6,208) TP,T1
  208 FORMAT(18H PES TEMPERATURE= ,F7.2,2H F,
     122H EVAP SIDE VAPOR TEMP=,F7.2,2H F)
      WRITE(6,209) X5,X6,LEFF,CLC
  209 FORMAT(10H SUM QIN= ,F8.2,19H BTU/HR, SUM QOUT= ,F8.2,7H BTU/HR,
     1 4X,6HLEFF= ,F6.2,8H  INCHES,2X,6HQLEFF=,F8.1,12H BTU-INCH/HR)
  420 CONTINUE
  220 CONTINUE
      RETURN
      END
C
C
C     THIS SUBROUTINE CALCULATE THE HEAT FLOW RATE INTO AND OUT OF
C     THE VAPOR NODE
C
      SUBROUTINE QMETER(TV,T,G,QOUT,QIN,N3)
      DIMENSION T(80),G(80)
      X5=0.
      X6=0.
      DO 100 I=1,N3
      X7=(TV-T(I))*G(I)
      IF(X7.LE.0.) X5=X5-X7
  100 IF(X7.GT.0.) X6=X6+X7
      QIN=X5
      QOUT=X6
      RETURN
      END
C
C
C     THIS FUNCTION CALCULATES THE Q*LEFFECTIVE(POWER-LENGTH)
C     CAPACITY, E.G., BTU/HR-INCH OR WATT-METER
C
C
      FUNCTION QL(A,B,C,D,E,Z)
      A1=D-C
      A2=D+B
      A3=A-B-D
      IF(C.GE.D.AND.C.LT.A) GO TO 100
      IF(C.GE.A) GO TO 101
      Z=A1/2.+B+A3/2.
      GO TO 102
  100 Z=(A-C)/2.
```

```
07240         GO TO 102
07250   101   Z=0.
07260   102   QL=Z*F
07270         RETURN
07280         END
07290 C
07300 C       THIS SUBROUTINE CALCULATES THE ROOTS OF A QUADRATIC EQUATION
07310 C       WHICH RESULTS FROM A QUADRATIC FIT OF THREE VALUES OF
07320 C       CALCULATED POWER-LENGTH CAPACITIES.
07330 C
07340         SUBROUTINE QUADRA(L1,L2,L3,LP,QLC1,QLC2,QLC3,QLCT)
07350         REAL L1,L2,L3,LP,L5
07360         F1=QLC1-QLCT
07370         F2=QLC2-QLCT
07380         F3=QLC3-QLCT
07390 C       CALCULATE THE COEFFICIENTS OF F(Z)=A+B*Z+C*Z**2
07400 C
07410         A1=(F1*(L2-L3)+F2*(L3-L1)+F3*(L1-L2))
07420         A2=(L1**2*(L2-L3)+L2**2*(L3-L1)+L3**2*(L1-L2))
07430         IF(A2.EQ.0.) PRINT 10,L1,L2,L3,F1,F2,F3
07440   10    FORMAT(1X,/3(E22.15,2X))
07450         A=A1/A2
07460         B=((F2-F3)-A*(L2**2-L3**2))/(L2-L3)
07470         C=F3-A*L3**2-B*L3
07480         A2=2.*A
07490         Y=SQRT(B**2-4.*A*C)
07500         Z1=(-B+Y)/A2
07510         Z2=-(B+Y)/A2
07520         IF(Z1.LT..0.OR.Z1.GT.L3) GO TO 100
07530         IF(Z1.LT.L1) GO TO 100
07540         LP=Z1
07550         GO TO 101
07560   100   LP=Z2
07570   101   CONTINUE
07580         RETURN
07590         END
07600 C
07610 C       THIS SUBROUTINE PERFORMS A QUADRATIC BINARY SEARCH OF THE
07620 C       REQUIRED POWER-LENGTH CAPACITY.
07630 C
07640         SUBROUTINE BINARY(L1,L2,L3,LP,QLC,QLC1,QLC2,QLC3,QLCT,IR)
07650         REAL L1,L2,L3,L4,L5,LP
```

```
07660         IF(IB.EQ.0) GO TO 200
07670         IB=0
07680         F1=QLC1-QLCT
07690         F2=QLC2-QLCT
07700         F3=QLC3-QLCT
07710         F4=QLC-QLCT
07720         IF(LP .GT.L2) GO TO 201
07730         L5=L3
07740         L3=L2
07750         L2=LP
07760         L4=L5
07770         F2=F4
07780         F3=QLC2-QLCT
07790         F4=QLC3-QLCT
07800         SIGN1=F1*F2
07810         SIGN2=F3*F2
07820         SIGN3=F2*F4
07830         IF(SIGN1.LT.0.) GO TO 202
07840         IF(SIGN2.LT.0.) GO TO 203
07850         IF(SIGN3.LT.0.) GO TO 204
07860   202   DX=(L2-L1)/2.
07870         L3=L2
07880         L2=L1+DX
07890         QLC3=QLC
07900         GO TO 300
07910   203   DX=(L3-L2)/2.
07920         L1=L2
07930         L2=L2+DX
07940         QLC1=QLC
07950         QLC3=QLC2
07960         GO TO 300
07970   204   DX=(L4-L2)/2.
07980         L1=L2
07990         L2=L2+DX
08000         L3=L4
08010         QLC1=QLC
08020         QLC3=QLC3
08030         GO TO 300
08040   201   L5=L3
08050         L3=LP
08060         L4=L5
08070         F3=QLC-QLCT
```

```
08080           F4=QLC3-QLCT
08090           SIGN1=F1*F3
08100           SIGN2=F2*F3
08110           SIGN3=F3*F4
08120           IF(SIGN2.LT.0.) GO TO 302
08130           IF(SIGN3.LT.0.) GO TO 303
08140           IF(SIGN1.LT.0.) GO TO 304
08150   302     DX=(L3-L2)/2.
08160           L1=L2
08170           L2=L2+DX
08180           QLC1=QLC2
08190           QLC3=QLC
08200           GO TO 300
08210   303     DX=(L4-L3)/2.
08220           L1=L3
08230           L2=L3+DX
08240           L3=L4
08250           QLC1=QLC
08260           GO TO 300
08270   304     DX=(L3-L1)/2.
08280           L2=L1+DX
08290           QLC3=QLC
08300           GO TO 300
08310   200     IB=1
08320           GO TO 301
08330   300     LP=L2
08340   301     RETURN
08350           END
```

VARIABLE CONDUCTANCE HEAT PIPE TEST CASE

********** TIME= 0.00000
DTIMEU= 0.00000 CSGMIN(33)= 9.76562E-03 TEMPCC(25)= 0.00000 RELXCC(26)= 8.49406E-02

T	23=-7.71369E+01	T	24=-6.36237E+01	T	25=-3.53098E+01	T	26= 1.76123E+01	T	27= 5.84899E+01
T	28= 6.02895E+01	T	29= 6.03695E+01	T	30= 6.03747E+01	T	31= 6.04130E+01	T	33= 8.83257E+01
T	34=-9.76865E+01	T	1=-9.34746E+01	T	2=-8.50323E+01	T	3=-7.57267E+01	T	4=-6.16585E+01
T	5=-3.19624E+01	T	6= 2.43206E+01	T	7= 6.86867E+01	T	8= 7.06592E+01	T	9= 7.07470E+01
T	10= 7.07528E+01	T	11= 7.07948E+01	T	12= 7.38431E+01	T	13= 7.48972E+01	T	14= 7.49431E+01
T	15= 7.94214E+01	T	16= 7.94468E+01	T	17= 7.94476E+01	T	18= 7.94477E+01	T	19= 7.94477E+01
T	20= 7.94478E+01	T	22=-8.60501E+01	T	32= 6.36764E+01	T	35=-1.20000E+02	T	36= 7.49055E+01

G	-1= 3.46000E-10	G	-2= 3.46000E-10	G	-3= 3.46000E-10	G	-4= 3.46000E-10	G	-5= 3.46000E-10
G	-6= 3.46000E-10	G	-7= 3.46000E-10	G	-8= 3.46000E-10	G	-9= 3.46000E-10	G	-10= 8.22000E-11
G	-11= 8.22000E-11	G	12= 5.00000E-01	G	13= 2.00000E+00	G	14= 2.00000E+00	G	15= 2.00000E+00
G	16= 2.00000E+00	G	17= 2.00000E+00	G	18= 2.00000E+00	G	19= 2.00000E+00	G	20= 2.00000E+00
G	21= 2.00000E+00	G	22= 5.00000E-01	G	23= 2.56000E+00	G	24= 2.56000E+00	G	25= 2.56000E+00
G	26= 2.56000E+00	G	27= 2.56000E+00	G	28= 2.56000E+00	G	29= 5.05000E-02	G	30= 2.52000E-02
G	31= 7.77000E-02	G	32= 2.52000E-01	G	33= 2.52000E-01	G	34= 2.52000E-01	G	35= 2.52000E-01
G	36= 2.52000E-01	G	37= 2.52000E-01	G	38= 2.52000E-01	G	39= 2.52000E-01	G	40= 7.77000E-02
G	41= 2.52000E-02	G	42= 2.52000E-02	G	43= 4.58000E-02	G	44= 2.52000E-01	G	45= 2.52000E-01
G	46= 2.52000E-01	G	47= 2.52000E-01	G	48= 2.52000E-01	G	-49= 5.48480E-11	G	50= 0.00000
G	51= 0.00000	G	52= 0.00000	G	53= 0.00000	G	54= 0.00000	G	55= 3.26717E-01
G	56= 5.00000E+00	G	57= 5.00000E+00	G	58= 5.00000E+00	G	59= 5.00000E+00	G	60= 5.00000E+00
G	61= 5.00000E+00	G	62= 5.00000E+00	G	63= 5.00000E+00	G	64= 5.00000E+00	G	65= 5.00000E+00
G	66= 5.00000E+00	G	67= 5.00000E+00	G	68= 5.00000E+00	G	69= 5.00000E+00		

HEAT PIPE NUMBER 1 CHARACTERISTICS

TOTAL LENGTH= 40.00IN GAS V/L= .115IN**3/IN RES VOLUME= 6.710 IN-3
GAS INVENTORY = .2530 FT-1B/R RESERVOIR IS WICKED
VAPOR TEMP = 74.91 F TOTAL PRESS = 141.45 PSIA GAS LGTH = 11.87IN DRY EVAP LGTH= 0.00 IN
RESERVOIR TEMP= -97.69 F RES GAS PRESS= 140.05 PSIA
SUM QIN= 136.32 BTU/HR, SUM QOUT= 136.32 BTU/HR LEFF= 16.32 INCHES QLEFF= 2224.1 BTU-INCH/HR
RESERVOIR GAS NR= .216148 HEAT PIPE NR= .036852 RESIDUAL= .000001

TOTAL HEAT EXCHANGE TO BOUNDARIES -1.35907E+02
QB 35=-1.35907E+02 QB 36=-1.47793E-10

VARIABLE CONDUCTANCE HEAT PIPE TEST CASE

********** TIME= 1.00000E+00
DTIMEU= 7.23656E-03 CSGMIN(33)= 9.76562E-03 TEMPCC(23)= 9.57947E-04 RELXCC(6)= 1.36499E-03

T	23=-7.65756E+01	T	24=-6.28810E+01	T	25=-3.41951E+01	T	26= 1.92357E+01	T	27= 5.86162E+01
T	28= 6.03491E+01	T	29= 6.04261E+01	T	30= 6.04312E+01	T	31= 6.04695E+01	T	33= 8.83903E+01
T	34=-9.75946E+01	T	1=-9.32712E+01	T	2=-8.46063E+01	T	3=-7.51467E+01	T	4=-6.[illegible]888E+01
T	5=-3.08186E+01	T	6= 2.60508E+01	T	7= 6.88196E+01	T	8= 7.07206E+01	T	9= 7.08052E+01
T	10= 7.08108E+01	T	11= 7.08527E+01	T	12= 7.39015E+01	T	13= 7.49557E+01	T	14= 7.50016E+01
T	15= 7.94820E+01	T	16= 7.95075E+01	T	17= 7.95083E+01	T	18= 7.95083E+01	T	19= 7.95083E+01
T	20= 7.95083E+01	T	22=-8.56384E+01	T	32= 6.37296E+01	T	35=-1.20000E+02	T	36= 7.49608E+01

G	-1= 3.46000E-10	G	-2= 3.46000E-10	G	-3= 3.46000E-10	G	-4= 3.46000E-10	G	-5= 3.46000E-10
G	-6= 3.46000E-10	G	-7= 3.46000E-10	G	-8= 3.46000E-10	G	-9= 3.46000E-10	G	-10= 8.22000E-11
G	-11= 8.22000E-11	G	12= 5.00000E-01	G	13= 2.00000E+00	G	14= 2.00000E+00	G	15= 2.00000E+00
G	16= 2.00000E+00	G	17= 2.00000E+00	G	18= 2.00000E+00	G	19= 2.00000E+00	G	20= 2.00000E+00
G	21= 2.00000E+00	G	22= 5.00000E-01	G	23= 2.56000E+00	G	24= 2.56000E+00	G	25= 2.56000E+00
G	26= 2.56000E+00	G	27= 2.56000E+00	G	28= 2.56000E+00	G	29= 5.05000E-02	G	30= 2.52000E-02
G	31= 7.77000E-02	G	32= 2.52000E-01	G	33= 2.52000E-01	G	34= 2.52000E-01	G	35= 2.52000E-01
G	36= 2.52000E-01	G	37= 2.52000E-01	G	38= 2.52000E-01	G	39= 2.52000E-01	G	40= 7.77000E-02
G	41= 2.52000E-02	G	42= 2.52000E-02	G	43= 4.58000E-02	G	44= 2.52000E-01	G	45= 2.52000E-01
G	46= 2.52000E-01	G	47= 2.52000E-01	G	48= 2.52000E-01	G	-49= 5.48480E-11	G	50= 0.00000
G	51= 0.00000	G	52= 0.00000	G	53= 0.00000	G	54= 0.00000	G	55= 3.51348E-01
G	56= 5.00000E+00	G	57= 5.00000E+00	G	58= 5.00000E+00	G	59= 5.00000E+00	G	60= 5.00000E+00
G	61= 5.00000E+00	G	62= 5.00000E+00	G	63= 5.00000E+00	G	64= 5.00000E+00	G	65= 5.00000E+00
G	66= 5.00000E+00	G	67= 5.00000E+00	G	68= 5.00000E+00	G	69= 5.00000E+00		

HEAT PIPE NUMBER 1 CHARACTERISTICS

TOTAL LENGTH= 40.000IN GAS V/L= .115IN**3/IN RES VOLUME= 6.710 IN-3
GAS INVENTORY = .2530 FT-LB/R RESERVOIR IS WICKED
VAPOR TEMP = 74.96 F TOTAL PRESS = 141.58 PSIA GAS LGTH = 11.86IN DRY EVAP LGTH= 0.00 IN
RESERVOIR TEMP= -97.59 F RES GAS PRESS= 140.18 PSIA
SUM QIN= 136.49 BTU/HR, SUM QOUT= 136.49 BTU/HR LEFF= 16.32 INCHES QLEFF= 2227.5 BTU-INCH/HR
RESERVOIR GAS NR= .216293 HEAT PIPE NR= .036707 RESIDUAL= -.000000

TOTAL HEAT EXCHANGE TO BOUNDARIES -1.36459E+02
QB 35=-1.36459E+02 QB 36=-1.60526E-10

VARIABLE CONDUCTANCE HEAT PIPE TEST CASE

********** TIME= 1.20000E+00
DTIMEU= 7.22656E-03 CSGMIN(33)= 9.76562E-03 TEMPCC(31)= 3.24291E+00 RELXCC(2)= 9.04152E-02

T	23=-8.05490E+01	T	24=-7.28250E+01	T	25=-6.10005E+01	T	26=-4.78218E+01	T	27=-3.61980E+01
T	28=-2.68526E+01	T	29=-1.77450E+01	T	30=-5.21865E+00	T	31= 1.48030E+01	T	33= 6.93290E+01
T	34=-9.76237E+01	T	1=-9.42290E+01	T	2=-8.75166E+01	T	3=-7.98901E+01	T	4=-7.23265E+01
T	5=-6.08279E+01	T	6=-4.79829E+01	T	7=-3.64410E+01	T	8=-2.68535E+01	T	9=-1.73171E+01
T	10=-4.39474E+00	T	11= 1.50650E+01	T	12= 6.72487E+01	T	13= 6.90027E+01	T	14= 6.90124E+01
T	15= 6.91184E+01	T	16= 6.91190E+01	T	17= 6.91190E+01	T	18= 6.91190E+01	T	19= 6.91190E+01
T	20= 6.91190E+01	T	22=-8.84529E+01	T	32= 5.76419E+01	T	35=-1.20000E+02	T	36= 6.90115E+01

G	-1= 3.46000E-10	G	-2= 3.46000E-10	G	-3= 3.46000E-10	G	-4= 3.46000E-10	G	-5= 3.46000E-10
G	-6= 3.46000E-10	G	-7= 3.46000E-10	G	-8= 3.46000E-10	G	-9= 3.46000E-10	G	-10= 8.22000E-11
G	-11= 8.22000E-11	G	12= 5.00000E-01	G	13= 2.00000E+00	G	14= 2.00000E+00	G	15= 2.00000E+00
G	16= 2.00000E+00	G	17= 2.00000E+00	G	18= 2.00000E+00	G	19= 2.00000E+00	G	20= 2.00000E+00
G	21= 2.00000E+00	G	22= 5.00000E-01	G	23= 2.56000E+00	G	24= 2.56000E+00	G	25= 2.56000E+00
G	26= 2.56000E+00	G	27= 2.56000E+00	G	28= 2.56000E+00	G	29= 5.05000E-02	G	30= 2.52000E-02
G	31= 7.77000E-02	G	32= 2.52000E-01	G	33= 2.52000E-01	G	34= 2.52000E-01	G	35= 2.52000E-01
G	36= 2.52000E-01	G	37= 2.52000E-01	G	38= 2.52000E-01	G	39= 2.52000E-01	G	40= 7.77000E-02
G	41= 2.52000E-02	G	42= 2.52000E-02	G	43= 4.58000E-02	G	44= 2.52000E-01	G	45= 2.52000E-01
G	46= 2.52000E-01	G	47= 2.52000E-01	G	48= 2.52000E-01	G	-49= 5.48480E-11	G	50= 0.00000
G	51= 0.00000	G	52= 0.00000	G	53= 0.00000	G	54= 0.00000	G	55= 0.00000
G	56= 0.00000	G	57= 0.00000	G	58= 0.00000	G	59= 0.00000	G	60= 7.61818E-03
G	61= 5.00000E+00	G	62= 5.00000E+00	G	63= 5.00000E+00	G	64= 5.00000E+00	G	65= 5.00000E+00
G	66= 5.00000E+00	G	67= 5.00000E+00	G	68= 5.00000E+00	G	69= 5.00000E+00		

HEAT PIPE NUMBER 1 CHARACTERISTICS

TOTAL LENGTH= 40.00IN GAS V/L= .115IN**3/IN RES VOLUME= 6.710 IN-3
GAS INVENTORY = .2530 FT-LB/R RESERVOIR IS WICKED
VAPOR TEMP = 68.88 F TOTAL PRESS = 127.08 PSIA GAS LGTH = 22.00IN DRY EVAP LGTH= 0.00 IN
RESERVOIR TEMP= -97.62 F RES GAS PRESS= 125.68 PSIA
SUM QIN= 8.55 BTU/HR, SUM QOUT= 8.55 BTU/HR LEFF= 11.25 INCHES QLEFF= 96.2 BTU-INCH/HR
RESERVOIR GAS NR= .193926 HEAT PIPE NR= .059075 RESIDUAL= -.000001

TOTAL HEAT EXCHANGE TO BOUNDARIES -6.65372E+01
QB 35=-6.65372E+01 QB 36=-6.09930E-11

VARIABLE CONDUCTANCE HEAT PIPE TEST CASE

********** TIME= 1.80000E+00
DTIMEU= 7.22656E-03 CSGMIN(33)= 9.76562E-03 TEMPCC(30)= 3.84640E-01 RELXCC(12)= 9.01424E-02

T	23=-1.06576E+02	T	24=-1.05874E+02	T	25=-1.04760E+02	T	26=-1.03336E+02	T	27=-1.01692E+02
T	28=-9.99056E+01	T	29=-9.80225E+01	T	30=-9.60041E+01	T	31=-9.35985E+01	T	33= 6.25676E+01
T	34=-1.00556E+02	T	1=-1.02685E+02	T	2=-1.07002E+02	T	3=-1.06508E+02	T	4=-1.05821E+02
T	5=-1.04720E+02	T	6=-1.03308E+02	T	7=-1.01673E+02	T	8=-9.98915E+01	T	9=-9.80017E+01
T	10=-9.59483E+01	T	11=-9.34561E+01	T	12=-8.17984E+01	T	13=-2.53019E+01	T	14= 3.11628E+01
T	15= 6.22303E+01	T	16= 6.25717E+01	T	17= 6.25824E+01	T	18= 6.25827E+01	T	19= 6.25827E+01
T	20= 6.25827E+01	T	22=-1.07348E+02	T	32=-8.29255E+01	T	35=-1.20000E+02	T	36= 6.25905E+01

G	-1= 3.46000E-10	G	-2= 3.46000E-10	G	-3= 3.46000E-10	G	-4= 3.46000E-10	G	-5= 3.46000E-10
G	-6= 3.46000E-10	G	-7= 3.46000E-10	G	-8= 3.46000E-10	G	-9= 3.46000E-10	G	-10= 8.22000E-11
G	-11= 8.22000E-11	G	12= 5.00000E-01	G	13= 2.00000E+00	G	14= 2.00000E+00	G	15= 2.00000E+00
G	16= 2.00000E+00	G	17= 2.00000E+00	G	18= 2.00000E+00	G	19= 2.00000E+00	G	20= 2.00000E+00
G	21= 2.00000E+00	G	22= 5.00000E-01	G	23= 2.56000E+00	G	24= 2.56000E+00	G	25= 2.56000E+00
G	26= 2.56000E+00	G	27= 2.56000E+00	G	28= 2.56000E+00	G	29= 5.05000E-02	G	30= 2.52000E-02
G	31= 7.77000E-02	G	32= 2.52000E-01	G	33= 2.52000E-01	G	34= 2.52000E-01	G	35= 2.52000E-01
G	36= 2.52000E-01	G	37= 2.52000E-01	G	38= 2.52000E-01	G	39= 2.52000E-01	G	40= 7.77000E-02
G	41= 2.52000E-02	G	42= 2.52000E-02	G	43= 4.58000E-02	G	44= 2.52000E-01	G	45= 2.52000E-01
G	46= 2.52000E-01	G	47= 2.52000E-01	G	48= 2.52000E-01	G	-49= 5.48480E-11	G	50= 0.00000
G	51= 0.00000	G	52= 0.00000	G	53= 0.00000	G	54= 0.00000	G	55= 0.00000
G	56= 0.00000	G	57= 0.00000	G	58= 0.00000	G	59= 0.00000	G	60= 0.00000
G	61= 0.00000	G	62= 0.00000	G	63= 0.00000	G	64= 9.97868E-01	G	65= 5.00000E+00
G	66= 5.00000E+00	G	67= 5.00000E+00	G	68= 5.00000E+00	G	69= 5.00000E+00		

HEAT PIPE NUMBER 1 CHARACTERISTICS

TOTAL LENGTH= 40.00IN GAS V/L= .115IN**3/IN RES VOLUME= 6.710 IN-3
GAS INVENTORY = .2530 FT-LB/R RESERVOIR IS WICKED
VAPOR TEMP = 62.57 F TOTAL PRESS = 113.62 PSIA GAS LGTH = 29.60IN DRY EVAP LGTH= 0.00 IN
RESERVOIR TEMP= -100.56 F RES GAS PRESS= 112.40 PSIA
SUM QIN= .34 BTU/HR, SUM QOUT= .34 BTU/HR LEFF= 5.20 INCHES QLEFF= 1.7 BTU-INCH/HR
RESERVOIR GAS NR= .174851 HEAT PIPE NR= .078148 RESIDUAL= .000001

TOTAL HEAT EXCHANGE TO BOUNDARIES -1.10248E+01
QB 35=-1.10248E+01 QB 36=-1.80425E-11

VARIABLE CONDUCTANCE HEAT PIPE TEST CASE

********** TIME= 2.00000E+00
DTIMEU= 7.22656E-03 CSGMIN(33)= 9.76562E-03 TEMPCC(30)= 2.09753E-01 RELXCC(12)= 8.48855E-02

T	23=-1.10685E+02	T	24=-1.10423E+02	T	25=-1.09866E+02	T	26=-1.09086E+02	T	27=-1.08128E+02
T	28=-1.07001E+02	T	29=-1.05645E+02	T	30=-1.03888E+02	T	31=-1.01345E+02	T	33= 6.09382E+01
T	34=-1.02045E+02	T	1=-1.04727E+02	T	2=-1.10158E+02	T	3=-1.10633E+02	T	4=-1.10383E+02
T	5=-1.09835E+02	T	6=-1.09060E+02	T	7=-1.08103E+02	T	8=-1.06967E+02	T	9=-1.05588E+02
T	10=-1.03783E+02	T	11=-1.01152E+02	T	12=-8.77315E+01	T	13=-2.95995E+01	T	14= 2.84702E+01
T	15= 6.04146E+01	T	16= 6.08954E+01	T	17= 6.09352E+01	T	18= 6.09385E+01	T	19= 6.09383E+01
T	20= 6.09382E+01	T	22=-1.10416E+02	T	32=-8.86609E+01	T	35=-1.20000E+02	T	36= 6.10084E+01

G	-1= 3.46000E-10	G	-2= 3.46000E-10	G	-3= 3.46000E-10	G	-4= 3.46000E-10	G	-5= 3.46000E-10
G	-6= 3.46000E-10	G	-7= 3.46000E-10	G	-8= 3.46000E-10	G	-9= 3.46000E-10	G	-10= 8.62000E-11
G	-11= 8.62000E-11	G	12= 5.00000E-01	G	13= 2.00000E+00	G	14= 2.00000E+00	G	15= 2.00000E+00
G	16= 2.00000E+00	G	17= 2.00000E+00	G	18= 2.00000E+00	G	19= 2.00000E+00	G	20= 2.00000E+00
G	21= 2.56000E+00	G	22= 5.00000E-01	G	23= 2.56000E+00	G	24= 2.56000E+00	G	25= 2.56000E+00
G	26= 2.56000E+00	G	27= 2.56000E+00	G	28= 2.56000E+00	G	29= 5.05000E-02	G	30= 2.52000E-02
G	31= 1.26000E-02	G	32= 2.52000E-01	G	33= 2.52000E-01	G	34= 2.52000E-01	G	35= 2.52000E-01
G	36= 5.04000E-01	G	37= 2.52000E-01	G	38= 2.52000E-01	G	39= 2.52000E-01	G	40= 7.77000E-02
G	41= 2.52000E-02	G	42= 2.52000E-02	G	43= 4.58000E-02	G	44= 2.52000E-01	G	45= 2.52000E-01
G	46= 2.52000E-01	G	47= 2.52000E-01	G	48= 2.52000E-01	G	-49= 5.48480E-11	G	50= 0.00000
G	51= 0.00000	G	52= 0.00000	G	53= 0.00000	G	54= 0.00000	G	55= 0.00000
G	56= 0.00000	G	57= 0.00000	G	58= 0.00000	G	59= 0.00000	G	60= 0.00000
G	61= 0.00000	G	62= 0.00000	G	63= 0.00000	G	64= 0.00000	G	65= 0.00000
G	66= 0.00000	G	67= 0.00000	G	68= 0.00000	G	69= 0.00000		

HEAT PIPE NUMBER 1 CHARACTERISTICS
TOTAL LENGTH= 40.00IN GAS V/L= .115IN**3/IN RES VOLUME= 6.710 IN**3
GAS INVENTORY= .2530 FT-LB/RRESERVOIR IS WICKED
LOCATION OF ICE PLUG= 4.00 IN POSITION OF GAS FRONT= 40.00 IN DRY EVAP LGTH= 0.00 IN
GAS IN RES SIDE= .186676 GAS IN EVAP SIDE= .066324 GAS RESIDUAL= 0.000000
TOTAL PRESSURE IN RES SIDE= 112.87 PSIA TOTAL PRESSURE ON EVAP SIDE= 111.32 PSIA PEV-PRE= -1.55 PSIA
RES TEMPERATURE= -102.04 F EVAP SIDE VAPOR TEMP= 60.94 F
SUM QIN= 0.00 BTU/HR, SUM QOUT= 0.00 BTU/HR LEFF= 0.00 INCHES QLEFF= 0.0 BTU-INCH/HR

TOTAL HEAT EXCHANGE TO BOUNDARIES -7.33479E+00
QB 35=-7.33479E+00 QB 36= 0.00000

VARIABLE CONDUCTANCE HEAT PIPE TEST CASE

********** TIME= 4.00000E+00
DTIMEU= 7.22656E-03 CSGMIN(33)= 9.76562E-03 TEMPCC(33)= 6.29288E-02 RELXCC(18)= 6.29812E-02

T	23=-1.19025E+02	T	24=-1.19121E+02	T	25=-1.19083E+02	T	26=-1.18897E+02	T	27=-1.18521E+02
T	28=-1.17876E+02	T	29=-1.16824E+02	T	30=-1.15145E+02	T	31=-1.12481E+02	T	33= 4.28057E+01
T	34=-1.13432E+02	T	1=-1.15018E+02	T	2=-1.18206E+02	T	3=-1.19006E+02	T	4=-1.19104E+02
T	5=-1.19063E+02	T	6=-1.18872E+02	T	7=-1.18486E+02	T	8=-1.17823E+02	T	9=-1.16742E+02
T	10=-1.15016E+02	T	11=-1.12278E+02	T	12=-9.81778E+01	T	13=-4.30292E+01	T	14= 1.20647E+01
T	15= 4.23155E+01	T	16= 4.27708E+01	T	17= 4.28085E+01	T	18= 4.28116E+01	T	19= 4.28114E+01
T	20= 4.28062E+01	T	22=-1.18252E+02	T	32=-9.87798E+01	T	35=-1.20000E+02	T	36= 4.28691E+01

G	-1= 3.46000E-10	G	-2= 3.46000E-10	G	-3= 3.46000E-10	G	-4= 3.46000E-10	G	-5= 3.46000E-10
G	-6= 3.46000E-10	G	-7= 3.46000E-10	G	-8= 3.46000E-10	G	-9= 3.46000E-10	G	-10= 8.22000E-11
G	-11= 8.22000E-11	G	12= 5.00000E-01	G	13= 2.00000E+00	G	14= 2.00000E+00	G	15= 2.00000E+00
G	16= 2.00000E+00	G	17= 2.00000E+00	G	18= 2.00000E+00	G	19= 2.00000E+00	G	20= 2.00000E+00
G	21= 2.00000E+00	G	22= 5.00000E-01	G	23= 2.56000E+00	G	24= 2.56000E+00	G	25= 2.56000E+00
G	26= 2.56000E+00	G	27= 2.56000E+00	G	28= 2.56000E+00	G	29= 5.05000E-02	G	30= 2.52000E-02
G	31= 7.77000E-02	G	32= 2.52000E-01	G	33= 2.52000E-01	G	34= 2.52000E-01	G	35= 2.52000E-01
G	36= 2.52000E-01	G	37= 2.52000E-01	G	38= 2.52000E-01	G	39= 2.52000E-01	G	40= 7.77000E-02
G	41= 2.52000E-02	G	42= 2.52000E-02	G	43= 4.58000E-02	G	44= 2.52000E-01	G	45= 2.52000E-01
G	46= 2.52000E-01	G	47= 2.52000E-01	G	48= 2.52000E-01	G	-49= 5.48480E-11	G	50= 0.00000
G	51= 0.00000	G	52= 0.00000	G	53= 0.00000	G	54= 0.00000	G	55= 0.00000
G	56= 0.00000	G	57= 0.00000	G	58= 0.00000	G	59= 0.00000	G	60= 0.00000
G	61= 0.00000	G	62= 0.00000	G	63= 0.00000	G	64= 0.00000	G	65= 0.00000
G	66= 0.00000	G	67= 0.00000	G	68= 0.00000	G	69= 0.00000		

HEAT PIPE NUMBER 1 CHARACTERISTICS
TOTAL LENGTH= 40.00IN GAS V/L= .115IN**3/IN RES VOLUME= 6.710 IN**3
GAS INVENTORY= .2530 FT-LB/RRESERVOIR IS WICKED
LOCATION OF ICE PLUG= 4.00 IN POSITION OF GAS FRONT= 40.00 IN DRY EVAP LGTH= 0.00 IN
GAS IN RES SIDE= .186676 GAS IN EVAP SIDE= .066324 GAS RESIDUAL= 0.000000
TOTAL PRESSURE IN RES SIDE= 108.90 PSIA TOTAL PRESSURE ON EVAP SIDE= 99.38 PSIA PEV-PRE= -9.53 PSIA
RES TEMPERATURE= -113.43 F EVAP SIDE VAPOR TEMP= 42.81 F
SUM QIN= 0.00 BTU/HR, SUM QOUT= 0.00 BTU/HR LEFF= 0.00 INCHES QLEFF= 0.0 BTU-INCH/HR

TOTAL HEAT EXCHANGE TO BOUNDARIES -1.65910E+00
QB 35=-1.65910E+00 QB 36= 0.00000

VARIABLE CONDUCTANCE HEAT PIPE TEST CASE

********** TIME= 4.20000E+00
DTIMEU= 7.22656E-03 CSGMIN(33)= 9.76562E-03 TEMPCC(31)= 6.08291E+00 RELXCC(9)= 6.51485E-02

T	23=-1.19138E+02	T	24=-1.19207E+02	T	25=-1.19124E+02	T	26=-1.18776E+02	T	27=-1.17693E+02
T	28=-1.14101E+02	T	29=-1.01889E+02	T	30=-6.29855E+01	T	31= 4.33758E+01	T	33= 9.13351E+01
T	34=-1.14093E+02	T	1=-1.15536E+02	T	2=-1.18428E+02	T	3=-1.19120E+02	T	4=-1.19186E+02
T	5=-1.19084E+02	T	6=-1.18661E+02	T	7=-1.17305E+02	T	8=-1.12826E+02	T	9=-9.81648E+01
T	10=-5.39366E+01	T	11= 6.21087E+01	T	12= 7.79318E+01	T	13= 7.92174E+01	T	14= 7.92605E+01
T	15= 8.33012E+01	T	16= 8.33241E+01	T	17= 8.33249E+01	T	18= 8.33249E+01	T	19= 8.33249E+01
T	20= 8.33249E+01	T	22=-1.18468E+02	T	32= 6.74087E+01	T	35=-1.20000E+02	T	36= 7.92237E+01

G	-1= 3.46000E-10	G	-2= 3.46000E-10	G	-3= 3.46000E-10	G	-4= 3.46000E-10	G	-5= 3.46000E-10
G	-6= 3.46000E-10	G	-7= 3.46000E-10	G	-8= 3.46000E-10	G	-9= 3.46000E-10	G	-10= 8.22000E-11
G	-11= 8.22000E-11	G	12= 5.00000E-01	G	13= 2.00000E+00	G	14= 2.00000E+00	G	15= 2.00000E+00
G	16= 2.00000E+00	G	17= 2.00000E+00	G	18= 2.00000E+00	G	19= 2.00000E+00	G	20= 2.00000E+00
G	21= 2.00000E+00	G	22= 5.00000E-01	G	23= 2.56000E+00	G	24= 2.56000E+00	G	25= 2.56000E+00
G	26= 2.56000E+00	G	27= 2.56000E+00	G	28= 2.56000E+00	G	29= 5.05000E-02	G	30= 2.52000E-02
G	31= 7.77000E-02	G	32= 2.52000E-01	G	33= 2.52000E-01	G	34= 2.52000E-01	G	35= 2.52000E-01
G	36= 2.52000E-01	G	37= 2.52000E-01	G	38= 2.52000E-01	G	39= 2.52000E-01	G	40= 7.77000E-02
G	41= 2.52000E-02	G	42= 2.52000E-02	G	43= 4.58000E-02	G	44= 2.52000E-01	G	45= 2.52000E-01
G	46= 2.52000E-01	G	47= 2.52000E-01	G	48= 2.52000E-01	G	-49= 5.48480E-11	G	50= 0.00000
G	51= 0.00000	G	52= 0.00000	G	53= 0.00000	G	54= 0.00000	G	55= 0.00000
G	56= 0.00000	G	57= 0.00000	G	58= 0.00000	G	59= 9.15553E-03	G	60= 5.00000E+00
G	61= 5.00000E+00	G	62= 5.00000E+00	G	63= 5.00000E+00	G	64= 5.00000E+00	G	65= 5.00000E+00
G	66= 5.00000E+00	G	67= 5.00000E+00	G	68= 5.00000E+00	G	69= 5.00000E+00		

HEAT PIPE NUMBER 1 CHARACTERISTICS
TOTAL LENGTH= 40.00IN GAS V/L= .115IN**3/IN RES VOLUME= 6.710 IN**3
GAS INVENTORY= .2530 FT-LB/RRESERVOIR IS WICKED
LOCATION OF ICE PLUG= 4.00 IN POSITION OF GAS FRONT= 20.00 IN DRY EVAP LGTH= 0.00 IN
GAS IN RES SIDE= .186676 GAS IN EVAP SIDE= .066324 GAS RESIDUAL= -.000000
TOTAL PRESSURE IN RES SIDE= 108.68 PSIA TOTAL PRESSURE ON EVAP SIDE= 153.45 PSIA PEV-PRE= 44.77 PSIA
RES TEMPERATURE= -114.09 F EVAP SIDE VAPOR TEMP= 79.82 F
SUM QIN= 105.03 BTU/HR, SUM QOUT= 105.03 BTU/HR LEFF= 12.25 INCHES QLEFF= 1286.8 BTU-INCH/HR

TOTAL HEAT EXCHANGE TO BOUNDARIES -2.86253E+01
QB 35=-2.86253E+01 QB 36=-5.09317E-11

VARIABLE CONDUCTANCE HEAT PIPE TEST CASE

********** TIME= 5.00000E+00
DTIMEU= 7.22656E-03 CSGMIN(33)= 9.76562E-03 TEMPCC(28)= 6.18198E-01 RELXCC(7)= 8.71805E-02

T	23=-1.09210E+02	T	24=-1.03930E+02	T	25=-9.23761E+01	T	26=-7.07886E+01	T	27=-3.20878E+01
T	28= 3.76153E+01	T	29= 8.72459E+01	T	30= 8.94233E+01	T	31= 8.95687E+01	T	33= 1.21813E+02
T	34=-1.15433E+02	T	1=-1.14114E+02	T	2=-1.11401E+02	T	3=-1.08626E+02	T	4=-1.03110E+02
T	5=-9.10588E+01	T	6=-6.85088E+01	T	7=-2.77775E+01	T	8= 4.71821E+01	T	9= 1.00685E+02
T	10= 1.03067E+02	T	11= 1.03228E+02	T	12= 1.07252E+02	T	13= 1.08630E+02	T	14= 1.08677E+02
T	15= 1.13073E+02	T	16= 1.13098E+02	T	17= 1.13099E+02	T	18= 1.13099E+02	T	19= 1.13099E+02
T	20= 1.13099E+02	T	22=-1.11625E+02	T	32= 9.39670E+01	T	35=-1.20000E+02	T	36= 1.08637E+02

G	-1= 3.46000E-10	G	-2= 3.46000E-10	G	-3= 3.46000E-10	G	-4= 3.46000E-10	G	-5= 3.46000E-10
G	-6= 3.46000E-10	G	-7= 3.46000E-10	G	-8= 3.46000E-10	G	-9= 3.46000E-10	G	-10= 8.22000E-11
G	-11= 8.22000E-11	G	12= 5.00000E-01	G	13= 2.00000E+00	G	14= 2.00000E+00	G	15= 2.00000E+00
G	16= 2.00000E+00	G	17= 2.00000E+00	G	18= 2.00000E+00	G	19= 2.00000E+00	G	20= 2.00000E+00
G	21= 2.00000E+00	G	22= 5.00000E-01	G	23= 2.56000E+00	G	24= 2.56000E+00	G	25= 2.56000E+00
G	26= 2.56000E+00	G	27= 2.56000E+00	G	28= 2.56000E+00	G	29= 5.05000E-02	G	30= 2.52000E-02
G	31= 7.77000E-02	G	32= 2.52000E-01	G	33= 2.52000E-01	G	34= 2.52000E-01	G	35= 2.52000E-01
G	36= 2.52000E-01	G	37= 2.52000E-01	G	38= 2.52000E-01	G	39= 2.52000E-01	G	40= 7.77000E-02
G	41= 2.52000E-02	G	42= 2.52000E-02	G	43= 4.58000E-02	G	44= 2.52000E-01	G	45= 2.52000E-01
G	46= 2.52000E-01	G	47= 2.52000E-01	G	48= 2.52000E-01	G	-49= 5.48480E-11	G	50= 0.00000
G	51= 0.00000	G	52= 0.00000	G	53= 0.00000	G	54= 0.00000	G	55= 0.00000
G	56= 0.00000	G	57= 4.06813E-01	G	58= 5.00000E+00	G	59= 5.00000E+00	G	60= 5.00000E+00
G	61= 5.00000E+00	G	62= 5.00000E+00	G	63= 5.00000E+00	G	64= 5.00000E+00	G	65= 5.00000E+00
G	66= 5.00000E+00	G	67= 5.00000E+00	G	68= 5.00000E+00	G	69= 5.00000E+00		

HEAT PIPE NUMBER 1 CHARACTERISTICS
TOTAL LENGTH= 40.00IN GAS V/L= .115IN**3/IN RES VOLUME= 6.710 IN**3
GAS INVENTORY= .2530 FT-LB/RRESERVOIR IS WICKED
LOCATION OF ICE PLUG= 4.00 IN POSITION OF GAS FRONT= 15.84 IN DRY EVAP LGTH= 0.00 IN
GAS IN RES SIDE= .186676 GAS IN EVAP SIDE= .066324 GAS RESIDUAL= .000001
TOTAL PRESSURE IN RES SIDE= 108.35 PSIA TOTAL PRESSURE ON EVAP SIDE= 244.10 PSIA PEV-PRE= 135.75 PSIA
RES TEMPERATURE= -115.43 F EVAP SIDE VAPOR TEMP= 108.76 F
SUM QIN= 130.09 BTU/HR, SUM QOUT= 130.09 BTU/HR LEFF= 14.33 INCHES QLEFF= 1864.4 BTU-INCH/HR

TOTAL HEAT EXCHANGE TO BOUNDARIES -1.17181E+02
QB 35=-1.17181E+02 QB 36=-1.11868E-10

VARIABLE CONDUCTANCE HEAT PIPE TEST CASE

********** TIME= 5.20000E+00
DTIMEU= 7.22656E-03 CSGMIN(33)= 9.76562E-03 TEMPCC(33)= 1.58935E+00 RELXCC(2)= 9.03780E-02

T	23=-5.56363E+01	T	24=-4.32380E+01	T	25=-2.34563E+01	T	26= 4.50673E+00	T	27= 5.28458E+01
T	28= 6.15088E+01	T	29= 6.18917E+01	T	30= 6.19099E+01	T	31= 6.19401E+01	T	33= 1.43798E+02
T	34=-1.09175E+02	T	1=-9.34923E+01	T	2=-6.19749E+01	T	3=-5.43996E+01	T	4=-4.22482E+01
T	5=-2.22415E+01	T	6= 7.40668E+00	T	7= 6.00703E+01	T	8= 6.95037E+01	T	9= 6.99232E+01
T	10= 6.99433E+01	T	11= 6.99765E+01	T	12= 7.23433E+01	T	13= 7.31535E+01	T	14= 7.34602E+01
T	15= 1.06835E+02	T	16= 1.40737E+02	T	17= 1.43545E+02	T	18= 1.43777E+02	T	19= 1.43797E+02
T	20= 1.43798E+02	T	22=-6.14764E+01	T	32= 6.45429E+01	T	35=-5.00000E+01	T	36= 7.31560E+01

G	-1= 3.46000E-10	G	-2= 3.46000E-10	G	-3= 3.46000E-10	G	-4= 3.46000E-10	G	-5= 3.46000E-10
G	-6= 3.46000E-10	G	-7= 3.46000E-10	G	-8= 3.46000E-10	G	-9= 3.46000E-10	G	-10= 8.22000E-11
G	-11= 8.22000E-11	G	12= 5.00000E-01	G	13= 2.00000E+00	G	14= 2.00000E+00	G	15= 2.00000E+00
G	16= 2.00000E+00	G	17= 2.00000E+00	G	18= 2.00000E+00	G	19= 2.00000E+00	G	20= 2.00000E+00
G	21= 2.00000E+00	G	22= 5.00000E-01	G	23= 2.56000E+00	G	24= 2.56000E+00	G	25= 2.56000E+00
G	26= 2.56000E+00	G	27= 2.56000E+00	G	28= 2.56000E+00	G	29= 5.05000E-02	G	30= 2.52000E-02
G	31= 7.77000E-02	G	32= 2.52000E-01	G	33= 2.52000E-01	G	34= 2.52000E-01	G	35= 2.52000E-01
G	36= 2.52000E-01	G	37= 2.52000E-01	G	38= 2.52000E-01	G	39= 2.52000E-01	G	40= 7.77000E-02
G	41= 2.52000E-02	G	42= 2.52000E-02	G	43= 4.58000E-02	G	44= 2.52000E-01	G	45= 2.52000E-01
G	46= 2.52000E-01	G	47= 2.52000E-01	G	48= 2.52000E-01	G	-49= 5.48480E-11	G	50= 0.00000
G	51= 0.00000	G	52= 0.00000	G	53= 0.00000	G	54= 0.00000	G	55= 0.00000
G	56= 1.96396E+00	G	57= 5.00000E+00	G	58= 5.00000E+00	G	59= 5.00000E+00	G	60= 5.00000E+00
G	61= 5.00000E+00	G	62= 5.00000E+00	G	63= 5.00000E+00	G	64= 2.87321E+00	G	65= 0.00000
G	66= 0.00000	G	67= 0.00000	G	68= 0.00000	G	69= 0.00000		

HEAT PIPE NUMBER 1 CHARACTERISTICS

TOTAL LENGTH= 40.00IN GAS V/L= .115IN**3/IN RES VOLUME= 6.710 IN-3
GAS INVENTORY = .2530 FT-1B/R RESERVOIR IS WICKED
VAPOR TEMP = 73.21 F TOTAL PRESS = 137.31 PSIA GAS LGTH = 13.21IN DRY EVAP LGTH= 10.85 IN
RESERVOIR TEMP= -109.17 F RES GAS PRESS= 136.47 PSIA
SUM QIN= 97.87 BTU/HR, SUM QOUT= 97.87 BTU/HR LEFF= 10.22 INCHES QLEFF= 1000.0 BTU-INCH/HR
RESERVOIR GAS NR= .217514 HEAT PIPE NR= .035488 RESIDUAL= -.000002

TOTAL HEAT EXCHANGE TO BOUNDARIES -8.98458E+01
QB 35=-8.98456E+01 QB 36=-5.86624E-11

VARIABLE CONDUCTANCE HEAT PIPE TEST CASE

********** TIME= 6.00000E+00
DTIMEU= 7.22656E-03 CSGMIN(33)= 9.76562E-03 TEMPCC(33)= 1.62094E+00 RELXCC(18)= 1.27446E-02

T	23=-3.90734E+01	T	24=-3.22309E+01	T	25=-1.84603E+01	T	26= 7.90362E+00	T	27= 5.88763E+01
T	28= 6.57098E+01	T	29= 6.60123E+01	T	30= 6.60271E+01	T	31= 6.60584E+01	T	33= 3.22351E+02
T	34=-8.28823E+01	T	1=-7.09827E+01	T	2=-4.71243E+01	T	3=-3.85016E+01	T	4=-3.13046E+01
T	5=-1.67551E+01	T	6= 1.13274E+01	T	7= 6.65825E+01	T	8= 7.40897E+01	T	9= 7.44230E+01
T	10= 7.44393E+01	T	11= 7.44738E+01	T	12= 7.69487E+01	T	13= 7.78084E+01	T	14= 7.96794E+01
T	15= 2.85532E+02	T	16= 3.19301E+02	T	17= 3.22097E+02	T	18= 3.22330E+02	T	19= 3.22349E+02
T	20= 3.22351E+02	T	22=-4.72502E+01	T	32= 6.87448E+01	T	35=-5.00000E+01	T	36= 7.78033E+01

G	-1= 3.46000E-10	G	-2= 3.46000E-10	G	-3= 3.46000E-10	G	-4= 3.46000E-10	G	-5= 3.46000E-10
G	-6= 3.46000E-10	G	-7= 3.46000E-10	G	-8= 3.46000E-10	G	-9= 3.46000E-10	G	-10= 8.22000E-11
G	-11= 8.22000E-11	G	12= 5.00000E-01	G	13= 2.00000E+00	G	14= 2.00000E+00	G	15= 2.00000E+00
G	16= 2.00000E+00	G	17= 2.00000E+00	G	18= 2.00000E+00	G	19= 2.00000E+00	G	20= 2.00000E+00
G	21= 2.00000E+00	G	22= 5.00000E-01	G	23= 2.56000E+00	G	24= 2.56000E+00	G	25= 2.56000E+00
G	26= 2.56000E+00	G	27= 2.56000E+00	G	28= 2.56000E+00	G	29= 5.05000E-02	G	30= 2.52000E-02
G	31= 7.77000E-02	G	32= 2.52000E-01	G	33= 2.52000E-01	G	34= 2.52000E-01	G	35= 2.52000E-01
G	36= 2.52000E-01	G	37= 2.52000E-01	G	38= 2.52000E-01	G	39= 2.52000E-01	G	40= 7.77000E-02
G	41= 2.52000E-02	G	42= 2.52000E-02	G	43= 4.58000E-02	G	44= 2.52000E-01	G	45= 2.52000E-01
G	46= 2.52000E-01	G	47= 2.52000E-01	G	48= 2.52000E-01	G	-49= 5.48480E-11	G	50= 0.00000
G	51= 0.00000	G	52= 0.00000	G	53= 0.00000	G	54= 0.00000	G	55= 0.00000
G	56= 2.44903E+00	G	57= 5.00000E+00	G	58= 5.00000E+00	G	59= 5.00000E+00	G	60= 5.00000E+00
G	61= 5.00000E+00	G	62= 5.00000E+00	G	63= 5.00000E+00	G	64= 4.45460E-01	G	65= 0.00000
G	66= 0.00000	G	67= 0.00000	G	68= 0.00000	G	69= 0.00000							

HEAT PIPE NUMBER 1 CHARACTERISTICS

TOTAL LENGTH= 40.00IN GAS V/L= .115IN**3/IN RES VOLUME= 6.710 IN-3
GAS INVENTORY = .2530 FT-LB/R RESERVOIR IS WICKED
VAPOR TEMP = 77.84 F TOTAL PRESS = 148.61 PSIA GAS LGTH = 13.02IN DRY EVAP LGTH= 11.82 IN
RESERVOIR TEMP= -82.88 F RES GAS PRESS= 146.09 PSIA
SUM QIN= 101.74 BTU/HR, SUM QOUT= 101.74 BTU/HR LEFF= 9.83 INCHES QLEFF= 999.9 BTU-INCH/HR
RESERVOIR GAS NR= .216617 HEAT PIPE NR= .036383 RESIDUAL= -.000000

TOTAL HEAT EXCHANGE TO BOUNDARIES -9.88990E+01
QB 35=-9.88990E+01 QB 36=-9.54969E-12

VARIABLE CONDUCTANCE HEAT PIPE TEST CASE

********** TIME= 7.00000E+00
DTIMEU= 7.22656E-03 CSGMIN(33)= 9.76562E-03 TEMPCC(33)= 1.56624E+00 RELXCC(18)= 1.23151E-02

T	23=-3.79085E+01	T	24=-3.14735E+01	T	25=-1.79354E+01	T	26= 8.30569E+00	T	27= 5.92305E+01
T	28= 6.85544E+01	T	29= 6.89668E+01	T	30= 6.89864E+01	T	31= 6.90189E+01	T	33= 5.41379E+02
T	34=-6.37102E+01	T	1=-5.69965E+01	T	2=-4.35372E+01	T	3=-3.72975E+01	T	4=-3.05242E+01
T	5=-1.62161E+01	T	6= 1.17374E+01	T	7= 6.69265E+01	T	8= 7.71947E+01	T	9= 7.76502E+01
T	10= 7.76719E+01	T	11= 7.77078E+01	T	12= 8.02603E+01	T	13= 8.11601E+01	T	14= 8.49658E+01
T	15= 5.04140E+02	T	16= 5.38294E+02	T	17= 5.41123E+02	T	18= 5.41358E+02	T	19= 5.41378E+02
T	20= 5.41379E+02	T	22=-4.38235E+01	T	32= 7.17607E+01	T	35=-5.00000E+01	T	36= 8.11454E+01

G	-1= 3.46000E-10	G	-2= 3.46000E-10	G	-3= 3.46000E-10	G	-4= 3.46000E-10	G	-5= 3.46000E-10
G	-6= 3.46000E-10	G	-7= 3.46000E-10	G	-8= 3.46000E-10	G	-9= 3.46000E-10	G	-10= 8.22000E-11
G	-11= 8.22000E-11	G	12= 5.00000E-01	G	13= 2.00000E+00	G	14= 2.00000E+00	G	15= 2.00000E+00
G	16= 2.00000E+00	G	17= 2.00000E+00	G	18= 2.00000E+00	G	19= 2.00000E+00	G	20= 2.00000E+00
G	21= 2.00000E+00	G	22= 5.00000E-01	G	23= 2.56000E+00	G	24= 2.56000E+00	G	25= 2.56000E+00
G	26= 2.56000E+00	G	27= 2.56000E+00	G	28= 2.56000E+00	G	29= 5.05000E-02	G	30= 2.52000E-02
G	31= 7.77000E-02	G	32= 2.52000E-01	G	33= 2.52000E-01	G	34= 2.52000E-01	G	35= 2.52000E-01
G	36= 2.52000E-01	G	37= 2.52000E-01	G	38= 2.52000E-01	G	39= 2.52000E-01	G	40= 7.77000E-02
G	41= 2.52000E-02	G	42= 2.52000E-02	G	43= 4.58000E-02	G	44= 2.52000E 01	G	45= 2.52000E-01
G	46= 2.52000E-01	G	47= 2.52000E-01	G	48= 2.52000E-01	G	-49= 5.48480E-11	G	50= 0.00000
G	51= 0.00000	G	52= 0.00000	G	53= 0.00000	G	54= 0.00000	G	55= 0.00000
G	56= 1.87813E+00	G	57= 5.00000E+00	G	58= 5.00000E+00	G	59= 5.00000E+00	G	60= 5.00000E+00
G	61= 5.00000E+00	G	62= 5.00000E+00	G	63= 5.00000E+00	G	64= 1.99426E-01	G	65= 0.00000
G	66= 0.00000	G	67= 0.00000	G	68= 0.00000	G	69= 0.00000		

HEAT PIPE NUMBER 1 CHARACTERISTICS

TOTAL LENGTH= 40.00IN GAS V/L= .115IN**3/IN RES VOLUME= 6.710 IN-3
GAS INVENTORY = .2530 FT-1B/R RESERVOIR IS WICKED
VAPOR TEMP = 81.16 F TOTAL PRESS = 157.12 PSIA GAS LGTH = 13.25IN DRY EVAP LGTH= 11.92 IN
RESERVOIR TEMP= -63.71 F RES GAS PRESS= 152.10 PSIA
SUM QIN= 103.37 BTU/HR, SUM QOUT= 103.37 BTU/HR LEFF= 9.67 INCHES QLEFF= 999.1 BTU-INCH/HR
RESERVOIR GAS NR= .214618 HEAT PIPE NR= .038382 RESIDUAL= -.000000

TOTAL HEAT EXCHANGE TO BOUNDARIES -1.02141E+02
QB 35=-1.02141E+02 QB 36=-4.72937E-11

VARIABLE CONDUCTANCE HEAT PIPE TEST CASE

********** TIME= 8.00000E+00
DTIMEU= 7.22656E-03 (SGMIN(33)= 9.76562E-03 TEMPCC(33)= 1.53594E+00 RELXCC(18)= 1.20770E-02

T	23=-3.74700E+01	T	24=-3.12652E+01	T	25=-1.78904E+01	T	26= 8.19984E+00	T	27= 5.89250E+01
T	28= 6.99811E+01	T	29= 7.04699E+01	T	30= 7.04930E+01	T	31= 7.05261E+01	T	33= 7.55141E+02
T	34=-5.40359E+01	T	1=-4.99756E+01	T	2=-4.18365E+01	T	3=-3.68409E+01	T	4=-3.03071E+01
T	5=-1.61698E+01	T	6= 1.16231E+01	T	7= 6.65850E+01	T	8= 7.87552E+01	T	9= 7.92950E+01
T	10= 7.93205E+01	T	11= 7.93570E+01	T	12= 8.19501E+01	T	13= 8.28751E+01	T	14= 8.85845E+01
T	15= 7.17670E+02	T	16= 7.52037E+02	T	17= 7.54883E+02	T	18= 7.55120E+02	T	19= 7.55139E+02
T	20= 7.55141E+02	T	22=-4.22002E+01	T	32= 7.32978E+01	T	35=-5.00000E+01	T	36= 8.28510E+01

G	-1= 3.46000E-10	G	-2= 3.46000E-10	G	-3= 3.46000E-10	G	-4= 3.46000E-10	G	-5= 3.46000E-10
G	-6= 3.46000E-10	G	-7= 3.46000E-10	G	-8= 3.46000E-10	G	-9= 3.46000E-10	G	-10= 8.22000E-11
G	-11= 8.22000E-11	G	12= 5.00000E-01	G	13= 2.00000E+00	G	14= 2.00000E+00	G	15= 2.00000E+00
G	16= 2.00000E+00	G	17= 2.00000E+00	G	18= 2.00000E+00	G	19= 2.00000E+00	G	20= 2.00000E+00
G	21= 2.00000E+00	G	22= 5.00000E-01	G	23= 2.56000E+00	G	24= 2.56000E+00	G	25= 2.56000E+00
G	26= 2.56000E+00	G	27= 2.56000E+00	G	28= 2.56000E+00	G	29= 5.05000E-02	G	30= 2.52000E-02
G	31= 7.77000E-02	G	32= 2.52000E-01	G	33= 2.52000E-01	G	34= 2.52000E-01	G	35= 2.52000E-01
G	36= 2.52000E-01	G	37= 2.52000E-01	G	38= 2.52000E-01	G	39= 2.52000E-01	G	40= 7.77000E-02
G	41= 2.52000E-02	G	42= 2.52000E-02	G	43= 4.58000E-02	G	44= 2.52000E-01	G	45= 2.52000E-01
G	46= 2.52000E-01	G	47= 2.52000E-01	G	48= 2.52000E-01	G	-49= 5.48480E-11	G	50= 0.00000
G	51= 0.00000	G	52= 0.00000	G	53= 0.00000	G	54= 0.00000	G	55= 0.00000
G	56= 1.60444E+00	G	57= 5.00000E+00	G	58= 5.00000E+00	G	59= 5.00000E+00	G	60= 5.00000E+00
G	61= 5.00000E+00	G	62= 5.00000E+00	G	63= 5.00000E+00	G	64= 1.18962E-01	G	65= 0.00000
G	66= 0.00000	G	67= 0.00000	G	68= 0.00000	G	69= 0.00000		

HEAT PIPE NUMBER 1 CHARACTERISTICS

TOTAL LENGTH= 40.00IN GAS V/L= .115IN**3/IN RES VOLUME= 6.710 IN-3
GAS INVENTORY = .2530 FT-1B/R RESERVOIR IS WICKED
VAPOR TEMP = 82.86 F TOTAL PRESS = 161.83 PSIA GAS LGTH = 13.36IN DRY EVAP LGTH= 11.95 IN
RESERVOIR TEMP= -54.04 F RES GAS PRESS= 154.94 PSIA
SUM QIN= 104.22 BTU/HR, SUM QOUT= 104.22 BTU/HR LEFF= 9.59 INCHES QLEFF= 999.9 BTU-INCH/HR
RESERVOIR GAS NR= .213417 HEAT PIPE NR= .039583 RESIDUAL= .000000

TOTAL HEAT EXCHANGE TO BOUNDARIES -1.03615E+02
QB 35=-1.03615E+02 QB 36=-2.50111E-11

APPENDIX A.5.1

POTENTIAL FOR BUBBLE FORMATION IN CTS HEAT PIPES: FUNDAMENTALS

TRW
DEFENSE AND SPACE SYSTEMS GROUP
ONE SPACE PARK • REDONDO BEACH • CALIFORNIA 90278

INTEROFFICE CORRESPONDENCE

8715.10.2-78-7

TO: E. E. Luedke

CC: D. Antoniuk
J. E. Eninger
B. D. Marcus

DATE: 27 October 1978

D.K.E. /for

SUBJECT: Potential for Bubble Formation in CTS Heat Pipes: Fundamentals

FROM: D. K. Edwards
BLDG 01 MAIL STA. 1230 EXT. 52850

INTRODUCTION

In the Anomalies Review and Program Plan of 19 October 1978, there is promised the following analysis: "Calculate number of critical size bubbles which can be generated due to supersaturation in rapid chilldown. Consider both temperature and pressure effects". In what follows the basis for making such a calculation is reviewed.

GAS SATURATION

For dilute solutions of gas in liquid, Henry's Law can be invoked: The partial pressure gas i in the vapor phase P_i and the mole fraction X_i or concentration c_i of gas i in the liquid phase are linearly related

$$P_i = C_i(T)\, X_i = \left[C_i(T)/c \right] c_i, \quad i > 2 \tag{1}$$

In the vapor phase the total pressure P is given by Dalton's Law for an ideal gas mixture

$$P = \sum_{i=1}^{n} P_i \tag{2}$$

where the vapor pressure of the solute species is given by

Raoult's Law

$$P_1 = P_{sat}(T)\, X_1 = C_1(T)\, X_1 \tag{3}$$

Often Henry's contant C_i (T) is so large that all X_i's other than X_1 are very small, and $X_1 \approx 1$. The mole fractions in the liquid sum to unity, of course.

$$1 = \sum_{i=1}^{n} X_i \qquad c = \sum_{i=1}^{n} c_i \tag{4}$$

If the liquid contacts a gas mixture of specified total pressure P and specified ratios of noncondensible gas mole fraction,

$$Y_i = P_i / \sum_{i=2}^{n} P_i = P_i / P_g \tag{5}$$

First, one finds the mole fraction of noncondensibles in the liquid

$$X_g = \frac{\sum_{i=2}^{n} (Y_i/C_i)\,(P - C_1)}{1 - \sum_{i=2}^{n} (Y_i/C_i)\,C_1} \tag{6}$$

The partial pressures in the vapor phase are

$$P_i = Y_i \left[P - C_1 (1 - X_g) \right] \tag{7}$$

The mole fractions in the liquid phase are

$$X_i = (Y_i/C_i) \left[P - C_1 (1 - X_g) \right] \tag{8}$$

CRITICAL BUBBLE SIZE

The preceeding relations are assumed to apply to gas at equilibrium within a critically-sized bubble when the total pressure in the bubble exceeds that in the surrounding liquid by an amount related to the surface tension σ and bubble size r

$$P - P_{\ell} = \frac{2\,\sigma\,(T)}{r} \tag{9}$$

Given a value of P_{ℓ}, σ (T), and r one can find P from Eq. (9) and then proceed as before to establish the set of X_i mole fractions in the liquid immediately surrounding the bubble (the effect of X_i on σ is neglected). Conversely given a set of X_i, one can use Eqs. (1), (2), and (3) to find P and Eq. (9) to find r.

PREVIOUS AND PRESENT STATE VARIABLES

For convenience we choose to set the composition of a (bubbly) liquid by its "Previous state variables" T'_e and T'_c plus the Y_i ratios. The quantity T'_e is the "Previous evaporator temperature". It sets the previous total pressure P'

$$P' = P_{sat}(T'_e) \tag{10}$$

The "Previous (gas-blocked) condenser temperature is T'_c". It sets the previous vapor pressure according to Eq. (3) and, as explained below Eq. (4) in Eqs. (5) - (8), with P' and P'_1 one can find the previous liquid composition X'_i.

Present state variables are T_e and T_c. The quantity T_e is understood to fix pressure P_ℓ by the relation

$$P_\ell = P_{sat}(T_e) \tag{11}$$

The quantity T_c fixes σ and P_1.

CRITICAL BUBBLE SIZE IN AN INFINITE LIQUID

Specification of the previous state variables, present state variables, and nonisothermal gas composition leads immediately to the critical size of a single bubble in contact with an infinite liquid. Variables T_e', T_c', and Y'_i leads to a set of X'_i which, in an infinite liquid, are identical to X_i. Then, as explained below Eq. (9), one can find P and r using the set of X_i and P_ℓ (from T_e) and σ and P_1 (from T_c).

$$r_{cr} = \frac{2\,\sigma\,(T_c)}{P - P_\ell} \tag{12}$$

Where P_ℓ comes from Eq. (11) and P from Eq. (2) with P_i from Eqs. (1) and (3).

NUMBER OF BUBBLES OF A SPECIFIED SIZE IN A FINITE LIQUID

Let the mole fractions in one mole of liquid mixture be specified by the previous state variables. Imagine that the liquid is supersaturated, that is, there exists a finite r_{cr}. Now choose a value of r greater than r_{cr}. Then Eq. (9), with P_ℓ fixed by T_e and σ by T_c, fixes total pressure P. Unfortunately the gas composition in the bubble is unknown so that Eq. (7) cannot be directly applied. However, one can write that the moles of species i remaining in the liquid plus

those in the gas sum to the original amount of species i.

$$X_i (1 - N) + N Y_i = X_i' \tag{13}$$

where N is the number of moles in the vapor phase. Introducing Eqs. (1), (2), and (3) gives

$$X_i + N P_i/P = X_i'$$

$$X_i + (N/P) C_i X_i = X_i \tag{14}$$

where C_1 is understood to be $P_{sat}(T_c)$. Solving for X_i gives

$$X_i = \frac{X_i}{1 + (N/P) C_i} \tag{15}$$

Multiplying both sides by $C_i(T_c)/P$ and summing over i gives a single equation which fixes the unknown N.

$$1 = \sum_{i=1}^{n} \frac{C_i X_i'}{P + N C_i} \tag{16}$$

For a single-species noncondensible gas Eq. (16) may be solved explicity via the quadratic equiation. For a binary noncondensible gas mixture, one can employ a computer-aided binary search for the normalizing value of N. Once N is determined the number of bubbles follows immediately

$$N_b = \frac{N R_u T_c}{P(\frac{4}{3} \pi r^3)} \qquad \frac{\text{Bubbles}}{\text{Mole}} \tag{17}$$

where R_u is the universal gas constant.

APPENDIX A.5.2

POTENTIAL FOR BUBBLE FORMATION IN CTS HEAT PIPES: SAMPLE CALCULATIONS

SYSTEMS GROUP
ONE SPACE PARK • REDONDO BEACH • CALIFORNIA 90278

INTEROFFICE CORRESPONDENCE 8715.10.2-78-8

TO: E. E. Luedke

CC: D. Antoniuk
J. E. Eninger
B. D. Marcus

DATE: 28 November 1978

SUBJECT: Potential for Bubble Formation in CTS Heat Pipes: Sample Calculations

FROM: D. K. Edwards
BLDG 01 MAIL STA. 1230 EXT. 52850

INTRODUCTION

It is desired to calculate the number and size of critical size bubbles which can be generated due to supersaturation. In Part I the fundamentals were developed. Here sample calculations are made for two test cases (1) a condenser depressurization case where evaporator temperature is dropped at constant gas-blocked condenser temperature and (2) a condenser chilldown where the gas-blocked condenser is cooled at constant total pressure.

HENRY'S CONSTANTS

Henry's constants are calculated from extrapolations of a solubility curve from Saaski. Saaski plots mole fraction of the gas in the liquid versus temperature on a log-log scale. Presumably the gas pressure is one atmosphere. Thus one has X_i for $P_i = 1$, and since $P_i = C_i X_i$, $C_i = P_i/X_i = 1/X_i$.

As a check, an Ostwald coefficient reported by Saaski for helium in methanol at 25°C is compared to the graphed value. Ostwald coefficient α at 25°C is reported to be 0.036. The graph shows $X_i = 6 \times 10^{-5}$. Hence we expect from the graph that $C_i = 1/6 \times 10^{-5} = 16670$ atm. Ostwald coefficient and Henry number are related by

$$C_i = \frac{c_\ell R_u T}{\alpha} = \frac{\rho_\ell R_u T}{M\alpha}$$

$$C_i = \frac{(0.785)(82.05)(298.15)}{(32)(0.036)} = 16670 \text{ atm}$$

The check is very satisfactory.

Table 1 gives Henry constant for helium and nitrogen at -100°C and -40°C. The values are hypothetical and extrapoluted, hypothetical in that liquid is

freezes at a temperature of -98°C, and extrapoluted in that Saaski's curves are extrapoluted. The values are chosen merely to exemplify trends.

TEST CASES

Table 2 shows the test-case conditions selected. Table 3 shows the property values needed for the test cases.

PREVIOUS STATE COMPOSITIONS

As detailed in Part I the calculation commences with Eq.(I-6) and proceeds to Eq.(I-8).

$$x_g = \frac{[(y_2/C_2) + (y_3/C_3][P-C_1]}{1-[(y_2/C_2) + (y_3/C_3)]C_1}$$

$$x_i=(y_i/C_i)[P-C_1(1-x_g)$$

Table 4 gives the values.

TABLE 1

Extraction of Henry's Constants From
A Solubility Curve

$C = 1/x_i$ atm

Gas	Temperature	Solubility in Methanol	Henry's Constant C atm
Helium	-100C (Hypothetical)	1×10^{-5}	100000
	-40C (Extrapolated)	2.6×10^{-5}	38500
Nitrogen	-100C (Hypothetical)	2.82×10^{-4}	3550
	-40C (Extrapolated)	2.69×10^{-4}	3720

TABLE 2

Hypothetical Test Cases

Test Case 1 Depressurization from Drop in Evaporator Temperature

Previous State Variables

Evaporator Temperature, T_e'	49C(120F)
Gas Blocked Condenser Temperature, T_c'	-40C(-40F)
Noncondensible Gas Composition, $y_{n,i}$	90% N_2 - 10% He

Present State Variables

Evaporator Temperature, T_e	21C(70F)
Gas Blocked Condenser Temperature, T_c	-40C(-40F)

Test Case 2 Chilldown in Gas-Blocked Condenser

Previous State Variables

Evaporator Temperature, T_e'	21C(70F)
Gas Blocked Condenser Temperature, T_c'	-40C(-40F)
Noncondensible Gas Composition, $y_{n,i}$	90% N_2 - 10% He

Present State Variables

Evaporator Temperature, T_e	21C(70F)
Gas Blocked Condenser Temperature, T_c	-100C(-148F)

TABLE 3

Vapor Pressure and Surface Tension

T C	$P_{sat}=C_1$ psia	T C	σ lb_f/ft
49	7.62	-40	2.1×10^{-3}
21	1.96	-100	2.4×10^{-3}
-40	0.02870		
-100	0.00012		

TABLE 4

Previous State Conditions

y_2	y_3	P atm	C_1 atm	C_2 atm	C_3 atm	x_g	x_1	x_2	x_3
.90	.10	0.519	.001953	3720	38500	1.264×10^{-4}	1.000	1.251×10^{-4}	1.34×10^{-6}
.90	.10	0.133	.001953	3720	38500	3.204×10^{-5}	1.000	3.170×10^{-5}	3.40×10^{-7}

TABLE 5

Critical Bubble Size in an Infinite Liquid

x_1	x_2	x_3	C_1 atm	C_2 atm	C_3 atm	σ lb_f/ft^2	P atm	P_ℓ atm	r_{cr} μm
1.000	1.251×10^{-4}	1.34×10^{-6}	.001953	3720	38500	2.1×10^{-3}	0.519	0.133	1.6 (0.6×10^{-4} in.)
1.000	3.170×10^{-5}	3.40×10^{-7}	8.17×10^{-5}	3550	10^5	2.4×10^{-3}	0.1466	0.133	50.8 (2×10^{-3} in.)

Critical Bubble Size in an Infinite Liquid

As explained in Part I, to compute the ciritical bubble size, one computes

$$P = \sum_{i=1}^{n} x_i' \, C_i(T_c)$$

and then

$$r_{cr} = \frac{2\sigma(T_e)}{P - P_{sat}(T_e)}$$

Table 5 shown the results. For depressurization (case 1) the critical bubble is small, 1.6 μm in radius, the size of nuclei expected to be active in nucleate surface boiling. However, the gas composition near the surface exposed to the gas would be more nearly in equilibrium. That is contact with the wick might be close to the composition assumed. For chilldown (case 2) the increase in Henry's constant for helium results in supersaturation, but the potential for nucleation is much less. A fifty-micron-radius nucleus would be required for bubble formation.

Number of Bubbles of a Specified Size

From Part I the equation which governs the amount of gas N within bubbles is

$$1 = \frac{C_1 \, x_1'}{P + NC_1} + \frac{C_2 \, x_2'}{P + NC_2} + \frac{C_3 \, x_3'}{P + NC_3}$$

where the total pressure within the bubble is

$$P = P_{sat}(T_e) + \frac{2\sigma}{r}$$

For case 1 and r = 50.8 μm the following values pertain:

$$P = 1.96 + \frac{2(2.1 \times 10^{-3}/12}{50.8/25400} = 2.135 \text{ psia} = 0.1453 \text{ atm}$$

$$C_1 x_1' = (0.001963)(1.000) = 0.001953 \text{ atm}$$

$$C_2 x_2' = (3720)(1.251 \times 10^{-4}) = 0.465 \text{ atm}$$

$$C_3 x_3' = (38500)(1.34 \times 10^{-6}) = 0.052 \text{ atm}$$

$$N = 8.96 \times 10^{-5} \text{ moles of bubbles/mole of original liquid}$$

The number of bubbles per mole is then

$$N_b = \frac{N R_u T_c}{P(\frac{4}{3}\pi r^3)} = \frac{(8.96 \times 10^{-5})(82.05)(233.15)}{(0.1453)(\frac{4}{3}\pi)(50.8 \times 10^{-4})^3}$$

$$N_b = 2.15 \times 10^7 \text{ Bubbles/g-mole of liquid}$$

Taking c_ℓ to be approximately 0.8 [g/cm^3]/32[g/g-mole] gives

$$N_b c_\ell = 537000 \text{ Bubbles/cm}^3 \text{ of liquid}$$

Conclusions

The sample calculations show the possibility for bubble formation upon (1) depressurization by reduction in heat pipe loading and reservoir chilling and (2) condenser chilldown. Depressurization shows greater potential, for 537000 bubbles/cm^3 are found possible, compared to only one of equal size from condenser chilldown.

APPENDIX A.5.3

BUBBLE NUCLEATION EXPERIMENTS

TRW
DEFENSE AND SPACE SYSTEMS GROUP
ONE SPACE PARK • REDONDO BEACH • CALIFORNIA 90278

INTEROFFICE CORRESPONDENCE

TO: B. Marcus

CC: D. K. Edwards
J. Eninger
E. E. Luedke

DATE: 8 December 1978

SUBJECT: Bubble Nucleation Experiments

FROM: D. Antoniuk

BLDG	MAIL STA.	EXT.
01	1230	52850

As part of the experimental program to investigate the potential of various mechanisms to cause artery depriming, a series of experiments have been conducted to examine bubble nucleation in methanol. The experiments were to determine whether gas bubbles could be generated in the bulk of liquid methanol saturated with either helium or nitrogen gas as it undergoes temperature and/or pressure reduction.

Prior to the experiments, a theoretical analysis of the potential for bubble formation in CTS heat pipes had shown that large numbers of bubbles could be generated in methanol due to supersaturation resulting from temperature and pressure reduction under conditions similar to those prevailing prior to the anomalies. An objective of these experiments was to verify, at least qualitatively, the theoretical results.

In addition the experiments considered the potential of a mesh screen artery to provide bubble nucleating sites.

The experimental set-up consisted of a glass flask half filled with 50cc of spectral grade methanol and instrumented to allow continuous monitoring of temperature and pressure. A sketch of the apparatus is attached. A needle valve located between the flask and a vacuum pump was used to control the pressure level or the rate of pressure reduction of the liquid. Cooling of the liquid was attained by immersion of the test flask in liquid nitrogen. This technique, however, did not allow for arbitrary control of the cooling rate. The liquid was saturated by bubbling either nitrogen or helium gas through the liquid using a frit glass tube. This process was allowed to be continued for at least two hours.

A typical pressure reduction experimental sequence was as follows:

1. Saturate methanol with either nitrogen or helium at ambient conditions.

2. Reduce temperature at atmospheric pressure. Two temperature levels, 21°C and -40°C, were used.

3. Drop into the liquid a dry section of mesh screen artery.

4. Reduce pressure from 14.7 psia to 4 psia. In some cases this pressure drop was accomplished in 10 seconds and in others in 5 minutes.

A typical temperature reduction experimental sequence was as follows:

1. Saturate methanol at ambient conditions.

2. Drop into the liquid a dry section of mesh screen artery.

3. Reduce pressure at ambient temperature. Pressure levels of 14.7 psia, 10 psia, and 4 psia were used.

4. Reduce temperature. In some cases the temperature was reduced from 21°C to -40°C in approximately 20 minutes. This was accomplished by placing the flask near the liquid nitrogen surface contained in a Dewar flask where cooling of the methanol occurred by natural convection. In other cases, the liquid was rapidly chilled by immersing the flask in liquid nitrogen for approximately 10 seconds at which point the liquid on the bottom of the test flask and inside the artery froze.

The experiments were repeated several times and the results were found reproducible. No bubbles were observed as the liquid, originally at a set temperature level, underwent pressure reduction. Similar results were obtained from temperature reduction experiments provided the liquid temperature did not drop below the freezing point (-98°C).

Experiments in which the liquid partially froze however, yielded significantly different results. A large number of small bubbles were observed streaming from the surface of the thawing ice. As the melting process went to competion the bubbles were reduced to a few originating from the bottom surface of the flask and from the outter surface of the mesh screen artery. About a dozen small bubbles were observed trapped inside the arteries after the ice melted. These bubbles were observed later to coalesce forming fewer but larger bubbles which continue to grow. The ultimate size of these bubbles depended on the pressure of the system. For example, at 4 psia the remaining bubbles inside the artery continue to grow for approximately 10 minutes as the liquid temperature rose from -40°C to 0°C, at which point the size of the bubbles was such that essentially all the liquid in the artery was displaced.

As the result of these experiments, freezing of supersaturated methanol in the arteries has been identified as a potential mechanism for bubble formation in the arteries owing to the fact that the ice surface is an excellent source of nucleating sites.

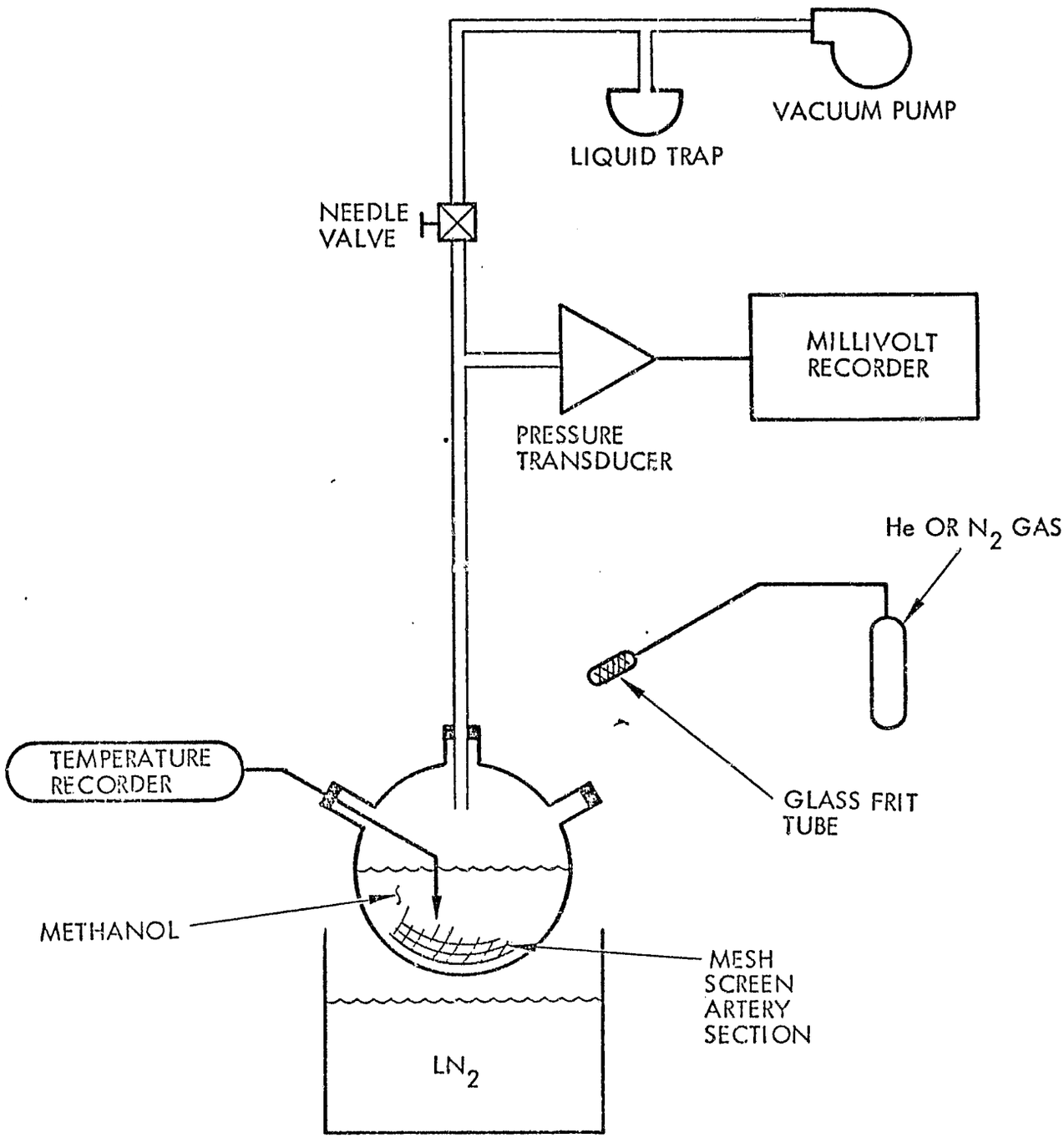
VACUUM PUMP
LIQUID TRAP
NEEDLE VALVE
MILLIVOLT RECORDER
PRESSURE TRANSDUCER
He OR N_2 GAS
TEMPERATURE RECORDER
GLASS FRIT TUBE
METHANOL
MESH SCREEN ARTERY SECTION
LN_2

APPENDIX A.5.4
GLASS HEAT PIPE BUBBLE NUCLEATION/MIGRATION EXPERIMENTS

A series of experiments were performed with an existing 1.07 meter long glass heat pipe. A cross section of this heat pipe is shown in Figure 1. The pipe contains a slab wick with a CTS-type artery attached to one side. A heater and cooling loop are attached to the other side of the wick in the evaporator and condenser sections, respectively. This arrangement permits observations on the behavior of the artery in an operational heat pipe.

The heat pipe was gas loaded with a 90% nitrogen — 10% helium mixture at a pressure equivalent to the conditions in the CTS pipes. The experiments simply involved visually observing the artery behavior as a result of freezing the methanol within it by passing liquid nitrogen through the cooling loop, and subsequently thawing the methanol by terminating the LN_2 flow.

The experiment was repeated several times with the following results:

- The methanol froze to an opaque white solid (frost), indicating it was full of gas bubbles.
- As the methanol thawed and warmed, numerous (up to 33) gas bubbles of varying size were observed along a 12-inch length of the artery.
- The bubbles slowly shrank and ultimately disappeared as the gas within them redissolved into the liquid and diffused through the artery wall into the surrounding vapor core under the pressure gradient established by their curvature and surface tension.
- The time required for the bubbles to disappear varied enormously, depending on their size. Very small bubbles (d $\sim$1/4 artery dia) dissolved within a few hours, while a large sausage-shaped bubble which filled the artery (2 artery diameters long) required several weeks.

It was believed that incorporation of these ice-generated bubbles into the active condenser could cause artery deriming. Accordingly, additional tests were conducted and a number of deprimings were observed, but they were sporadic (probabilistic in nature). On some occasions, as the active

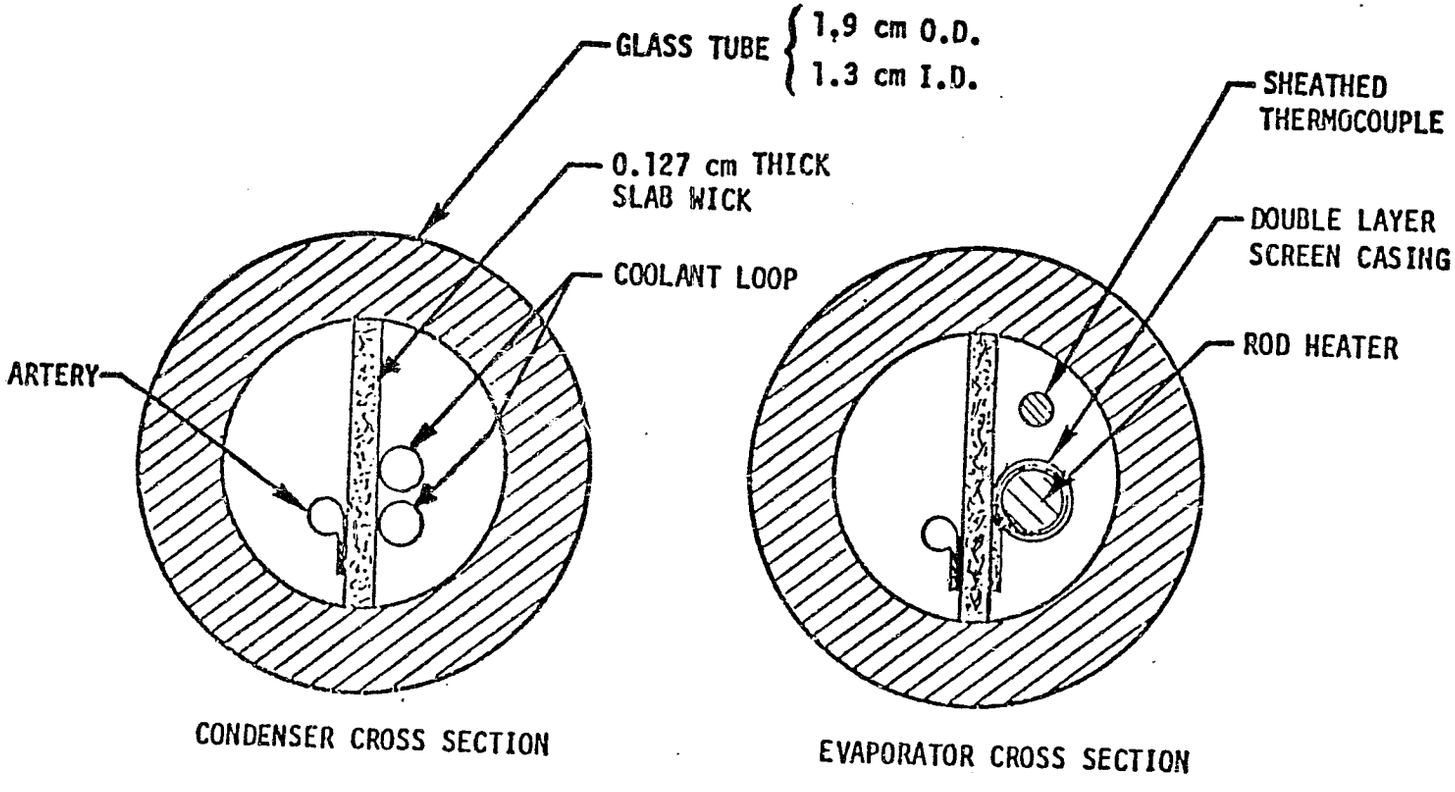

Figure 1. Cross Section of the Glass Heat Pipe in the Condenser and Evaporator Regions

condensation front was brought into the previously gas-blocked condenser, no depriming occurred. On two occasions, freezing generated a bubble in the adiabatic section; on both these occasions, advancement of the front to the bubble caused depriming. On another occasion, a rather large bubble formed in the center of the condenser, and advancement of the front to this bubble caused depriming.

These results conclusively demonstrated that: 1) control gas is liberated from saturated methanol every time the heat pipe goes through a freeze-thaw cycle, and 2) the number, size, and durability of gas bubbles generated within the arteries is a statistical phenomena influenced by bubble coalescence. Arterial bubbles are known to lead to depriming if they are convected into the active region of the pipe under high load conditions. Thus, it is clear that freezing and thawing of the condenser can, but does not necessarily, lead to artery depriming, depending on subsequent history. That is, do the bubbles dissolve and diffuse away before they are convected into a high stress region where they would deprime the artery?

This mechanism appears to be a prime candidate for explaining the CTS anomalies. It is consistent with their seasonal occurrence (eclipse seasons may be necessary to experience condenser freezing), sporadic occurrence (statistical nature of bubble population) and the lack of freezing prior to the anomaly on day 253 (bubbles were generated during day 252).

APPENDIX B.1

SPHERICAL BUBBLE MODEL COMPUTER PROGRAM LISTING

This appendix contains the main program and sample input.

```
00100       PROGRAM SMLBUB(INPUT,OUTPUT,TAPE5=INPUT,TAPE6=OUTPUT,TAPE9)
00110 C     -------> FILE:SMLBUB INPUT FILE:SBUBDAT<------
00120       DIMENSION A(100),B(100),C(100),ASTR(100),BSTR(100),A22(3),
00130      1B22(3),C22(3),XBBC(3),XEBC(3),FG1(100),FG2(100),
00140      2FGG1(100),FGG2(100),DIFF(3)
00150       COMMON/MAIN/X(100,3),XSTR(100,3),XSTR2(100,3),R(100),Y(100),
00160      1Z(100),R1,R2,N,TIME,TC,TE,PVC,PVE,WG1,WG2,YE1,YE2,PB,TCNOT,
00170      2XB1,XB2,XE1,XE2,YB1,YB2,IPRINT,KPLOT,YB0,IPLOT,IDPLOT,TENOT,RATE
00180       COMMON/SUBDAT/CMOLE,RHOL,RHOV,RU,EMW
00190       COMMON/DATPLO/FTIME(1000),FTE(1000),FTC(1000),FPVE(1000),
00200      1              FPVC(1000),FYB0(1000),FYB1(1000),FYB2(1000),
00210      2               FR1(1000),FPBUBLE(1000)
00220       COMMON/SCLDIF/DF11,DF21,DF12,DF22,COS11,COS12,COS21,COS22,
00230      1NG1,NG2
00240       DATA PI,RU/3.1416,82.06/
00250       NAMELIST/BUBDAT/R10,R20,NDIV,GAMA,DT,IDPRNT,RFILLET,FBY1,FBY2,
00260      1                FEY1,FEY2,EMW,TCNOT,TENOT,NSTPMX,IDPLOT,RATE,
00270      2DF11,DF12,DF21,DF22,COS11,COS12,COS21,COS22,NG1,NG2
00280 C
00290 C     INPUT DATA
00300 C
00310       READ(5,BUBDAT)
00320       WRITE(6,BUBDAT)
00330 C
00340 C     CALCULATE CONSTANT COEFFICIENTS
00350 C
00360       TIME=-1.0
00370       CALL TPCNDI
00380       CALL SUBRHO(TC,RHOL,RHOV)
00390       CMOLE=RHOL/EMW
00400       PI43=4./3.*PI
00410       VLIQ2=R20**3-R10**3
00420       VLIQ1=VLIQ2*PI43
00430       N=NDIV+2
00440       DZ=1./FLOAT(NDIV)
00450       DZ2=DZ+DZ
00460       DZDZ=DZ*DZ
00470       BIGGAM=EXP(GAMA)-1.0
00480 C
00490 C    INITIALIZE SPECIES AND BUBBLE RADIUS
00500 C
00510       CALL TENSION(TC,SIGMA)
```

```
00520         PLIQ=PVE-2.*SIGMA/RFILLET
00530         YE0=PVC/PVE
00540         YE1=(1.-YE0)*FEY1
00550         YE2=(1.-YE0)*FEY2
00560         CALL OSWALT(TC,HENRY1,HENRY2)
00570         X1NOT=YE1*PVE/HENRY1
00580         X2NOT=YE2*PVE/HENRY2
00590         X1PX2=X1NOT+X2NOT
00600         FBY1=X1NOT/X1PX2
00610         FBY2=X2NOT/X1PX2
00620         DO 100 I=2,N
00630         X(I,1)=X1NOT
00640         X(I,2)=X2NOT
00650         XSTR(I,1)=X1NOT
00660         XSTR(I,2)=X2NOT
00670         XSTR2(I,1)=X1NOT
00680         XSTR2(I,2)=X2NOT
00690   100   CONTINUE
00700         R1=R10
00710         R1STR=R10
00720         R1STR2=R10
00730         DR1DT=0.
00740         DDRDT=0.
00750         R1MIN=0.1*R1
00760 C
00770 C       INITIALIZE TIME AND FLAGS
00780 C
00790         TIME=0.
00800         DTU=0.
00810         IPRINT=0
00820         IPLOT=0
00830         KPLOT=0
00840         NSTEP=0
00850 C
00860 C       CALCULATE INITIAL AMOUNT OF GAS IN BUBBLE
00870 C
00880         CALL TPCONDI
00890         CALL TENSION(TC,SIGMA)
00900         PLIQ=PVE-2.*SIGMA/RFILLET
00910         PG=PLIQ+2.*SIGMA/R1-PVC
00920         PB=PG+PVC
00930         WGT=PG*PI43*R1**3/RU/TC
```

```
00940         WG1=WGT*FBY1
00950         WG2=WGT*FBY2
00960 C
00970 C       CALCULATE CONSTANT GEOMETRIC FUNTIONALS
00980 C
00990         Z(1)=-DZ
01000         DO 200 I=2,N
01010         Z(I)=Z(I-1)+DZ
01020         FG1(I)=BIGGAM*Z(I)+1.0
01030         FG2(I)=ALOG(FG1(I))
01040         Y(I)=FG2(I)/GAMA
01050  200    CONTINUE
01060 C
01070 C       ENTER TIME LOOP
01080 C
01090         CALL PRINT
01100  9999   CONTINUE
01110         TIME=TIME+DT
01120 C
01130 C       SET COEFFICIENTS FOR TEMPORAL DERIVATIVES APPROXIMATION
01140 C
01150         IF(DTU.NE.DT) GO TO 300
01160         COT1=1.5
01170         COT2=-2.
01180         COT3=0.5
01190         GO TO 400
01200  300    CONTINUE
01210         COT1=1.0
01220         COT2=-1.0
01230         COT3=0.
01240  400    CONTINUE
01250 C       DTU=DT
01260         IPRINT=IPRINT+1
01270 C
01280 C       CALCULATE EXTERNAL PRESSURE,TEMPERATURE AND GAS CONCENTRATION
01290 C
01300         CALL TPCONDI
01310         CALL SUBRHO(TC,RHOL,RHOV)
01320         CALL TENSION(TC,SIGMA)
01330         P[illegible]*PVE-2.*SIGMA/RFILLET
01340         YL[illegible] VC/PVE
01350         YE1[illegible].-YEO)*FEY1
```

```
01360          YE2=(1.-YE0)*FEY2
01370          CALL OSWALT(TC,HENRY1,HENRY2)
01380          XE1=YE1*PVE/HENRY1
01390          XE2=YE2*PVE/HENRY2
01400 C
01410 C        SET B.C.'S AT EXTERNAL INTERFACE
01420 C
01430          XEBC(1)=XE1
01440          XEBC(2)=XE2
01450 C
01460 C        CALCULATE B.C.'S AT BUBBLE INTERFACE
01470 C
01480          WG1=WG1+DWG1DT*DT
01490          WG2=WG2+DWG2DT*DT
01500          WG12=WG1+WG2
01510 C
01520 C        CALCULATE NEW BUBBLE RADIUS
01530 C        SOLVE A*X**3+B*X+C=0 BY QUASILINIEARIZATION
01540 C
01550          CAB1=RU*TC*(WG1+WG2)/PI43
01560          CAB2=-2.*SIGMA
01570          CAB3=-(PLIQ-PVC)
01580          ZR=1./R1
01590          DO 500 ITER=1,50
01600          ZRU=ZR
01610          ZR2=ZR*ZR
01620          ZR3=ZR2*ZR
01630          FACTOR=CAB3+CAB2*ZR+CAB1*ZR3
01640          FACTOR=-FACTOR/(3.*CAB1*ZR2+CAB2)
01650          ZR=ZR+FACTOR
01660          ERROR=ABS(1.0-ZR/ZRU)
01670          IF(ERROR.LT.1.E-4) GO TO 501
01680    500   CONTINUE
01690    501   R1=1./ZR
01700          IF(R1.LE.0.) GO TO 51
01710          VOL=PI43*R1**3
01720          PG1=WG1*RU*TC/VOL
01730          PG2=WG2*RU*TC/VOL
01740          PB=PVC+PG1+PG2
01750          YB0=PVC/PB
01760          YB1=PG1/PB
01770          YB2=PG2/PB
```

```
      XB1=PG1/HENRY1
      XB2=PG2/HENRY2
C
C     SET B.C.'S AT BUBBLE INTERFACE
C
      XBBC(1)=XB1
      XBBC(2)=XB2
C
C     CALCULATE BUBBLE RADIUS TEMPORAL DERIVATIVES
C
      DR1DT=(COT1*R1+COT2*R1STR+COT3*R1STR2)/DT
      R1SQ=R1*R1
      R1CU=R1SQ*R1
      R2=(VLIQ2+R1CU)**(1./3.)
      R2SQ=R2*R2
      DR2DT=R1SQ/R2SQ*DR1DT
      DR=R2-R1
      DDRDT=DR2DT-DR1DT
      COF1=GAMA/DR/BIGGAM
      COF2=DR/GAMA
      COF2P=DDRDT/GAMA
      COF4=DR1DT*R1**2*COF1
C
C     CALCULATE COEFFICIENTS FOR PARTIAL DIFFERENTIAL
C     SPECIES EQUATIONS
C
      DO 600 K=NG1,NG2
      CALL DIFFCO(K,TC,DIFF(K))
      COF3=2.*DIFF(K)*COF1
      COF5=-DIFF(K)*GAMA/DR*COF1
      COF6=-DIFF(K)*COF1*COF1
      DO 700 I=2,N
      FGG1(I)=COF1*FG1(I)*(COF2P*FG2(I)+DR1DT)
     1         +COF3*FG1(I)*1.0/(COF2*FG2(I)+R1)
     2         -COF4*FG1(I)*1.0/((COF2*FG2(I)+R1)**2)
     3         -COF5*FG1(I)
      FGG2(I)=-COF6*FG1(I)*FG1(I)
      R(I)=DR*Y(I)+R1
  700 CONTINUE
C
C
C     RESET FSTR'S AND FSRT2'S
```

```
C
      DO 800 I=2,N
      XSTR2(I,K)=XSTR(I,K)
      XSTR(I,K)=X(I,K)
  800 CONTINUE
C
C     CALCULATE COEFFICIENTS A(I),B(I),C(I) FOR KTH ALGEBRAIC
C     SPECIES EQUATION. X(I)=A(I)*X(I+1)+B(I)*X(I-1)+C(I)
C
      DO 900 I=2,N
      DENOM=COT1/DT+2.0*FGG2(I)/DZDZ
      A(I)=(FGG1(I)/DZ2+FGG2(I)/DZDZ)/DENOM
      B(I)=(FGG2(I)/DZDZ-FGG1(I)/DZ2)/DENOM
      C(I)=-(COT2*XSTR(I,K)/DT+COT3*XSTR2(I,K)/DT)/DENOM
  900 CONTINUE
C
C     AT NODE ≡2≡:
C     1) SAVE COEFFICIENTS A(2),B(2) AND C(2)
C     2) RESET THE ABOVE
C
      A22(K)=A(2)
      B22(K)=B(2)
      C22(K)=C(2)
      A(2)=0.
      B(2)=0.
      C(2)=XBBC(K)
C
C     AT NODE ≡N≡:
C     RESET COEFFICIENTS A(N),B(N),AND C(N)
C
      A(N)=0.
      B(N)=0.
      C(N)=XEBC(K)
C
C     CALCULATE COEFFICIENTS ASTR(I) AND BSTR(I) FOR
C     X(I)=ASTR(I)*X(I+1)+BSTR(I)
C
C     AT NODE ≡2≡
C
      ASTR(2)=0.
      BSTR(2)=C(2)
C
```

```
C      FOR NODES 3 THRU N
C
       DO 1000 I=3,N
       DENOM=1.0-B(I)*ASTR(I-1)
       ASTR(I)=A(I)/DENOM
       BSTR(I)=(B(I)*BSTR(I-1)+C(I))/DENOM
 1000  CONTINUE
C
C      ELIMINATION ALGORITHM TO CALCULATE NEW SPECIES PROFILE
C
       DO 1100 J=2,N
       I=N+2-J
       X(I,K)=ASTR(I)*X(I+1,K)+BSTR(I)
 1100  CONTINUE
C
C      CALCULATE  IMAGE MOLAR FRACTION X(1,K)
C
       X(1,K)=(X(2,K)-A22(K)*X(3,K)-C22(K))/B22(K)
  600  CONTINUE
C
C      CALCULATE MOLAR FLUXES AT BUBBLE INTERFACE
C
       DX1DZ=(X(3,1)-X(1,1))/DZ2
       DX2DZ=(X(3,2)-X(1,2))/DZ2
       FACTOR=4.*PI*R1SQ*GAMA/BIGGAM/DR
       DWG1DT=FACTOR*CMOLE*DIFF(1)*DX1DZ
       DWG2DT=FACTOR*CMOLE*DIFF(2)*DX2DZ
C
C      ADVANCE TIME BY DT
C
       IF(R1.LE.R1MIN) GO TO 50
       IF(NSTEP.EQ.IPLOT) CALL SETPLOT
       NSTEP=NSTEP+1
C
C      RESET R1STR AND R1STR2
C
       R1STR2=R1STR
       R1STR=R1
       IF(IPRINT.EQ.IDPRNT) CALL PRINT
       IF(NSTEP.GT.NSTPMX) GO TO 50
       DTMAX=0.1*ABS(R1/DR1DT)
       IF(DT.GT.DTMAX) DT=DTMAX
```

```
03040          GO TO 9999
03050    50    CALL SETPLOT
03060    51    CALL TRACE(FTIME,FTE,KPLOT,1.0)
03070          CALL TRACE(FTIME,FTC,KPLOT,2.0)
03080          CALL ENDPLT(9HTE AND TC,9HTIME(SEC),7HTEMP(K),5HPARAM)
03090          CALL TRACE(FTIME,FPVE,KPLOT,3.0)
03100          CALL TRACE(FTIME,FPVC,KPLOT,4.0)
03110          CALL TRACE(FTIME,FPBUBLE,KPLOT,5.0)
03120          CALL ENDPLT(10HPE,PC,PBUB,9HTIME(SEC),9HPRES(ATM),5HPARAM)
03130          CALL TRACE(FTIME,FR1,KPLOT,6.0)
03140          CALL ENDPLT(10HBUBLE SIZE,9HTIME(SEC),10HRADIUS(CM),
03150         15HPARAM)
03160          CALL TRACE(FTIME,FYB0,KPLOT,7.0)
03170          CALL TRACE(FTIME,FYB1,KPLOT,8.0)
03180          CALL TRACE(FTIME,FYB2,KPLOT,9.0)
03190          CALL ENDPLT(8HX0,X1,X2,9HTIME(SEC),10HMOLE FRCTN,5HPARAM)
03200          CALL ENDALL
03210          CALL PRINT
03220          STOP
03230          END
03240          SUBROUTINE SETPLOT
03250 C
03260 C        SAVE VARIABLES FOR PLOTING
03270 C
03280          COMMON/MAIN/X(100,3),XSTR(100,3),XSTR2(100,3),R(100),Y(100),
03290         1Z(100),R1,R2,N,TIME,TC,TE,PVC,PVE,WG1,WG2,YE1,YE2,PB,TCNOT,
03300         2XB1,XB2,XE1,XE2,YB1,YB2,IPRINT,KPLOT,YB0,IPLOT,IDPLOT,TENOT,RATE
03310          COMMON/DATPLO/FTIME(1000),FTE(1000),FTC(1000),FPVE(1000),
03320         1              FPVC(1000),FYB0(1000),FYB1(1000),FYB2(1000),
03330         2               FR1(1000),FPBUBLE(1000)
03340          IPLOT=IPLOT+IDPLOT
03350          KPLOT=KPLOT+1
03360          FTIME(KPLOT)=TIME
03370          FTE(KPLOT)=TE
03380          FTC(KPLOT)=TC
03390          FPVE(KPLOT)=PVE
03400          FPVC(KPLOT)=PVC
03410          FYB0(KPLOT)=YB0
03420          FYB1(KPLOT)=YB1
03430          FYB2(KPLOT)=YB2
03440          FR1(KPLOT)=R1
03450          FPBUBLE(KPLOT)=PB
```

```
03460  100  RETURN
03470       END
03480       SUBROUTINE OSWALT(XT,CH1,CH2)
03490 C
03500 C     SUBROUTINE TO CALCULATE GAS SOLUBILITY IN A LIQUID
03510 C
03520       COMMON/SUBDAT/CMOLE,RHOL,RHOV,RU,EMW
03530       COMMON/SCLDIF/DF11,DF21,DF12,DF22,COS11,COS12,COS21,COS22,
03540      1NG1,NG2
03550 C
03560 C     COEFFICIENTS FOR SOLUBILITY EQUATION
03570 C     F(T)=COS1*T**COS2 IN 1./ATM
03580 C     WHERE T=TEMPERATURE IN DEGREES KELVIN
03590 C
03600       CH1=COS11*XT**COS21
03610       CH1=1./CH1
03620       CH2=COS12*XT**COS22
03630       CH2=1./CH2
03640  100  RETURN
03650       END
03660       SUBROUTINE TPCONDI
03670 C
03680 C     UPDATE EXTERNAL PRESSURE AND TEMPERATURE
03690 C
03700       COMMON/MAIN/X(100,3),XSTR(100,3),XSTR2(100,3),R(100),Y(100),
03710      1Z(100),R1,R2,N,TIME,TC,TE,PVC,PVE,WG1,WG2,YE1,YE2,PB,TCNOT,
03720      2XB1,XB2,XE1,XE2,YB1,YB2,IPRINT,KPLOT,YBO,IPLOT,IDPLOT,TENOT,RATE
03730       TC=180.+RATE*TIME
03740       TE=300.
03750       IF(TIME.GT.0.0.AND.TC.GE.TCNOT) TC=TCNOT
03760       IF(TIME.GE.0.) GO TO 50
03770       TC=TCNOT
03780       TE=TENOT
03790  50   CONTINUE
03800 C
03810 C     COEFFICIENTS FOR METHANOL VAPOR PRESSURE
03820 C
03830       DATA CP1,CP2,CP3,CP4,CP5
03840      1      /15.05411,-9.24063,3.366136,-1.9692,3.389658E-1/
03850       TRC=1000./1.8/TC
03860       TRC2=TRC*TRC
03870       TRC3=TRC2*TRC
```

```
03880         TRC4=TRC3*TRC
03890         PVC=CP1+CP2*TRC+CP3*TRC2+CP4*TRC3+CP5*TRC4
03900         PVC=EXP(PVC)/14.696
03910         TRE=1000./1.8/TE
03920         TRE2=TRE*TRE
03930         TRE3=TRE2*TRE
03940         TRE4=TRE3*TRE
03950         PVE=CP1+CP2*TRE+CP3*TRE2+CP4*TRE3+CP5*TRE4
03960         PVE=EXP(PVE)/14.696
03970   100   RETURN
03980         END
03990         SUBROUTINE DIFFCO(ISPICE,TEMP,DIFCO)
04000         COMMON/SOLDIF/DF11,DF21,DF12,DF22,COS11,COS12,COS21,COS22,
04010        1NG1,NG2
04020 C       COEFFICIENTS FOR DIFFUSIVITY EQUATION OF GASES IN METHANOL
04030 C       D(T)=DF1*EXP(DF2/T) IN SQCM/SEC
04040 C       WHERE T=TEMPERATURE IN DEGREES KELVIN
04050         IF(ISPICE.GT.1) GO TO 10
04060         DIFCO=DF11*EXP(DF21/TEMP)
04070         GO TO 100
04080   10    DIFCO=DF12*EXP(DF22/TEMP)
04090   100   RETURN
04100         END
04110         SUBROUTINE TENSION(TEMP,FTEMP)
04120 C
04130 C       COEFFICIENT FOR SURFACE TENSION EQN FOR METHANOL
04140 C
04150         DATA CT1,CT2,CT3,CT4,CT5
04160        1      /5.79025E-3,-1.404494E-5,1.20562E-8,3.516629E-12,
04170        2       -8.67029E-15/
04180         TR=TEMP*1.8
04190         TR2=TR*TR
04200         TR3=TR2*TR
04210         TR4=TR3*TR
04220         FTEMP=CT1+CT2*TR+CT3*TR2+CT4*TR3+CT5*TR4
04230         FTEMP=FTEMP*1.44E-2
04240   100   RETURN
04250         END
04260         SUBROUTINE PRINT
04270         COMMON/MAIN/X(100,3),XSTR(100,3),XSTR2(100,3),R(100),Y(100),
04280        1Z(100),R1,R2,N,TIME,TC,TE,PVC,PVE,WC1,WG2,YE1,YE2,PB,TCNOT,
04290        2XB1,XB2,XE1,XE2,YB1,YB2,IPRINT,KPLOT,YBO,IPLOT,IDPLOT,TENOT,RATE
```

```
04300         IF(TIME.GT.0.) GO TO 51
04310         WRITE(6,50)
04320         WRITE(6,60)
04330   60    FORMAT(1X,5H(SEC),7X,4H(CM),8X,5H(ATM),7X,
04340        18H(KELVIN),4X,8H(KELVIN),4X,5H(ATM)//)
04350   50    FORMAT(1H1,4HTIME,8X,10HBUBBLE RAD,2X,11HBUBBLE PRES,1X,
04360        13HTCO,9X,3HTEV,9X,3HPEV,9X,7HXHELIUM,5X,9HXNITROGEN)
04370   51    WRITE(6,100) TIME,R1,PB,TC,TE,PVE,YB1,YB2
04380   100   FORMAT(1X,8(E11.4,1X))
04390         NP1=N+1
04400         IF(TIME.LT.1.E20) GO TO 509
04410         WRITE(6,70)
04420   70    FORMAT(1X,5HR(CM),7X,8HX-HELIUM,4X,10HX-NITROGEN//)
04430         DO 300 I=1,NP1
04440         WRITE(6,71) R(I),X(I,1),X(I,2)
04450   71    FORMAT(1X,3(E11.4,1X))
04460   300   CONTINUE
04470   509   IPRINT=0
04480   200   RETURN
04490         END
04500         SUBROUTINE SUBRHO(XT,YL,YV)
04510 C
04520 C       CALCULATE LIQUID AND VAPOR MASS DENSITY
04530 C
04540 C
04550 C       COEFFICIENTS FOR LIQUID DENSITY RHO(LB/CUFT)
04560 C       T(KELVIN), RHO=C1+C2*T+.....
04570 C
04580         DATA CRL1,CRL2,CRL3,CRL4,CRL5
04590        1      /19.079,5.2791E-1,-2.72739E-3,5.69277E-6,-4.51924E-9/
04600 C
04610 C       COEFFICIENTS FOR VAPOR DENSITY RHO(LB/CUFT)
04620 C       T(KELVIN), R=EXP(C1+C2/T+.....)
04630 C
04640         DATA CRV1,CRV2,CRV3,CRV4,CRV5
04650        1     /15.93164,-1.17172E4,3.53187E6,-7.33649E8,5.53411E10/
04660         TR=XT
04670         TR2=TR*TR
04680         TR3=TR2*TR
04690         TR4=TR3*TR
04700         YL=CRL1+CRL2*TR+CRL3*TR2+CRL4*TR3+CRL5*TR4
04710         YL=YL*1.6E-2
```

```
04720         YV=CRV1+CRV2/TR+CRV3/TR2+CRV4/TR3+CRV5/TR4
04730         YV=1.6E-2*EXP(YV)
04740   100   RETURN
04750         END
04760         SUBROUTINE TRACE(V, F, NV, PVAL)
04770 C       SAVE 1 TRACE (SET OF (V(I),F(I))) OF DATA ON TAPE9.
04780 C       ALSO COLLECT EXTREMA INFO
04790         COMMON /PLOTC/ TITLE,VNAME,FNAME,PNAME,VMIN,FMIN,PMIN
04800        1,   VMAX,FMAX,PMAX,NP,NPLTS,LOCHED(63),PA(256),NA(256)
04810         DIMENSION V(1),F(1),BLK(1026),INDX(1080)
04820         DATA VMIN,FMIN,PMIN,VMAX,FMAX,PMAX /3*1.E30,3*-1.E30/
04830        1,   NP,NPLTS,LOCHED(1) /0,1,1/
04840        2,   IPASS1/1/
04850 C
04860 C       SKIP IF NOT 1ST PASS
04870         IF (IPASS1 .EQ. 0)  GO TO 10
04880         IPASS1 = 0
04890 C       DONT WANT TO ADD RECORDS TO AN EXISTING FILE.  RETURN OLD
04900         CALL RETFILE(9)
04910         CALL OPENMS(9, INDX, 1080, 0)
04920 C
04930 C       AFTER INC, LOCHED(NPLTS)=RECORD NUMBER TO STORE THIS TRACE
04940    10   LOCHED(NPLTS) = LOCHED(NPLTS) +1
04950         IF (LOCHED(NPLTS) .GT. 1077)  X = SQRT(-1.)
04960 C       NUMBER OF PARAMETER VALUES (TRACES) IN THIS PLOT
04970         NP = NP+1
04980         IF (NP .GT. 256)  X= ACOS(2.)
04990 C       SAVE RECORD SIZE(/2)
05000         NA(NP) = NV
05010         IF (NV .GT. 513)  X=ASIN(2.)
05020 C       SAVE PARAMETER VALUE
05030         PA(NP) = PVAL
05040 C       FIND EXTREMA OF PARAMETER, VARIABLE, FUNCTION
05050         PMIN = AMIN1(PMIN, PVAL)
05060         PMAX = AMAX1(PMAX, PVAL)
05070         DO 20  I=1,NV
05080         X = V(I)
05090         VMIN = AMIN1(VMIN, X)
05100         VMAX = AMAX1(VMAX, X)
05110 C       PACK VARIABLE, THEN FUNCTION PRIOR TO WRITE
05120         BLK (I) = X
05130         Y = F(I)
```

```
05140        FMIN = AMIN1(FMIN, Y)
05150        FMAX = AMAX1(FMAX, Y)
05160     20 BLK(I+NV) = Y
05170 C      WRITE (V(I),I=1,NV),(F(I),I=1,NV)
05180        CALL WRITMS(9, BLK, 2*NV, LOCHED(NPLTS))
05190        RETURN
05200        END
05210        SUBROUTINE ENDPLT(TI, VN, FN, PN)
05220 C      TERMINATE CURRENT PLOT, SET UP FOR NEXT
05230        COMMON /PLOTC/ TITLE,VNAME,FNAME,PNAME,VMIN,FMIN,PMIN
05240       1,   VMAX,FMAX,PMAX,NP,NPLTS,LOCHED(63),PA(256),NA(256)
05250        EQUIVALENCE (IPA,PA)
05260        DIMENSION IPA(1)
05270 C
05280 C      MOVE CALLING SEQ INTO STORAGE BLOCK
05290        TITLE = TI
05300        VNAME = VN
05310        FNAME = FN
05320        PNAME = PN
05330 C      NEXT IS FINAL SETTING OF LOCHED(NPLTS).  NOTE LOCHED(I) IS
05340 C      RECORD NUMBER OF HEADER FOR PLOT I
05350        LOCHED(NPLTS) = LOCHED(NPLTS) + 1
05360 C      WRITE HEADER REC--INCLUDES VARIABLES IN /PLOTC/ FROM TITLE TO NP
05370        CALL WRITMS(9, TITLE, 11, LOCHED(NPLTS))
05380 C      PACK LIST OF RECORD LEN/2 RIGHT AFTER LIST OF PARAMETER VALUES
05390 C      NOTE EQU (IPA,PA)
05400        DO 10  I=1,NP
05410     10 IPA(I+NP) = NA(I)
05420 C      WRITE PARAMETER, LENGTH LISTS AFTER HEADER
05430        CALL WRITMS(9, PA, 2*NP, LOCHED(NPLTS)+1)
05440 C      NUMBER OF NEXT PLOT
05450        NPLTS = NPLTS+1
05460        IF (NPLTS .GT. 63)  X = ALOG(-1.)
05470 C      (CHECK TRACE) NOTE TRACES FOR NEXT PLOT START RIGHT AFTER
05480 C      HEADER, LIST RECORDS FOR THIS ONE
05490        LOCHED(NPLTS) = LOCHED(NPLTS-1) + 1
05500 C      INITIALIZE SCALING, NUMBER OF PARAM VALUES FOR NEXT PLOT
05510        BIG = 1.E30
05520        VMIN = BIG
05530        FMIN = BIG
05540        PMIN = BIG
05550        VMAX = -BIG
```

```
05560         FMAX = -BIG
05570         PMAX = -BIG
05580         NP = 0
05590         RETURN
05600         END
05610         SUBROUTINE ENDALL
05620 C       WRAP UP PLOT DATA FILE
05630         COMMON /PLOTC/ TITLE,VNAME,FNAME,PNAME,VMIN,FMIN,PMIN
05640        1,   VMAX,FMAX,PMAX,NP,NPLTS,LOCHED(63),PA(256),NA(256)
05650 C
05660         NPLTS = NPLTS-1
05670 C       WRITE NUMBER OF PLOTS ON FILE AND REC NUMBER OF HEADER FOR EACH
05680         CALL WRITMS(9, NPLTS, 64, 1)
05690         CALL CLOSEMS(9)
05700         RETURN
05710         END
```

Sample Input

```
$BUBDAT
COS11=2.5091E-12
COS21=2.9665
COS12=2.6367E-4
COS22=0.0
DF11=5.92E-3
DF21=-1034.2
DF12=2.09E-3
DF22=-1070.5
NG1=1
NG2=2
NSTPMX=8000
IDPLOT=30
R10=0.02
R20=0.08
NDIV=90
GAMA=-2.0
DT=5.
IDPRNT=200
RFILLET=10.
FBY1=1.0
FBY2=0.
FEY1=0.1
FEY2=0.9
EMW=32.0
TCNOT=250.
TENOT=300.
RATE=0.0
$END
```

APPENDIX B.2

SN009 HEAT PIPE CYCLIC TEST DATA

This appendix presents plots of temperatures along the SN009 heat pipe versus time for selected freeze/thaw test cycles not shown in Section 3.3.

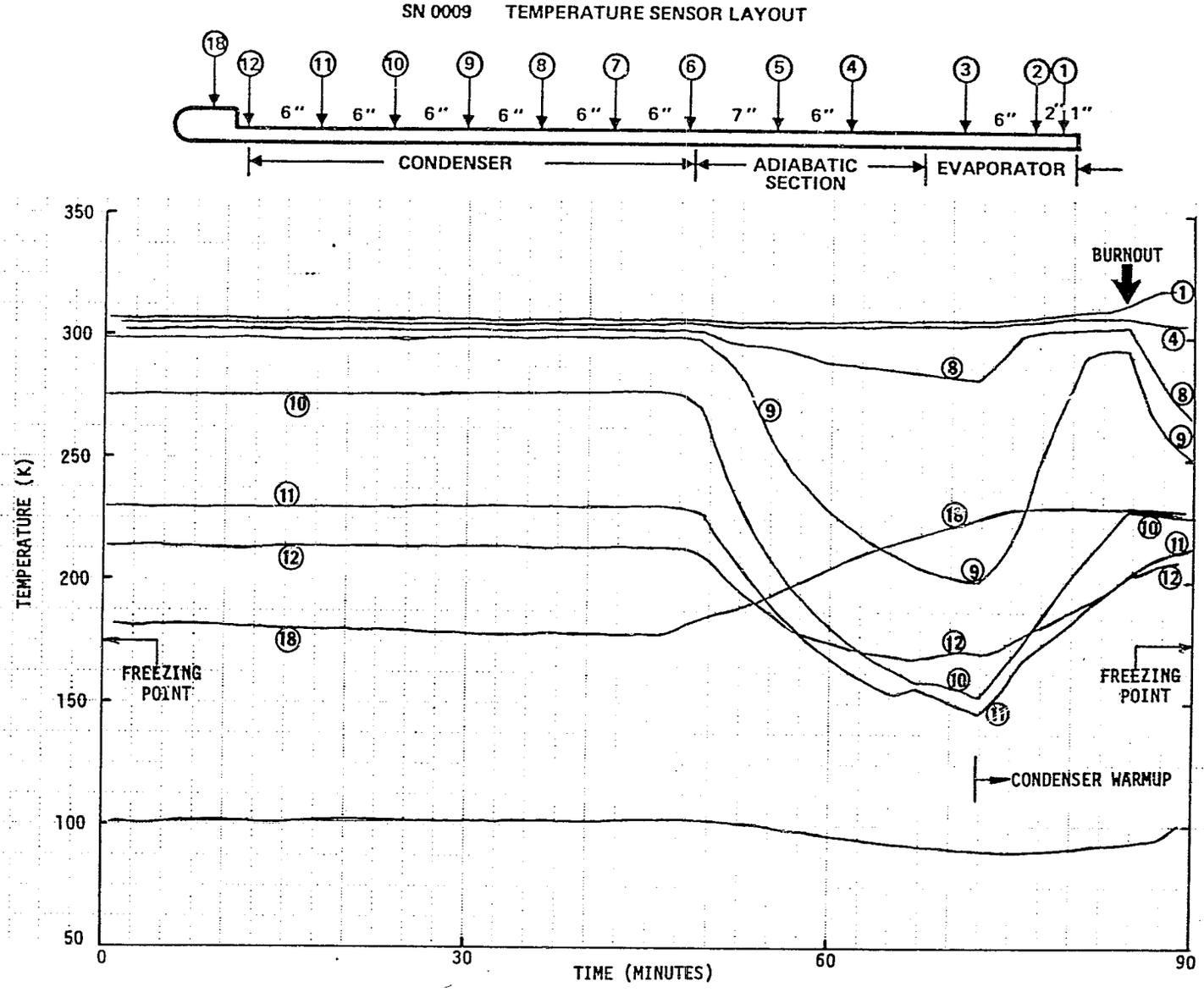

Figure B.2-1 Temperature Histories During SN009 Heat Pipe Cyclic Test No. 3

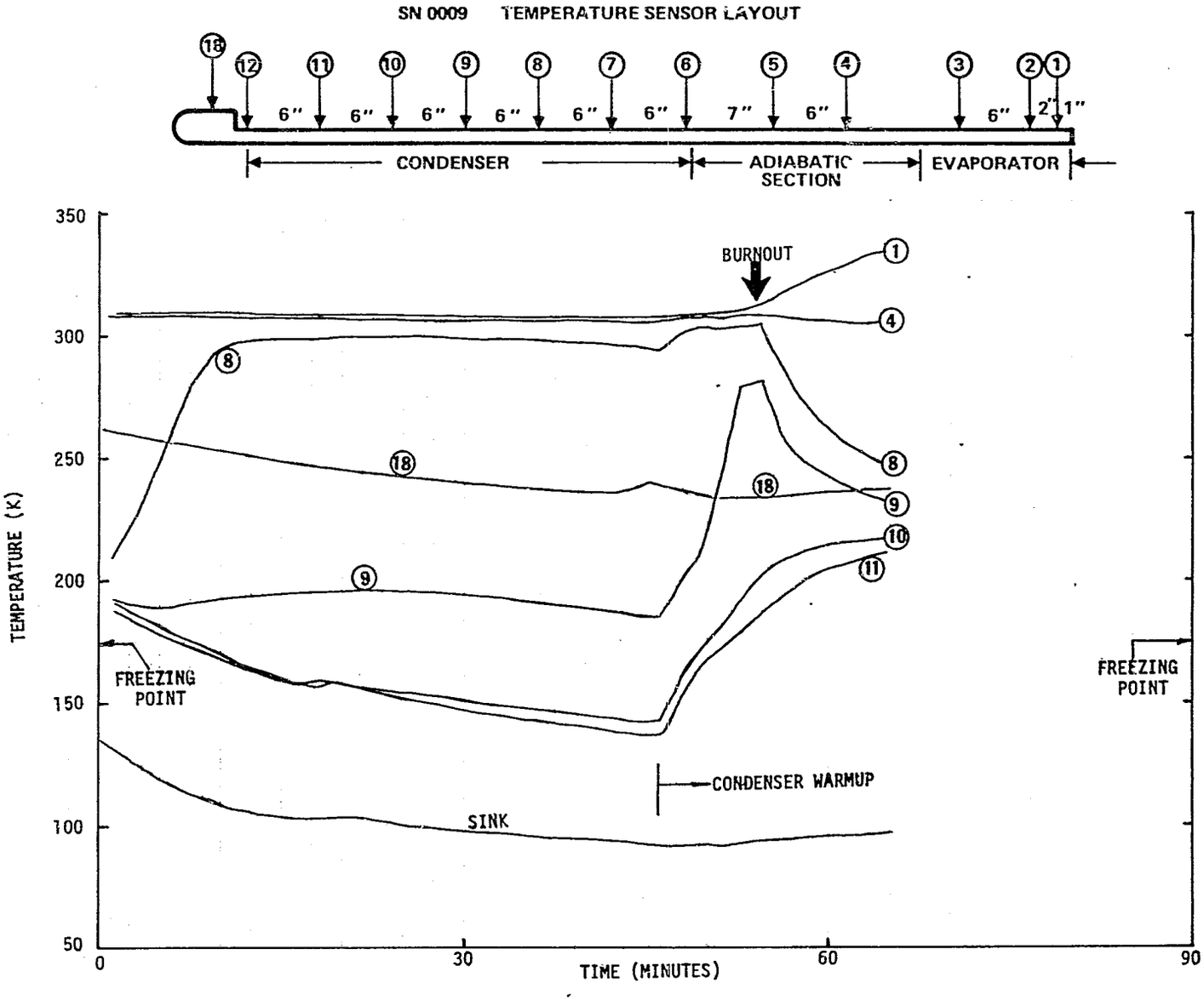

Figure B.2-2 Temperature Histories During SN009 Heat Pipe Cyclic Test No. 5

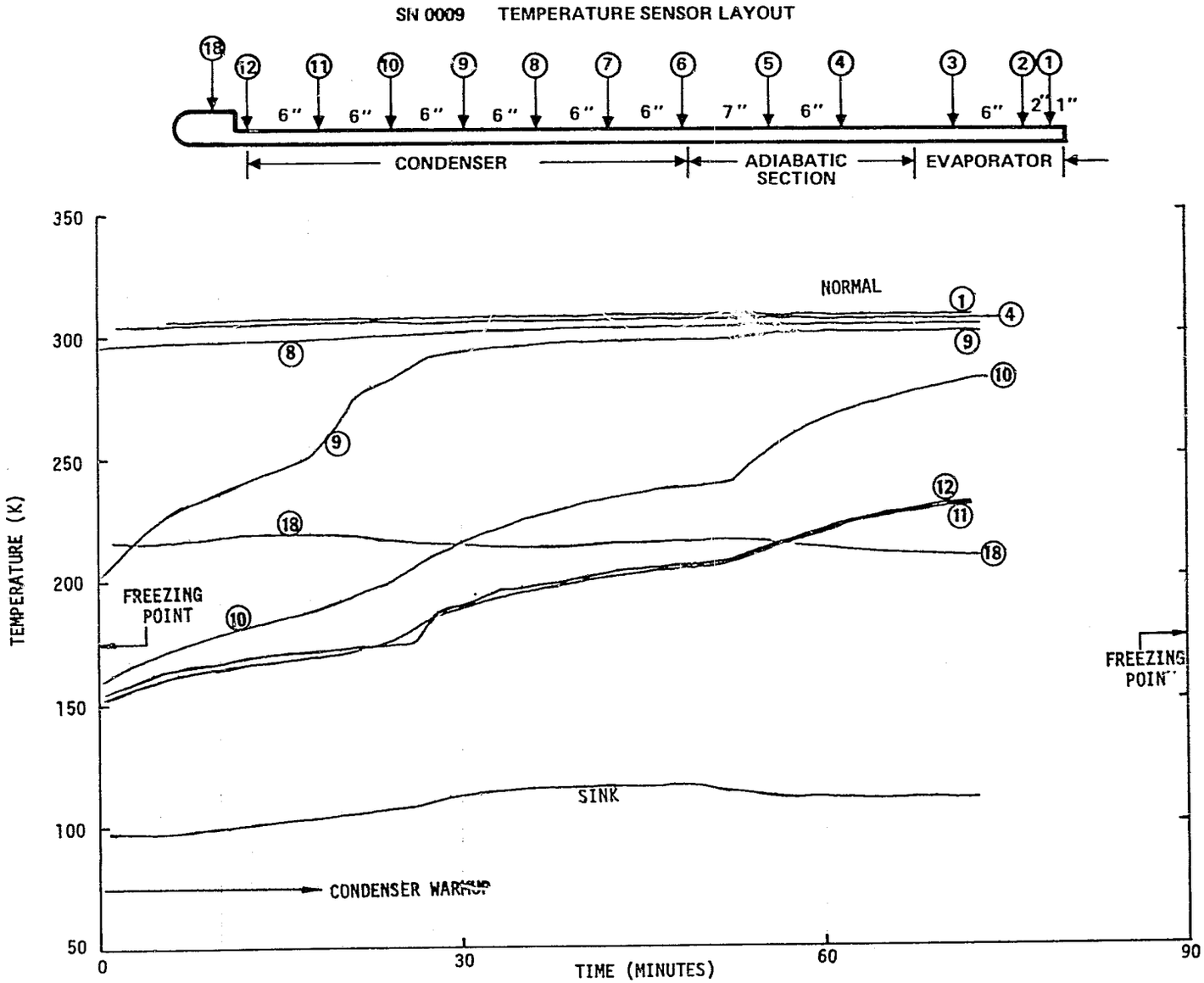

Figure B.2-3 Temperature Histories During SN009 Heat Pipe Cyclic Test No. 7

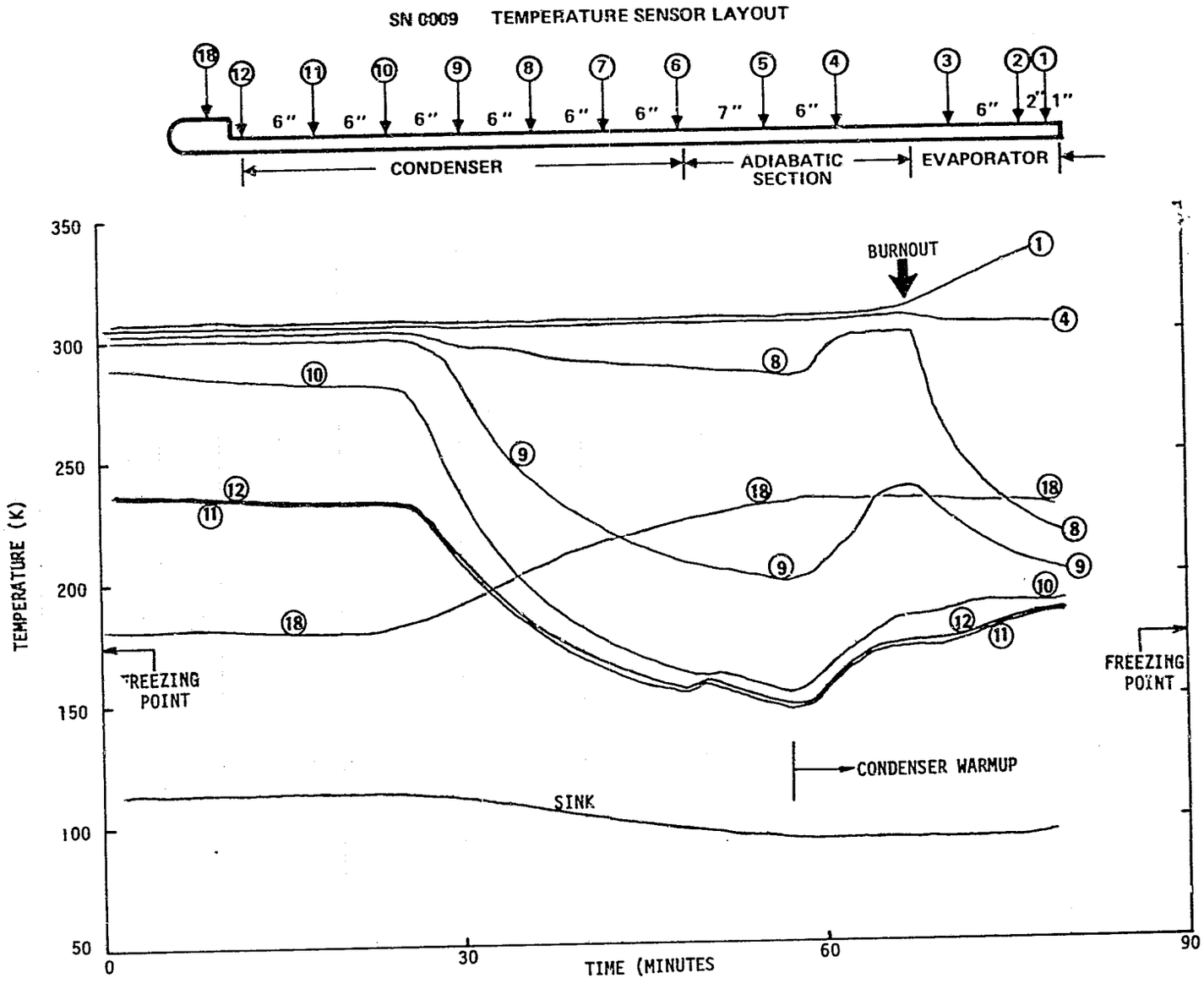

Figure B.2-4 Temperature Histories During SN009 Heat Pipe Cyclic Test No. 8

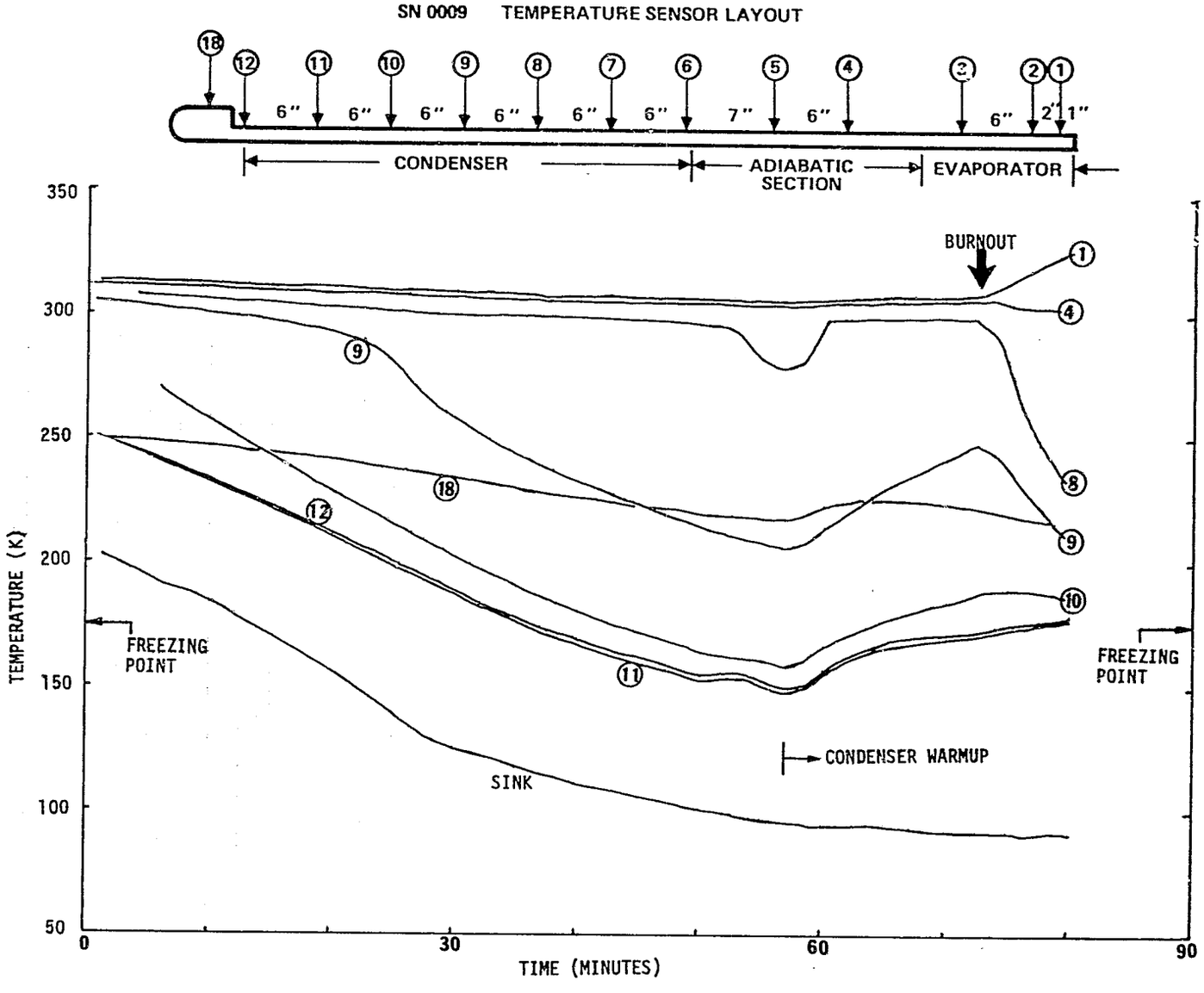

Figure B.2-5 Temperature Histories During SN009 Heat Pipe Cyclic Test No. 10

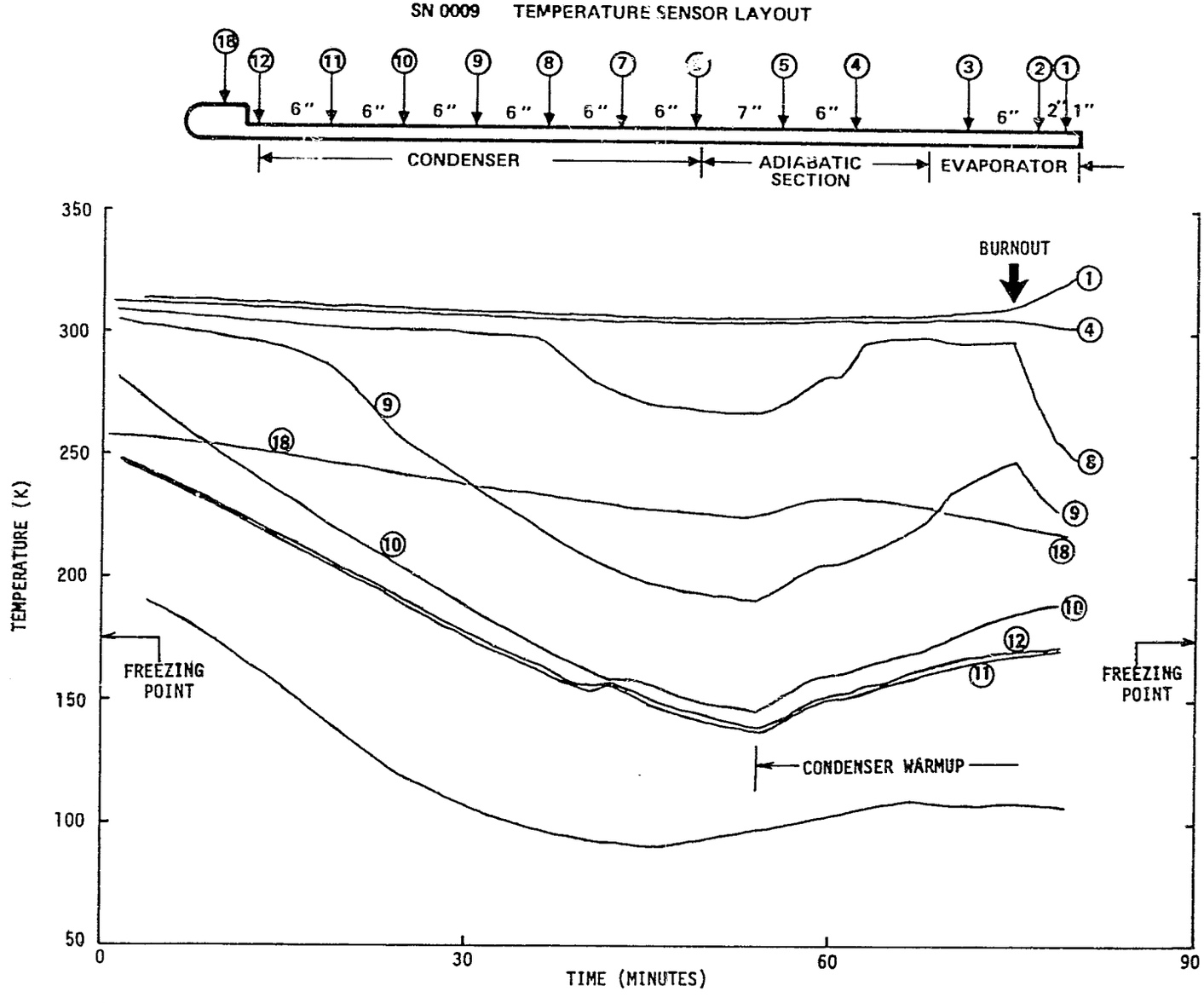

Figure B.2-6 Temperature Histories During SN009 Heat Pipe Cyclic Test No. 12

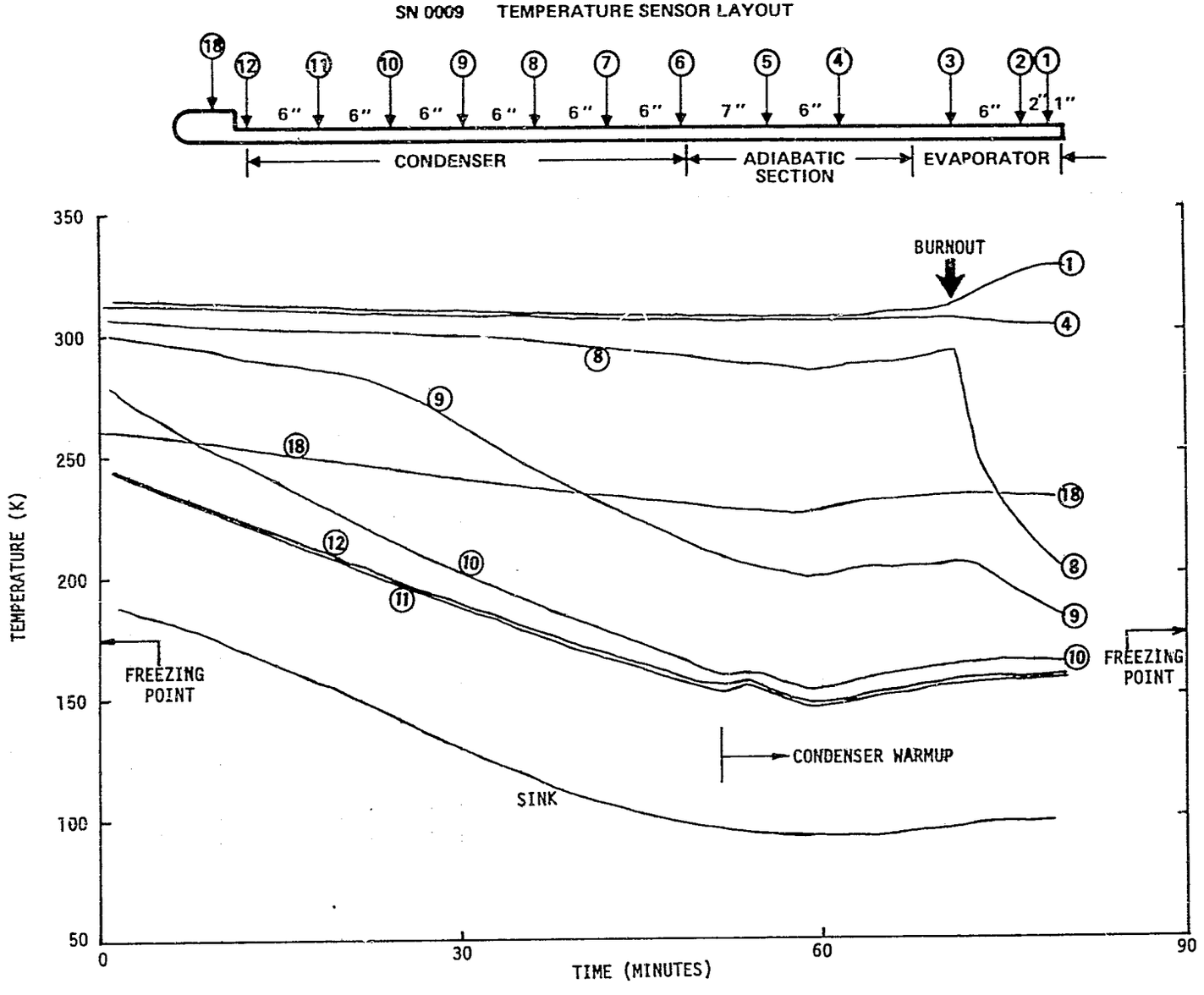

Figure B.2-7 Temperature Histories During SN009 Heat Pipe Cyclic Test No. 14

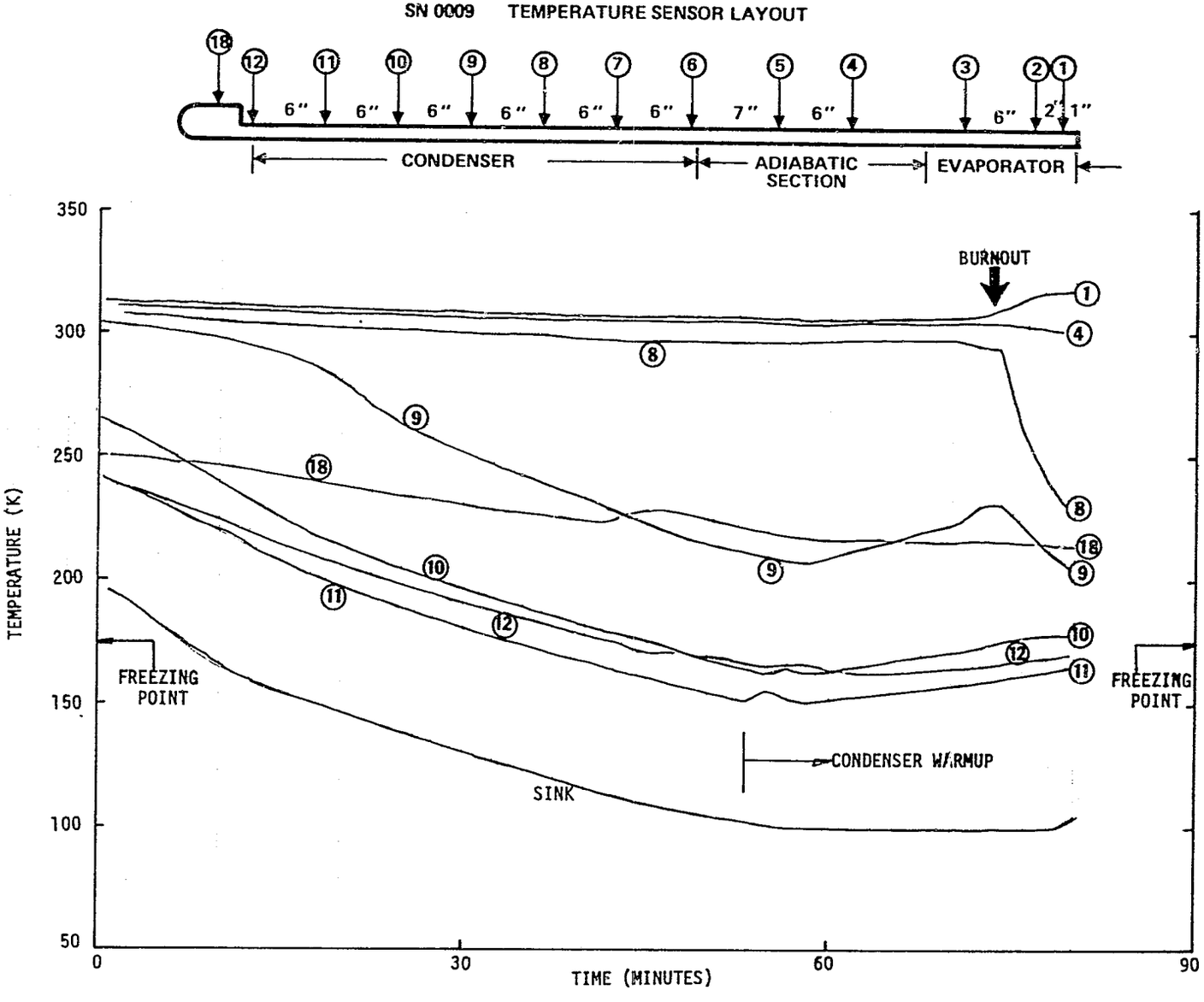

Figure B.2-8 Temperature Histories During SN009 Heat Pipe Cyclic Test No. 16

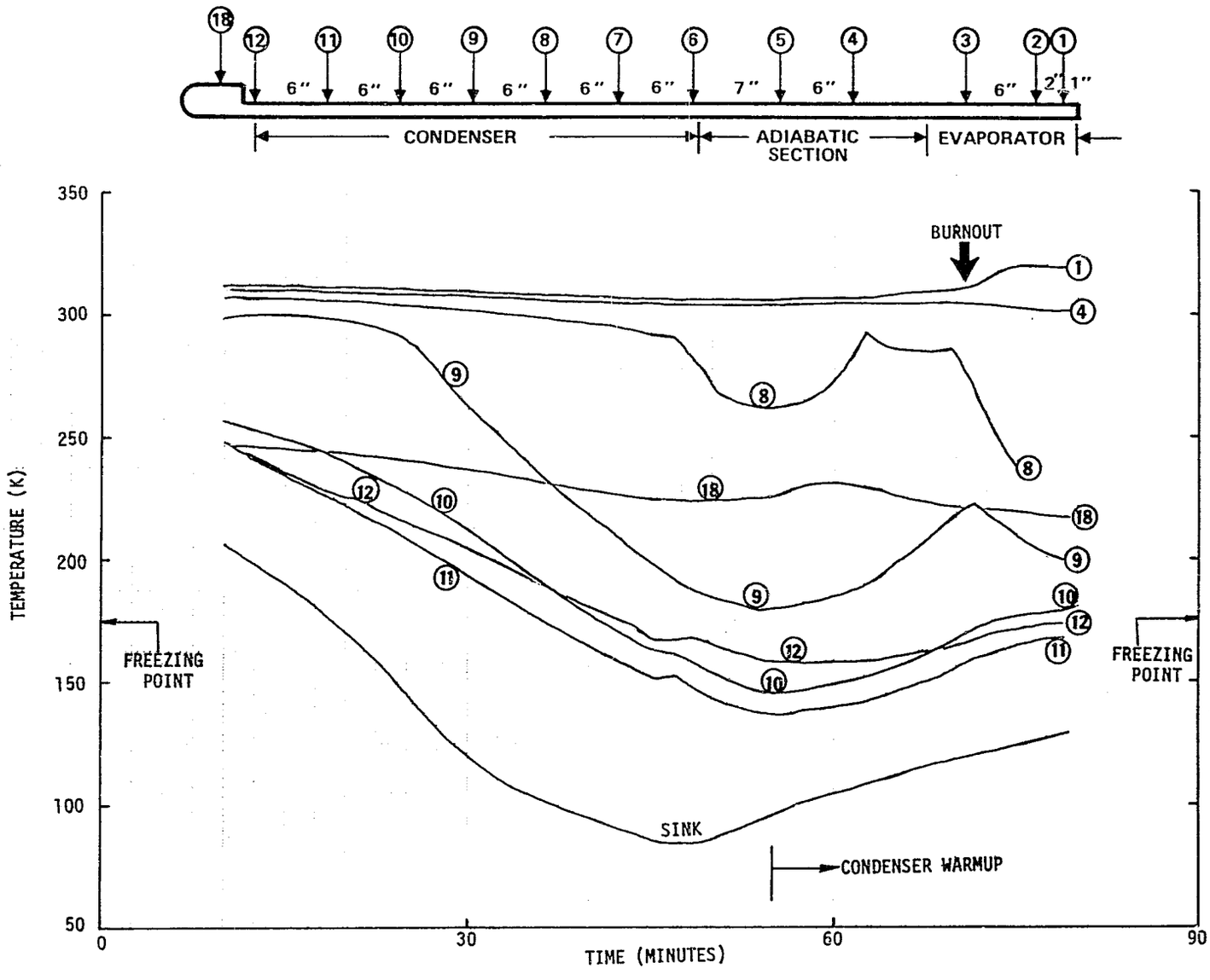

Figure B.2-9 Temperature Histories During SN009 Heat Pipe Cyclic Test No. 17

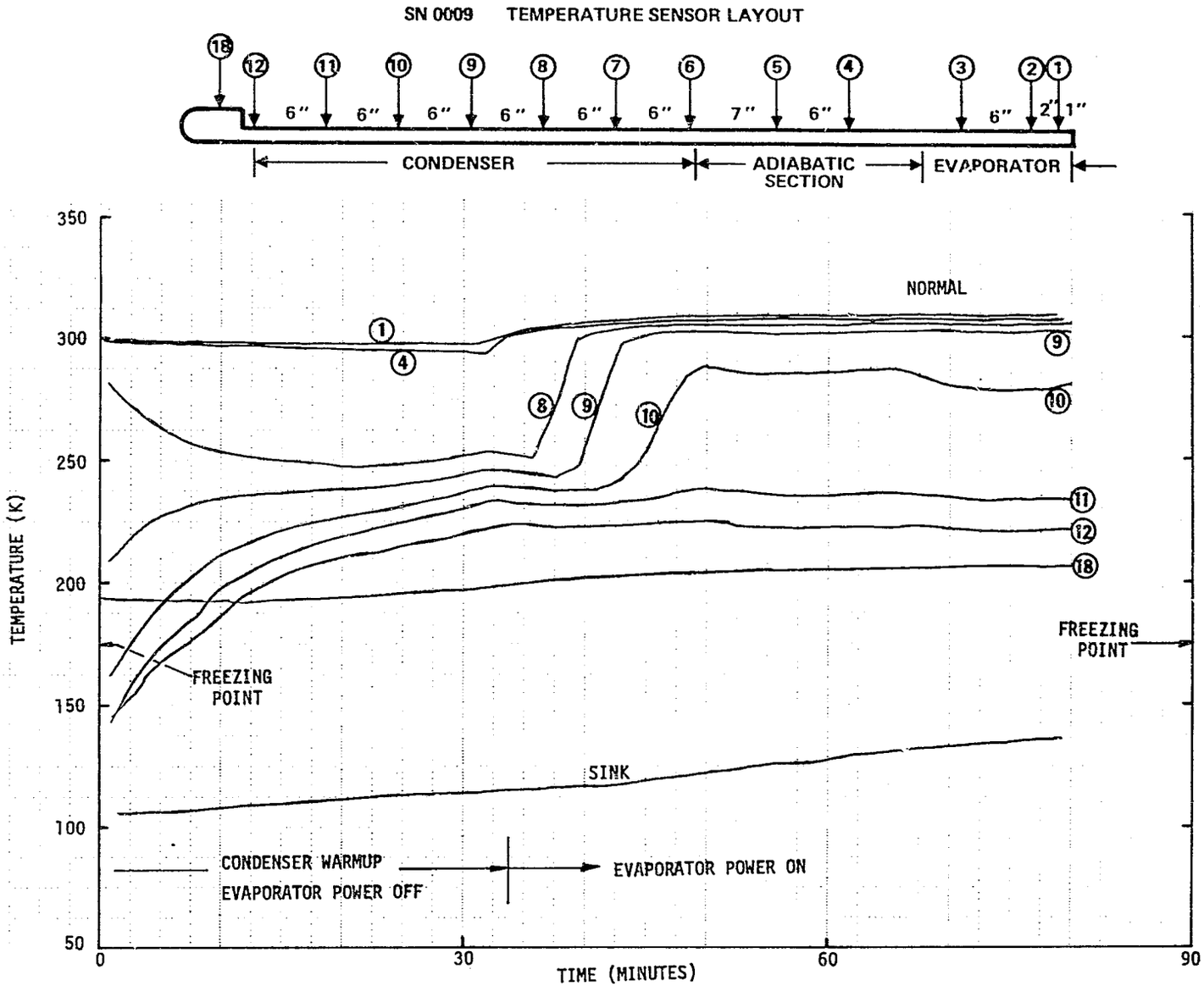

Figure B.2-10 Temperature Histories During SN009 Heat Pipe Cyclic Test No. 22

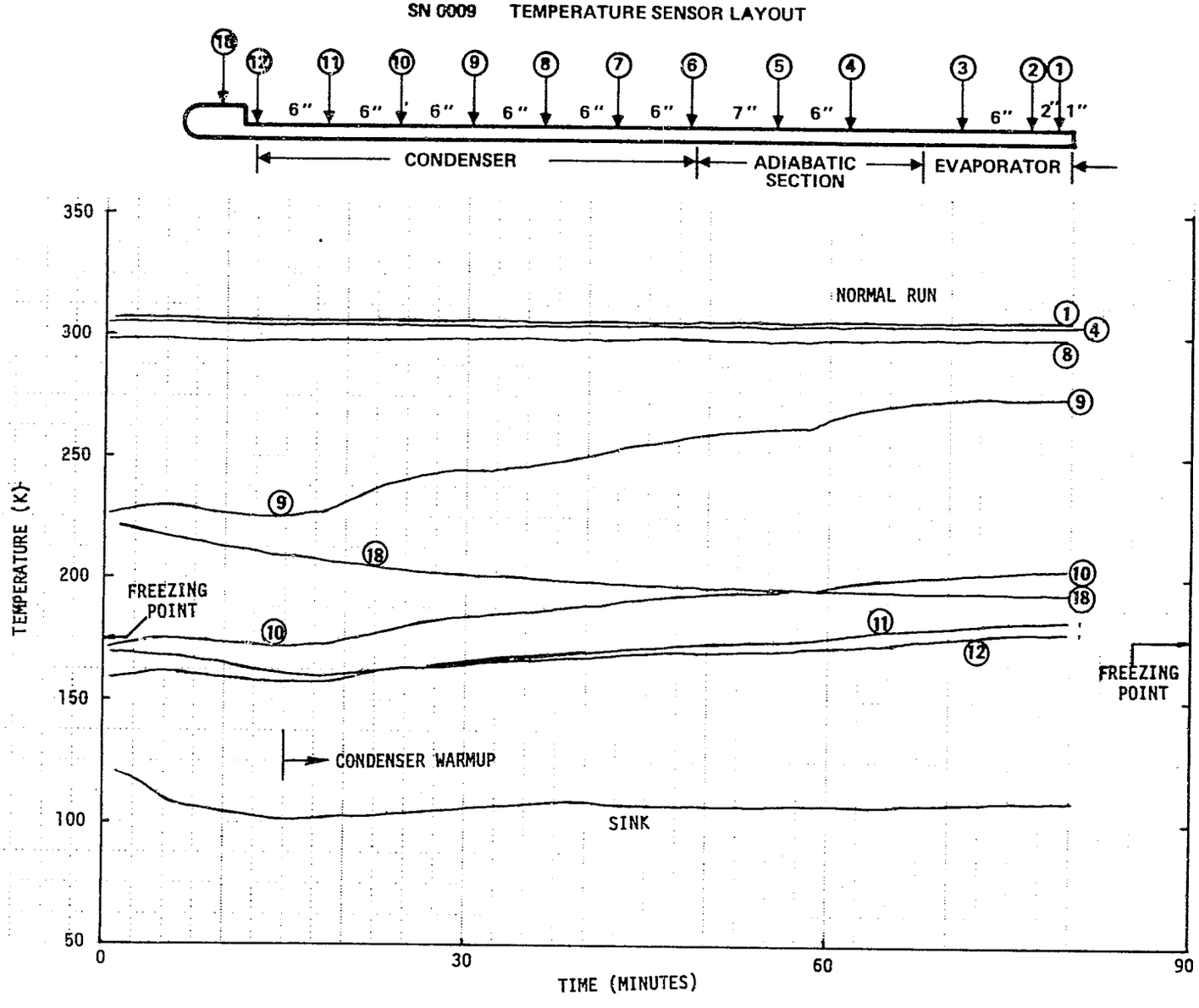

Figure B.2-11 Temperature Histories During SN009 Heat Pipe Cyclic Test No. 25

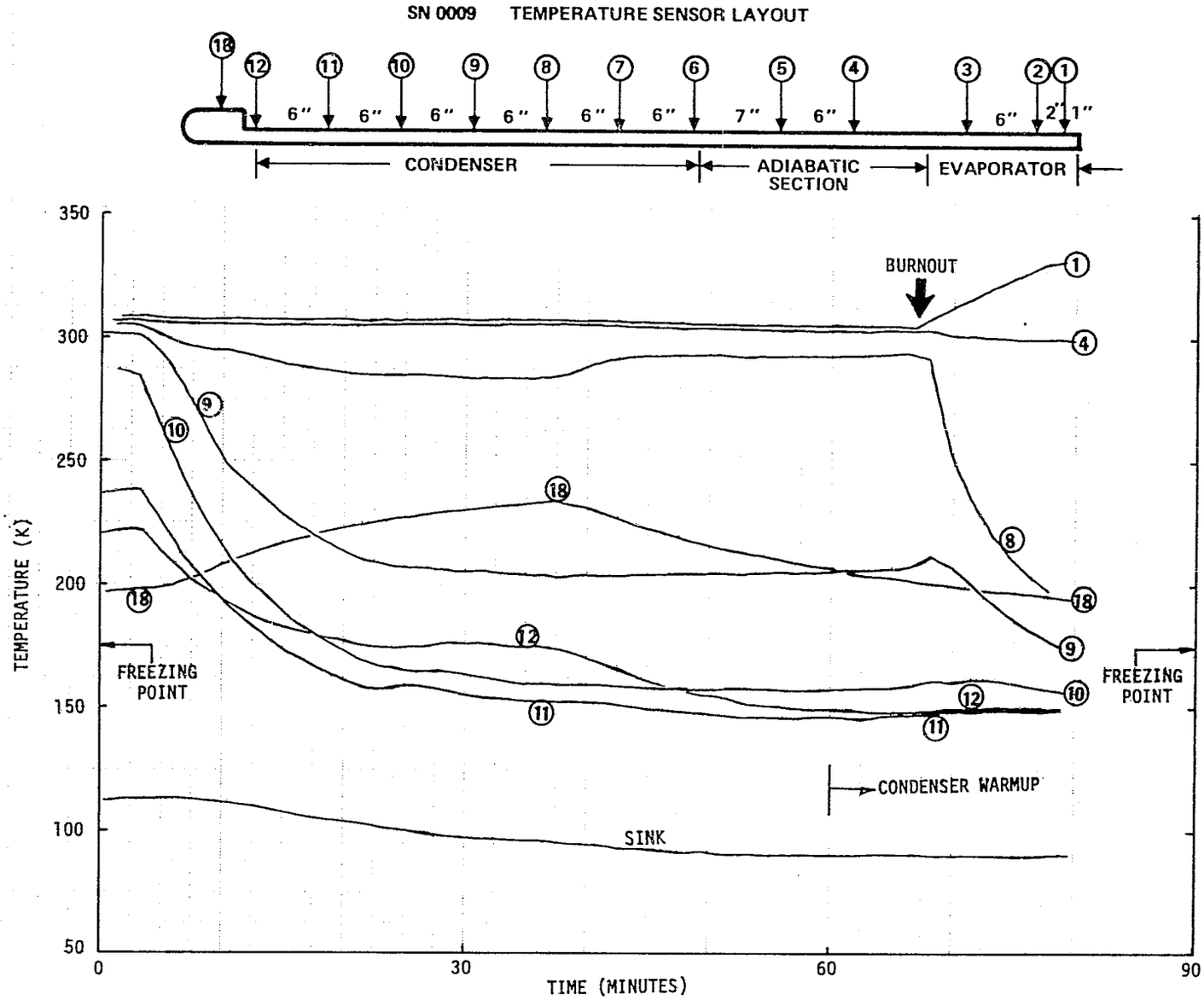

Figure B.2-12 Temperature Histories During SN009 Heat Pipe Cyclic Test No. 26